

HYDROGEOLOGICAL CHARACTERISTICS OF CARBONATE FORMATIONS OF THE CUDDAPAH BASIN, INDIA

A thesis submitted to the

University of Hyderabad

**in Partial Fulfillment of the
Requirements for the Award of the Degree of**

DOCTOR OF PHILOSOPHY

In Earth and Space Sciences



By

Farooq Ahmad Dar

July, 2013

DECLARATION

Center for Earth and Space Sciences
University of Hyderabad
HYDERABAD, 500134

Dated: 15th July, 2013

This is to certify that I, *Farooq Ahmad Dar* have carried out the research work embodied in the present thesis entitled “*Hydrogeological Characteristics of Carbonate Formations of the Cuddapah Basin, India*” for the full period prescribed under Ph.D ordinances of the University.

I declare to the best of my knowledge that the work has not been submitted previously in part or in full for any degree in this or any other university/institute. All the sources used or quoted in the thesis have been indicated and properly acknowledge.

Name: **Farooq Ahmad Dar**
Enrollment No. **09ESPE01**
University of Hyderabad

Dr. Shakeel Ahmed
Chief Scientist and Team Leader
Indo-French Center for Groundwater Research,
CSIR-National Geophysical Research Institute,
Hyderabad, 500007

Prof. A. C. Narayana
Professor and former Director,
Centre for Earth and Space Sciences,
University of Hyderabad,
Hyderabad, 500134

Head of the Department

*Dedicated
to
My Family*

ACKNOWLEDGEMENTS

Firstly, with soul deep veneration and humble submission, I bow to Almighty for everything.

*I am deeply indebted and highly thankful to my supervisor **Dr. Shakeel Ahmed**, Chief Scientist and team leader Indo-French Centre for Groundwater Research, CSIR-NGRI, Hyderabad for his unique guidance and inspirations. This thesis was possible only because of his very kind and helping nature. He provided me all the necessary facilities to carry out the research. I would take this opportunity to thank **Prof. A.C. Narayana**, Prof. and former director Centre for Earth and Space Sciences, University of Hyderabad for his all valuable help. Both have critically reviewed drafts of the thesis and made valuable suggestions and improvements that significantly enhanced the clarity and content.*

*I fall short of words for expressing my deep sense of gratitude to **Dr. Jerome Perrin** for his help and insight with this project. It was an enriching experience to work with him. Ideas expressed have been constructively and critically reviewed and suggested by him from time to time. He has, in fact been instrumental in my evolution as a groundwater researcher.*

*I wish to express my gratitude and debt to Director NGRI, **Prof. Mrinal K. Sen** for providing all kinds of necessary facilities. He has always been a source of encouragement to the young researchers. All the necessary facilities were provided by CSIR-NGRI. I am also thankful to former director NGRI **Dr. V.P. Dimri** who encouraged me when I joined NGRI as JRF.*

*I would like to thank **Prof. Ramakrishna Ramaswami**, Vice Chancellor, University of Hyderabad for making the administrative formalities easier.*

*I take this opportunity to thank **University Grants Commission (UGC) and Council of Scientific and Industrial Research (CSIR)** for financial support as Junior Research Fellowship and Senior Research Fellowship without which this thesis was impossible. Financial assistance provided by UGC-CSIR **vide F. No. 33-50/2007: JRF/SRF**). **Embassy of France in India** is gratefully acknowledged for offering me 4 months Research fellowship that provided me the opportunity to work with internationally renowned scientists and an exposure to the advance research at Montpellier, France.*

*I feel overwhelmedly indebted to **Dr. Nathalie Dörfliger** for providing me introductory ideas about the karst hydrogeology and sharing her experience and insights at the esteemed laboratory BRGM in France. Special thanks to **Mr. Jean Louis, Dr. Beneoit, Dr. Perrin and others at Montpellier, BRGM** for their much needed help and support during my stay at France.*

*I am also thankful to **Dr. Chakarvarty** Director, Centre for Earth and Space Sciences, University of Hyderabad for his valuable support. I would especially like to thank **Mr. Waju-du-din, Mr. Ahmed-ud-din and Mr. Irshad Ahmad** for meticulous assistance during field work in hot climate with lot of chilli foods. Many thanks to **Dr. Krishnaiah, Nagmunya, Babu and other** Belum cave employees for their valuable support during field visits.*

*I am indebted to **Dr. Alexandre Boisson, Dr. Muralidharan, Dr. Rangarajan** for their valuable comments and suggestions. I am also grateful to **Dr. V.K. Somwamshi, Dr. Subhash Chandra, Dr. Tanvi Arora, Dr. N.C. Mondal, Dr. Haris Khan, Dr. Adil Nabi, Dr. P.D. Sridevi Dr. Saheb Rao, Dr. Fakhre Alam** for providing continuous encouragement and useful inputs regarding my research. It is my pleasure to thank **Ms. Sara, Mrs. Mehnaz, Mr. Mehjoor Ahmad, Mr. Muneer Ahmad and Ms. Zahida** who were always a source of encouragement and motivation during my research. My special thanks to **Md. Khalil Junior** for his unparalleled support and pains he took for me during my research at IFCGR, NGRI. My colleagues **Mr. Syed Ali, Mr. Khaleel, Dr. Surendra Atal, Dr. E Nagaiah, Dr. Purushottam, Dr. NV Sheshama, Mr. Tarun Gour, Mr. Raghavendra, Ms. Visa Zapu, Ms. Kissa Fatima, Mrs. Deepa Negi, Mr. Nasish Rana and others** support and encouragements are thankfully acknowledged. Sincere thanks to **Mr. Surya Narayana**, my colleagues at UCESS, University of Hyderabad especially **Ms. Sravanti, Mr. Bijan Debnath, Mr. Sandeep Chintu, Mr. Anjaiah, Mrs. Vani, Ms. Varalakshmi, Mr. Shiva Kumar and office bearers** for their worthwhile support.*

*I am thankful to Geological Survey of India and Osmania University for providing me access to the literature pertinent to study. Different organizations, particularly APGWD, and Central Groundwater Board are thankfully acknowledged. Thanks are due to **Dr. Jean Riotte** at IISC Bangalore, **Dr. Nagabushnam** at Isotope Lab and other people at NGRI and CRIDA, Hyderabad for sample analysis and other valuable help. **Dr. Mani** of Birds NGO is gratefully acknowledged. I am also thankful to all office bearers in CSIR-NGRI who directly or indirectly helped me during the research period.*

*My brother-like friends, **Riyaz Ahmad, Ali Mohd, Zameer Ahmad, Shamim Ahmad, Sajad Ahmad, Imran Khan, Late Mukhtar Ahmad, Mohd. Iqbal, Ashaq Hussain and others** deserve my sincere thanks whose love and appreciation is valuable to me forever. Many of my colleagues, **Mahmood Alam, Tabish Raza, Mohd Rafiq, Waseem Raza, Nagaraju, Fuzail Akhtar** and many others at NGRI or outside deserve a special mention. Also thanks to **Chauhan** family for the kind help in returning my laptop and documents when I lost them during the final stage of my thesis.*

*Mere thankful words cannot compensate for the noble sacrifices of my parents **Mr. and Mrs. Ab. Rashid Dar**, my loving sister, family members and relatives. This acknowledgement will be incomplete without thanking for their love, care and support throughout all my endeavors in my life. Your prayers, wishes and blessings gave me re-birth. Whenever I was at ebb their blessings en-route me to shore. I have no words except being in your thoughts and with you all the time. The prayers and wishes from all my relatives particularly those very close to me helped and encouraged me from time to time.*

At last, I take this opportunity to once again thank Almighty to Whom all this research is indebted to.

(Farooq Ahmad Dar)
IFCGR, CSIR-NGRI, Hyderabad

ABSTRACT

Title: Hydrogeological Characteristics of Carbonate Formations of the Cuddapah Basin, India

Karst hydrogeology is an important field of earth sciences as the aquifers in carbonate formations represent vital resource of groundwater that feeds a large part of the world population particularly in semi-arid climates. These unique aquifers possess peculiar characteristics developed by dissolutional activities of water. Karst aquifers possess a typical hydrogeological setup from surface to subsurface. The aquifers are governed by slow groundwater flow in matrix porosity, a medium to fast flow in fractures and rapid flow in conduits and channels. This large variability in their properties makes the prediction and modeling of flow and transport very cumbersome and data demanding. The aquifers are vulnerable to contamination as the pollutants reach the aquifer very fast with little or no attenuation. The geomorphological and hydrogeological properties in these aquifers demand specific techniques for their study. The carbonate aquifers of the semi-arid Cuddapah basin were characterized based on geomorphological, hydrogeological and hydrochemical investigations. All the formations are highly karstified possessing one of the longest and deepest caves of India and few springs along with unique surface features. Karstification is still in progress but at deeper levels indicated by growing speleothems of different architectural size. Model of karstification indicates that lowering of base level of erosion resulted in the dissolution of deeper parts of the limestone as represented by paleo-phreatic conduits in the region. Moist conditions of the past were responsible for the karst development which has been minimized due to the onset of monsoon conditions. Karst has developed at various elevations representing the past base levels in the region.

The recharge processes in these aquifers are complex due to climatic and karst specificities. Point recharge is the major contributor which enters the aquifer as allogenic water. It replenishes the groundwater very rapidly. Diffuse recharge travels through soil and epikarst zone. Average annual recharge of semi-arid Narji limestone aquifer is 29% of the rainfall which occurs during 5-7 rain events in the year.

The hydrogeochemical characteristic of karst aquifers is quite variable. A significant difference is observed in hydrochemistry. High concentrations of SO_4^{2-} , Cl^- , NO_3^- suggests the anthropogenic source particularly from agriculture. Local Meteoric Water Line of $\delta^2\text{H}$

and $\delta^{18}\text{O}$ isotopes of rain and groundwater shows a slope of 7.02. Groundwater isotope data shows more depletion in heavy isotopes -a result of high evaporation of the area. Groundwater samples show a trend with a slope of 4 and 3.1 for $\delta^2\text{H}$ and $\delta^{18}\text{O}$ respectively. Groundwater during dry months gets more fractionated due to higher temperature and little rainfall. The irrigated water becomes more enriched and then recharges the aquifer as depleted irrigation return flow. The isotopes show large variation in spring water. Few springs are diffuse or mixed type and not purely of conduit type in the area. Tracer results indicate that the tracer output at the sampling location depends on the hydrogeological setup and the nature of karstification.

The study has significantly dealt with in disclosing the typical characteristics of such aquifer systems and bringing out a reliable as well as detailed assessment of various recharges to the system. The groundwater chemistry has been elaborated to establish the nature of possible hydrochemical processes responsible for water chemistry variation in semi-arid karst aquifer. Such study has thrown light on the aquifers that are on one hand very important from social and strategic point of view and on the hand were left unattended from the detailed scientific studies.

Key words: carbonate formations, karst aquifers, Belum Cave, Narji limestone, dissolution, karstification, epikarst, groundwater flow, spatio-temporal variability, isotopes, tracers, vulnerability.

CONTENTS

Acknowledgements.....	i-ii
Abstract.....	iii-iv
Contents.....	v-vii
List of Tables.....	viii-ix
List of Figures.....	x-xvi
List of Appendices.....	xvii-xviii
CHAPTER 1. KARST FORMATIONS: GENERAL INTRODUCTION...	1-26
1.1. Origin and Historical Evolution.....	1
1.2. Processes.....	2
1.3. Characteristic Features.....	9
1.4. Conceptualization.....	13
1.5. Distribution of Karst Formations.....	19
1.5.1. World Scenario.....	19
1.5.2. Indian Scenario.....	21
1.6. Objectives of Present Study.....	22
1.7. Scope of Present Study.....	24
1.8. Summary.....	25
CHAPTER 2. STUDY AREA.....	27-50
2.1. Introduction.....	27
2.1.1. Location.....	27
2.1.2. Climate.....	29
2.1.3. Topography and Geomorphology	33
2.1.4. Soils, Vegetation and Land-use/land-cover.....	34
2.1.5. Geology and Stratigraphy.....	36
2.2. Regional Hydrogeology.....	45
2.2.1. Aquifer Systems.....	45
2.2.2. Groundwater Exploitation.....	47
2.3. Summary.....	49
CHAPTER 3. METHODS AND APPROACHES.....	51-73
3.1. Introduction.....	51
3.2. Data Acquisition.....	53
3.2.1. Field Investigations.....	53
3.2.2. Field Sampling and Procedures.....	54
3.2.3. Laboratory Analysis.....	59
3.3. Hydrogeological Investigations.....	61
3.4. Hydrochemical Studies.....	62
3.4.1. Physico-chemical Analysis of Groundwater.....	62
3.4.2. Stable Isotope Study.....	63
3.4.3. Tracer Study.....	64
3.5. Recharge Estimation.....	66
3.5.1. Point Recharge.....	70

3.5.2. Diffuse Recharge.....	71
3.5.3. Tritium Method.....	72
3.6. Statistical Approach.....	72
CHAPTER 4. KARSTIFICATION IN THE CUDDAPAH BASIN.....	74-115
4.1. Introduction.....	74
4.2. Karstified Formations.....	74
4.2.1. Karstification in the Vempalle Dolomite.....	75
4.2.2. Karstification in the Narji Limestone.....	79
4.2.3. Karstification in the Koilkuntla Limestone.....	91
4.3. Proposed Model of Karstification.....	96
4.3.1. Karst Evolution.....	97
4.3.2. Regional Karstification in Southern Andhra Pradesh.....	103
4.4. Hydrodynamics and Hydrochemistry of Narji Limestone.....	106
4.4.1. Groundwater Flow.....	106
4.4.2. Hydrochemistry of Spring Water: A Means to Characterize Karst System.....	111
4.5. Summary.....	114
CHAPTER 5. GROUNDWATER RECHARGE IN KARST AQUIFERS.....	116-138
5.1. Introduction.....	116
5.2. Recharge Estimation.....	118
5.2.1. Point Recharge (Q_{run})	119
5.2.2. Diffuse Recharge (Q_r)	121
5.2.3. Calibration of the Model.....	129
5.2.4. Validation of Recharge Results by Tritium Injection Method.....	134
5.3. Impact of Anthropogenic Activities on Groundwater and Recharge.....	135
5.4. Summary	137
CHAPTER 6. HYDROGEOCHEMICAL CHARACTERISTICS OF KARST AQUIFER.....	139-165
6.1. Introduction.....	139
6.2. Physical Parameters.....	142
6.3. Chemical Parameters.....	144
6.4. Spatial Variability of Water Quality.....	145
6.5. Seasonal (PRM-POM) Variability of Water Quality.....	149
6.6. Temporal Variability of Water Quality.....	152
6.7. Hydrochemical Evolution.....	155
6.8. Water-rock Interaction in Karst Aquifer.....	157
6.9. Summary.....	164
CHAPTER 7. CHARACTERIZATION OF KARST AQUIFER USING ISOTOPES AND TRACERS.....	166-189
7.1. Introduction.....	166
7.2. ^2H and ^{18}O Isotopes.....	170

7.2.1. Rainwater and Local Meteoric Water Line.....	170
7.2.2. Groundwater.....	173
7.2.3. Deuterium Excess and Groundwater Recharge.....	178
7.2.4. Isotopic Time Series of Karst Springs.....	180
7.3. Karst Aquifer Characteristics Inferred from Tracer Study.....	183
7.4. Summary.....	188
CHAPTER 8. CONCLUSIONS AND RECOMMENDATIONS.....	190-200
8.1. Conclusion.....	190
8.2. Recommendations.....	199
REFERNCES.....	201-233
APPENDICES.....	234-249

LIST OF TABLES

- Tab.1.1. Limestone erosion rates as measured in different climatic regions of the world.*
- Tab.1.2. Triple permeability media in karst and their characteristics (after white, 2003 and Gillieson, 2009).*
- Tab.2.1. Annual rainfall, monsoon and non-monsoon rainfall amount and number of rainy days at Kolimigundla station from 1999-2011.*
- Tab.2.2. Statistical analysis of rainfall at different station in the area, from 1999-2009 (SD, standard deviation; CV, coefficient of variation).*
- Tab.2.3. Characteristics of different Proterozoic Intra-Cratonic basin of India (after Kale, 1991). #exposed to maximum thickness. For location refer to insert in Fig. 2.1.*
- Tab. 3.1. Parameters measured from different sampling locations from the study area. Physical parameters (Q, pH, T, EC) were measured in-situ while major ions and isotopes were measured in laboratory. For sample locations of springs and caves refer to Appendix 5 and 6 and for bore wells refer to Appendix 10 and 11.*
- Tab.4.1. Statistics of 1-year bimonthly data (static water levels (SWL), pumped water levels, abstraction rates (Q)) from 84 irrigation wells in the Koilkuntla limestone*
- Tab.5.1. Land use classes and hydrological soil groups of the study area based on soil map. * indicates the infiltration rate in mm/hour for each soil type.*
- Tab.5.4. Annual rainfall and recharge in mm for the study area. The data is from Kolimigundla and Belum stations.*
- Tab.5.3. Average monthly rainfall, Q_{run} , Q_r and AE for the study area from 2002-2011. Data is from Belum and Kolimigundla station. All values are in mm.*
- Tab. 5.4. Annual recharge rates calculated in different semi-arid karst aquifers of the world against annual rainfall. *Concentrated+diffuse, ** Diffuse*
- Tab.5.5 . Values of specific yield computed from pumping tests and annual recharge and rainfall of carbonate rocks in India. *Average annual groundwater level fluctuation in meters. ** percent of point+diffuse recharge.*
- Tab. 5.6. Natural recharge calculated at the injection sites in the area. The site numbers are also the serial number of scatter plots of Fig.5.9 .*
- Tab. 6.1. Statistical analysis of chemical parameters of groundwater for PRM and POM seasons. Number in brackets indicates the number of samples. T in °C, EC in μ/cm*

and ion concentration in mg/l except $\text{Ca}^{2+}/\text{Mg}^{2+}$ ratio. Number of samples is given in braces.

Tab. 6.2. Water types as observed in the spring and bore well waters for the two seasons.

Tab. 6.3. Difference in ionic concentration in percent from PRM to POM (Pre minus Post/Pre*100). Positive values indicate a decrease in concentration and negative values indicate an increase in concentration during POM season.

Tab. 6.4. Mean and coefficient of variation of different ions in spring and bore well samples during PRM and POM. Mean is expressed in mg/l and CV as percentage. Number of samples is given in parenthesis.

Tab. 6.5. Correlation matrix between different groundwater chemical parameters. The top value in each row represents PRM season and bottom values POM season. TH is total hardness as CaCO_3 .

Tab. 6.6. Mean and coefficient of variation CV (%) of different physico-chemical parameters showing intra-site temporal variability in karst springs. Q in L/s, T in $^{\circ}\text{C}$, EC in $\mu\text{S}/\text{cm}$ and ion concentration in mg/l.

Tab.7.1. LMWL equations for different station of India based on various studies.

Tab.7.2. Statistical parameters of isotopic composition of springs, bore well and rain water collected during PRM and POM 2011 period.

Tab.7.3. Statistical analysis of isotopic composition of spring and rain water collected during 2009 to 2011 period. Water samples were collected three to four times a year.

LIST OF FIGURES

- Fig.1.1. Comprehensive schematic representation of a karst system indicating the processes responsible for karstification (Ford and Williams, 2007).*
- Fig.1.2. Karstification and its dependence on different processes (Clemens, et. al., 1999, modified after Kiraly, 1975).*
- Fig.1.3. Equilibrium curves for the dissolution of calcium carbonate and its dependence on the temperature, pCO₂, CaCO₃ saturation (modified after Jennings, 1971).*
- Fig.1.4. A typical well developed karst model with its physiographic and hydrologic features (source; Kentucky Geological Survey, <http://www.uky.edu/KGS/water/general/karst/>).*
- Fig.1.5. Conceptual models of karst system according to different authors: [(a) Drogue, 1971 (b) Mangin, 19745 (c) Dörfliker & Zwahlen, 1995 (d) Marsaud, 1996 (e) Lee and Krothe, 2001 (f) Klimchouk, 2004 (g) White, 2003 (h) Bakalowicz, 2003].*
- Fig.1.6. Variability of hydraulic conductivity in karst aquifer with scale of measurement; (a) after Kiraly, 1975 and (b) after Sauter, 1992).*
- Fig.1.7. A three cascading sub-system model to represent karst spring hydrographs (Hobbs and Smart, 1986).*
- Fig.1.8. Representation of epikarst (subcutaneous) zone by different authors; (a) William 1983, (b) Gunn 1983 and (c) Klimchouk 2004.*
- Fig.1.9. Global carbonate rock outcrops (Ford and Williams, 2007) source, www.circleofblue.org.*
- Fig.1.10. Map of India showing major aquifer systems. Carbonate formations with potential for karstification are also shown, (source CGWB, 2012).*
- Fig.2.1. Geological map of Proterozoic Cuddapah Basin (CB) southern India, showing the distribution of three karstified formations, modified after GSI, 1997. Map of India shows location of different Proterozoic Basins. Study are has been shown in inset for clarity.*
- Fig.2.2. Long term (10 year) average monthly variation of different climatic parameters at Kurnool station (temperature, wind speed and humidity from Kurnool station, source IMD).*
- Fig.2.3. Percentage contribution of seasonal rainfall to the annual amount at Kolimigundla from 1999-2011.*

- Fig.2.4. Percentage of long term normal rainfall showing climatic conditions in the area. Data from Kolimigundla mandal.*
- Fig.2.5. Trilinear diagram showing granulometric composition of soils of the area. Soils fall in the field of clay.*
- Fig.2.6. Major stratigraphic successions of the Cuddapah Basin. Vertical scale has been exaggerated for clarity.*
- Fig.2.7. Geological cross-section across the Cuddapah sedimentary basin showing three karstified formations (cross-section through the centre of CB).*
- Fig.2.8. Growth rate of groundwater development in Andhra Pradesh from 1980-2010 (Jain et. al., 2009).*
- Fig. 3.1. Flow chart showing the detailed account of data sets used for this study.*
- Fig. 3.2. Flow chart of the methodology used for the characterization of the karst aquifer.*
- Fig.3.3. Field photograph showing the measurement of the water level in the study area (left). A dug wells in the Narji Limestone is also shown (right) which is currently being used for irrigation purposes.*
- Fig.3.4. Meteorological station at Belum (5 km from Kolimigundla village) installed for monitoring daily rainfall and evaporation in the study area.*
- Fig.3.5. Picture of field measurements of infiltration rates in the soils of the study area.*
- Fig.3.6. Groundwater flow in karst springs monitored during the study period. Left one is the photograph of Belum spring, S1 during flowing condition and right one shows the Kona spring S2 flowing through a conduit. For location refer to Fig. 2.1.*
- Fig.4.1. Geological cross-section across the Vempalle dolomite along Rayala Cheruvu showing the main cave and inferred piezometric surface based on observations in the cave and existing borewells in the surroundings (refer to Fig. 2.1 for location).*
- Fig.4.2. Picture taken at the bottom of Kuruva Bali Guha (C8), showing the phreatic shaped conduit and sediment accumulation on the floor.*
- Fig.4.3: Geological cross-section across Vempalle dolomite along Chillavaripalle Cave (C25) area (refer to Fig. 2.1) showing typical geomorphological features.*
- Fig.4.4. Fracture orientation around Chillavaripalle Cave plotted as frequency in Rose Diagram.*

- Fig.4.5. Geological and geomorphological map of the Narji limestone terrain in Kolimigundla sector (refer to Fig. 2.1) showing observed karst features.
- Fig.4.6. Picture showing typical mesa and butte geomorphic features, overlying the Narji limestone in Kolimigundla area.
- Fig.4.7. Geological cross-section across Narji limestone terrain near Belum area. The trace of the cross-section is indicated in Fig. 4.6.
- Fig.4.8. Sinkhole in the Narji limestone; (a) developed near Belum cave and (b) that has opened in 2003 probably as a consequence of increased aquifer pumping in Nossam area.
- Fig. 4.9. Field photograph, showing (a) epikarst development in the Narji limestone near Belum and (b) secondary calcite deposition in the area.
- Fig.4.10. Fracture orientation plotted as frequency in Rose Diagram around Belum Cave (a) and around Banderlapalle Cave (b). N is the number of sample points.
- Fig.4.10. Fracture orientation plotted as frequency in Rose Diagram around Belum Cave (a) and around Banderlapalle Cave (b) Banderlapalle. N is the number of sample points.
- Fig.4.11. Field photograph, showing the top of the Uppalapadu Plateau along Yadiki area. Paniam quartzite is shown overlying the Narji limestone.
- Fig.4.12. Geological cross-section through Yadiki karstified area showing cave and spring locations and tectonic features.
- Fig.4.13. Photographs showing currently developing speleothems inside Yadiki cave.
- Fig.4.14. Karst spring discharge of the Narji Limestone at Yaganti spring (S8) through conduits.
- Fig.4.15. Geological cross-section of the Koilkuntla limestone formation. The indicated quarry is also the location of Fig. 4.16.
- Fig.4.16. Karrenfield underlying the soil cover in the Koilkuntla limestone as an indicator of epikarst development.
- Tab.4.1. Statistics of 1-year bimonthly data (static water levels (SWL), pumped water levels, abstraction rates (Q)) from 84 irrigation wells in the Koilkuntla limestone
- Fig.4.17. Plot between specific capacity and static water level in Koilkuntla limestone in pre- and post-monsoon. (Red dots indicate deeper water table and blue dots for shallower water table).

- Fig.4.18. Plot between specific capacity and percentage of wells in Koilkuntla limestone. (Red dots are for pre-monsoon data and blue dots for post-monsoon data).
- Fig.4.19. Planimetric view of different cave patterns identified in the area (maze, dendritic and meander), which had developed in three karstified formations.
- Fig.4.20. A karstification conceptual model of the Narji limestone; 1) initial phase with development of maze cave system in a confined setting; 2) following tectonic uplift, the limestone is progressively exposed to the surface and anastomosing phreatic cave systems develop; 3) the water table gets progressively lower inducing a lower level of karstification (present state).
- Fig.4.21. Hydrograph and chemographs of the Belum spring (S1) showing a sharp response to the rainfall events typical of a karst aquifer:
- Fig.4.22. Hydrograph of an observation well in Narji limestone near Kolimigundla, showing a sharp response to the rainfall events typical of a karst aquifer.
- Fig.4.23. Scatter plot showing the temporal variability of groundwater discharge from different karst springs of the Narji limestone. For location and description of springs refer to Fig. 2.1.
- Fig. 4.24. Water level (masl) maps of the Narji limestone aquifer (left PRM and right POM) for the year 2011. Drainage and surface reservoirs are also shown.
- Fig.4.25. Hydro-chemographs of Kona spring Yadiki (S2 and S3). For location and description of springs refer to Fig. 2.1 and Appendix 6.
- Fig.4.26. Hydro-chemograph of Yaganti karst spring (S8). For location and description of spring refer to Fig. 2.1.
- Fig.5.1. Location of the area showing (a) geology, drainage, water level and surface elevation in masl and (b) land use of the area. The area has been selected for recharge estimation.
- Fig.5.2. Recharge model of the semi-arid karst aquifer; Q_{rum} , Q_r , and Q_{intr} are point recharge, diffuse recharge and internal runoff respectively. Q_{quarry} , Q_{irf} , Q_{pump} are the water stored in quarry depressions, irrigation return flow and pumping water that represents the impact of anthropogenic conditions in the area.
- Fig.5.3. Bar plot of the total monthly values for three years against rainfall (AE actual evapotranspiration, Q_{rum} concentrated recharge and Q_r diffuse recharge). All parameters are in mm.

- Fig.5.4. Diagrams showing daily based recharge calculations as a function of intensity and duration of rainfall (Q_{run} concentrated recharge and Q_r diffuse recharge).
- Fig.5.5. Scatter plot showing the linear correlation of different recharge types with rainfall.
- Fig.5.6. Monthly water level, recharge ($Q_{run}+Q_r$) and change in storage of Kolimigundla bore well as shown against monthly rainfall.
- Fig.5.7. Scatter plot of annual ($Q_{run}+Q_r$) and water level fluctuation of Kolimigundla bore well showing good correlation.
- Fig.5.8. The effect of daily rainfall on water level variation of Belum spring for two years; left 2009 and right 2010. Horizontal axis is plotted as number of days in a year to show the time lag in water level.
- Fig. 5.9. Tritium concentration in counts per minute (CPM) and soil moisture in weight percent measured with depth from the soils cores.
- Fig. 6.1. Geological map of the karstified area. Three karstified formations of Cuddapah Basin are also shown (modified after GSI, 1997). Black dashed contours represent the water level in masl. Spring and bore well samples are represented by solid circles. Major surface drainage is shown by blue lines.
- Fig. 6.2 Geological cross-section along the karstic terrain, showing the Narji limestone aquifer and location of some springs and bore wells.
- Fig.6.3. Scatter plot showing cations sum Vs anions sum for pre-monsoon (PRM) and post-monsoon (POM) samples. Good correlation indicates the quality of water chemistry analysis.
- Fig. 6.4. Hydrochemical facies showing the spatial variability of spring and bore well waters on Piper Diagram (a) PRM and (b) POM samples.
- Fig. 6.5. Intra-site temporal variability of physico-chemical parameters in springs (S1, S2, S8). Water level was used for Belum spring (S1) whereas discharge was compared for others springs.
- Tab. 6.6. Mean and coefficient of variation CV (%) of different physico-chemical parameters showing intra-site temporal variability in karst springs. Q in (L/s, T in $^{\circ}C$, EC in $\mu S/cm$ and ion concentration in mg/l.
- Fig. 6.6. Temporal variability as indicated by the coefficient of variation CV (%) of physico-chemical parameters in karst springs.

- Fig. 6.7. Hydrogeochemical evolution of groundwater during PRM and POM using LL-Diagram. The pink lines indicate the possible shift of chemistry from mixed character to Ca-Mg dominated field.
- Fig. 6.8. Scatter plots between various cations and anions that can indicate the possible nature of equilibrium reactions between rock and water in the area during PRM (black dots) and POM (blue dots). Less scatter is observed between $\text{Ca}^{2+} + \text{Mg}^{2+}$ Vs $\text{HCO}_3^- + \text{SO}_4^{2-}$.
- Fig. 6.9. Plot of $\text{SO}_4^{2-} / (\text{SO}_4^{2-} + \text{HCO}_3^-)$ vs. $\text{Ca} / (\text{Ca} + \text{Mg})$ for the PRM and POM samples of the area.
- Fig. 6.10. Plot of SO_4^{2-} vs. Ca^{2+} and SO_4^{2-} vs. Mg^{2+} for the PRM and POM samples of the area.
- Fig. 6.11. Gibbs plot showing the mechanism that controls the chemistry of groundwater (a) cations and (b) anions.
- Fig. 6.12. Na^+ Vs K^+ plots for PRM and POM showing the processes of water rock interaction.
- Fig.7.1. Rainout effect on $\delta^2\text{H}$ and $\delta^{18}\text{O}$ values (based on Hoefs, 1997 and Coplen et. al., 2000).
- Fig.7.2. Generalized diagram showing how common hydrologic processes affect oxygen and hydrogen isotopic composition of water, (source: <http://cierzo.sahra.arizona.edu/programs/isotopes/oxygen.html> and insert from Toran, 2006).
- Fig.7.3. Plot of $\delta^2\text{H}$ versus $\delta^{18}\text{O}$ for rainwater samples. GMWL and LMWL (Mumbai) represent the global meteoric line of Craig (1961) and the local meteoric water line from Mumbai, respectively.
- Fig.7.4. Step plot showing the weighted monthly isotopic signature as a function of total monthly rainfall for the study period.
- Fig.7.5. Plot of $\delta^2\text{H}$ Vs $\delta^{18}\text{O}$ for groundwater samples for PRM (left) and POM 2011 (right). GMWL and LMWL represent the global meteoric line of Craig (1961) and the local meteoric water line, respectively. Blue line is a trend line through water sample data.
- Fig.7.6. Box-Whisker plot showing the variability of $\delta^2\text{H}$ (a) and $\delta^{18}\text{O}$ (b) isotopic composition of spring compared with rainwater during 2010 to 2011.

Fig.7.7. Temporal evolution of $\delta^2\text{H}$ and $\delta^{18}\text{O}$ of groundwater collected from Belum spring (S1). For spring location, refer to Fig. 2.1.

Fig.7.8. Temporal evolution of $\delta^2\text{H}$ and $\delta^{18}\text{O}$ of groundwater collected from different springs (Kona1, S2; Kona2, S3; Rati, S6 & Yaganti, S8). For spring location and characteristics refer to Fig.2.1 and Appendix 4.

Fig.7.9. A scatter plot of $\delta^{18}\text{O}$ Vs d-excess for PRM (left) and POM (right) samples of 2011.

Fig.7.10. Figure shows a hypothetical single-peaked tracer breakthrough curve with its different parts and interpretation.

Fig.7.11. Geological map of Yadiki area showing the dye injection point and sampling locations. Dashed contours are surface elevations in meters above sea level. (For Cave and spring locations refer to Fig.2.1). Inset shows the subsurface profile of Munagamanu Gavi (C8) for more details refer to chapter 4.

Fig. 7.12. Geological cross-section of Yadiki area showing the cave and spring location.

LIST OF APPENDIX

- Appendix 1. Stratigraphic record of Indian Geology showing the major carbonate units in the country. (Compiled from Wadia, 1919; Murty, 1981; GSI, 1997; Kumar, 2006). Three karstified units of Cuddapah basin are highlighted.*
- Appendix 2. Data of monthly rainfall from 1999-2011 at Kolimigundla from Mandal Revenue Office, Kurnool District, A.P.*
- Appendix 3. Rainfall and Pan Evaporation data collected at Belum Cave station from 2009-2011.*
- Appendix 4. Stratigraphic classification of Cuddapah Basin after GSI, 1997. Three karstified units are shown in color.*
- Appendix 5. Description of the caves located in the different carbonate rocks of the CB. (N.L., Narji Limestone; V.D., Vempalle Dolomite.*
- Appendix 6. Description of the springs of the carbonates and quartzites of the CB. (N.L., Narji Limestone; V.D., Vempalle Dolomite; Q. Quartzite). (*) Gebauer 1984; (**) Shibasaki, 1985; (#) Gowd, 2005; (TS) This study; (\$) Toposheets.*
- Appendix 7. Statistical analysis of the spring flow and their physico-chemical parameters as measured during the study period (2009-2011).*
- Appendix 8. Monthly water level of an observation bore well in Narji Limestone at Kolimigundla village (data source GWD, 2010).*
- Appendix 9. Analyzed chemical data of rainwater during the study period. All concentrations in mg/l.*
- Appendix 10. Results of the Pre-monsoon (PRM) water chemistry analysis in mg/l for representative samples of the study area.*
- Appendix 11. Results of the Post-monsoon (POM) water chemistry analysis in mg/l for representative samples of the study area.*
- Appendix 12. Stable isotope data of rainfall samples collected at Belum station during the study period.*
- Appendix 13. Stable isotope data of bore wells and springs of the area during pre-monsoon (PRM) season, 2011.*
- Appendix 14. Stable isotope data of bore wells and springs of the area during post-monsoon season (POM season), 2011.*

Appendix 15. Time series of stable isotope data of springs of the Narji Limestone aquifer analyzed during the study period.

CHAPTER 1

KARST FORMATIONS: GENERAL INTRODUCTION

1.1. Origin and Historical Evolution

The term karst is a German translation of the original Slavic “krs” or “kras” meaning ‘stony ground’. Karst is a near-surface landscape formed from the dissolution of soluble rocks. The surface landscape extends to underground caves and subterranean drainage possessing a network of conduits. Thus, the landscape with exo- and endo-karst features is called a “karst landscape”. A typical karst has characteristic surface and subsurface morphological features like, karren and karrenfield, sinkholes, dry valleys, poljes, ouvalas, blind valleys, dolines, swallow holes, underground drainage systems, caves and a number of depositional features. Ford and William, (2007) presented a comprehensive work on all the surface and subsurface processes that result in the formation of different landforms of karst (Fig. 1.1). Karst mainly occurs in carbonate rocks, like limestones and dolomites, gypsum and halite (true karst of Bakalowicz, 2005). Sometimes quartzites are also prone to karstification, provided the special hydro-geochemical conditions prevail (Ford and William, 2007).

The first known publication, *Das Karstphanomen* (Cvijic, 1893 recognised as the father of Karst geomorphology) confirmed the existence of distinct landscapes of dissolutional origin (Ford, 2006). Ford and Williams, (2007) and Andreo et. al., (2010) presented karst in their text books that provide a detailed account of different aspects of karst study (geomorphology, hydrogeology, evolution of caves, groundwater flow,

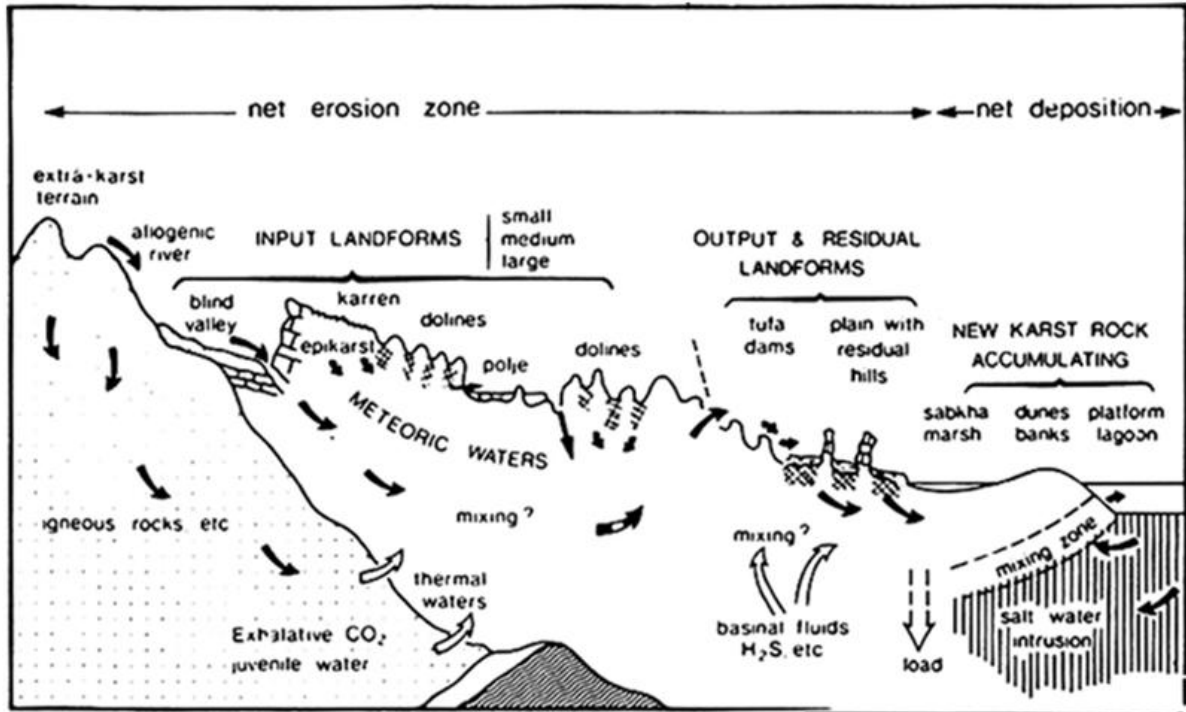


Fig. 1.1. Comprehensive schematic representation of a karst system indicating the processes responsible for karstification (Ford and Williams, 2007).

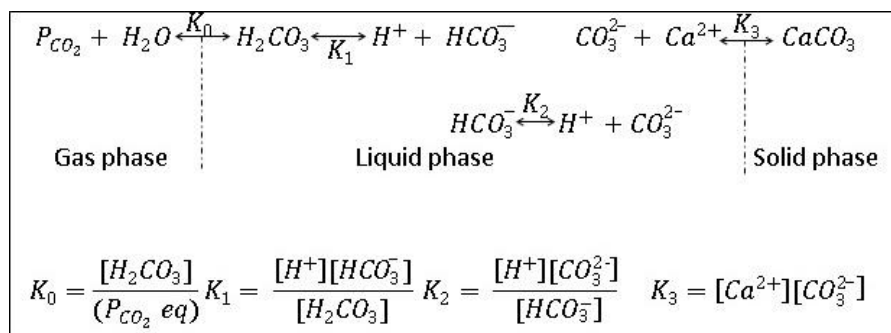
engineering aspects, etc). Karst, in other terms acts as a large reservoir for groundwater resources. The nature of the landform and the movement and composition of water in karst systems is mainly controlled by the structure and rock type. The term Karst system (Mangin, 1975) is more adapted than karst aquifer. The importance of karst aquifers lies in its valuable groundwater resources particularly in arid and semi-arid climates. It acts as an important geological agent in mass and energy transport within the earth. Karst is also important due to its beautiful and useful depositional speleothems.

1.2. Processes

Karst landscape is a result of dissolutional processes occurring in soluble rocks. The whole mechanism of karst development is termed as “Karstification” or Potential for Karst

Development. Thus, karstification is a geological process of differential chemical and mechanical erosion on soluble rock. Karstifiability is the ease with which a particular rock yields to karstification processes. The solubility of carbonate rocks is very low in chemically pure waters but readily dissolves in acidic solutions. Carbonic acid is the most important acid which is formed from the dissolution of gaseous CO₂ generally of edaphic origin (Drever, 1997). Dissolution of calcite is a relatively fast process than dolomite (Palmer and Cherry, 1984) and mostly takes place a few hours after infiltration and mainly close to the land surface (existence of exo-karst and epikarst zone) and to a lesser extent, in deeper zones within the network of karstic conduits.

As rainwater passes through the atmosphere and the soil layer, it combines with carbon dioxide and forms a weak, carbonic acid (H₂CO₃). During its movement into the rock, the acidified water begins to dissolve the limestone (CaCO₃). This carbonate solution equilibrates according to a set of reactions (Peyraube, et al., 2012) summarised as:



Thus, karst development is a part of the global Carbon Cycle. The dissolution proceeds as groundwater flows into other parts of the rock and create voids and dissolution fractures, which progressively organise into a hierarchical structure - the conduit system or karst network. The dissolution leads to the development of typical karstic features like,

sinkholes, sinking streams, springs and caves, etc which act as windows in certain cases to investigate the subterranean processes (e.g., insitu groundwater flow behaviour). Apart from dissolution, erosion and gravitational collapse also contribute towards karst development (Palmer, 1991).

The karstification is governed by two factors- geological factor; porosity, joints/fractures (Sauter, 1992) and hydrogeological-hydrogeochemical factor (karstification potential). Karst is well developed on thick, fractured and pure limestones. The purer the limestone the better will be the karst morphological development (Jennings, 1971; Herak, 1972). For example, highly developed Dinaric karst (origin of the term karst) limestones of Yugoslavia are 95 to 100% pure while less karstified white limestone in Jamaica is less than 98% pure. The thickness of a carbonate rock and its beds and lateral facies variations in geology also affect the karstification degree. A minimum thickness of one to two meters is necessary for the karst development (White et. al., 2003). The presence of impermeable interbeds (e.g., shale) limits the depth of karstification.

Geological structures (fractures, faults, etc) affect the carbonate rocks and cause brittle deformation in them which is directly or indirectly responsible for development of secondary porosity and hence karstification. Joints and vertical fractures at the surface usually focus the dissolutional processes to the depth. Large openings tend to enlarge more by solution compared to small ones which are usually disconnected from infiltration pathway (Legrand and Stringfield, 1971).

Global sea-level (base level) variations and regional geodynamics also affect the processes of karst development. Abandoned conduits located in the unsaturated zone have developed during high base-level; while those located within the saturated zone develop during low base-level. During Quaternary period important sea level variations have occurred that have developed significant changes in karstification degree. Hardenbol et. al., (1998) have shown that the periods favourable for karst development are correlated with the regional geodynamics and global sea-level. Tectonics has also a major role on rates and degree of karst development. Uplift and deformation of a carbonate terrain can have many side effects that accelerate karstification; fracture density increases, increased elevation usually increases precipitation, more the relief more the gradients in piezometric surfaces, etc, (Häuselmann, et al., 1999; Sauro et. al., 2013; Tîrlă, and Vijulie, 2013).

Hydrogeology has a leading role in karst development as it involves the interrelationships of geologic materials and water (Fetter, 1980). Thus, the change in any of the two parameters leads to a counter change in karst development. Aggressive water (under-saturated with respect to dissolved carbonate) has more capability of dissolving limestone. To reach its saturation equilibrium it take time (minutes to a few hours) varying considerably and depending on many factors (temperature, turbulence, pCO₂, dilution, presence of other acids and surface area of limestone. Organic acids from soils, sulfuric and nitric acids from acid rain also contribute to dissolution. The temporal evolution of recharge and discharge and the boundary conditions influence the karstification processes (Kovacs, 2003).

Karstification is a function of time and depends on many factors like, nature of rock, soil and water pCO₂, with climate being the driving factor (Smith and Atkinson, 1976). Climate and nature of rock is important in developing karst (e.g. Gypsum karst develops almost equally in semiarid and humid climate and halite karst develops best in arid (Jennings, 1983). Dissolutional erosion is intense in tropics and temperate climates (Smith and Atkinson, 1976) where the surface and subsurface is highly modified due to abundant rainfall and higher production of CO₂ in soils due to higher temperatures. However, in cold humid regions more carbon dioxide is absorbed by water due to low temperatures which may enhance karstification. In hot and dry as well as semi-arid climates, this climate related geomorphology is nearly stable (Ford and Williams, 2007) and thus less erosion rates. Smith and Atkinson, (1976) have calculated the erosion rates that vary widely even within the same climatic zone for many karst area of the world (Tab. 1.1).

Location	Erosion rate (m ³ /km ² /yr)	Climate	Reference
Florida USA	35, 5, 8	Tropical	<i>Smith and Atkinson, 1976</i>
Jamaica	69, 39, 86, 96	Do	<i>Smith and Atkinson, 1976</i>
Yucatan, Mexico	30, 16	Do	<i>Smith and Atkinson, 1976</i>
Guangxi, S China	120-300 (surface)	Do	<i>Daoxian, 1981</i>
Dinaric karst, Yugoslavia	43, 63, 55, 67	Temperate	<i>Smith and Atkinson, 1976</i>
Nullarbor Plain, Australia	5 (surface)	Semi-arid	<i>Lowry and Jennings, 1974]</i> <i>(in Short and Blair, 1998</i>
Cuddapah Basin, Southern India	3.7 mm/ka	Do	<i>Dar et. al., 2011</i>

Tab. 1.1. Limestone erosion rates as measured in different climatic regions of the world.

Vegetation is also important in karst development. In arid regions, sparse vegetation and thin soils lead to slower rate of karstification. While, in dense vegetation areas intensified surface and subsurface karstification occurs. The biogenic carbon dioxide from

plant roots and bacterial decay has most important control on dissolutional erosion of limestones. Finally, karst development is time dependant like other erosional processes. An overview of all the factors that govern karstification has been given in Fig. 1.2.

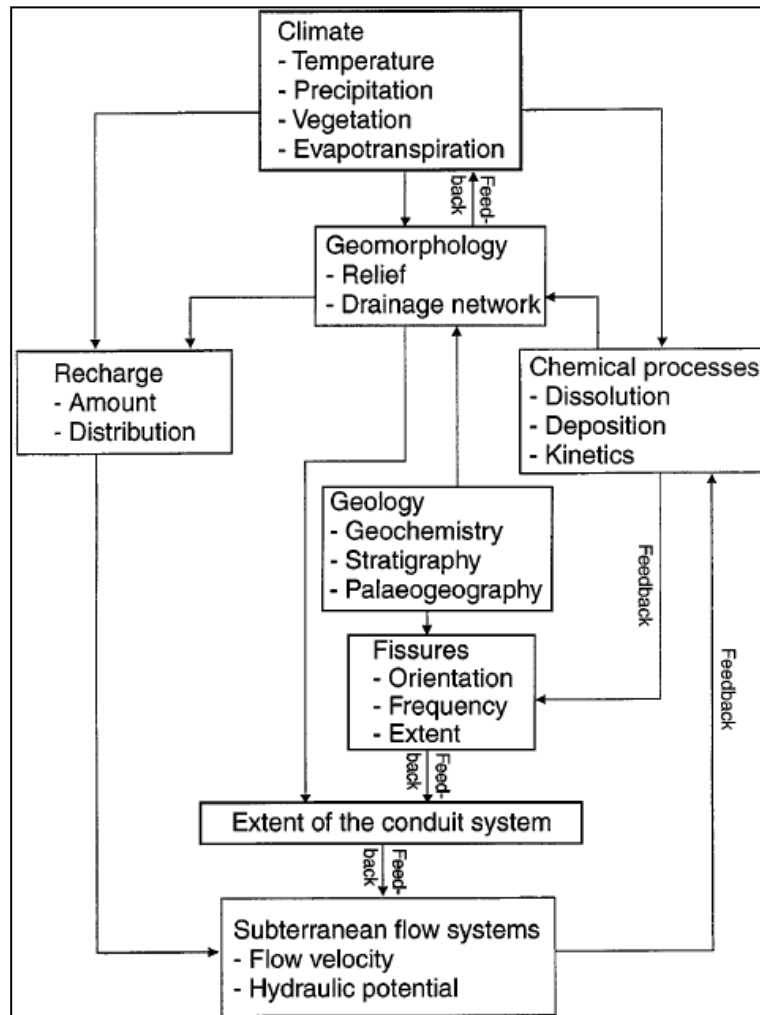


Fig. 1.2. Karstification and its dependence on different processes (Clemens et. al., 1999 modified after Kiraly, 1975).

These changes can take place very rapidly in geologic time scale and in few thousand years (generally less than 50ky) a well integrated karst network may get developed (Bakalowicz, 1975; Dreybrodt, 1998; Ford and Williams, 2007). The mixing of calcite

saturated and newly added water increases the aggressivity and causes more dissolution of limestone (Gabrovšek and Dreybrodt, 2001; Dreybrodt and Gabrovšek, 2002). Carbon dioxide dissolution in water depends on temperature. The cooler water dissolves more CO_2 than warmer waters. Increase in water temperature (Fig. 1.3) will decrease the CO_2 saturation level. The partial pressure of CO_2 is more important than temperature as it changes in soil cover. Thus, the presence and nature of soil affects karstification more than temperature itself.

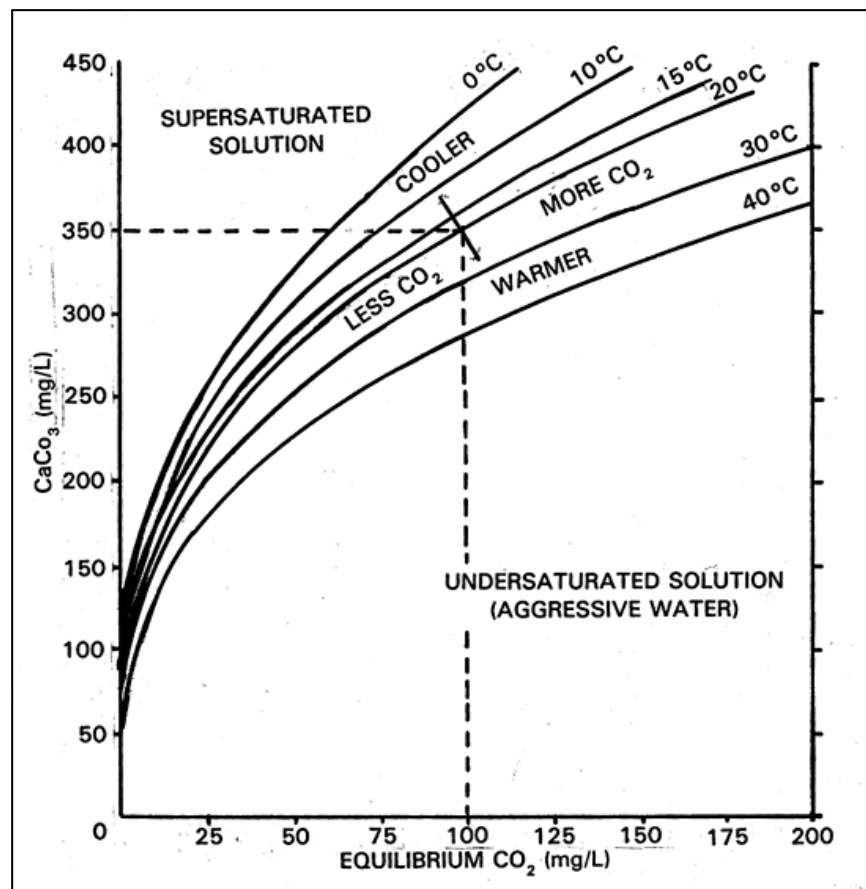


Fig. 1.3. Equilibrium curves for the dissolution of calcium carbonate and its dependence on the temperature, $p\text{CO}_2$, CaCO_3 saturation (modified after Jennings, 1971).

There are two views regarding the initiation of karstification. The concepts of legacy karst (Wright and Smart, 1994) believed that present or past dissolution is controlled by an

earlier (paleo) karst system. While, according to the inception concept (Lowe and Gunn, 1997; Lowe, 2000) karstification is guided by the presence of weaknesses in the carbonate rocks during or after their deposition along which cave formation initiates. The inception horizon may be physical or chemical (fracture, fault, weak bed or change in limestone chemistry). These horizons are preferred loci of initiation in few caves. Thus, karst development is a polycyclic and polygenetic process (Bosák, 2003). Karst dating includes the definition of the beginning of karstification and study of preservation of the products. Karst developed during shorter time is easily preserved in the stratigraphic record with less exposure to geomorphic and other agents.

1.3. Characteristic Features

Karst aquifers are different from classical aquifers because of their specific characteristic (organised heterogeneity) and thus, need to be studied differently. Typical karst morphology (Fig. 1.4) along with the related hydraulic/hydrodynamic processes, are the main features of karst aquifers.

They are characterised by two or three types of porosity as given in Tab. 1.2 - intergranular matrix porosity, fracture and conduit porosity (Smart and Hobbs, 1986, White, 1988). Conduit porosity can be connected to surface water through cavernous opening (sinkholes and sinking streams).

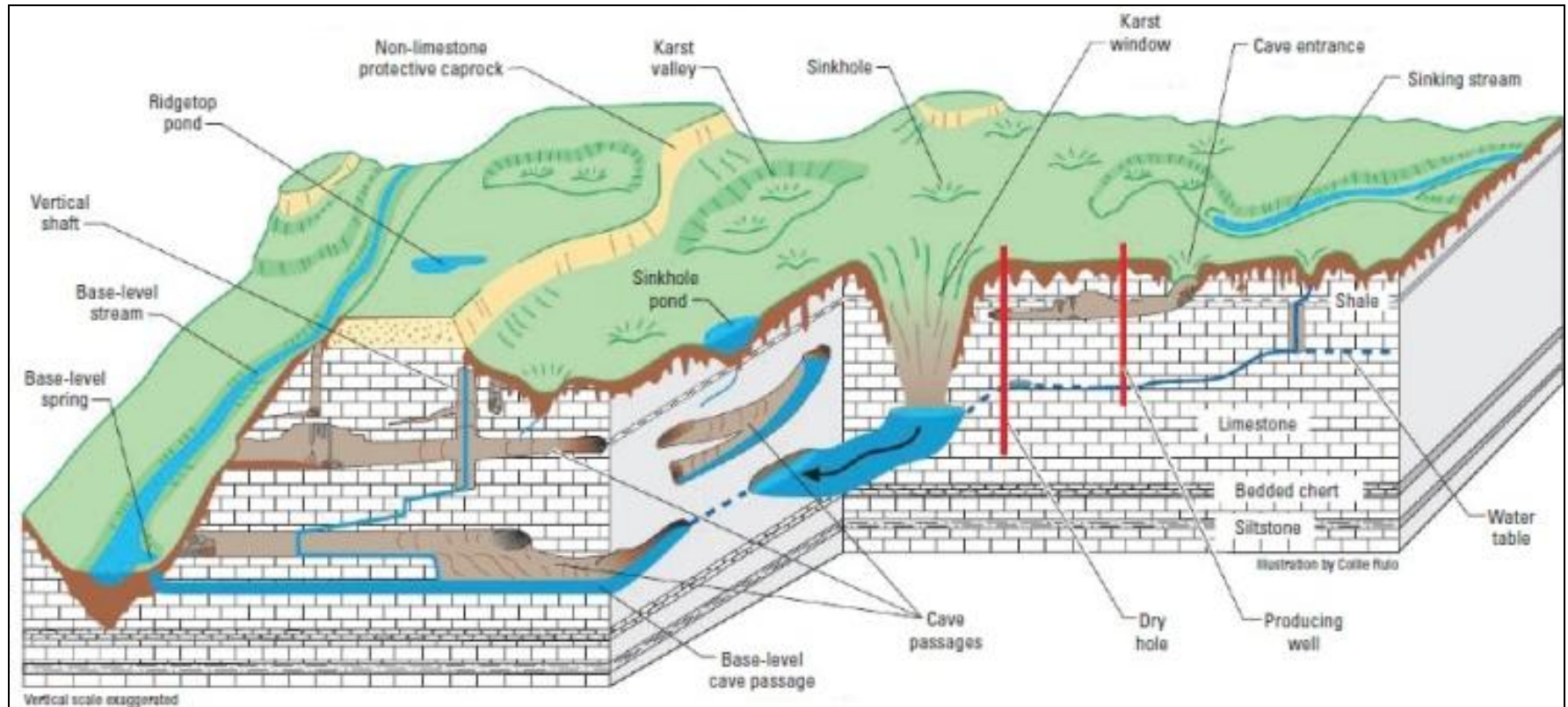


Fig. 1.4. A typical well developed karst model with its physiographic and hydrologic features (source; Kentucky Geological Survey, <http://www.uky.edu/KGS/water/general/karst/>).

Porosity	Dimension	Travel time/response to input	Governing Law/Flow mechanism	Distribution
Primary/ Matrix	Pore/vugs (μm to mm)	Slow/ <1mm/day	Darcy law/laminar flow	Continuous medium
Secondary/ Fracture	Joints, fractures (10 μm to 10 mm)	Intermediate/ 1-100 m/day	Hagen-Poiseuille (cube- law)/Laminar to just turbulent	Localized
Tertiary/ Conduit	Open channels, pipes (>10 mm)	Short/ 100s of m/day	Darcy-Weisbach/open channel and pipe flow, turbulent flow	Localized

Tab. 1.2. Triple permeability media in karst and their characteristics (after white, 2003 and Gillieson, 2009).

The unsaturated and saturated zones are not necessarily superimposed as in other aquifers. The vadose zone (infiltration zone and epikarst) is particularly important (Bakalowicz, 2003). The epikarst acts as skin of the karst where most of the processes of karstification dominate. The recharge area of the aquifer can include both karstic and a non-karstic part of the catchment area. Unary and binary karst systems are differentiated on the basis of their recharge areas. A unary karst system exclusively extends over limestone with no non-karstic part and the recharge is autogenic. A binary system has a non-karstic part providing an allogenic recharge to the karst aquifer. The nature of conduit pattern, its functioning, exploitation and protection of karst depend on both karstic and non-karstic parts. Most groundwater discharge takes place through one or few springs, which may be (perennial or underflow springs) carrying the base-flow discharge while, others (intermittent or overflow springs) flow only during periods of high discharge (Taylor and Greene, 2008). Karst aquifers have also a characteristic feature provided by the nature of its groundwater flow. Highly karstified aquifers have a hierarchical structure of conduits which provide short

distance and low resistance pathways for groundwater flow. This heterogeneity results in the duality of fundamental hydraulic processes in the aquifer (Király, 1998);

Duality of the recharge; (diffuse or slow recharge through low permeability volumes, concentrated or rapid recharge through channel network).

Duality of storage; storage and transport can occur in matrix or Low Permeability Volume (LPV), conduits or both. Storage is low in solutionally developed fractures and conduits and high in LPV rock matrix with primary and secondary pores (Atkinson, 1977 b; Mudry, 1990; Király, 1997).

Duality of groundwater flow -low flow velocities in the fractured volumes, high flow velocities in the channel networks (Liedl et. al., 2003). Sometimes, intense rain events cause subsurface flooding as the conduit system does not accommodate the excess infiltrating water which causes backfilling of channels with fresh under-saturated water. These events lead to flash flooding in many karst areas of the world (e.g. Maréchal et. al., 2009b).

Karst areas usually have absence of surface drainage; show typical spring hydrograph (rapid and violent floods, rapid falling and slow tailing); rapid water level variation in some wells and a slow response in others and rapid variations in hydro-chemistry (Dörfliger et. al., 1999). Sinkholes and other surface openings allow rapid and extensive mixing of waters, commonly cause sharp changes in the chemical composition of groundwater and increase its vulnerability to contamination and anthropogenic activities (e.g., Field, 1993; Bakalowicz, 2005).

1.4. Conceptualization

Conceptualisation of a real system is the first step in karst groundwater study. It helps in visualising the processes (recharge, storage, transmission and discharge) of the system. Karst aquifers are usually not defined by representative elementary volume (REV) for the whole aquifer due to the presence of cavities and hierarchically organised flow between them. According to Teutsch and Sauter, (1991) karst system is one of the advanced and complex systems where modelling is not easy. Since water flow is a combination of diffuse, fracture and conduit flow, their flow modelling is dealt with mixture of surface and groundwater hydrology concepts (White, 2002). Taking their heterogeneity and duality into consideration karst aquifers have been conceptualized by many researchers as discussed below and given in Fig. 1.5.

According to Shuster and White, (1971) and Quinlan and Ewers, (1985) conduit flow aquifers contain well developed conduit systems and diffuse flow aquifers have a mixture of flow. Smart and Hobbs, (1986) included recharge source and aquifer storage as additional parameters for conceptualisation. Conduit systems develop along one, well defined horizon near the unsaturated and saturated interface (Mangin, 1975). The main conduit system transmits infiltration water towards the karst spring(s), but is poorly connected to large voids in the adjacent rocks (annex-to-drain system; ADS). The ADS acts as a main storage part of karst aquifers. The epikarst (upon the karst) is a shallow, high permeability karstified zone below the soil zone. Presence of surface karst features, like sinkholes reflect the development of the epikarst. It hampers the runoff and absorbs and stores it, a characteristic in karst areas. Concentrated recharge occurs

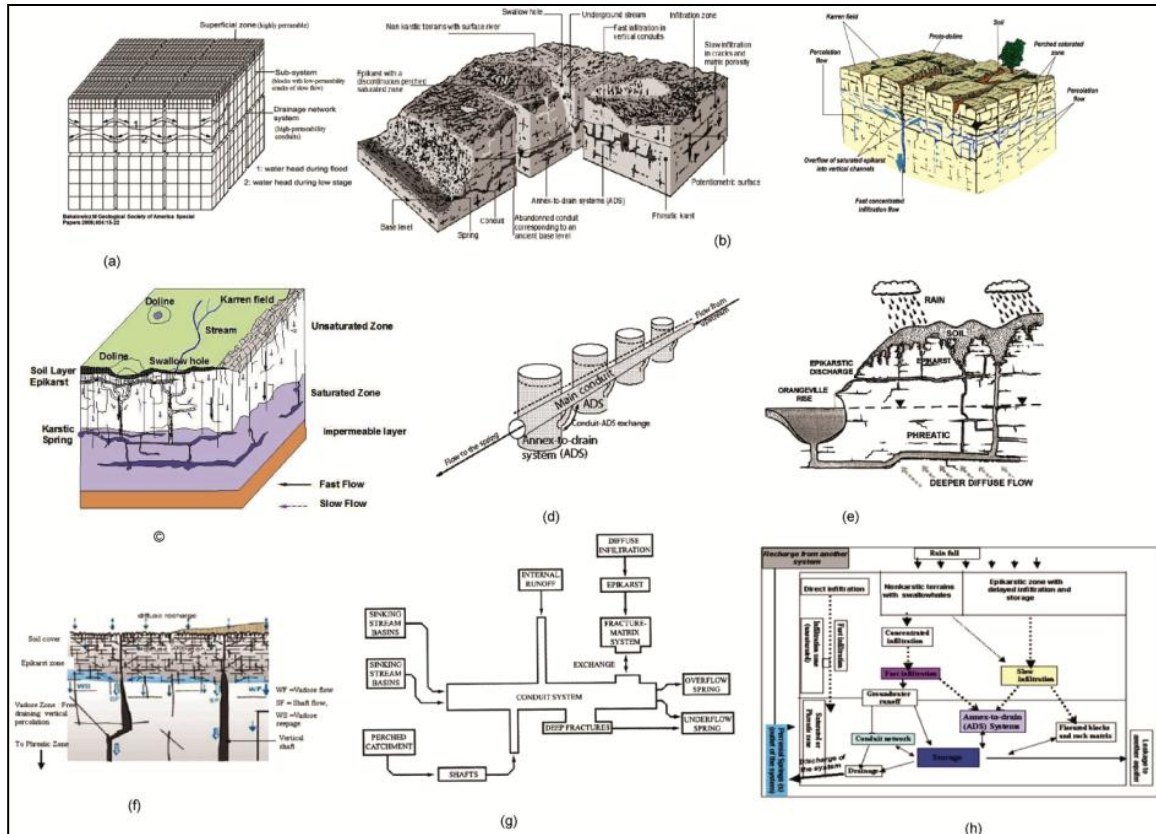


Fig. 1.5. Conceptual models of karst system according to different authors: [(a) Drogue, 1971 (b) Mangin, 1975 (c) Dörfliger and Zwahlen, 1995 (d) Marsaud, 1996 (e) Lee and Krothe, 2001 (f) Klimchouk, 2004 (g) White, 2003 (h) Bakalowicz, 2003].

by rapid infiltration of the water through the highly karstified epikarst. After the saturation of epikarst water hole discharges as perched (overflow) springs.

Drogue, (1980) proposed a double-fissured porosity model of karst consisting of fissured blocks of different size with high permeability and low storage conduits in between. The conduit/cave patterns are determined by the type of porosity and recharge (Palmer, 1991) and are predetermined by the fracture pattern. The main conduits develop along main fractures and the smaller ones on fissures. Sometimes the karst network is different from the fracture pattern. The conduit development follows initial rock fractures by increasing the

hydraulic conductivity of certain fractures. The blocks are dissected by small fractures which considerably storage large water.

Rock matrix (primary and secondary pores) acts as a main storage unit with most of the flow drained by conduits (Atkinson, 1977b; Király, 1997). According to Mangin, (1994), karstic voids connected to conduits are the main storage units with negligible volume in matrix. Some researchers believe that groundwater storage in the phreatic zone is altogether absent. The epikarst delays the recharging water, plays an important role in storage and later drains through karst network directly (Lastennet et. al., 1995). The fissured rock matrix and the dissecting hierarchically organized channels provide two interactive hydraulic properties to the system. White, (2003) attempted to conceptualize karst aquifers based on geologic settings and their influence on groundwater hydraulics. Király, (2003) proposed a model that takes the epikarst and Drogue's, (1980) concept into account. The triple porosity and their relative proportions cause permeability to span many orders of magnitudes (scale-effect Fig. 1.6). The turbulent flow is associated with pipes and fissures in karst (Ford and Williams, 2007). A Wide range is observed in flow rates in such aquifers. Numerical modelling (Király and Morel, 1976b) and vulnerability mapping (Dörfliger and Zwahlen, 1995) quantitatively verified the Király's, (1975) concept.

It is believed that base flow represents either the low permeability volume of the phreatic zone (Drogue 1971) or at least a fraction of the epikarst storage (Williams 1983, Sauter 1992, Klimchouk, 2000). Karst aquifer hydrograph can be divided into different parts (Blavoux and Mudry, 1983; Vervier, 1990; Bonacci, 1993, etc). It includes freshly

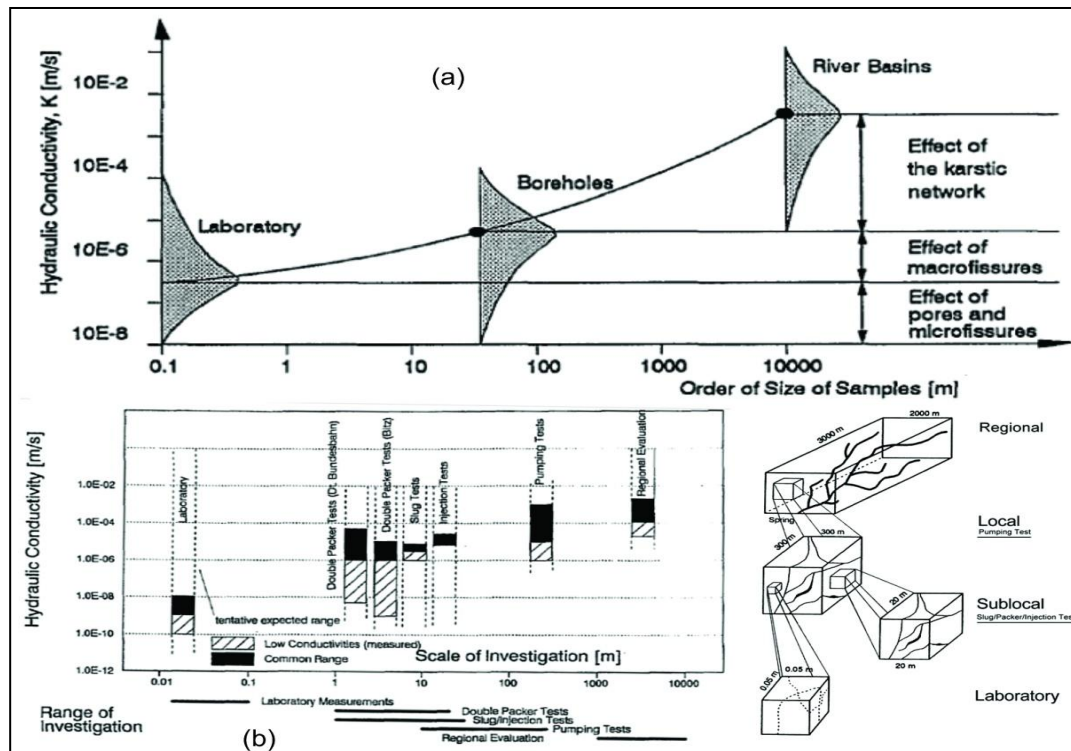


Fig. 1.6. Variability of hydraulic conductivity in karst aquifer with scale of measurement; (a) after Kiraly, 1975 and (b) after Sauter, 1992).

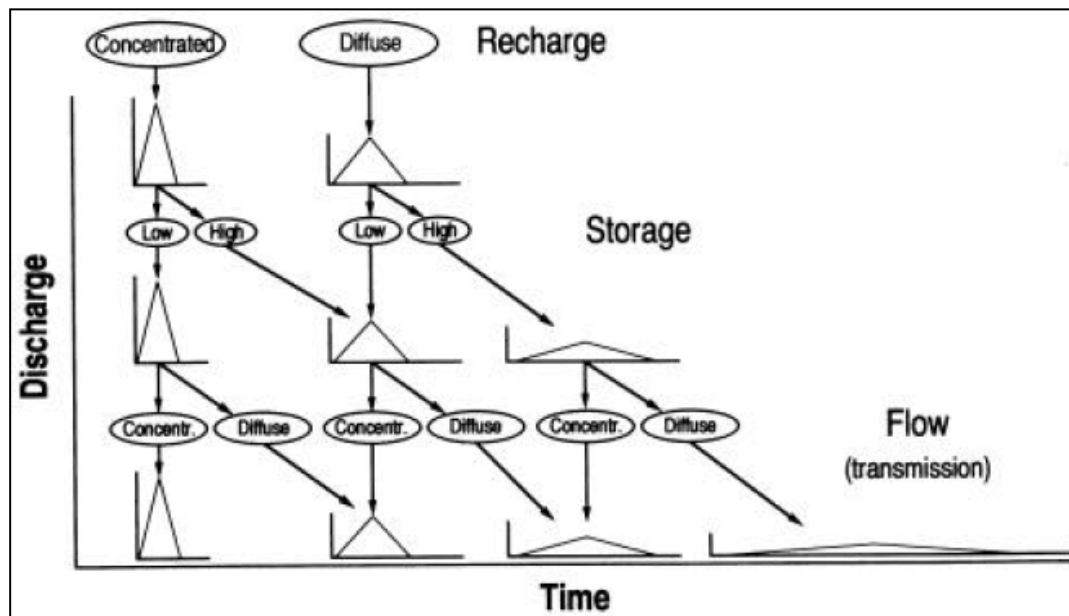


Fig. 1.7. A three cascading sub-system model to represent karst spring hydrographs (Hobbs and Smart, 1986).

infiltrated water, epikarst water and conduit water (Williams, 1983, Sauter, 1992); mixed fresh infiltrated water, soil water, epikarst water and phreatic water (Lee and Krothe, 2001); mixed water from several tributaries (Hess and White, 1988). Bakalowicz, (2003) conceptualized karst systems by including various recharge and flow mechanisms and functions in the vadose and phreatic zones. Hobbs and Smart, (1986) produced different shaped hydrographs by combining recharge (diffuse or concentrated), storage (low or high) and flow (diffuse or concentrated) characteristics of the aquifer using a cascading model (Fig. 1.7).

Cave morphologies have been grouped into two broad end-members- Epigene caves are usually attributed to the dissolution of calcite by infiltrating meteoric water (Dreybrodt, 1990; Palmer, 1991) and hypogene caves are formed by processes involving sulphate, sulphide and/or thermal waters (Ford and Williams, 2007). More than 90% of the caves are epigene, where sulphur involving reactions are negligible (Palmer, 1991). Hypogene caves often have maze patterns and spectacular mineral precipitates. Based on the conceptual models, karst systems consist of following vertical sub-systems (White, 2002):

Infiltration zone- where recharge is autogenic, allogenic, diffuse or concentrated.

Soil and epikarst zone- is a storage zone where runoff and infiltration processes occur. Epikarst (subcutaneous zone, Williams, 1983) is a shallow, most weathered and high permeability karstified zone within first few meters below the soil (Mangin, 1975; Williams, 1983; Perrin et. al., 2003a; Aquilina et. al., 2006). It extends to a variable depth depending on many factors. It has slow percolation of water into narrow fissures (water storage) and rapid drainage through connected pipes (concentrated flow). The soil and epikarst plays a role in the generation of overland flow, underground lateral flow before final infiltration of

water through the vadose zone. In this exchange zone, CO₂ mixes and transports with infiltrating water (Ford and William, 2007). The development of conduits in the phreatic zone partly depends on the temporal evolution of recharge process in the epikarst. In semi-arid areas, epikarst storage is more (up to years or more) than in humid zones (Ford and Williams, 2007). Different conceptual models of epikarst have been proposed as given in Fig. 1.8.

Unsaturated or vadose zone- connects the former subsystems to the saturated groundwater zone.

Phreatic zone- lies below the water table and includes a network of high permeability conduits and low permeability matrix blocks with a high storage capacity.

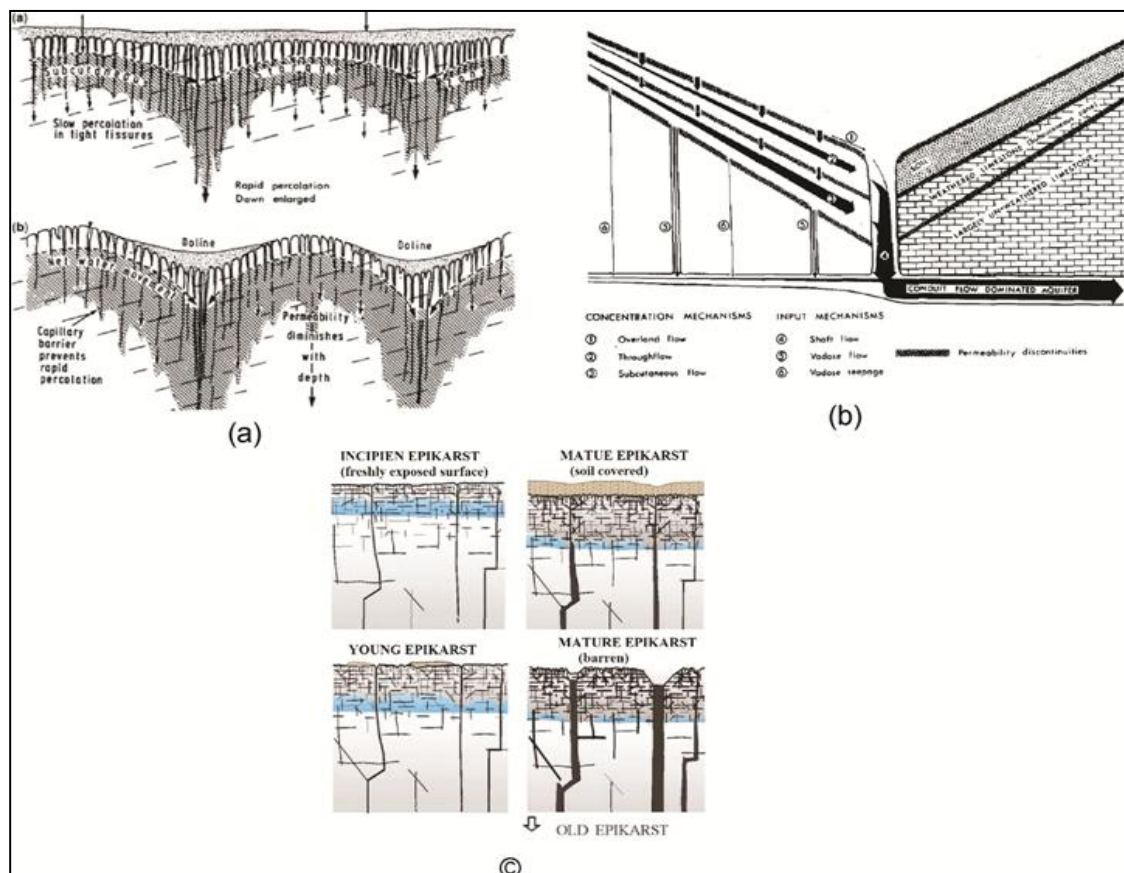


Fig. 1.8. Representation of epikarst (subcutaneous) zone by different authors; (a) William 1983, (b) Gunn 1983 and (c) Klimchouk 2004.

1.5. Distribution of Karst Formations

1.5.1. World Scenario

Karst regions are widespread across the globe and present unique geomorphological characteristics which have specific consequences on land and water resources management (e.g. White et. al., 1997; Ford and Williams, 2007). They represent about 12.5% of the world's continental landmass (Martin and White, 2007) and are home for nearly 17% of the world's population. Karst water resources have been important for millennia all over the world for a number of purposes as many cities depend heavily on their resources (Ford and Williams, 2007). In many European countries, karst waters contribute about 50% of the total drinking water supply (Cost Action 65, 1995) while it is the sole source of fresh water in other areas.

Mapping of karst features at local and global scale has been undertaken by world scientists but the recent publication of Ford and Williams, (2007) has integrated all known data into a meaningful map of karst regions of the world (Fig. 1.9). Sedimentary rocks, which include 10 to 20% limestones or dolomite, cover 75 percent of the Earth's surface (Pettijohn, 1975). According to Ford and Williams, (2007) carbonate rocks cover 20% of the world's continents. Karst groundwater constitutes a crucial freshwater resource for many countries, regions and cities of the world. About 20-25% of the human population feeds on karst waters directly or indirectly (Ford and Williams, 2007). These figures however, differ from region to region.

Karst aquifers are found worldwide from extreme hot and dry climates to karst of extreme cold. Like other climates, the determinants of karstification are same in arid and

semi-arid regions. But the relative influence of various factors varies: short, erratic, violent rainfall and very high evapotranspiration characterize these regions. The research has been carried out in different continents under varied climates particularly humid and temperate regions as discussed by Andreo et. al., (2010). However, in arid and semi-arid areas karst aquifers are more vulnerable to over-exploitation for water and economic developments (Martín, 2006).

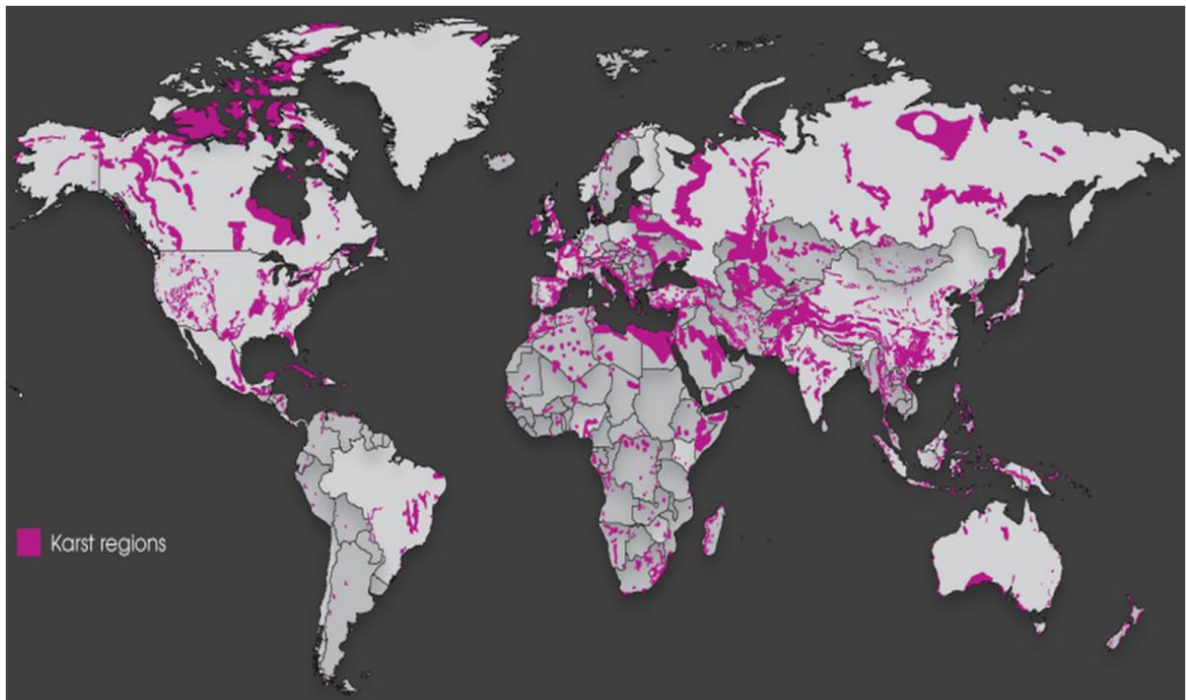


Fig. 1.9. Global carbonate rock outcrops (Ford and Williams, 2007) source, www.circleofblue.org.

The karst of semi-arid and arid climates is extremely different than karst of temperate warm and humid climates. Semi-arid and arid climate is an extreme type with hot and dry conditions. They are represented by short and violent rainfall with very high evapotranspiration. The intense rainfall gets accumulation in depressions. The karst is usually bare; absent or interrupted, very thin and less developed soil cover. The limestone is usually dissected into tectonic blocks and fissures. This affects karst development as soils

regulate runoff and act as a source of additional CO₂. These areas have more frequent collapse dolines than solution dolines. Less number of caves is observed which are usually truncated with dry, inactive lying above than active ones representing the change in moisture availability for karst development (Kranjc, 2010).

1.5.2. Indian Scenario

While, karst landscapes are scarcely common in India, they are well developed in certain locations. The stratigraphic record reveals the presence of carbonate rocks from Precambrian (Vindhyan Super Group) to Tertiary age (Appendix 1). Limestone aquifers, potentially karstified are present in various parts, particularly within different sedimentary basins (Cuddapah, Vindhyan, Chattisgarh, etc) in different geomorphological and climatic zones. In certain parts of the Indian sub-continent these aquifers may become a great resource for water supply. Consequently, karst rocks may prove as one of the most important aquifers along with other rocks.

The karstified aquifers of India have not been comprehensively characterized except few studies that have not taken the specificities of karst into consider. The rocks have been studied for hydro-geomorphology (Sankar et. al., 2001), hydrogeology (Coward et. al., 1972; Singh, 1985; Venkatanarayana et. al., 1999; Ruggieri et. al., 2011), karstification processes (Shibasaki et. al., 1985), groundwater quality and pollution (Dubey et. al., 2006), speleology (Gebauer, 1985 and 1986) and cave biology (Prasad, 1996). Few studies have also been taken in other fields, like application of geophysics in detecting solution channels (Dutta et. al., 1970, Chandra et. al., 1987; Venkatanarayana and Rao, 1989), climate change

effect on water resources (Jeelani, 2008), protection and management of limestone areas (Singh, 1985; Rande, 2007) salt water intrusion problems (Pujari and Soni, 2009).

In context of semi-arid karst in India, the main carbonate rocks are located in the Proterozoic sedimentary Cuddapah Basin (CB) (Fig. 1.10) which includes Vempalle Formation of the Cuddapah Supergroup and the Narji and Koilkuntla Formations of the Kurnool Group. The carbonate formations show a non-homogeneous composition from bottom to top. Usually, the middle massive part is welded between the lower and upper flaggy units. The flaggy part is thinly bedded. Of the total area of the basin (44,500 km²), 17% (i.e. 7,690 km²) shows the exposure of these potentially-karstified rocks. The areal extent of Vempalle, Narji and Koilkuntla Formations is 1,830, 4,333 and 1527 km² respectively. The most extensive carbonate rock in the basin is 0-200m thick Narji limestone outcropping mainly in the central plains of Kundu valley.

The research on karst in such areas is limited. Thus, a need arises in such areas to find a balance between aquifer resources, environmental protection and economic development which demands a detailed research in such karst areas as well.

1.6. Objectives of Present Study

The literature review suggests that very limited studies have been carried out on the groundwater characteristics in karst terrain and the karstification processes in Indian context. These aquifers therefore, need to be fully characterized for understanding the system, its set-up, aquifer geometry, various fluxes and so that an adequate management of their water resources is guaranteed with no future depletion of quantity and quality of the reserves.

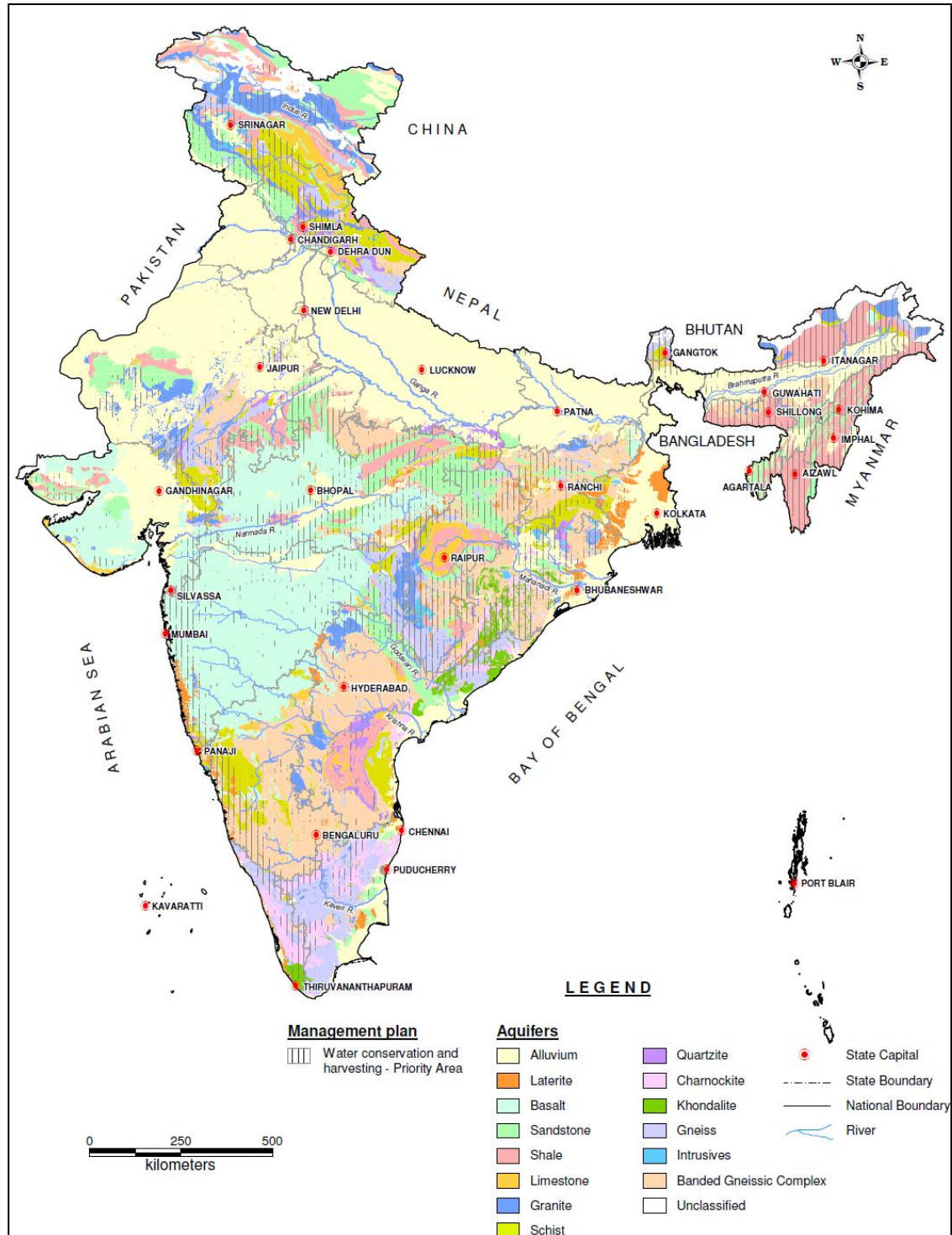


Fig. 1.10. Map of India showing major aquifer systems. Carbonate formations with potential for karstification are also shown, (source CGWB, 2012).

Against this background, it is proposed in this study to understand the karst hydrogeological processes of limestone terrain in semi-arid region of southern Andhra Pradesh. The study envisages the following main objectives;

- Conceptualization and Characterization of the karst aquifers using geomorphological, geological, hydrological and hydrochemical applications,
- Analyze the nature of different recharge mechanisms in the area and, estimate the recharge.
- Assess chemical characteristics of groundwater using different quality parameters during monsoon and non-monsoon seasons, and
- Characterise the aquifer system by stable isotopes and tracer tests

1.7. Scope of Present Study

The scope of the study is to understand the characteristics of karst aquifers of semi-arid, drought prone area of Southern India, where groundwater is the main source of utilization..

The study focuses on the nature of recharge mechanisms and chemical evolution of the groundwater using the supporting parameters in semi-arid areas. The present study will compliment the karst studies of the semi-arid region carried out elsewhere, which are still outnumbered (Jennings, 1983; Hughes et. al., 2008). The study will also provide the scope to understand the management of groundwater aquifers in limestone terrains using detailed hydrogeological studies in India. It will provide a possibility to revise previous studies on limestone aquifers of India.

1.8. Summary

Karst is a unique landform developed in carbonate and other soluble lithologies by the dissolutional action of groundwater. It develops both on surface and underground with characteristic karst geomorphological landforms. The Karst aquifers are complex due to the fact that it contains all possible hydrogeological structures and features e.g., weathering, fracturing, faulting, cavities and the karstification of various degrees. Karstification is a dependent process influenced by a variety of factors like, climate, $p\text{CO}_2$, nature of rock, presence of weak zones in rocks, etc.

Karst acts as a large reservoir for groundwater resources particularly in semi-arid areas where groundwater is the sole source of water supply for the population. These aquifers are different from classical aquifers because of their specific characteristic (highly heterogeneous and anisotropic character). Karst areas have no permanent surface drainage; runoff lost through sinking streams, swallow holes and other depressions. The aquifers are characterised by triple porosity, duality of recharge, storage and groundwater flow with high velocity of groundwater in highly organised channels and conduits and low velocity in fractures and matrix porosity.

Due to their specific geomorphological and hydrogeological peculiarities, these aquifers are most complex to study as they are not represented by elementary volume. The presence of cavities and hierarchically organised flow between them make any modelling technique difficult. Hydraulic properties in these aquifers are highly scale dependent. Conceptualisation of the system has been carried out using many approaches in different geological terrains of the world. The models have highlighted the nature of karst from

surface to subsurface and have included the infiltration, flow and discharge processes. Vertical zonation of the aquifer includes epikarst layer which acts as an important infiltration and storage unit in the aquifer.

Karst aquifers are widespread across globe in many climatic regimes but the nature of karst and the processes in semi-arid areas are still less understood particularly in terms of hydrogeology. These rocks form potential groundwater aquifers in the many areas of Indian sub-continent as well. In Proterozoic sedimentary Cuddapah Basin, the karstified rocks cover about 17% of the basin area and form important groundwater reservoirs in the many drought prone areas of southern Andhra Pradesh. The karst aquifers are important in the sense that they represent a part of the semi-arid karst of the world. This thesis therefore, focuses on the hydrogeological characterization of these karst aquifers and using the approaches applied in other karst areas of the world.

CHAPTER 2 **STUDY AREA**

2.1. Introduction

The carbonate formations of the Proterozoic Cuddapah basin have been chosen for the hydrogeological characterization. The study area has therefore, been discussed in this context (Fig. 2.1). The CB is geologically, stratigraphically, structurally and economically unique as it represents the onset of sedimentation after great Eparchean interval. It is the second largest sedimentary basin in Indian plateau and has the thickest sediment cover (12,000m) than the rest of the basins. The presence of a variety of economic minerals and building stones gave it an economic importance. Mineral deposits of barite, asbestos, iron, copper, lead-zinc and steatite are widespread (Murthy, 1950; Kasipathi, 2008, Raju, 2009). The conglomerates of the Kurnool System are the sources of diamond (Crawford et. al., 1973). Hydrogeologically the basin rocks particularly carbonates are the major source of groundwater in many drought prone areas.

2.1.1. Location

The crescent-shaped CB is situated in the eastern part of the Dharwar Craton in south-central Andhra Pradesh, India (Fig. 2.1). The basin extends between 13⁰30' to 17⁰N and 78⁰ to 80⁰ E covering parts of Chittore, Anantapur, Cuddapah, Kurnool, Mahabubnagar, Nalgonda, Guntur and Krishna districts of Andhra Pradesh. Spreading over a large area it is one of the extensive sedimentary basins of India. The basin convexes towards west and extends for a length of about 400 km in north–south direction with a maximum width of 145 km in the middle. The total area of the basin is 44,500 km² out of which about 17% is occupied by the carbonate rocks (Dar et. al., 2011). The study area has been chosen from the

west central portion of the basin which possesses a number of karst features. The study area is shown as an inset in Fig. 2.1 for clarity. The area is well connected by rail and road and covers many parts of Kurnool, Cuddapah and Anantapur districts.

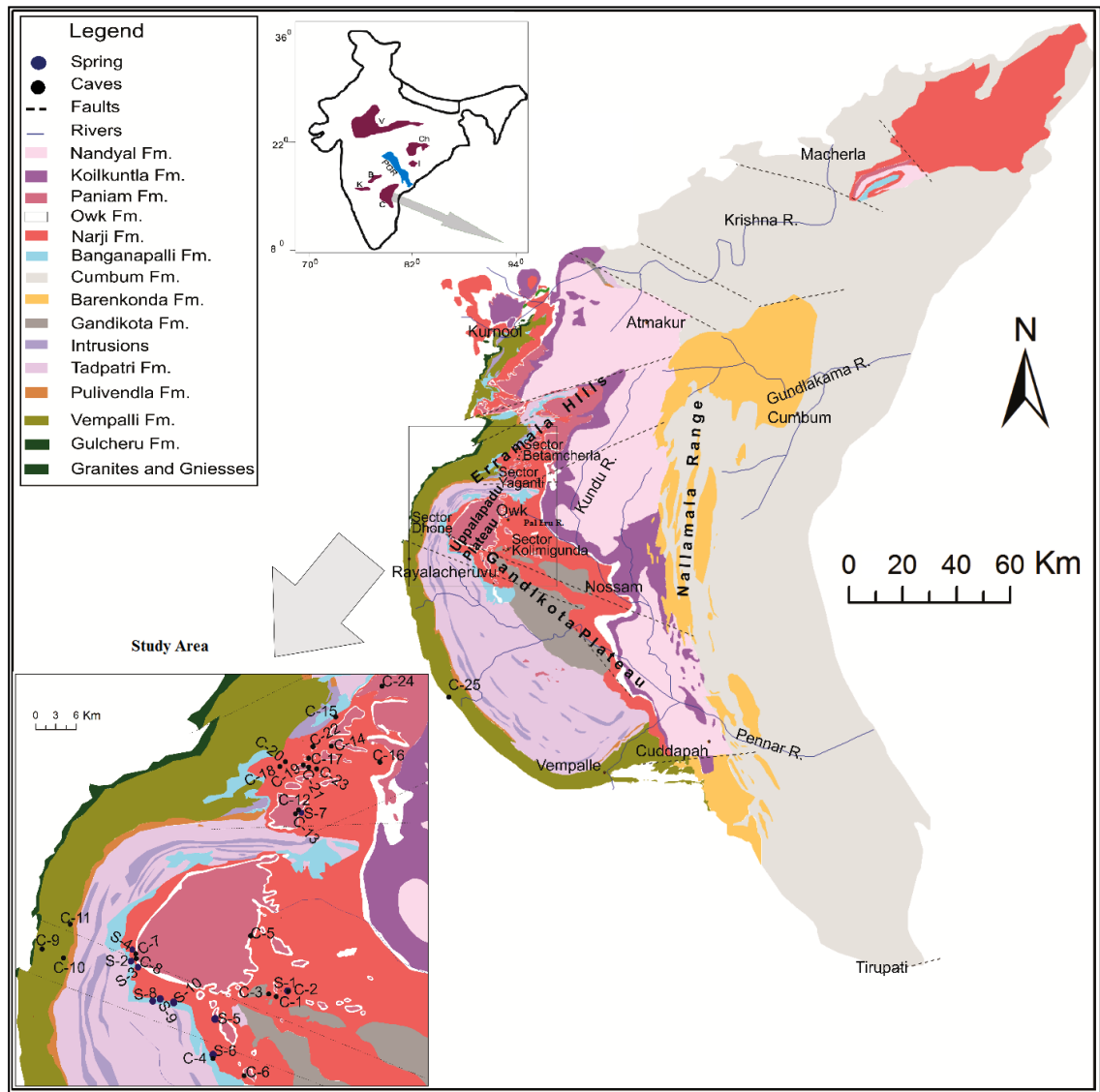


Fig. 2.1. Geological map of Proterozoic Cuddapah Basin (CB) southern India, showing the distribution of three karstified formations, modified after GSI, 1997. Map of India shows location of different Proterozoic Basins. Study are has been shown in inset for clarity.

2.1.2. Climate

The study area lies in a semi-arid region with long, hot and dry summers when day temperature reaches 45⁰C and a well-defined monsoon season. High temperature and evapotranspiration along with less and periodic rainfall characterise the area. The area lies in the scarce rainfall zone (Planning Commission, 1990) characterized by the lowest rainfall-evapotranspiration ratio. Large seasonal and annual temporal variability in rainfall is observed which is characteristic of the semiarid climates is.

Climatically four seasons are distinguished; south-west monsoon season (June-September), north-east retreating-monsoon (October-November), long hot summer season (March to mid-June) and mild, dry, comparatively cool pleasant winter season (December-February). Temperature varies from minimum 17⁰C to a maximum of 45⁰C in months of April and May (Fig. 2.2).

The area receives a mean annual rainfall of ~709 mm with monthly totals ranging from 0 to more than 300 mm. Annual rainfall for different years is given in Appendix 2 for Kolimigundla area. Most rainfall occurs unevenly as high intensity events. South west monsoons contribute ~467 mm (63.7 %), post-monsoons 162.5 mm (22.8 %) and winter rains 87 mm (12.5 %) to the average annual rainfall (Tab. 2.1 and Fig. 2.3). The average annual number of rainy days varies from 23 to 56 with an average value of 37 days (Tab. 2.1). A rainy day receives ~2.5 mm a day (India Meteorological Department). The monthly climatic data measured at Belum station is given in Appendix 3.

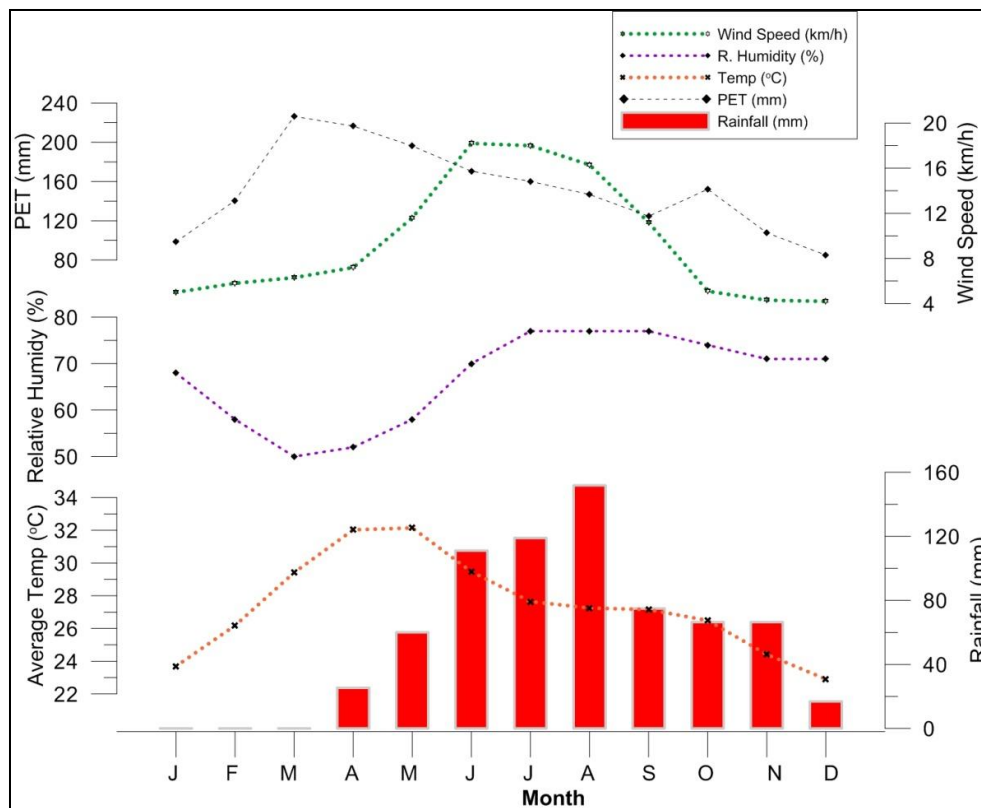


Fig. 2.2. Long term (10 year) average monthly variation of different climatic parameters at Kurnool station (temperature, wind speed and humidity from Kurnool station, source IMD).

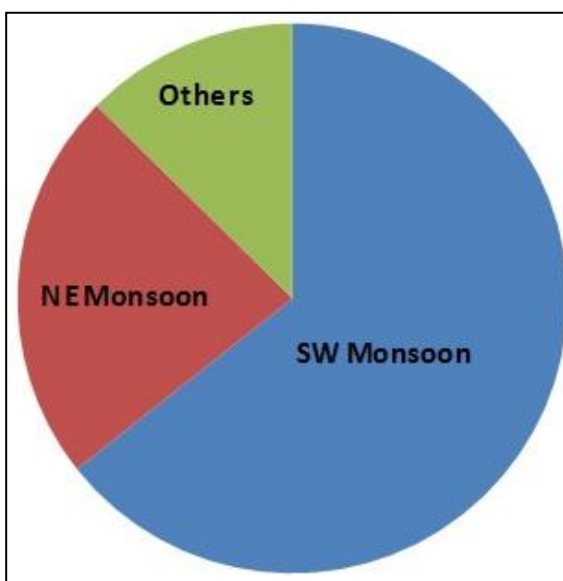


Fig. 2.3. Percentage contribution of seasonal rainfall to the annual amount at Kolimigundla from 1999-2011.

Year	Annual rainfall	SW Monsoon	NE Monsoon	Non Monsoon	Rainy days
1999	706.3	564.5	82.0	59.8	29
2000	1023.4	784.2	157.6	100.0	47
2001	758.0	311.2	298.0	148.8	34
2002	407.6	187.6	216.2	3.8	24
2003	516.0	280.8	209.6	25.6	23
2004	543.0	379.0	0.0	164.0	34
2005	933.2	573.6	234.0	125.6	42
2006	667.2	434.4	208.4	24.4	32
2007	884.0	761.8	78.2	44.0	44
2008	636.4	300.6	164.2	171.6	51
2009	626.0	422.2	126.4	77.4	32
2010	966.6	577.0	242.0	111.6	56
2011	554.5	613.0	95.6	73.9	25
Mean	709.4	476.1	162.5	87.0	37

Tab. 2.1. Annual rainfall, monsoon and non-monsoon rainfall amount and number of rainy days at Kolimigundla station from 1999-2011.

Compared with the normal rainfall at Kurnool district (India Meteorological Department) the year with <50% rainfall is considered as severe drought, drought up to 75%, high rainfall 125% and extremely high rainfall will be 150% of the normal rainfall (Fig. 2.4). Mandal-wise spatial variability of rainfall is negligible. Seasonal variability at Belum has a coefficient of variation of 0.35 (Tab. 2.2).

The average monthly PET losses at Belum station of Kolimigundla mandal vary from 118-314mm, with a mean of 210 mm respectively. Annual evapotranspiration is 1825 mm. Annual rainfall makes only 38.8% of total annual PET demand, which indicates an aridity index of 0.38, corresponding to the semi-arid class of (UNEP, 1999). The relative

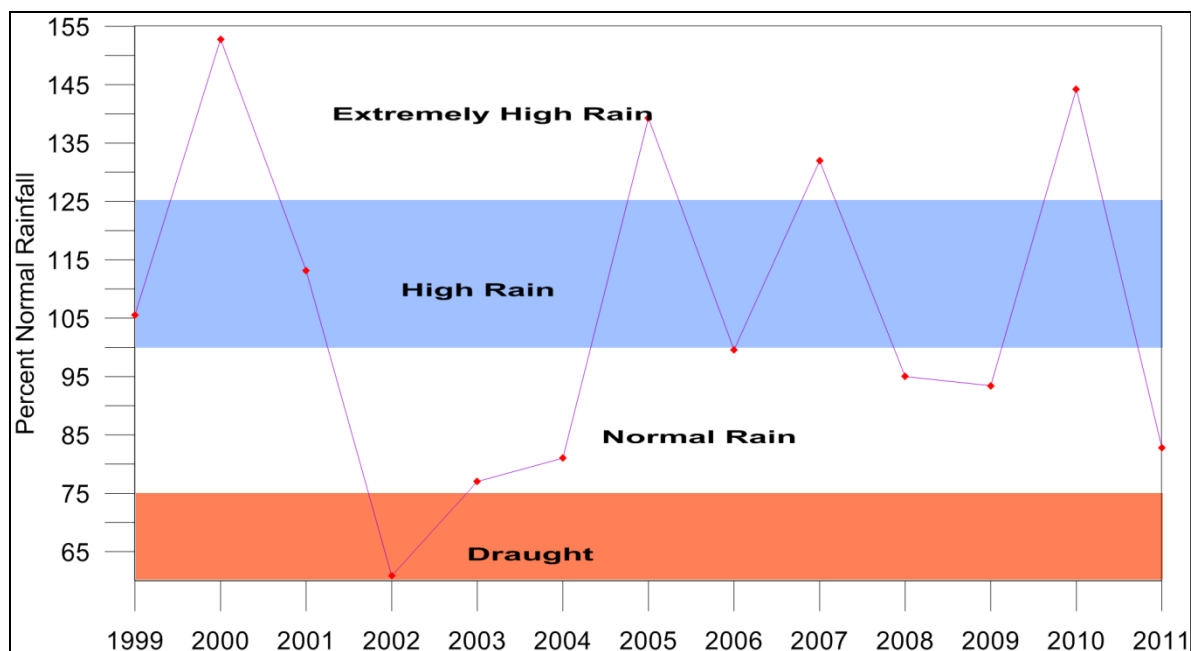


Fig. 2.4. Percentage of long term normal rainfall showing climatic conditions in the area. Data from Kolimigundla mandal.

Station	Annual Mean	C V (%)	Dry Year	Wet Year
Kolimigundla	701.8	27	2002 (407.6)	2000 (1041.8)
Koilkuntla	706.7	33	2006 (497.8)	2007 (1118.2)
Owk	599.6	29	2003 (310.5)	2007 (873.4)
Banganapalle	703.0	23	2004 (443.3)	2005 (910.6)
Allagadda	754.9	46	1999 (284)	2000 (1386.2)
Chagalamarri	648.5	45	2004 (306.2)	2000 (1296.6)
Sanjamala	616.9	32	1999 (384.2)	2000 (1022.8)
Dornipadu	641.6	47	1999 (91.8)	2000 (1263.4)

Tab. 2.2. Statistical analysis of rainfall at different station in the area, from 1999-2009, (SD, standard deviation; CV, coefficient of variation).

humidity fluctuates seasonally and shows variations with rainfall and temperature (Fig. 2.2).

The average relative humidity is 66.9 %. The monsoon season is also characterized by higher wind speed of 18 km/h.

2.1.3. Topography and Geomorphology

The physiographic studies of an area are vital in groundwater studies. Geomorphology helps in understanding the characteristics of an aquifer and enhances the knowledge of the many processes.

Geomorphologically, the area is characterised by rolling topography from west to east, (e.g., Vaidyanadhan, 1964; Bhagavan and Rao, 1985). The centre of the CB corresponding to a carbonate massif is nearly flat plain (pediplain) bounded on west by flat topped quartzitic Erramala Hills, plateaus of Uppalapadu and Gandikota and on east by the steep N-S trending rugged Nallamala range. The plain descends from an elevation of 260 m at Atmakur in north to 130m near Cuddapah in south. The western and eastern hills generally trend WSW–ENE to NNE–SSW. This central valley is dissected by a number of scattered, plateau type low series of quartzite hills, (e.g., mesa and butte as discussed in chapter 4). This flat valley is drained by the Kundu River with a watershed area of 512 km² (Fig. 2.1). Majority of the streams are ephemeral and are relatively short with dendrite and parallel to sub-parallel drainage pattern. High density of hydrographic network is observed over the hilly terrains, while the low density in central area. Ephemeral Pal-Eru Watershed covers most of the Narji limestone plain (Fig. 2.1). The maximum height in the Kundu basin is 840 m corresponding to the western and eastern hilly areas and the lowest is 130 m, with a relief of 691 m. The low scattered hills raise 350 to 500 masl. Relief (difference between the lowest and the highest altitudes) is an important factor in defining the denudational characteristics of the area. Based on the ASTER-30m DEM, the slope of the Kundu watershed varies from ~0° to 11° with a mean slope of 6.68°.

2.1.4. Soils, Vegetation and Land-use/land-cover

The soils of the area are influenced by climate, geology, topography and the degree of weathering. Soil properties affect the recharge processes. Generally, soils are shallow (limited by rock outcrops), granular with high gravel and rock content. The soils are immature with no well developed horizons, typical of arid and semi-arid climates. Two main soil types are defined; Vertic Inceptisols (Deep Black) and Alfisols (Red Sandy) along with a mixed type. Black soils (typical limestone soils) are very gentle to flat, calcareous with high proportion of swelling montmorillonite clay (NBSS and LUP, 2000). The remarkable swell and shrink phenomena during wetting and drying forms deep cracks in drier seasons that helps in infiltration. Black soils are rich in nutrients, poorly to imperfectly drained and suitable mainly for paddy and many deep rooting crops like, cotton. They have high production potential. Alfisols or brown sandy soils are relatively shallow, gently to very gently sloping and free draining. Alfisols are derived from material associated with shale and quartzite. The thickness of red soils (less than few cm) is less as compared with black soil. However, the thickness of black soils increases up to 9m at places towards south (Chand et. al., 2006). Red soils are suitable particularly for upland crops. Mixed soils are usually derived from transported mixed colluvial material from hilly terrains of quartzite, shale and limestone/dolomite. The soils have an average clay content of 73.76%, sand 17.4%, and silt 8.9 (Fig. 2.5). Of the total clay content in both black and red soils in southern India, fine clay constitutes more than 50% (Pal and Deshpande, 1987). Soils have average saturated soil moisture content (at field capacity) of 27.9 % and residual moisture content (at permanent wilting point) of 16.5 %. The soils have an average pH of 8.5 and organic carbon of 1.04%. The soil moisture remains only for one rain event that may vary up to few days.

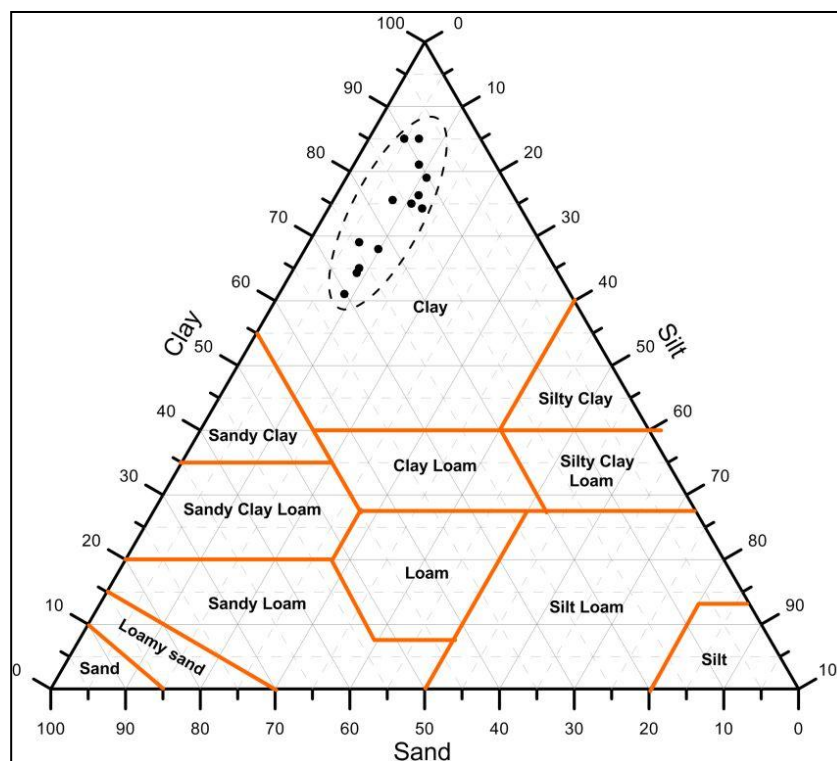


Fig. 2.5. Trilinear diagram showing granulometric composition of soils of the area. Soils fall in the field of clay.

The main vegetation in the form of open scrub type jungles is scattered. The natural vegetation, comprising of tropical, dry deciduous and thorn forests is meagre. However, areas of relatively dense forests cover high altitudes of the Nallamala and western hill range. The native vegetation has a dormant period while the soils are dry (Rossiter, 2002). Cultivated vegetation includes the rain-fed and irrigated crops grown in the flat soil-covered plains of Kundu valley. During Kharif (monsoon season) agricultural activities take place both in rain-fed and irrigated areas. The major Kharif crops grown are sorghum, cotton, pigeon pea, rice, groundnut and castor with vegetables and some fruits. In the Rabi season (winter months) agricultural activities take place mostly in the irrigated areas between October and June. Most important Rabi crops are sorghum, sunflower, paddy and some oilseeds. Canal irrigation for many crops particularly paddy is provided by water bodies, like

Owk and Pal-Eru reservoirs. The average rain-fed cropping season is 165 to 175 days for the Vertisol areas and 130 to 150 days for the Alfisol areas. The chief economic activities include agriculture, mineral exploitation (cement, construction slabs), rearing of domestic animals, fisheries and sericulture. Limestone quarrying for building stones and cement construction spreads over a large area. Quarry waste is dumped also over a large area.

2.1.5. Geology and Stratigraphy

Dharwar Craton of Southern Indian was exposed to large scale weathering, erosion and volcanism after Archaean Eon about 2500 m.y ago. This intensely brittle deformation formed unique rift-basins in the rigid crust of Indian Shield and the deposition of preponderance of endogenic source material (sedimentation) in them. The whole event represents the Proterozoic Eon (2500-540 Ma) with more sedimentation during Middle to Late Proterozoic. Cuddapah, Kaladgi, Bhima, Vindhyan, Chattisgarh and Pakhal (Pranhita-Godavari) include these intra-cratonic basins (Fig. 2.1 and Tab. 2.3). These basins preserved the earliest sedimentary-volcanic sequences (Dutt, 1975; McKenzie et. al., 1980). The basins were called 'Purana Basin and their rocks as Puranas. The time gap (~800 yrs) between Archaean and the Proterozoic is called the "*Great Eparchean Interval (unconformity)*". It is represented by a granite pebble-conglomerate between the Archean and the younger Bairenkonda Quartzite of the Cuddapah.

The age of the Cuddapah basin and its sedimentation has been estimated from radiometric and isotopic methods (e.g., Aswathanarayana, 1964; Crawford and Compston, 1973; Bhaskar. et. al., 1995). Aswathanarayana, (1962a) suggested its age as 780-840ma however, the base could be 1,700ma older.

Basin	Area (1000 km ²) #	Thickness (m) max.	Shape
Vindhyan	60-160	4,500	Arcuate
Chattisgarh	33-40	200	Semicircular
Baster	15-50	800	Disjointed patchy outcrops
Pakhal	15-30	6,000	Linear belt
Cuddapah	45-50	12,000	Crescent
Bhima	5-10	200	Array of narrow strips
Kaladgi	8-20	3800	Elliptical to actuate

Tab. 2.3. Characteristics of different Proterozoic Intra-Cratonic basin of India, (after Kale, 1991). #exposed to maximum thickness. For location refer to insert in Fig. 2.1.

The peninsular gneissic complex forms the basement. The sediments of west steeply dip towards east and are relatively undisturbed. Sedimentation was thicker towards east (Ramam et. al., 1997). The provenance of sediments was west and southwest (Balakrishna and Vijayam, 1968; King 1872). The shallow sub-marine shelf environment prevailed during the sedimentation of the basin (Shibasaki et. al., 1985) whose depocenter was successively migrating towards east (Singh and Mishra, 2002). The CB itself got developed in the form of many sub-basins separated by the prominent faults (Narayanaswami, 1966; Ramam and Murthy, 1997).

Geology and stratigraphy of the basin has been discussed by various geologists (e.g., King, 1872; Meijerink. et. al., 1984; GSI, 1997; etc). Kadapah and Kurnool Formations in the Madras Presidency (King, 1872) was the first known publication. King, (1872) divided the basin sequence into two main geological units while, others retained this classification with slight modifications. Narayanaswami, (1966) revised the stratigraphy proposing a five-fold classification. A comparative description of different stratigraphic classifications is

found elsewhere (Sen and Narsimha, 1968; Nagaraja Rao, 1987; Sing et. al., 2002). However, the stratigraphic nomenclature proposed by GSI, (1997) will be followed for this work.

The sedimentation is divided into two distinct lithostratigraphic units with a different rock assemblage: Cuddapah 'Kadapah' Supergroup and the overlying Kurnool 'Karnul' Group separated by an unconformity (Fig. 2.6 and Appendix 4). The Cuddapah Supergroup occupies almost the entire basin while, the Kurnool Group was deposited in two discrete sub-basins: the Kurnool in the western part and the Palnad in the northeastern part. There was contemporaneous igneous activity in the form of sills, flows and other intrusive rocks in lower units of Cuddapah Supergroup mainly in the western part of the basin (Sen and Narsimha, 1968; Crawford et. al., 1973; Ramam et. al., 1997; Anand et. al., 2003). The volcanic activity started intensively at the end of Vempalle Formation (Jhanwar, 1964). Rocks are slightly metamorphosed from west to east (Wadia, 1939). Narrow kimberlite type dykes intrudes the Cumbum shales and phyllites (Sen et. al., 1968) which are the source of diamonds. Intrusion of coarse-grained granites has caused contact metamorphism of the surrounding rocks (Narayanaswami, 1966). The density of the Cuddapah Supergroup is higher due to dolomitic and quartzitic facies than Kurnool rocks.

Litholog	Formation	Lithology	Age
	Nandyal Fm.	Shale, Limestone	Upper Proterozoic
	Koilkuntla Fm.	Limestone with shale	
	Paniam Fm.	Quartzite	
	Owk Fm.	Shale	
	Narji Fm.	Massive limestone, Flaggy limestone	
	Banganapalle Fm.	Quartzite with conglomerate	Middle Proterozoic
	Cumbum Fm.	Shale with phyllites, quartzite, dolomite/limestone	
	Barenkonda Fm.	Quartzite	
	Gandikota Fm.	Quartzite, shale	
	Tadpatri Fm.	Shale and tuff, dolomite/limestone, quartzite, basic sill	
Pulivendla Fm.	Quartzite with shale/limestone /dolomite intercalations, basic flow		
Vempalle Fm.	Dolomite/chert/mudstone, quartzite		
Gulcheru Fm.	Quartzite/arkose with conglomerate		
Basement		Granite–Gneisses, basic dykes, amphibolites and mica schist	

Fig. 2.6. Major stratigraphic successions of the Cuddapah Basin. Vertical scale has been exaggerated for clarity.

The Cuddapah Supergroup has comparatively steeper dips than the easterly dipping Kurnool Group (Fig. 2.7). The general thickness of the whole sedimentary sequence is of the order of 6,000–12,000m. The thickness of the Cuddapah Supergroup is more with the greatest thickness of about 6400m (King, 1872). The Kurnool System is thin, with maximum thickness of 370m but it is superficially very extensive (Fig. 2.1). The shallowest depth to the crystalline basement is around 200m (Reddy et. al., 2004). The Cuddapah Supergroup is composed predominantly of a cyclic repetition of two quartzite-shale sequences with a carbonate unit (Ramam et. al., 1997). The Kurnool Group is more carbonate-rich with less clastics.

Four stratigraphy groups are discussed (GSI, 1997); Papaghni, Chitravati and Nallamalai of the Cuddapah Supergroup and Kurnool (Appendix 4). Papaghni Group consists of Gulcheru and Vempalle Formations. Gulcheru Formation represents the base of the Cuddapah sedimentation and represents the Eparchean unconformity. It consists of the 35 to 320 m thick conglomerate unit of quartzitic composition. The beds dip generally 8°-15° towards north (Basu et. al., 2007).

The Gulcheru Formation is conformably overlain by the thick Vempalle Formation constituted predominantly of dolomite. The contact is gradational from quartzite to flaggy quartzite to dolomite, with minor argillaceous sediments (Roy, 1947). The lower part of the Vempalle sequence comprises of purple shale with interbedded layers of dolomite, succeeded by grey, greenish or brown dolomite with interbedded laminae of purple shale and beds of chert and intraformational conglomerates, which in turn is overlain by a purple and buff shale with thin dolomite layers and chert beds (Dutt, 1962). The thickness of the

Vempalle Formation varies from 1,250 to 1,900m (Roy, 1947; Jhanwar et. al., 1964). The rocks generally dip 15–25° towards east (Fig. 2.7). The rocks are unfossiliferous except the presence of stromatolites (Vaidhyanadan, 1961; Gururaja, and Chandra, 1987). Their presence indicates the evolutionary trend of cyanobacteria towards Palaeozoic (Riding et. al., 1998). Small-scale syndepositional slumping features associated with the rocks indicate the relief of the basin (Meijerink et. al., 1984). A number of listric faults with no large displacements cut obliquely through the strike of the beds. The areal extent of Vempalle formation in the basin is 1,830, km².

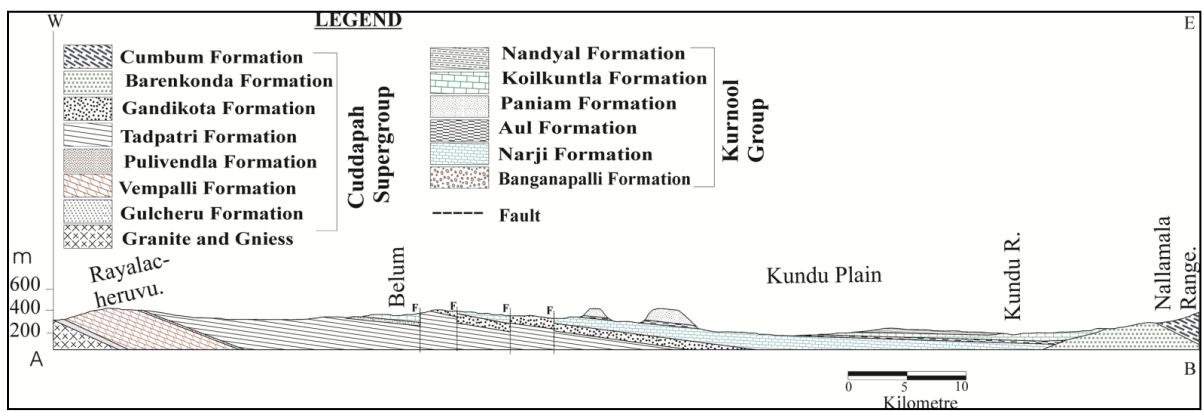


Fig. 2.7. Geological cross-section across the Cuddapah sedimentary basin showing three karstified formations (cross-section through the centre of CB).

Chitravati Group consists of Pulivendla, Tadpatri and Gandikota Formation. Vempalle Formation is overlain by quartzites of Pulivendla Formation. The formation is 1-75 m thick and grades to Tadpatri shale. Tadpatri Formation consists of nearly 5,000m thick argillaceous sediments with thin intercalated beds of quartzite and volcanogenic sediments. It consists of dull brown earthy shales with few intercalations of limestone, chert and jasper. The formation is intruded by numerous igneous rocks (Crawford et. al., 1973). The bedding planes are traversed by some low-angles listric faults like those of Vempalle rocks

(Meijerink et. al., 1984). The shale beds again grade to silicic shale and quartzite of the Gandikota Formation.

The Nallamalai Group consists of the Bairenkonda Quartzite and Cumbum slates which are absent in the western half of the Basin (King, 1872). The quartzite and shale succession show ripple marks and current bedding (Meijerink et. al., 1984). The rocks are metamorphosed (Aswathanarayana, 1962a). A long span of volcanics and folding of the Cuddapahs was followed by the deposition of the Kurnool Group, which was controlled by the re-activation of the basement-rooted faults (Meijerink et. al., 1984). The thickness of the Kurnool Group varies from 300 m to 600 m (Dutt, 1962; King, 1872). Banganapalle Formation marks a change in the nature of the sediments from arenaceous to argillaceous character. It comprises of diamondiferous basal conglomerates of marine origin with some local boulder beds of fluvial origin (Meijerink et. al., 1984). The conglomerates comprise of boulders and pebbles.

The base of the Narji Formation starts with a highly siliceous pink and purple shale/shaly-limestone with thin lenticular lenses of ferruginous sandstone. It grades into bluish-grey, high-grade massive limestone. The upper part of the limestone is flaggy (very regular 5–10 cm beds) that is mined for flooring and roofing material. The lower part of the limestone shows interbedded shale, quartzite and intraformational conglomerates in several places (Dutt, 1962). The massive limestone is extremely fine grained, compact and gives a metallic sound. Narji limestone shows a dip of 0–10° towards NE (Fig. 2.7) with a strike varying from NNW–SSE to NW–SE. The thickness of the Narji Limestone is quite variable: 0–192 m (Dutt, 1962), 100–200 m (Murthy et. al., 1979; Murthy, 1981; Nagaraja et. al.,

1987) up to 100 m thick around Kurnool (Kamal, 1974; Kamal and Vijayam, 1981; Vijayam et. al., 1981). The rocks have an average carbonates of ~60.5% as $\text{CaCO}_3 + \text{MgCO}_3$ and average CaO and MgO ~34.6% and ~0.5% respectively (Kumar, 1983). Some micro- and macro-stylolitic structures are also present. Towards east it is partly or wholly confined by upper Owk Shale and lower Banganapalle Quartzite/Tadpatri Shale.

The Narji Formation is overlain by the buff colored shale of the Owk Formation (Fig. 2.6). These rocks extensively outcrop in the western part of the Kundair valley, where the remnants of the overlying shale and quartzite occur in the form of small hillocks (mesas) and plateaus. It is well-laminated, thinly-bedded, with shales, siltstones and silty-clay stones. The shales are non-calcareous, light grey and buff in colour. The carbonaceous compression and impressions are found in abundance on bedding planes (Sharma and Shukla, 1999). At places the Kurnool's directly overlie the older Cuddapah formations like, Gandikota Formation (Fig. 2.7). Paniam Formation, overlying Owk shale mainly constitutes of quartzites locally ranging from lower well-jointed (Pinnacled Quartzite) to an upper medium to coarse-grained Plateau Quartzite (King, 1872). The two are separated by thinly laminated finer grained quartzites (Meijerink et. al., 1984).

The Koilkuntla Limestone is light to dark grey-colored, compact, massive and flaggy in nature, overlying the Paniam quartzite. Extensively exposed in the Kundair valley, the formation spreads to the east up to the foot of the Nallamala range (Fig. 2.1). The flaggy beds differ from Narji by possessing imperfect, wavy planes of bedding. The lower part of the formation includes the intercalation of shale and weathers to buff platy bits. The middle part of the formation is more calcareous, well bedded and tough. The thickness ranges from

0–90 m (Dutt, 1962). The purple Nandyal Shale with earthy calcareous intercalations, 50–100 m thick, overlies the Koilkuntla limestone. Towards the top, the color of the limestone changes to purple and pass into Nandyal shale. The purple Nandyal Shale with earthy calcareous intercalations, 50–100 m thick, overlies the Koilkuntla limestone.

The structural history of the basin is highly complex (Kaila and Tewari, 1985). While, the western half of the basin remained more or less undisturbed, the tectonic movements from east severely folded and metamorphosed the eastern part during the Eastern Ghat Orogeny. The Cuddapah sediments were deformed, slightly tilted to the northeast and intruded by the dykes prior to the deposition of the Kurnool sediments (Kher et. al., 1989; Narayanaswami, 1966). A thrust fault limiting the western flank of the Nallamalai Range had played an important role in the basin evolution which is called *Rudravaram line* (Meijerink et. al., 1984). The important structural features in the south central part of the basin include the ENE-WSW trending Kalava fault (Fig. 2.1) (Coulson, 1933; Meijerink et. al., 1984; Kher et. al., 1989). This pre-Kurnool deformation was rejuvenated during post-Kurnool times and formed Gani-Kalava anticline (Meijerink et. al., 1984). This led to the folding and faulting of all the pre-Paniam formations of the Kurnool Group (e.g., Kamal, 1974; Kher et. al., 1989). While the axes of minor folds in the Kurnool's trend NE-SW, those in Cuddapahs trend NE-SW to NW-SE through E-W (Kher et. al., 1989). The post-Kurnool compressive forces from the east probably have affected and tilted the Kurnool Group to the northeast (e.g. Narayanaswami, 1966, Sen and Narsimha Rao, 1968). This caused an increase in dip amount ($\sim 20^\circ$) of limestones at the faulted contacts. Minor vertical movements and dips in the flexure zone of the Paniam Quartzite indicate such faulting (Meijerink, et al., 1984).

2.2. Regional Hydrogeology

Geologically the state of Andhra Pradesh is underlain by rock types ranging in age from Archaean to Recent. Major part of the state is covered by hard rocks comprising of igneous, volcanic, metamorphic and hard sedimentary rocks. These rocks cover about 85% of the state while the rest part of its area is covered by other rock types. Most of the southern part of the Andhra Pradesh is occupied by the Cuddapah Basin which spreads over many districts. Major hydrogeological units of this part of the state are discussed below.

2.2.1. Aquifer Systems

The major aquifer systems of the Cuddapah basin include limestones, dolomites, quartzites and shales. Ground water occurs in all the geological formations with varying quantity and quality. A hydrogeological cross-section of the basin shows three major carbonate aquifers along with other sedimentary rocks that also form local aquifers. Highly fractured and karstified Vempalle dolomite, Narji and Koilkuntla Limestones possessing typical karst features form potential aquifers because of the dissolution activity. Secondary porosity developed due to tectonic deformations and bedding planes facilitates the groundwater occurrence and movement along with dissolution porosity in carbonates rocks. Limestones and dolomites cover a large part of the drought prone areas (CWC, 2009). A major part of Kurnool, the third largest district of Andhra Pradesh is underlain by such aquifers providing water for a population of 2973024 people out of which 74.1 percent lies in rural areas and depend on agriculture. The unconfined Narji aquifer becomes confined towards east by overlying impervious shale. The average specific capacity of the wells is 1.3 l/s/m with an average yield of 5 l/s and transmissivity of 68 m²/day (CGWB, 2007). A number of

temporary and permanent springs emerge from this karstified formation which yields 0 (dry months) to more than 50 l/s in monsoon period.

Koilkuntla limestone acts as unconfined aquifer in the top weathered zone and karstified horizons. The average yield of wells from Koilkuntla Limestone varies from 7.8 to 11.7 l/s. The average specific capacity varies from 1.7-2.8 l/s/m from dry months to wet months. According to CGWB, 2007 transmissivity of such aquifers vary from 67 to 1910 m²/day.

Compact Vempalle dolomite is a main aquifer occupying large part of the western part of the Cuddapah Basin. Groundwater in this highly karstified aquifer occurs in dissolution modified bedding planes, fractures and conduits. Surface water in the form of confluence lakes (Reddy et. al., 2000) is utilized for many months in many parts of Cuddapah district. Dug wells up to a depth of 15m and borewells up to 100m yield up to 1.5 l/s and 7 l/s water respectively in many areas.

According to Karanth, 1987 the specific yield of carbonate rocks of Cuddapah, Kurnool and Vindhyan Groups is 3%. Hydraulic conductivity varies from 0.1 to 83 with an average of 6.3 m/day. The rocks have a range of transmissivity of 1.3-1910 m²/day with an average value of 173 m²/day (Karanth, 1987).

Quartzites are hard and compact, but are more water-bearing than shales, (Janardhana et. al., 1996). Aquifers are exploited through dugwells, dug-cum-borewells and borewells up to varying depths. Generally, the depth to water level varies from 1.9 to 23.5m

in many areas (CGWB, 2007). Fissile Tadpatri shale forms good aquifer locally down to 60m depth with yield up to 2.1 l/s and specific capacity up to 6.6 l/s/m (CGWB, 2007). Nandyal shales also form potential aquifer up to shallow depths. Trap sills yield good quantity at the contact zones (Reddy et. al., 2000).

In Paniam Quartzite groundwater occurs under unconfined and semi-confined conditions in weathered zone, joints and beddings. The depth to water level ranges from 4 to 9 mbgl. The yield of wells ranges from 0.34-1.2 l/s (CGWB, 2007). Groundwater also discharges through some temporary springs emerging from bedding planes and fractures with discharge varying from 0 to more than 10 l/s.

Springs are quite common in the karstified rocks (fractured and karst springs), quartzites (fractured and fault springs). Springs also originate in the vicinity of many streams and rivers (Reddy et. al., 2000). However, some spring have dried up due to large scale groundwater exploitation and due to changes in the hydrogeological set up. A number of springs are also used for irrigation through spring channel irrigation.

2.2.2. Groundwater Exploitation

Groundwater overexploitation has posed serious threats, like water table depletion, drying of aquifers, groundwater pollution, salinity and seawater encroachment, water logging and, etc in many parts of India (Singh and Singh, 2002). Intense irrigation has also a major role in creating a number of such problems. Groundwater in Andhra Pradesh presently meets ~85% of the domestic needs in rural areas and ~30% of urban and 50% of industrial demands (Jain et. al., 2009). Demand for groundwater is increasing very fast day-by-day for many

purposes. Increase in well density due to more financial support for drilling wells and free electricity has increased the demand for groundwater which caused over-exploitation in many semi-arid parts of the state. Agricultural area irrigated through groundwater in Andhra Pradesh is increasing at a rate of 0.08 million hectare/year since 80's. While as, groundwater development is increasing (Fig. 2.8) at an average rate of 0.6% per year (Jain et. al., 2009). The increasing dependency on groundwater is felt by the fact that the well population in the state has increased from 800,000 in 1997 to 2,200,000 in 2001 (GEC, 2002). Irrigation is the major consumer of groundwater in India, with 46% of irrigation water fed by groundwater (CWC, 2000). As per 2005-06, 52% of water used for irrigation is supplied by groundwater (CGWB, 2007). According to CGWB, (2007) majority of the wells (83.5%) in Kurnool district have shown a decreasing trend in water level since 1996 which reveals the increase in stage of groundwater development with present value being 42%.

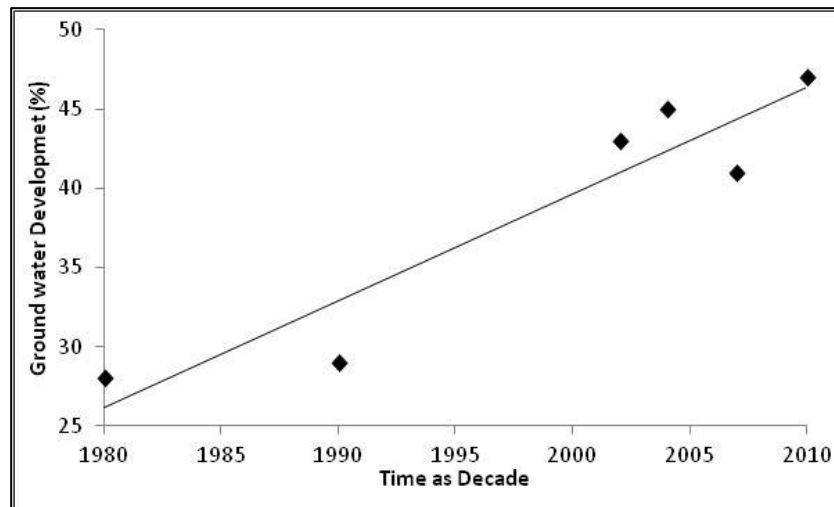


Fig. 2.8. Growth rate of groundwater development in Andhra Pradesh from 1980-2010 (Jain, et al., 2009).

The area is mainly dependent on water from carbonate aquifers. According to GWD, (2002) average groundwater draft for domestic and industrial uses in Pal-Eru and Pedavanka

watersheds will increase from present 1 to 2.8 MCM by 2025. Surface water is limited to some reservoirs and temporary tanks. The Owk reservoir built in 1946 has an area about 4 km² with an effective storage capacity of 2.46 MCM (NRLD, 2009). The water is mostly utilized for irrigation purpose with some pipelines supplying domestic water to the nearby villages. Some problems are associated with groundwater quality in Andhra Pradesh as well in Cuddapah and Kurnool rocks (Jain et. al., 2009).

2.3. Summary

For the hydrogeological characterisation of karst aquifers of the semi-arid India the carbonate formations of the Proterozoic Cuddapah Basin, southern Andhra Pradesh have been selected. The area is geologically, stratigraphically and economically very important. Hydrogeologically the carbonate rocks are the major source of groundwater in many drought prone areas. The area is characterized by low rainfall-evapotranspiration ratio (aridity index of 0.38) with a large temporal and seasonal variability in rainfall. Rainfall occurs mainly in monsoon months (June-September). Average annual rainfall of the studied area is 709mm in which 63% of rainfall is contributed by monsoons. Temperature in non-monsoon months reaches as high as 45°C.

The area is characterised by rolling topography with a large variation in elevation from west to east in the basin. The carbonate massif in the centre of the basin is nearly flat plain bounded by flat topped quartzitic plateaus and hills. This plain area is drained by the tributaries of Kundu River with majority of streams being ephemeral. The soils of the basin vary from place to place but the most part of this central plain is overlain by thin, less developed black and red soils. Vegetation is mostly in the form of scattered open scrub type

plants in the plain areas. The chief economic activities include agriculture, mineral exploitation (cement, construction slabs), rearing of domestic animals and sericulture. Limestone quarrying for building stones and cement construction spreads over a large area.

Geologically the karst areas are complex where tectonics has also played a vital role in karstification. Major fractures and faults coincide with the tectonic history of the southern India. The karstified units vary in thickness and other properties and cover 17% of the basin area. The units represent major aquifer systems of the area. The aquifers are not properly studied for their water resources and need to be characterised by including their heterogeneities developed from rock solubilities.

CHAPTER 3

METHODS AND APPROACHES

3.1. Introduction

Karst aquifers are hydrogeologically different from other groundwater systems. Therefore, the methods and approaches needed to study these important geological formations are also different. So it is important to first give a literary introduction of the methodology applied in karst studies.

Karst systems are characterized by using two approaches- the functional and the structural approach. The **functional** approach analyses the temporal behaviour of the system using spring time series data (Mangin, 1975). The concept considers karst as black-box model (known recharge as input and discharge as output) without knowing about the internal behaviour (Zhang et. al., 1996; Fleury et. al., 2007). This concept is widely used in local and global karst studies (e.g., Mudry, 1990; Andreo et. al., 2002; Perrin, 2003; Aquilina et. al., 2004). The structure of the system (storage, degree of karstification, type of infiltration) is inferred using hydrodynamics, hydrochemistry, hydrothermics, tracers and isotopes (Quinlan and Ewers, 1985; Bonacci, 1993). The method depends on less data and takes field observations into consider and making predictions. The drawback is that spatially distributed hydraulic parameters are not linked with aquifers response. However, the overall results depend on the structure of the system and its recharge conditions (Eisenlohr et. al., 1997).

The **structural approach** proposed by Drogue, (1971) and Király (1975) explains that karst systems can be studied using a hypothetical conceptual structural model, consisting of network of high permeability conduits embedded in a low permeability

fissured media. It is adapted to simulate karst spring hydrographs, recharge and groundwater flow. The method is able to study spatially distributed aquifer properties. It needs detailed data source and good knowledge of the aquifer geometry (dimensions and conduit location) for meaningful spatial results (Scanlon et. al., 2003).

Groundwater modelling in karst is a complex and data demanding process. However, many lumped or spatially distributed models have been used worldwide (Király, 1998; Contreras et. al., 2008; Padilla and Pulido-Bosch, 2008; Aguilera and Murillo, 2009; Martínez-Santos and Andreu, 2010). The assumptions in numerical models are controversial in karst (Scanlon et. al., 2003; Fleury et. al., 2007). But additional geological information can include preferential flows (Eisenlohr et. al., 1997). Modelling in many regional-scale carbonate aquifers (Dufresne and Drake, 1999; Scanlon et. al., 2003; Quinn et. al., 2006) has given acceptable results.

The highly time variable, non-stationary and scale-dependent property of karst systems demands the use of specific investigation techniques (Ford and Williams, 2007). The specific methodology for karst aquifers includes a check-up and diagnosis (Bakalowicz, 1999) which includes their structural characterisation, regional and local functioning. A detailed account of different methods applied in karst has been given in Goldscheider and Drew, (2007). Keeping in view the above methods and approaches, the methodology used for this study is discussed below (Fig 3.1 and 3.2).

3.2. Data Acquisition

Before carrying field investigations desk study was carried out by reviewing the relevant available information including, literature on different aspects of karst and previous studies. It also includes collection of literature, toposheets, existing maps, reports, satellite images and other available data from different organizations (Fig 3.1). Literature on geology, hydrogeology, karst, soils, etc was compiled from libraries from National Geophysical Research Institute, Osmania University, Geological Survey of India and University of Hyderabad. The Survey of India (1983) toposheets of 1:50,000 scale were used as base maps for the field data collection. Geological maps published by Geologic Survey of India of 1:250,000 scale were used for geological reconnaissance. Soil maps of National Bureau of Soil Survey were used for soil study.

3.2.1. Field Investigations

Geological and geomorphological field reconnaissance was a starting step for this study. The detailed geological investigations were carried out in selected areas (refer to sectors in Fig 2.1) from the three karstified formations along cross-sections, road cuts, quarry walls, cave interiors, spring locations, etc. The data on attitude of bedding planes, stratigraphy, fracturing, faults, etc were superimposed on the available maps. Karst geomorphological investigations include location and identification of the karst features (sinkholes/swallow holes, depressions, palaeokarst features, springs, caves, etc). Fracture orientation data was collected from outcrops, road cuts, quarry sites, cave and spring locations.

Data collected from field includes spatial and temporal measurements. Data from point measurements includes location, elevation, depth, water table and discharge of wells

and springs. Soil samples were collected from different areas to represent all soil types. The point data was collected by the use of a hand-held GPS with an accuracy of ± 7 m. The data was collected using a metric system of measurement. The field data was later transferred to a GIS data base and interpreted with the existing data.

Water level measurements were made at available bore wells, dug wells and springs (Fig. 3.3). Water level data of Koilkuntla Limestone was obtained from BIRDS NGO for monitoring wells for 2006-07 year. Monthly water level data of observation well at Narji limestone was obtained from groundwater department, A.P. Water level of the Narji limestone area from available bore wells was measured for pre- and post-monsoon seasons in 2011 using a water level indicator. The elevation data was also obtained in field and from ASTER 30m DEM data. Pumping data was measured from available wells using a bucket and stopwatch.

3.2.2. Field Sampling and Procedures

The rainfall data from 2002-2011 was obtained from Kolimigundla Mandal Revenue Office, Kurnool. Rain and evaporation data was manually collected at the Belum cave station using a rain gauge and evaporation pan with the help of APTDC cave employees (Fig. 3.4). The rainfall data was collected after each rain event and pan evaporation data was collected at the evening time each day.

Soil samples (13 in number) were collected by using a hand-held auger as the soil thickness in the area is less than 1m. Samples were collecting in plastic bags from the cores. Infiltration measurements were carried out in all soil types. The infiltration was carried out

with a 15 cm diameter infiltration ring (Fig. 3.5). The test was carried for 1 hour or more at a single site.

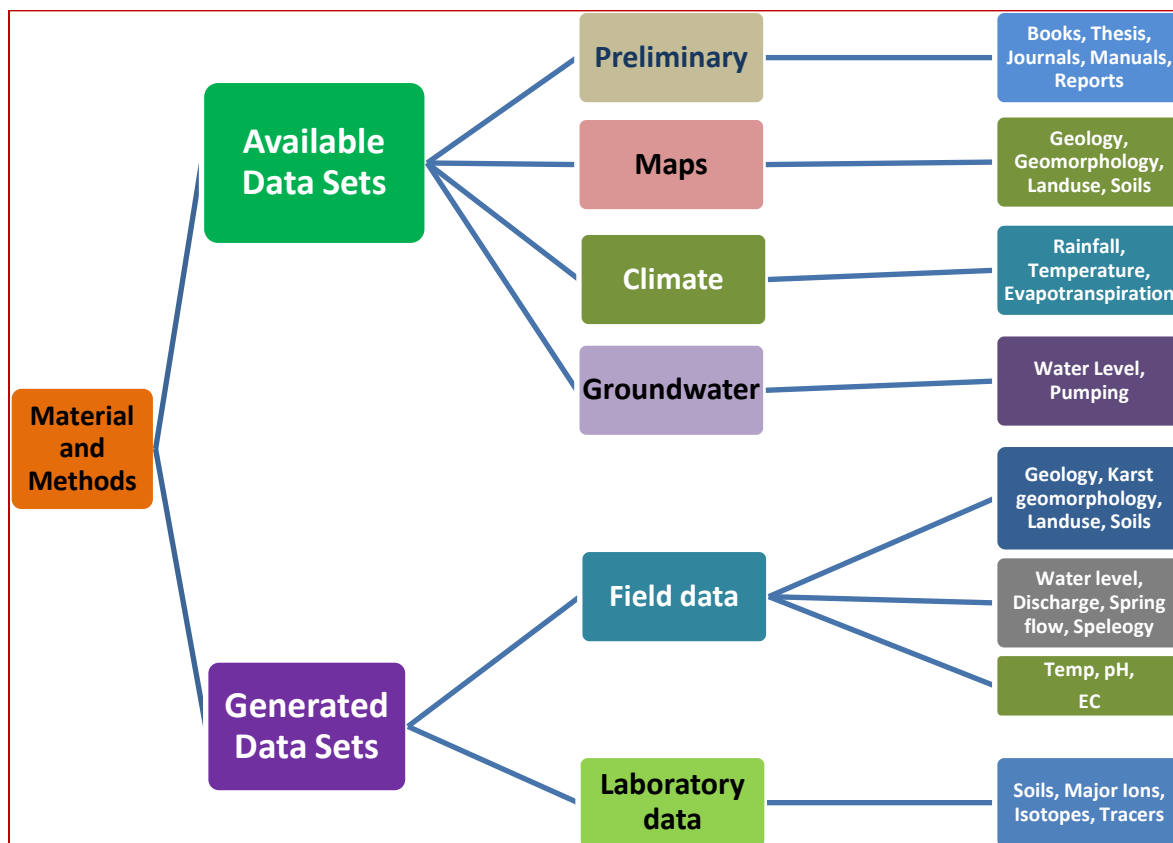


Fig. 3.1. Flow chart showing the detailed account of data sets used for this study.

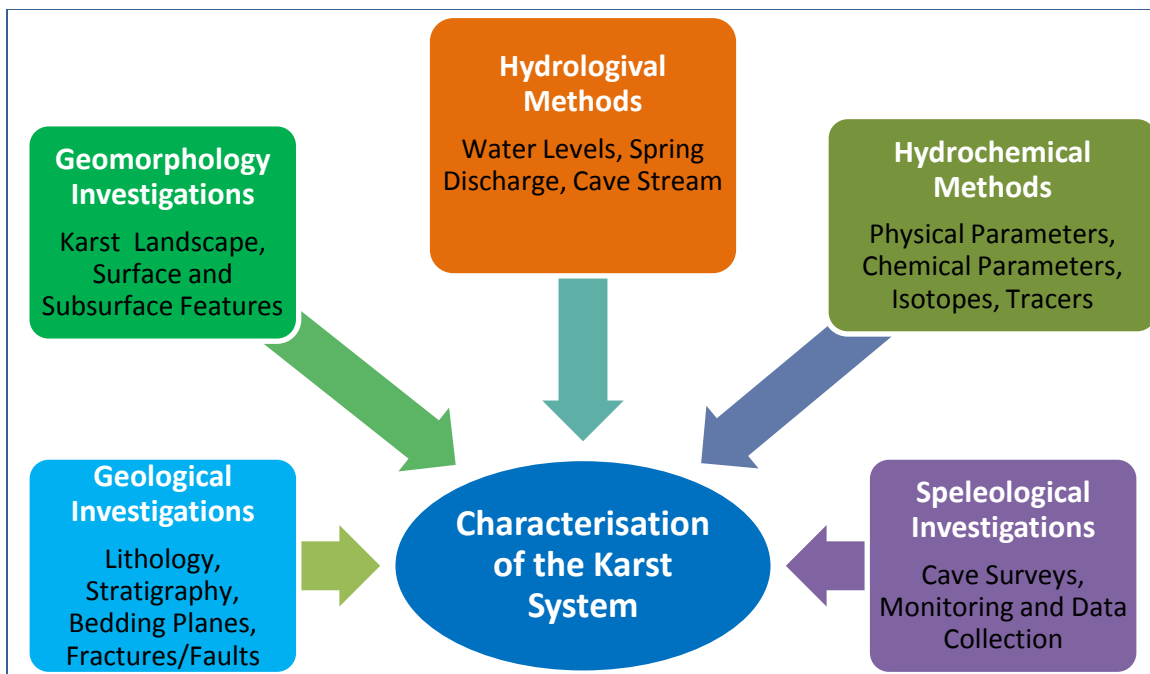


Fig. 3.2. Flow chart of the methodology used for the characterisation of the karst aquifer.



Fig.3.3. Field photograph showing the measurement of the water level in the study area (left). A dug wells in the Narji Limestone is also shown (right) which is currently being used for irrigation purposes.

Hydrogeological data was collected at the discharge point of karst springs. Discharge was measured from the outlets using a bucket of known volume and stopwatch. The in-situ

measurement of EC, pH and temperature were taken with portable field conductivity and pH meters that were calibrated for each field survey. Water sampling was done during 2009-11 for all springs (Fig. 3.6). Few cave streams were also sampled during different visits to the underground. Springs were sampled at their major outlets to avoid any human influence. Groundwater samples were also collected from available bore wells, springs and one cave stream for pre- and post-monsoon season of 2011 for spatio-temporal variability of groundwater chemistry in the carbonate area. Water sampling was done according to the procedure used in karst areas. Borewells and hand pumps were sampled after pumping water for at least 15 minutes. Water samples were filtered through a 0.45 μm membrane at collection sites and stored in plastic bottles for laboratory analysis. The samples were properly capped and marked to avoid any confusion in the laboratory.



Fig.3.4. Meteorological station at Belum (5 km from Kolimigundla village) installed for monitoring daily rainfall and evaporation in the study area.



Fig.3.5. Picture of field measurements of infiltration rates in the soils of the study area.



Fig.3.6. Groundwater flow in karst springs monitored during the study period. Left one is the photograph of Belum spring, S1 during flowing condition and right one shows the Kona spring S2 flowing through a conduit. For location refer to Fig. 2.1.

The samples from major springs were collected from 2009-2011 to represent a time series. Water was collected at the main spring outlets so as to avoid atmospheric influence on the isotope analysis. Samples for isotope concentration were also collected during pre- and post-monsoon season of 2011 from springs and bore wells in the limestone aquifer. This will help to assess the spatio-temporal evolution of the isotopic signature of groundwater.

Stable isotopes of hydrogen and oxygen are widely used as a tool for addressing hydrological problems in water resource development, planning and management. Stable isotope samples from rain and groundwater were collected in 10ml glass vials with air tight screw and putted with a parafilm on the cap. Rainfall samples were collected from major rain events (more than 50mm) at the rain gauge, (Tab. 3.1).

3.2.3. Laboratory Analysis

The analysis of soil samples for grain-size composition was done using the Unified Classification System of ASTM, 1982 at CRIDA, Central Research Institute for Dryland Agriculture, Hyderabad. During field studies, groundwater samples were analyzed for physical and chemical characteristics. The unfiltered samples were analyzed for bicarbonates shortly after returning from field by titration with 0.1 M HCl to a pH of 4.5. The anions were analyzed with an ion chromatograph Dionex DX 600 at Indo-French Cell at IISC Bangalore. The detection limit was about 1 μ mol/L and usual precision 5%. Cations were measured with an ICP-OES Jobain-Yvon with same detection limit and precision except for Ca and Mg due to conditioning of samples (oversaturation regarding to carbonates). All samples were analyzed within 1 month after collection. Chemical

parameters determined include major cation (Ca^{2+} , Mg^{2+} , Na^+ and K^+), major anion (F^- , Cl^- , NO_3^- and SO_4^{2-}).

ID	Name	Measured parameters
S1	Belum spring	Water level, Q, major ions, isotopes
S2	Kona spring 1	Q, major ions, isotopes
S3	Kona spring 2	Q, major ions, isotopes
S6	Rati spring	Q, major ions, isotopes
S7	Bugga spring	Q, major ions, isotopes
S8	Yaganti spring	Q, major ions, isotopes
BC	Belum cave stream	Major ions
R	Rain water	Amount, major ions, isotopes
BW	Bore wells	Major ions, ions
QS	Quartzite springs	Q, major ions
Drips	Cave drip water	Major ions
Surface water	Runoff, abandon quarries	Major ions

Tab. 3.1. Parameters measured from different sampling locations from the study area during 2009-2011. Physical parameters (Q, pH, T, EC) were measured in-situ while major ions and isotopes were measured in laboratory. For sample locations of springs and caves refer to Appendix 5 and 6 and for bore wells refer to Appendix 10 and 11.

Deuterium and oxygen-18 concentration were analyzed at NGRI by isotope ratio mass Spectrometer. The analysis is based on separation of gas molecules according to their mass. The analytical precisions for $\delta^2\text{H}$, $\delta^{18}\text{O}$ measurements were ± 1.5 and $\pm 0.1\%$, respectively. The concentration of the isotopes in a sample and in a standard is compared; the results of which are given by the delta (δ) notation in parts per thousand or permil i.e., ‰ (Criag, 1961a). For hydrogen and oxygen in water, standard mean ocean water (VSMOW), an average value for the isotopic composition (Vienna) of ocean water is most commonly used. The ratio of isotopes ($^{18}\text{O}/^{16}\text{O}$ or $^2\text{H}/^1\text{H}$) in a sample is given by delta (δ) notation with respect to a standard in parts per thousand or permil (‰) (Criag, 1961a).

$$\delta^2H \text{ or } \delta^{18}O (‰) = \left(\frac{R_{\text{sample}}}{R_{\text{standard}}} - 1 \right) \times 1000$$

here, R_{sample} and R_{standard} are the isotope ratios ($^2\text{H}/^1\text{H}$ or $^{18}\text{O}/^{16}\text{O}$) in a sample and the standard respectively.

3.3. Hydrogeological Investigations

The study of karst geomorphology and understanding of karstification processes are important for an adequate land and water resource management because specific problems are known to occur in karst regions such as, ground subsidence, sinkhole collapse, ground-water contamination and unpredictable water supply. Karst systems were characterized using the hydrogeological and hydrochemical methods. The methodology discussed in Goldscheider and Drew, (2007) was followed. Karst geomorphology and hydrogeology provided a better idea of the aquifer structure. Geological cross-sections were prepared for each of the formation at different location in order to compare the geomorphological setup in three karstified formations. The information on karst geomorphology, caves and springs and other karst features and water levels were included. Cave patterns were identified from the existing maps and reports along with the cave data collected from different speleological surveys in different caves of the area. A model of karstification was developed based on these studies. Time series data (flow, water level) helped in analysing local functioning as discussed in separate chapters. This gave an idea of the internal behaviour of the system.

3.4. Hydrochemical Studies

3.4.1. Physico-chemical Analysis of Groundwater

Groundwater chemistry is used as a means to understand the characteristics of karst aquifers. A number of studies are related to the relationships between physico-chemical properties of karst waters (e.g., Scanlon and Thrailkill, 1987; Scanlon, 1990; Vesper et. al., 2003; Karimi et. al., 2005; Krawczyk and Ford, 2006; Wu et. al., 2009). Study of hydrochemical characteristics of karst aquifers have helped in solving many karst related problems. The chemographs of springs can indicate the proportion of diffuse or conduit flow in discharging water (Shuster and White, 1971; Jacobson and Langmuir, 1974a). These studies need a high-frequency, flow-dependent sampling of karst waters (Quinlan and Alexander, 1987). Springs dominated by conduit flow show highest variability of chemistry (Ryan and Meiman, 1996). Hydrochemistry of karst aquifers indicate groundwater flow and residence time, interaction and exchange of components with different waters, recharge or discharge mechanisms, etc (e.g., Herczeg et. al., 1997; Wicks and Engeln, 1997; Barbieri, et. al., 2005; Falcone et. al., 2008; Azzaz et al., 2008). Water in extraordinarily pure limestones will show relatively high Mg^{2+}/Ca^{2+} ratios and a long residence time (Edmunds et. al., 2000). Calcite sub-saturated water of karst springs may indicate conduit flow with less residence time while the saturated spring water with respect to calcite represents predominant diffuse flow (Shuster and White, 1972).

Spatial and temporal variability of karst water chemistry has also been studied worldwide (e.g., Shuster and White, 1971; Scanlon, 1990; Mayer, 1999; Perrin et. al., 2003; Musgrove and Banner, 2004; Karimi et. al., 2005; Krawczyk and Ford, 2006; Wu et. al., 2009). The chemical signature has been interpreted in terms of recharge types (Scanlon and

Thraillkill, 1987; Hess and White, 1988; Vervier, 1990; Mayer, 1999), nature of storage (Williams, 1983), quick-flow and matrix-flow (Blavoux and Mudry, 1983), tributary mixing (Perrin et. al., 2006). Thus, understanding the geochemical processes that control the water quality is important for water resource management and protection of karst aquifers.

After locating and verifying various springs in the area water samples were collected to represent the time series data of spring waters from 2009 to 2011. Groundwater of the karst area was analyzed for physico-chemical analysis during pre- and post-monsoon season of 2011. Water samples from bore wells, springs and cave stream were analyzed for this purpose. The validity of chemical analysis was checked by the ion balance so that equivalent sum of the positive ions (cations) must equal the equivalent sum of the negative ions (anions). Thus, the error in a cation-anion balance was determined as:

$$\% \text{ Balance Error} = \frac{\sum \text{Cations} - \sum \text{Anions}}{\sum \text{Cations} + \sum \text{Anions}} \times 100$$

The charge balance of analysis (acceptable range 0-5%) was found to be 3.9%. The ratio of total anions to cations is also an indicator of validity. The linear regression of cation sum to anion sum gives $R^2 = 0.91$ also indicate that the quality of the data was good.

3.4.2. Stable Isotope Study

Stable isotopes of hydrogen and oxygen are widely used as a tool for addressing hydrological problems in water resource development, planning and management because ^{18}O and ^2H ratios are not modified by water-rock interactions at biospheric temperatures (Sidle, 1998; Marfia, et. al., 2004).

The stable oxygen and hydrogen isotopes have also widely been used in karst hydrogeological studies (e.g., Lakey, and Krothe, 1996; Vallejos, et. al., 1997; Perrin et. al., 2003). Isotopic investigations provide a clear picture of their functioning (Kattan, 2001; Larsen et. al., 2001; Vandenschrick et. al., 2002; Marfia et. al., 2004; Barbieri et. al., 2005; Blasch and Bryson, 2007) and contribution of preferential flow to groundwater system (Leaney et. al., 1993). The isotope application valuably help to understand the functioning of karst aquifer systems in semi-arid environments (Marfia et. al., 2004; Azzaz et al., 2008) and calculating the recharge (El-Quali et. al., 1999). Isotopic data is used to calculate the volume of water stored in the aquifer (Ford and Williams, 2007). They help in hydrograph separation (e.g., Larsen, et al., 2001; Shi et. al., 2001; Yehdegho and Reichi, 2002; Marfia et. al., 2004). Isotope data provides additional linkage to water chemistry studies (Aquilina et. al., 2005; Azzaz et. al., 2008). Isotopes can also be used as a tool for modeling of karst aquifers (El-Kashouty, 2010). The isotopic data of secondary cave deposits have been used to study many processes in carbonate environments (Mcdermott et. al., 2006). The isotope data of water and calcium carbonate reveals the palaeo-temperature under which CaCO_3 was precipitated.

Water samples were collected from springs during the study period (2009-2011) for isotope studies in this karst area. Groundwater was also analyzed during pre- and post-monsoon period of 2011 for spatial variability of major isotopes.

3.4.3. Tracer Study

A groundwater tracer is used to study a number of hydrogeological processes. Tracer can be natural or gets accidentally introduced or is intentionally used (e.g., dyes). An ideal tracer

should be non-toxic, inexpensive, easily detected, non-reactive and conservative (Davis et. al., 1980). Goldscheider, (2008) has given a review of the properties and limitations of different tracers in karst groundwater studies along with the procedure of injection, sampling, monitoring and analysis.

Dyes are used as powerful tracers in karst studies (e.g., Atkinson et. al., 1973; Perrin, 2003; Goldscheider et. al., 2003; Zare, 2007). Fluorescent dyes (e.g., rhodamine, uranine, etc.) are the most commonly used because of their conservative (resistant to adsorption and degradation) and non-toxic nature. Detectable at low concentrations, they also remain stable over time (Smart and Laidlaw, 1977; Smart, 1988; Raeisi et. al., 1999; Smart and Karunaratne, 2002). The dye will break down if exposed to direct sunlight, so needs proper care in sampling and transport to labs.

A tracer test is more efficient in karst aquifers than other techniques (Quinlan and Ewers, 1985). This well-developed and powerful tool enables delineation of catchment boundaries, identification of recharge areas and sources of pollution (Ford and Williams, 2007). The quantitative analysis of tracer data helps in determining the structure and transport properties of karstic systems (Wang et. al., 1987; Uliana et. al., 2001; Meigs et. al., 2001; Maloszewski et. al., 2002). These tests can help in the finding the groundwater-surface water connectivity (Crandall et. al., 1999) and assessing the role of different karst morphologies (channels, pools, rapids) on the karst hydrodynamics (Hauns, et, al., 2001; Massei et. al., 2006). They provide detailed information about groundwater flow (Katz, 2002; Goldscheider et. al., 2008), about the geometry and volume of active and often inaccessible the conduits of cave (e.g., Mohammadi et. al., 2007).

In an attempt to study the karst system functioning in the Yadiki area four kg of common salt NaCl (90:10 proportions) was introduced into the Munagamanu Gavi stream at 10:00 am on 7th January, 2010. The spring water of S2 was monitored with time for EC, temp and few water samples were also analyzed for major ions with time. For another tracer test one kg of uranine dye was introduced in the cave stream water at 06:56 pm on 10-08-10. This test was done during monsoon season during high flow conditions in the cave stream and spring. Water was monitored and samples collected at spring location (S2 and S3) for a time period of 21 hours for any change in color. The samples were not analyzed due to financial reasons.

3.5. Recharge Estimation

Groundwater in semi-arid areas is often the sole water source where aquifers are vulnerable to contamination, frequent droughts and depletion. It provides water for domestic use and economic activities (irrigated agriculture). To maintain the efficient and sustainable supply of this resource groundwater must get sufficiently recharged by rain and surface water (Scanlon et. al., 2002). Recharge is a process by which rain and surface water reaches the phreatic zone through the unsaturated zone (e.g., Freeze and Cherry, 1979; Lerner et. al., 1990).

Identification and quantification of recharge in highly heterogeneous karst aquifers is difficult. Abundant literature is devoted to the estimation of recharge in karst aquifers (e.g., Gunn, 1983; Jones et. al., 2000; Andreo et. al., 2008; Santos and Andreu, 2010; Canton et. al., 2010) however, few studies deal with karst in semi-arid environment (e.g., Hughes et. al., 2008; Hoetzl, 1995; De Vries and Simmers, 2002; Leduc et. al., 1997; Herczeg et. al.,

1997). The low rainfall and high potential evapotranspiration in such areas increases the necessity of replenishing groundwater through recharge. It is therefore, important to develop and test methodologies for estimating groundwater quantitatively for better water management. Recharge in semi-arid karst is a function of many processes that include intensity and time variability of rainfall (Lerner et. al., 1990), presence of depressions (Leduc et. al., 1997), nature of percolation (Wood et. al., 1997) and interaction between processes of the hydrological cycle. The amount of recharge is generally low compared to the average annual rainfall or evapotranspiration (Beekman, 1996; Scanlon et. al., 2002). Recharge also depends on the epikarst and its degree of development as it is an important storage zone. Vegetation cover reduces recharge by a factor of 2 to 30 from humid to arid areas (Keese et. al., 2005). Soil textural variability also causes a change in recharge amount.

Recharge in karst aquifer generally occurs in two ways -Allogenic and Autogenic (Gunn, 1983; Lerch et. al., 2005). The allogenic recharge usually takes place through concentrated dissolutional linear/point inputs (like, sinking streams) where the surface runoff drains areas of insoluble rock or low permeability soils and then reaches the limestone. In case of allogenic recharge water is collected outside the limestone area and reaches the aquifer very fast. In case of autogenic type recharging water is derived solely from precipitation falling on the limestone outcrop itself. The autogenic recharge can be separated into a diffuse recharge (entering the aquifer through the soil zone, fractures and fissures or closed depressions on the karst surface) and a discrete recharge or internal runoff (entering the aquifer quickly through the sinkhole drains). Closed depressions collect and concentrate the autogenic water (e.g., Gunn, 1983). A well integrated karst system can also

develop in limestone terrains with dominant surface depression landscapes (Williams, 1972) by autogenic recharge and because of the significant role of the epikarst. Point recharge is generally intermittent that may occur only for short span of time and only after a threshold of sustained rainfall gets exceeded (e.g., in Australia, greater than 2.5 mm day^{-1} for more than 3 days leads to point recharge, Herczeg et. al., 1997). The fast recharge (allogenic type) is the most common mechanism in karst (Ford and Williams, 2007). It causes a large variation in physico-chemical parameters of water and has shorter flow time than the slow infiltrating water. It provides an understanding of the connectivity between matrix and conduit porosity.

Groundwater recharge is measured through many methods in arid and semi-arid areas. Scanlon et. al., 2006 has discussed the recharge findings globally from many regions and has provided information regarding recharge rates, controls and processes. The dependence and limitations in terms of applicability and reliability vary with method, geology, climate and data sets needed. The following section will focus on the methods applied for estimating the recharge in semi-arid karst areas, which are usually adapted or derived from the classical ones.

Depending on available data, recharge in karst can be estimated with water balance method or with more complex hydrological models (e.g. Geyer et. al., 2008; Jukic and Denic-Jukic, 2009). The resolution of water balance methods is too low in semi-arid regions (Gee and Hillel, 1988; De Vries and Simmers, 2002). Water table fluctuation measurements in karst may not accurately estimate the aquifer parameters and storage changes due to their highly heterogeneous properties.

While, the physical methods only provide data over the monitoring period, an advantage of the chemical methods is that the data collected produce a historical record over many years (Allison et. al., 1985). Punctual measurements like, injection methods are not representative at larger scale. Certain chemical techniques like, CMB method represent a spatially uniform value (e.g., Lerner et. al., 1990). Chloride mass balance is most widely used in semi-arid areas where concentration through evaporation is significant (Wood, 1999; Allison et. al., 1985; Sharma and Hughes, 1985; Gee et. al., 2004; Scanlon et. al., 2002, 2006; Phillips, 1994). The method relies on a single data set and is time and cost effective in both unsaturated and saturated zones but is based on many assumptions. Signatures of stable isotopes of ^{18}O and ^2H are growingly used in recharge estimation (Ellins, 1992; Dutton, 1995; Vallejos et. al., 1997; Jones et. al., 2000; Andreu et. al., 2011). Spring hydrograph analysis is an effective way to estimate groundwater recharge (Korkmaz, N, 1990; Ford and William, 2007). The hydrochemistry of cave seepage (stalactite dripping) can be used to identify and quantify the mechanism of infiltration through the soil and epikarst zone (e.g., Yonge et. al., 1985; Sanza and Lopeza, 2000). Environmental as well as injected tracers have been applied in various aquifers of semi-arid India by many researchers (eg., Sukhija and Rama, 1973; Athavale et. al., 1980; Sharma and Gupta, 1987; Sukhija et. al., 1996; Rangarajan and Athavale, 2000). However, no such study has been carried out in karst aquifers.

Conceptualization of recharge processes and identification of flow mechanisms is important before choosing a recharge model. It reduces the uncertainty, time and cost of recharge quantification (Scanlon et. al., 2002; USGS, 2008). The classical recharge methods

consider a uniform condition in the aquifer and don't consider the type of recharge. Therefore, the methods need to be modified according to the heterogeneity of the karst aquifers and the semi-arid nature of the study area. Based on the field observations and geological mapping, two principle recharge components were identified; point recharge (runoff issued from the quartzite hills and entering the groundwater) and diffuse recharge enters across the soil and epikarst layers. The area for recharge estimation was defined on the basis of topography, geology, structure (fracture/faults) and groundwater flow.

3.5.1. Point Recharge (Q_{run})

With the hypothesis that no significant infiltration occurs through rock outcrops (Li et. al., 2011) like quartzites i.e., excess rainfall is lost only as evaporation, point recharge (Q_{run}) results from local fractures, dissolution features and depressions. The runoff becomes recharge and the only loss is through evapotranspiration. The ephemeral streams flow for a short distance and also enter the groundwater system, which is valid in highly karstified semi-arid areas (Frot and van Wesemael, 2009; Ingram et. al., 2012). Point recharge occurs rapidly through preferred paths and bypasses the soil zone in carbonate rocks. It is a major contributor of total recharge in well developed karst aquifers and other bare fissured areas in semi-arid and arid regions (e.g., Wood et. al., 1997; Andreo et. al., 2008). This bypass infiltration increases groundwater levels in short time. The runoff from quartzite areas reaches the limestone plateau and gets localized in the depressions and dissolution fractures. This amount was calculated from daily rainfall by the versatile and well established empirical curve number (SCN) approach (SCS, 1972). It is a procedure for direct runoff estimation in small watersheds (e.g., Hawkins, 1975; Boughton, 1989; Ponce et. al., 1996; NIH, 1997; Baltas et. al., 2007; Ebrahimian, et al., 2009; GEC, 2009; Kumar et. al., 2010).

3.5.2. Diffuse Recharge (Q_r)

Diffuse or direct recharge (Q_r) is the rain that reaches the aquifer by direct vertical percolation through the soil and unsaturated zone. Diffuse recharge infiltrates through soil and vadose zone. It is a slow process mostly affected by evapotranspiration and soil properties. Diffuse recharge impacts water budget and affects the dissolution processes of mineral and thus, cannot be neglected in karst (e.g., Ritorto et. al., 2009; Langston et. al., 2012). In case of temperate and humid climates with thick well developed soils, diffuse recharge prevails (Marechal et. al., 2009a). However, in semi-arid regions, this amount remains very little compared to rainfall. Diffuse recharge is accurately estimated at small scales through daily soil water content variation (Scanlon et. al., 2006; Marechal et. al., 2009). Diffuse recharge Q_r reaches groundwater in excess of soil moisture deficit and evapotranspiration by vertical percolation through the unsaturated zone. It was computed through soil water balance model (e.g., Rushton, 2003; Rushton et. al., 2006) that calculates the effective amount of water which ultimately reaches the aquifer due to rainfall or irrigation through the free draining soils at their field capacity. The method has been applied in semi-arid karst aquifers (Cantón et. al., 2010).

In addition to this, internal runoff (i.e., overland flow within the limestone plateau itself) may take place after heavy rainfall and then disappear into karst groundwater system (Wanfang and Beck, 2011) thus, generating a third type of recharge; Q_{intr} . It is the discrete autogenic recharge that enters the aquifer quickly through sinkholes other than diffuse recharge (Lerch et. al., 2005). It may occur in two forms; excessive runoff reaching the limestone outcrop and excessive saturation runoff. This part of recharge occurs only during

short and high intensity events of the rainfall. However, this term has a very limited impact on the overall groundwater balance.

3.5.3. Tritium Injection Method

Tritium (tracer) injection method was applied for evaluating annual natural recharge due to rainfall and rainfall+applied irrigation during monsoon season. The Tritium injection method of recharge estimation is based on Piston-Flow model for movement of moisture in the unsaturated zone (Munnich, 1968). Tritium has a half-life of 12.43 years and has negligible toxicity in handling as it emits soft beta particles possessing energies of 18Kev. This technique has been used in different hydrogeological provinces of India (Rangarajan and Athavale, 2000). The moisture was tagged with tritiated water at a depth of 0.6m in the soil profile before start of monsoon. The tracer moves downward along with the infiltrating moisture, due to subsequent rainfall of the monsoon months or irrigation water. A soil core from the injected site was measured for the moisture content and Tritium concentration at various depths in counts per minute (CPM). The peak in tracer concentration indicates the displaced position of the tracer. Moisture content of the soil column between the injection depth and displaced depth of the tracer is the measure of recharge to groundwater over the time interval between injection of tracer and collection of soil profile.

3.6. Statistical Approach

Different sets of data were analyzed using descriptive statistics. Range, mean, standard deviation and coefficient of variation (SD/mean and expressed as percent) were calculated for different parameters and for seasonal variations. Spatial data was converted to GIS based maps which were overlaid over other information to assess the spatial variability in

parameters. Temporal variability of different parameters and samples was analyzed using scatter, line and trilinear plots, bar charts, box-whisker plots, etc. Correlation matrix was developed to assess the relation between different parameters. Different software's were used for developing maps and plotting of graphs. Statistical analysis was mostly done using Microsoft Excel.

CHAPTER 4

KARSTIFICATION IN THE CUDDAPAH BASIN (CB)

4.1. Introduction

Karst regions are widespread across the globe and present unique geomorphological characteristics which have specific consequences on land and water resources management. In India, karstified carbonate rocks are distributed across the country in different geomorphological, geological and climatic contexts (Himalayan region, North-eastern hills, and sedimentary basins in peninsular India, etc.). Regionally, these karstic zones play a vital role for the society both as a primary water supply and in economic terms (water resource for irrigated agriculture, quarrying for construction and cement production). There are only a few studies on the characteristics and the role of karst in Indian carbonate terrains as discussed in chapter 1. This chapter therefore, aims at discussing the karstification of the carbonate units of the CB, southern Andhra Pradesh (Fig. 2.1). A model of karstification and evaluating the role of karstification on the groundwater resource are discussed. The results will provide new insights on the global karstification in southern India during geological time.

4.2. Karstified Formations

The main carbonate rocks of the basin are the Vempalle Formation of the Cuddapah Supergroup and the Narji and Koilkuntla Formations of the Kurnool Group. A detailed geological setup of the basin has been presented in chapter 2. Of the total 44,500 km² area of the basin 17% (i.e. 7,690 km²) shows the exposure of these potentially-karstified rocks. The areal extent of Vempalle, Narji and Koilkuntla Formations is 1,830, 4,333 and 1527 km² respectively.

Field observations indicate the extensive karstification of the three carbonate formations. Solution features in these rocks vary in scale from enlarge bedding planes, sinkholes to large cave openings. Few karst features are well developed in the Narji limestone, like grikes and grooves, karrenfield, etc. The karstification has been discussed separately for the three formations in different sectors of the basin (refer to Fig. 2.1).

4.2.1. Karstification in the Vempalle Dolomite

Vempalle Formation consists predominantly of dolomite with minor argillaceous sediments. The detailed geology of the formation is described in chapter 2. The dolomite is karstified with existence of a few caves of limited extension. Geomorphologically, the formation shows a typical landscape of hills dissected by valleys; the hills have an asymmetric geometry with a gentle slope that follows the dip of the beds ($5-18^{\circ}$) and a steeper slope on the opposite side (Fig. 4.1). The origin of these geomorphic features is not understood clearly. In the area north of Rayala Cheruvu, these hills are elongated along a W-E axis, width ranging between 400–800 m and length between 1,000-2,000 m. Slope on the western side is $>25^{\circ}$, whereas on the eastern flank it is $<10^{\circ}$ (dip-slope). The hill height is between 100–150 m. Field studies were carried out in two sectors in this formation (Done and Chillavaripalle sectors, refer to Fig. 2.1) where a number of karst features are present as discussed below.

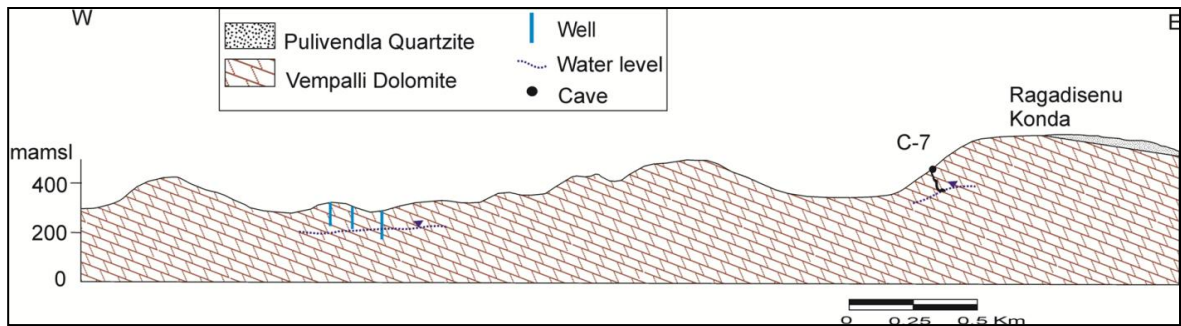


Fig. 4.1. Geological cross-section across the Vempalle dolomite along Rayala Cheruvu showing the main cave and inferred piezometric surface based on observations in the cave and existing borewells in the surroundings (refer to Fig. 2.1 for location).

In Dhone sector one of the important caves is the Kuruva Bali Guha (C7 of Fig. 4.1). It is located in Boyawandlapalli village of Kurnool district and is also called Shepherd Bali Cave (Gabauer, 1985). The geological cross-section of the area (Fig. 4.1) shows that the cave ends near the bottom of the valley which constitutes the base level. The characteristic features of few more caves of this formation are given in Appendix 5. Dolomite beds have a dip of 25° towards NE. The cave entrance (a 3m diameter shaft) has an elevation of about 427 masl; the length of the cave is more than 318m with a depth of 77m. It is the deepest known cave in southern India (Gebauer, 1985) and perhaps the second deepest cave in India that requires proper speleological equipments for exploration. A small pond is located at its bottom. It shows a bunch of stalagmites resting under a fine formation of pure white calcite flags resembling a colorful flower under the ceiling. The cave shows signs of water infiltration during monsoon period. From observations on the soil of the deepest part, it seems that a stream is meandering through the clay/silt deposits and possibly some water filling occurs after intense recharge (Fig. 4.2).

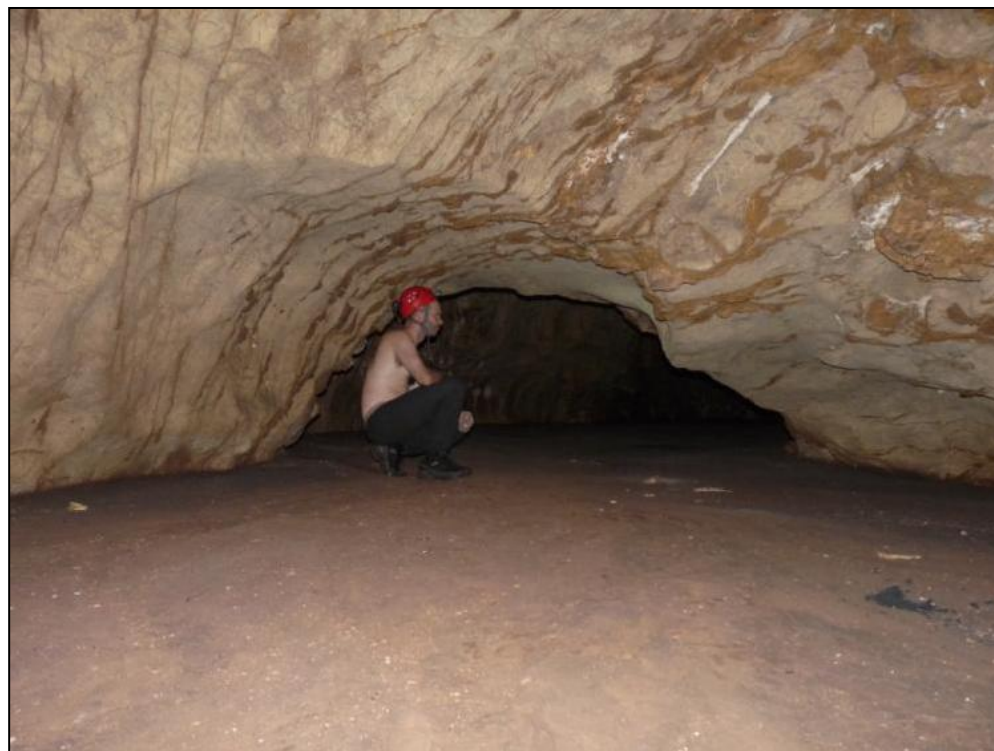


Fig. 4.2. *Picture taken at the bottom of Kuruva Bali Guha (C7) showing the phreatic shaped conduit and sediment accumulation on the floor.*

The dolomite valleys are used mainly for cultivation of rain fed crops with some bore well irrigated crops, like banana, groundnut, etc. Most of the borewells have depth between 40-50m. According to the drillers, the drill bits fall sharply during drilling, indicating the presence of underground conduits in the formation. In the valleys, irrigation wells exhibit quite variable discharge and some wells are dry. This is typical of a highly heterogeneous aquifer. Though, Reddy et. al., (2000) find a stable water level in the dolomite, but the data since 1976 shows a declining trend (0.3m/year) in water level. Recharge occurs seasonally on the hills and feeds the fissured-karstified dolomite aquifer with a water table close to the valley bottom. No karst springs are known and it is possible that natural discharge occurs within the alluvial deposits of the main valleys. However, certain springs have been found in the dolomite karstified terrain (fractured and cave springs), in quartzites

(fractured and fault springs) and in the vicinity of streams and rivers in the southern side of Cuddapah district (Reddy et. al., 2000). Temporary springs (S10, S11 and S12) have been found at dolomite/quartzite contacts in Rayalacheruvu and Pyapali areas during rainy seasons. Some springs have dried up due to upstream tank construction and large scale exploitation of groundwater in the vicinity of these springs (Reddy et. al., 2000). The spring-channel system is used for irrigating the low-lying agricultural lands.

Vempalle dolomite in Chillavaripalle sector (between Tadpatri and Anantapur) shows typical geomorphology in the form of valleys, ridges and cuestas (cliffs). Ridges have mostly NW to SE direction with 400-1050 m width. The valleys show a gentle slope ($\sim 40^\circ$) towards northeast (Fig. 4.3) and steep slope (more than 60° as cliffs) towards southwest. The gentle dip-slope corresponds to the dipping ($8-15^\circ$) of Gulcheru quartzite, while the steep cuestas (cliffs) correspond to the outcropping of 10 to 30 cm thick dolomite beds. Dip of the dolomite beds along road cuts and cave interior vary from $20-45^\circ$ towards NE-SE directions.

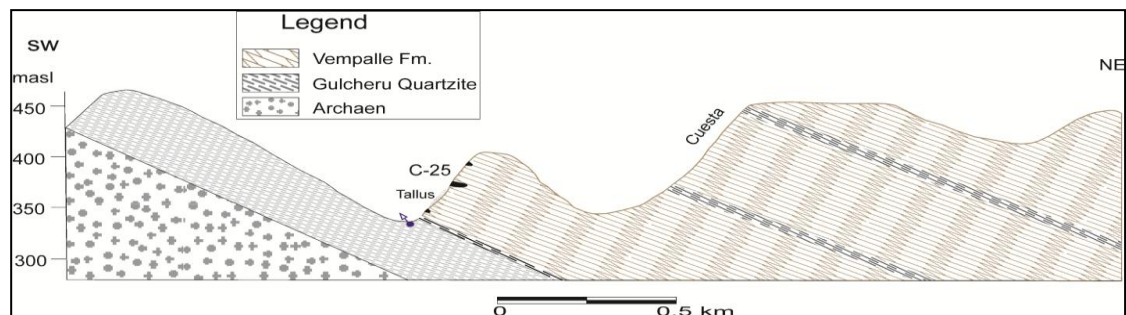


Fig. 4.3: Geological cross-section across Vempalle dolomite along Chillavaripalle Cave (C25) area (refer to Fig. 2.1) showing typical geomorphological features.

Chillavaripalle cave (C25) is located on a ~ 40 m high dolomite cliff at an elevation of 375 masl that is accessible by climbing stairs. This fossil cave formed in a phreatic

conduit (Shibasaki et. al., 1985) is 86m in length. Other conduits at the same or different elevations from the current base level seem either to narrow or filled near their entrances. One entrance may lead to a longer cave but needs proper equipments to access from top of the cliff. A seasonal spring (S9, Appendix 6) issuing from quartzite is a habitat for lot of monkeys. There is no visible flow which is limited by pumping.

Fractures vary in orientation from NE-SW to NW-SE (Fig. 4.4). Some faults in the area are dipping with NW side shifted down with a vertical displacement of up to 50m. One major fracture seems connected to other side of valley along the cave entrance in N80E direction. Karstification in the dolomite seems to be initiated along fractures and three sets of joints are observed at some levels at Chillavaripalle site. This is also supported by the fact that caves cut the bedding planes obliquely (Shibasaki et. al., 1985).

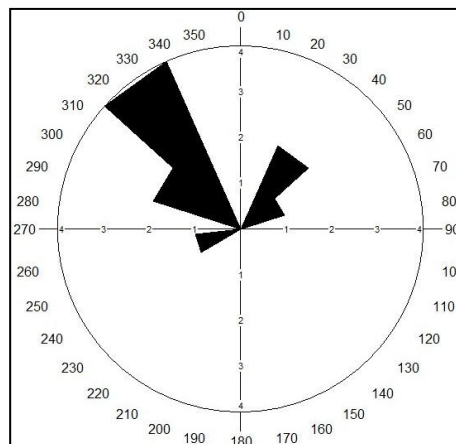


Fig. 4.4. Fracture orientation around Chillavaripalle Cave plotted as frequency in Rose Diagram.

4.2.2. Karstification in the Narji Limestone

The Narji limestone occupies a vast planar region (Fig. 4.5) surrounded by smooth topped hills of Gandikota quartzite (mostly in the Western part) and from place to place, by mesas

and butte of Owk shale and Paniam quartzite (Fig. 4.6). The massive limestone is well karstified and contains the major springs and caves of southern India (Appendix 5 and 6). This mostly bare semi-arid karst is dissected into blocks by fissures. Karst geomorphology has been studied in different sectors (Kolimigundla, Banderlapalle, Yadiki, Betamcherla and Yaganti, Fig. 2.1) and is discussed below.

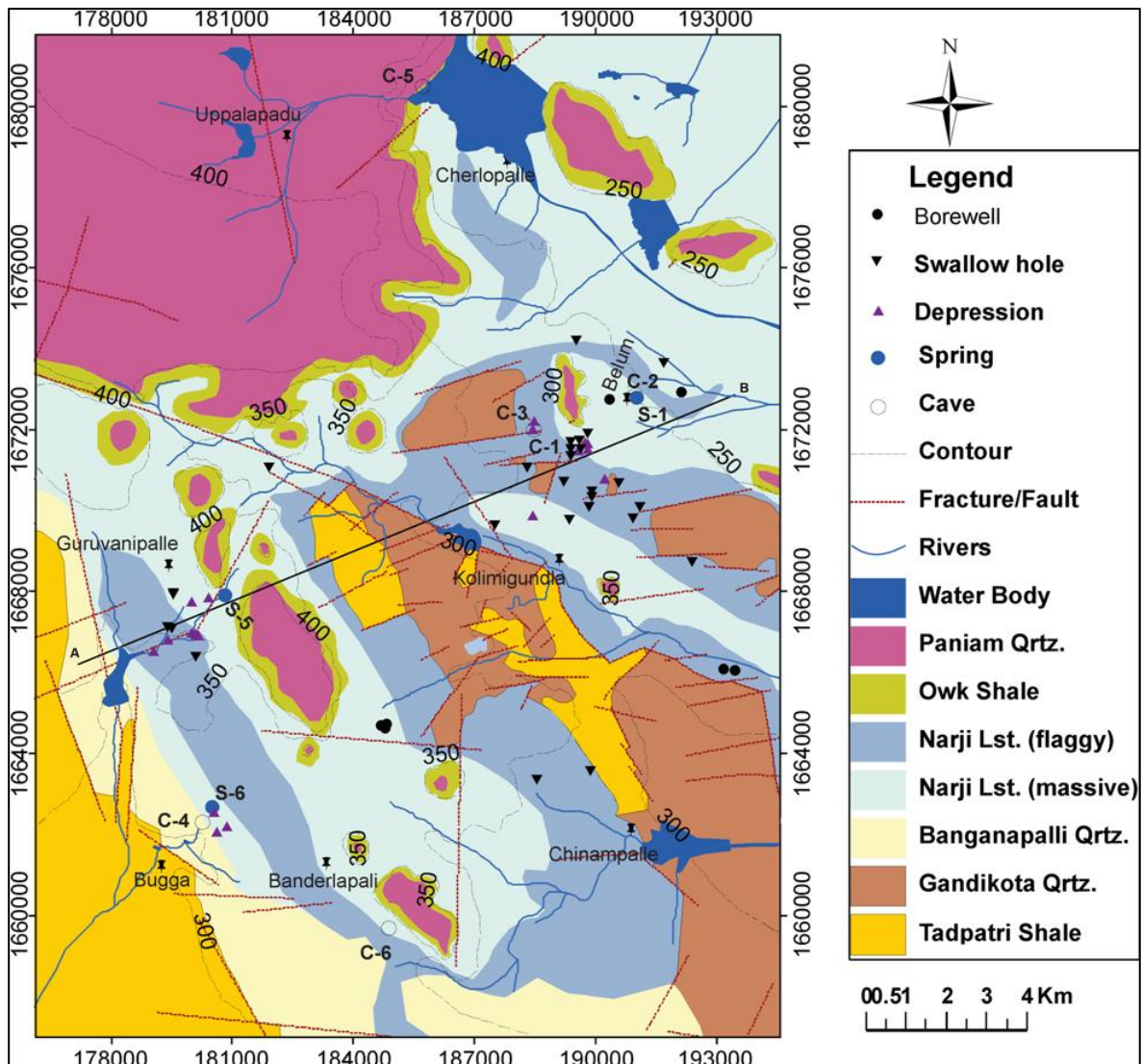


Fig. 4.5. Geological and geomorphological map of the Narji limestone terrain in Kolimigundla sector (refer to Fig. 2.1) showing observed karst features.

The most extensively surveyed area in the Narji limestone is the Kolimigundla sector (Fig. 4.5) which is a repository of different karst features. A number of karst features were observed including caves, springs, sinking streams, sinkholes, etc.



Fig. 4.6. Picture showing typical mesa and butte geomorphic features overlying the Narji limestone in Kolimigundla area.

The geology of the area is more complex than already mapped. The contact between limestone and Gandikota quartzite (Cuddapah supergroup) is apparently caused by faults (Fig. 4.5 and 4.7). Younger Paniam quartzites are separated from the Narji Limestone by Owk shale. Some evidence of palaeokarst in the Narji limestone have been observed in the form of pisolithic infills.

Bilam or Belum Cave (C1, Fig. 4.5 and 4.7) is the famous cave in Belum village of Kolimigundla Mandal of the Kurnool District. It is one of the longest caves of India with a linear development of 3.2km and a depth of 29m (Gebauer, 1985). It extends over a large

area and is developed in the form of many conduits and chambers which have been given different local names. The most promising gallery is locally called as Parvatamma Guha. The deepest point of the cave is called as Patalaganga.

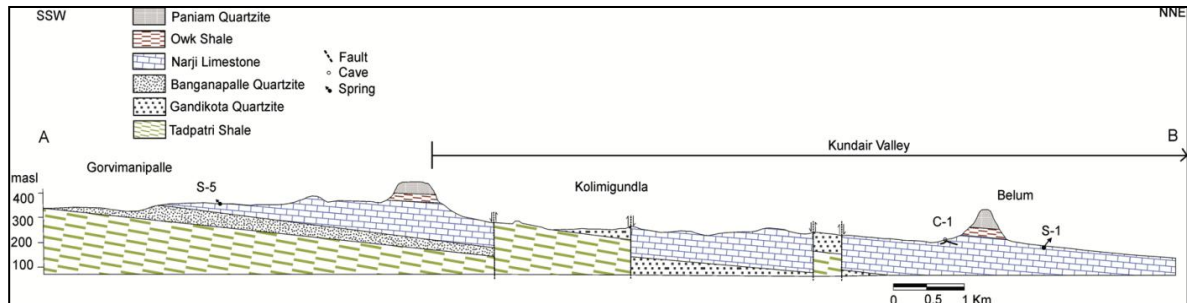


Fig. 4.7. Geological cross-section across the Narji limestone terrain of Belum area. The trace of the cross-section is indicated in Fig. 4.6.

In the upstream part of deepest point in the Belum cave (not accessible to public) a phreatic conduits is followed over several hundred meters filled with fine sediments. It is the origin of a small temporary streamlet (discharge ~10 l/min, EC: 824 uS/cm, Jan 2010). It flows after each recharge event (several l/s) but dries up quite rapidly after rain events. Sediment and millimeter to centimeter sized limestone fragments, a few centimeter sized reddish brown poorly rounded quartzite fragments are found in these conduits. The cave is famous from tourism point of view and is a good source of income (about 0.2 million people visit the caves annually). It is maintained by APTDC since its discovery and development.

Chirutipuli Guha, a small cave (C3, Fig. 4.5) located nearly 1 km southwest from the Belum cave is almost blocked/inaccessible and seems to be connected to it. Nela Bilam cave (C5, Fig. 4.5) is located in the slopes of the Uppalapadu plateau along the side of the Owk

reservoir. It is a water filled cave and the depth to water table is around 6 m which matches the reservoir water level.

A number of shallow depressions (sinkholes) are widespread on massive limestone in the area (Fig. 4.5 and 4.8a). They are filled with soil or rock fragments naturally or artificially. These natural depressions/sinkholes are very small in extent and very shallow. Five natural depressions/sinkholes (between 20-50 m diameter and 1-3 m depth) have been verified in the field (Fig. 4.8a) around Belum cave. Most of them are located at the contacts between quartzite and limestone and some located in the massive limestone (Fig. 4.5).



Fig. 4.8. Sinkhole in the Narji limestone; (a) developed near Belum cave and (b) that has opened in 2003 probably as a consequence of increased aquifer pumping in Nossam area.

Another important karst feature is the sinking streams that carry surface runoff and lot of soil with them to underground during heavy rains. According to farmers the soil remains water logged only for 2-3 hours during the rainfall. Part of the soil eroded by stream water is recollected in the conduits of the Belum cave. In Nossam area, a few sinkholes have developed since 2003-2004 with diameter between 2-5 m and depth 2-3 m, partly filled with water after monsoon (Fig. 4.8b). The process of subsidence started 5-6 years ago and seems

to increase with time (more sinkholes every year). Some show an increase in diameter and depth with time. Subsidence occurs during monsoon; up to 2 m diameter sinkhole subsides every year. The development of such landforms is likely related to human activities, like pumping, mining and changes in the subsurface drainage (e.g., Newton, 1987) which has developed over the past 15 years in the area. Most of these depressions guide the surface (recharging) waters to underground and are called input forms (Gunn, 1983; Ford and Williams, 2007). This indicates that the limestone aquifer is mostly recharged by the fast or concentrated flow with less or absence of the diffuse flow through the epikarst (as discussed in chapter 5). The presence of dripping water at very few places inside the cave also indicates the absence of well developed epikarst zone of the aquifer, an important part of the aquifer. However, there a number of places that shows epikarst development (Fig. 4.9a). Some evidences for palaeokarst in the Narji limestone have been observed in the form of quartzite and secondary calcite filled depressions in the limestone (Fig. 4.9b).



Fig. 4.9. Field photograph showing (a) epikarst development in the Narji limestone near Belum and (b) spongy secondary calcite deposition in the area.

Frequency of fractures mapped in the limestone along quarries and outcrops are plotted on rose diagrams (Fig. 4.10a). The fracture pattern seems to corroborate with the

fracture orientation mapped from satellite images. A number of small faults (100-150 m long) have NE-SW and NW-SE direction. The fault surfaces are filled with secondary calcitic material.

Another cave (Banderlapalle cave C6, Fig. 4.5) was explored during the field survey in the Banderlapalle sector. The cave lies in the highly quarried area and starts with a 17 m vertical shaft (rope and vertical equipment needed). The conduit leads to a permanent lake fed by a small stream arriving from another, surely water-flooded gallery on the opposite side. Total length of the cave is 117 m. The underground drainage followed in a phreatic conduit over 100 m between two sumps is in the form of a stream with a discharge of 1-2 l/s (Jan 2010) which may increase during the monsoon season. This seasonal stream (sound heard at surface) was not known to the local people two years back, which indicate that the underground drainage has been modified. A borehole has been drilled at the entrance shaft to pump water from the lake two years before. It is obvious that the lake level may increase by 3-4m above the observed conditions indicated by mud deposits on the cave wall.

Technical crossing of the lake (to remain dry and safe) leads to the gallery decorated by flowstones deposited by the stream. After climbing, reaches a more flat part of the cave with lot of mud and silt deposited on the ground and walls at places. The cave stream exits across these muddy deposits. A small meander-shaped conduit connects to the main gallery on the left side with a seasonal streamlet (dry in Jan 2010) that brings rock-dust issued from the quarries at the surface. This meander must have connection to the surface as air flow and nesting of bats is observed. About 2 m above the stream level, two opposite conduits are

seen which are difficult to reach without specific equipment. The fracture orientation (Fig. 4.10b) is in same direction (NE-SW to NW-SE) as observed in the Belum area.

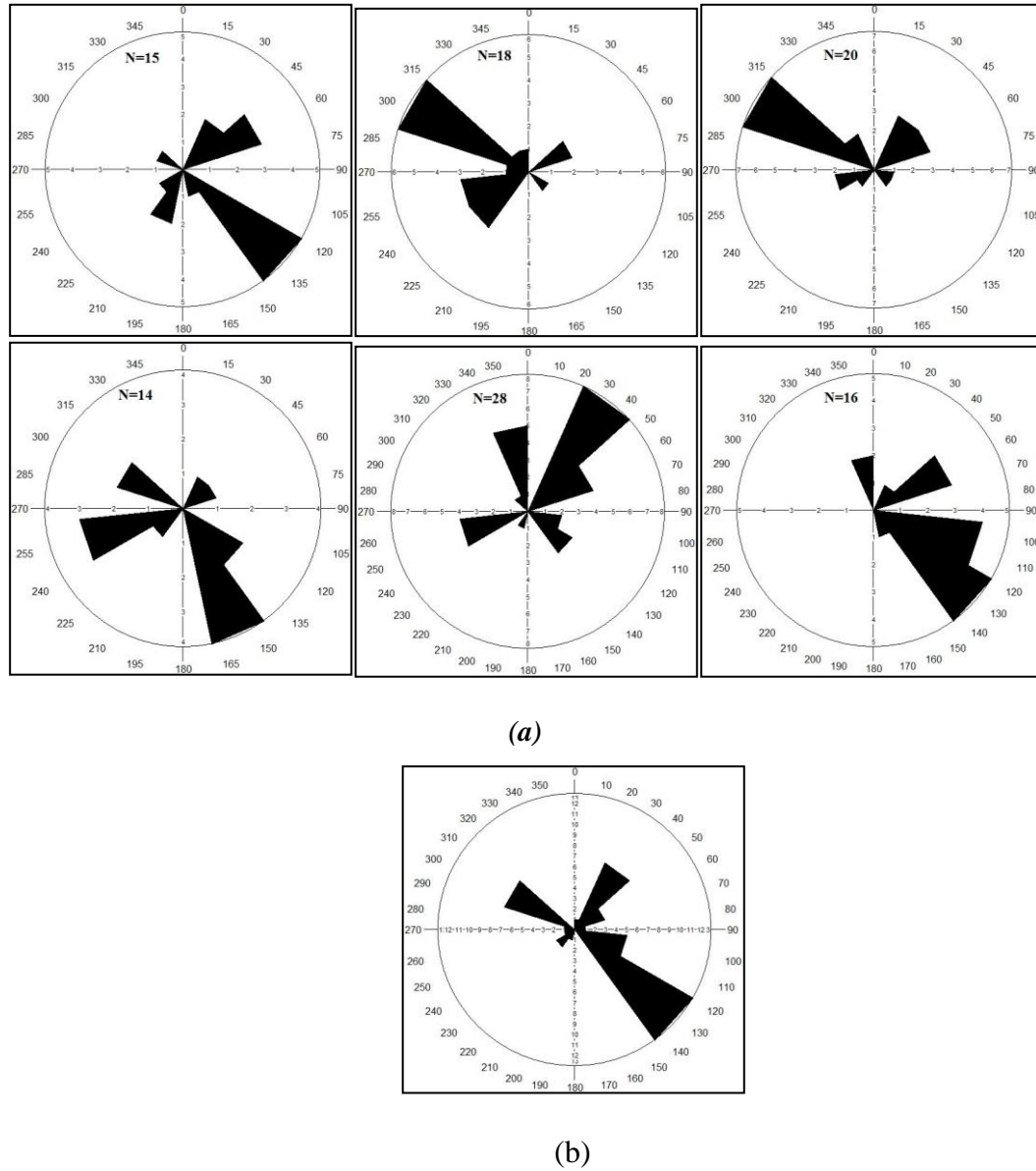


Fig. 4.10. Fracture orientation plotted as frequency in Rose Diagram around Belum Cave (a) and around Banderlapalle Cave (b) Banderlapalle. N is the number of sample points.

Many karst features, like sinkholes, depressions filled with palaeokarst/secondary calcitic material or rock fragments (conglomerates of limestones/quartzite in cement matrix) and temporary springs are observed in Guruvanipalle area (Fig. 4.5). During rainy season the sinkholes are the points of soil loss from the agriculture fields that gets collected underground. Rati Spring (S6, Fig. 4.5) issuing through the bedding planes of the massive limestone is an overflow spring. During high water levels two or more springs join the main spring and flow downstream with a varying discharge. Another small temporary spring (Bugga spring S7, Fig. 4.5) is located at the bottom of a valley 2m below the cave entrance. Bugga Cave (C4) is a small cave located at the base of Narji limestone having 10° dip towards SE.

In Yadiki sector, the horizontal Kurnool rocks unconformably overlie the tilted brown Tadpatri shale and forms flat topped plateaus and hills. The Narji limestone consists of reddish brown shale and an alternation of shale, sandstone and carbonate rock at the base, with a major massive and flaggy limestone. The Owk shale exposes along the scarps of the hills and is capped by Paniam quartzite (Fig. 4.11). Thin Banganapalle, white quartzitic sandstone forms an unconformity layer between Tadpatri shale and Narji limestone and shows thin basal conglomerate. The area is also influenced by tectonic activity. A major fault of N60W direction coincides with river course as observed from the displacement of rocks. The northern side of the fault has moved vertically down by 60m (Fig. 4.12). The valley has steep slopes at height of 90 to 100m above the river level and extends from northwest to southeast.

Munagamanu cave (C8, Fig. 4.12) is located in the Uppalapadu Plateau at an elevation of 475 masl. The cave exposes as a pitch-like entrance which is 5-10m in diameter. The linear development of the cave is 444.5m (still going) with a depth of 16.4 m. Seasonal streamlet has been observed in the middle of the cave that can be followed over several hundreds of meters in a canyon-type vadose gallery. The peak discharge should be several l/s and flow is maintained by more than 0.1 l/s after the end of the monsoon (6-10 l/min; EC 442 μ S/cm, Jan 2010). The interior of the cave distinctly exhibits a variety of impressive speleothems of various sizes and architecture in the form of stalactites and stalagmites (Fig. 4.13). The drip points from ceiling indicate a source of diffuse recharge.

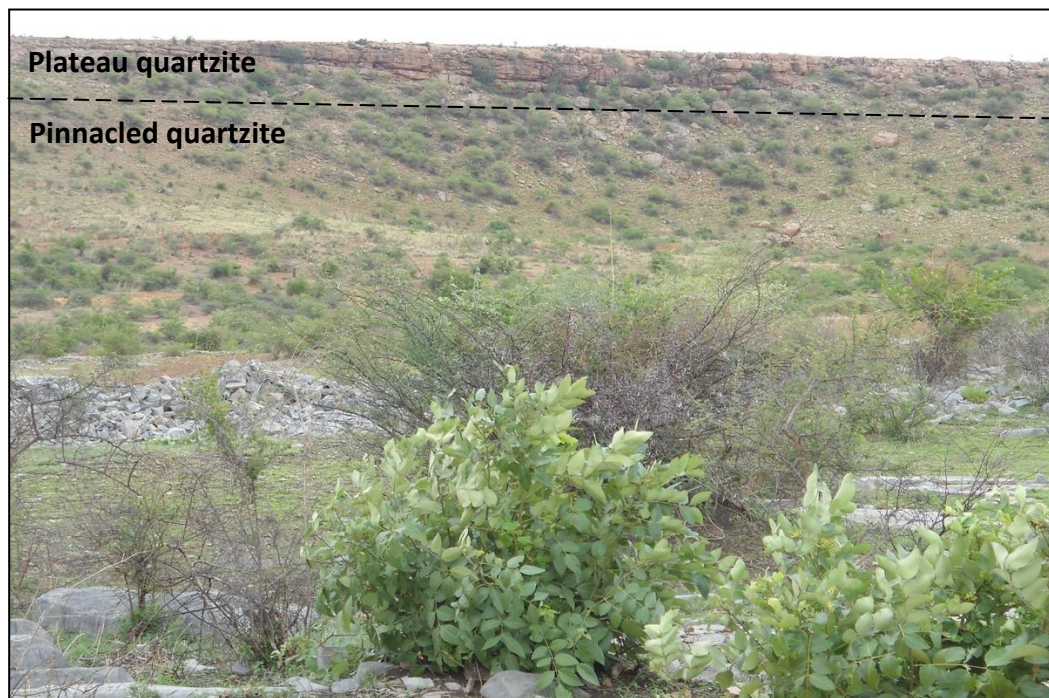


Fig. 4.11. Field photograph showing the top of the Uppalapadu Plateau along Yadiki area. Paniam quartzite (pinnacled and plateau) is shown overlying the Narji limestone.

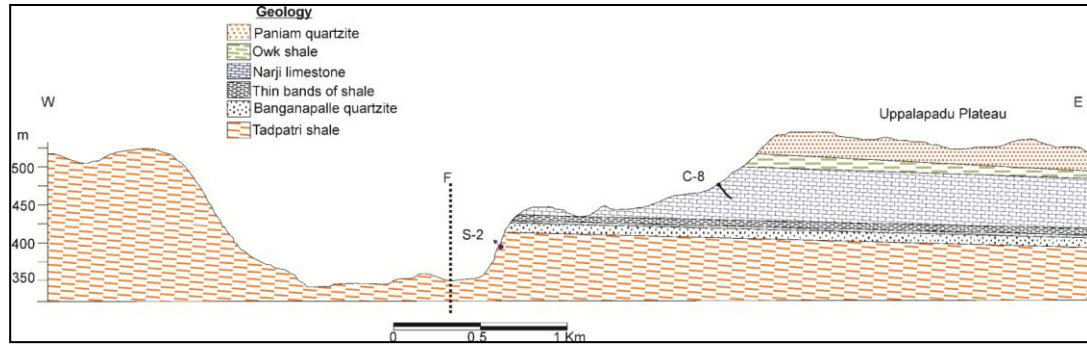


Fig. 4.12. Geological cross-section through Yadiki karstified area showing cave and spring locations and tectonic features.

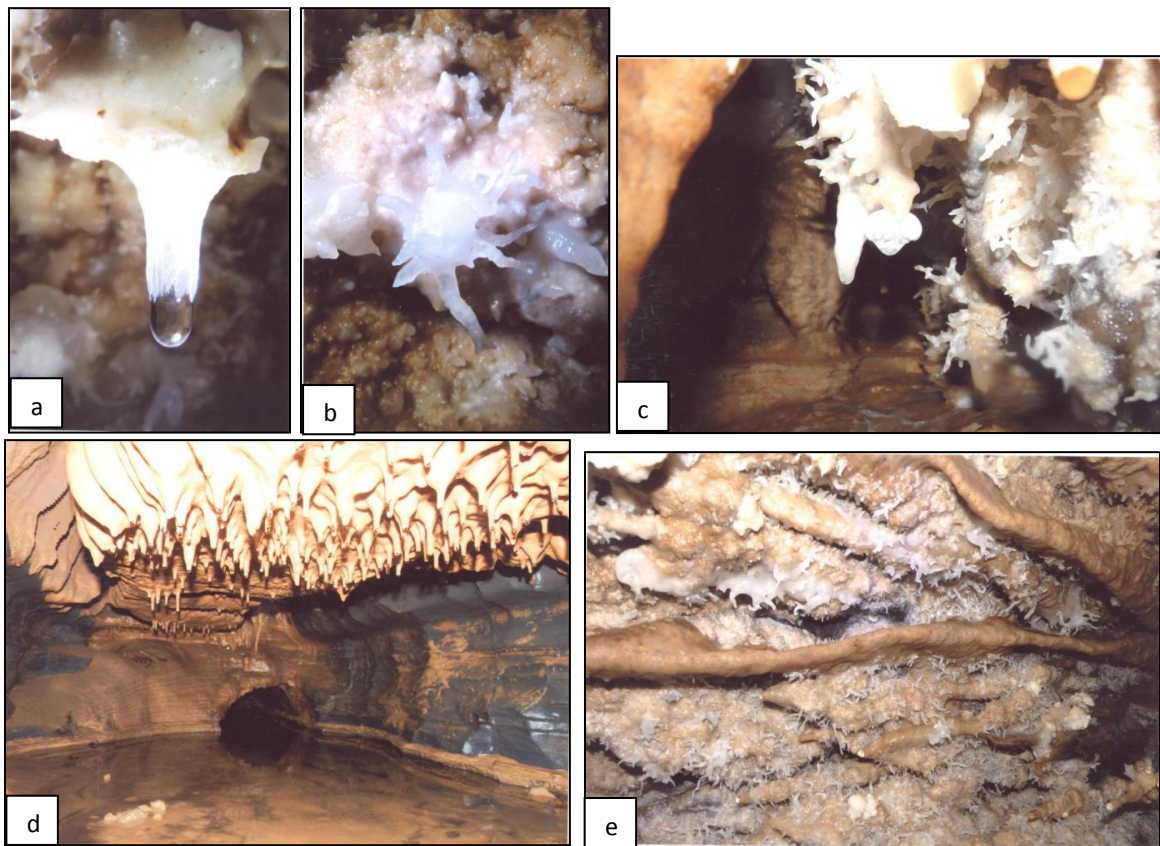


Fig. 4.13. Photographs showing currently developing speleothems inside carbonate caves of the study area. a) drip stone -the most common way of stalactite formation; b and c) deposition of calcium in flower shaper pattern; d) dripping from ceiling at multiple points at a time; e) Frost-like deposition- dripping through small multiple cracks causes calcite to get precipitated easily as frost.

The aquifer here discharges from a 20 cm diameter permanent phreatic conduit (Kona spring S2, Appendix 6) 4 m high in the limestone cliff in addition to the limited water issued from 2-3 other small conduits at lower levels. The spring location shows many travertine (secondary calcite) depositions. Another small diffuse permanent karst spring flows along the road side (Kona spring S3).

In the Betamcherla area, Narji limestone has few caves. Nemmalasilla Gavi (C17) is a small cave (Gebauer, 1997) located at the bottom of ~30 m massive limestone cliff with 8 m length and 50 m on side. Thin-bedded limestone and Paniam quartzite lie on the top. The area is faulted with one >100 m vertical fault in the N140 direction. Faulting has influenced the bedding dip.

Another cave (L~ 20 m) is located a few meters above the main Betamcherla–Banganapalle road on the left side of a small canyon. The fossil cave shows meander-shaped gallery (mean dimension w: 0.5m, h: 1.7m) and is the habitation of bats. The cave has been formed mainly under vadose conditions in the massive limestone with sub-horizontal bedding. At the entrance of the cave massive fossil speleothems are present. This setting gives an idea that the present open canyon was a main underground drainage and the visited caves are the remnant tributaries of now collapse cave system (small tributary on the left side of the main drainage gallery). Other cave entrances and fossil speleothems are visible elsewhere in the vicinity. The caves are disconnected from present drainage system that flows at the bottom of thalwegs following major fracture directions. The present base level is in shale below limestone. The caves have formed during phreatic conditions. In Yaganti

area a spring (S8, Fig. 4.14) and few caves (C12 to C16) are found in the limestone cliffs. Most caves have a religious purpose.



Fig. 4.14. Karst spring discharge of the Narji Limestone at Yaganti spring (S8) through two major conduits.

4.2.3. Karstification in the Koilkuntla Limestone

The Koilkuntla limestone has an average thickness of 90 m and bedding is nearly horizontal (Fig. 4.15); it is underlain by Paniam quartzite and overlain by Nandyal shale (as described in chapter 2).

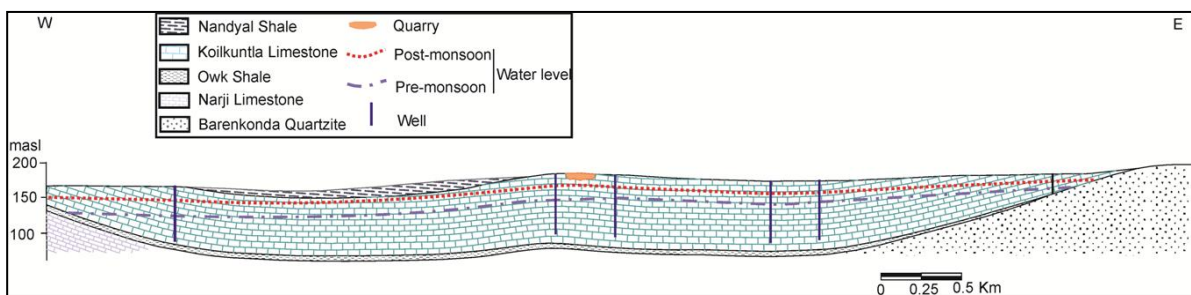


Fig. 4.15. Geological cross-section of the Koilkuntla limestone formation. The indicated quarry is also the location of Fig. 4.16.

The limestone contains numerous interconnected fractures and crevices. Karst features in the form of karrenfield and epikarst has developed in the formation (Fig. 4.16). The unit is well karstified covered by soils of 0.5 to >2m thickness (sub-soil karst of White, 1998) and contains abundant pisoliths. However, no caves and springs are known possibly because of the absence of hilly terrains and the location of the water table close to the surface.



Fig. 4.16. Karrenfield underlying the soil cover in the Koilkuntla limestone as an indicator of epikarst development.

The Koilkuntla aquifer is intensively exploited for irrigation as well as domestic use. The piezometric data displays a general SW flow in the Koilkuntla area. The area is depressed as a result of continuous pumping for agricultural activities. A periodic pumping database of 84 irrigation wells located in the limestone show high average discharge of ~9 l/s (Tab. 4.1) and a very significant water table fluctuation between post-monsoon (average water table 12.8 mbgs) and pre-monsoon (average water table 26.5 mbgs).

		<i>Average</i>	<i>Stand. Deviation</i>	<i>Coeff. Of Variation</i>	<i>N</i>
	Q_{mean} [l/s]	9.4	2.6	0.27	84
	Q_{min} [l/s]	7.8	2.1	0.27	84
	Q_{max} [l/s]	11.7	3.9	0.33	84
Post- monsoon 2005	SWL [mbgl]	12.8	8.0	0.63	79
	Drawdown [m]	7.7	5.6	0.72	79
	Sp. Capacity [l/s/m]	2.8	3.2	1.15	79
Pre- monsoon 2006	SWL [mbgl]	26.5	11.7	0.44	79
	Drawdown [m]	8.4	6.1	0.73	79
	Sp. Capacity [l/s/m]	1.7	1.6	0.98	79

Tab. 4.1. Statistics of 1-year bimonthly data (static water levels (SWL), pumped water levels, abstraction rates (Q)) from 84 irrigation wells in the Koilkuntla limestone

The specific capacity data (i.e. the discharge divided by the drawdown) shows a wide scatter which indicates aquifer heterogeneity due to enhanced permeability (e.g., McCoy and Kozar, 2008). The wells can be segregated into two groups; specific capacity in wells with shallow water table (< 25 mbgs) and specific capacity in wells with deeper water table (> 25 mbgs) (Fig. 4.17).

In addition to the drop in water table, the average specific capacity of the wells decreases significantly from post- to pre-monsoon (Fig. 4.18). This decrease may be partly due to larger head differentials which reduces pump discharge and also partly due to the desaturation of the upper part of the limestone aquifer. For instance, out of all dataset 14 wells have a specific capacity higher than 5 l/s/m. For 13 of these wells, the static water level (SWL) is <20 mbgs, for 8 of them the SWL is <11 m. These data suggest a quite high permeability in the top 10 m of the limestone, possibly corresponding to the epikarst layer. The importance of this data in limestone is that pumping tests may describe the hydraulic

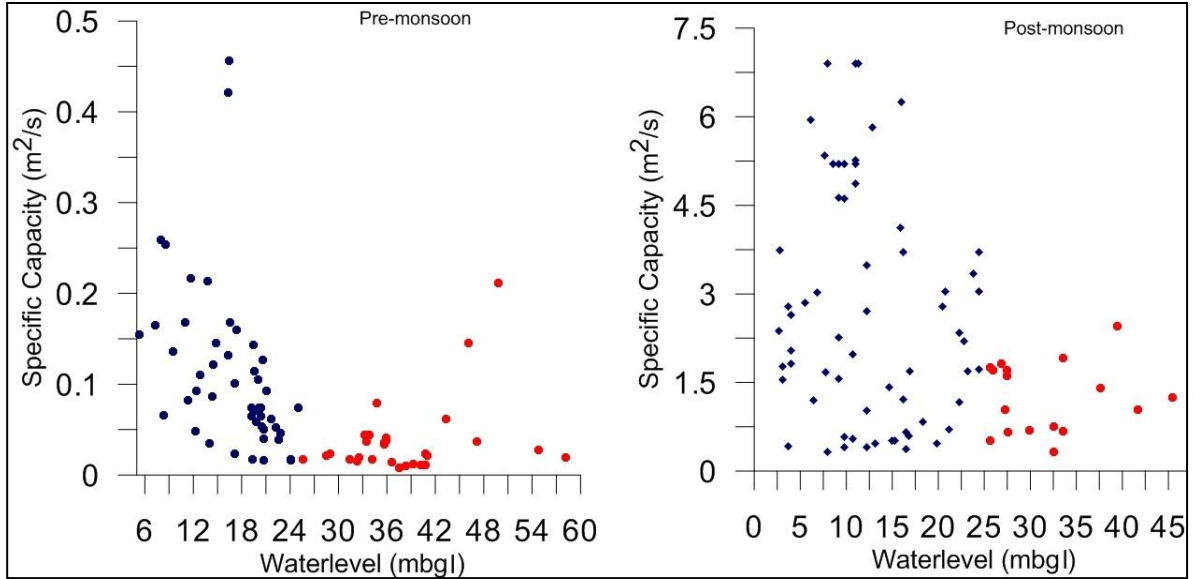


Fig. 4.17. Plot between specific capacity and static water level in Koilkuntla limestone in pre- and post-monsoon. (Red dots indicate deeper water table and blue dots for shallower water table).

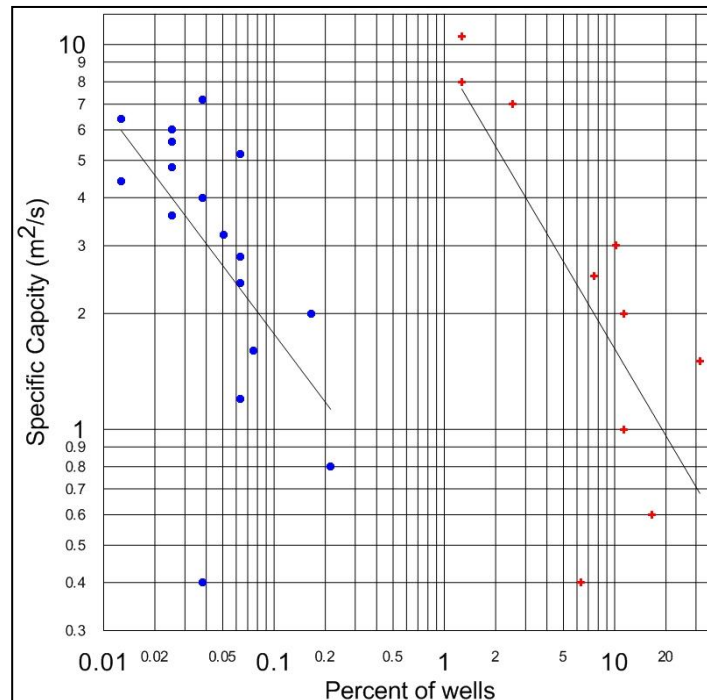


Fig. 4.18. Plot between specific capacity and percentage of wells in Koilkuntla limestone. (Red dots are for pre-monsoon data and blue dots for post-monsoon data).

properties of carbonate aquifers areally, but does not accurately describe the drawdown in the immediate vicinity of a well (Sandor, 1967).

The coefficient of transmissibility can be estimated from specific capacity (measure of pumping rate per unit drawdown) data easily than pumping data (e.g, Ahmed et. al., 1987; McCoy and Kozar, 2008). More or less marked draw down during high rate of pumping may indicate the well connection of the groundwater reservoirs. Transmissivity of confined and unconfined karst aquifers, like other aquifers can also be estimated from specific capacity data when aquifer test data is not enough (Sandor, 1967; Eagon and Johe, 1972b; Huntley et. al., 1992; El-Naqa, 1994; Mace, 1997; McCoy and Kozar, 2008; Rotzoll and El-Kadi, 2008; Verbovsek, 2008) by using an equation;

$$T = A \times Sc^D$$

where A and D are the regression coefficients. In a similar way, the hydraulic conductivity K can be estimated from specific capacity index $Si = Sc / \text{saturated thickness of aquifer}$ (Verbovsek, 2008). Based on the experimental studies from the karst aquifers of the world, an average value of A and D were defined as 1.67 and 1.02 respectively for T Vs Sc and 0.83 and 0.95 for K Vs Si calculations. From these estimates the coefficient of transmissibility, T varies from 27 to 2211 m²/day in the Koilkuntla limestone.

It seems clear that the fracture system provide significant permeability. The role of conduit flow is unclear but probably contributes to the larger yields observed on some wells. Data show that a significant part of well discharge is provided by the upper part of the limestone aquifer, which is indicative of a higher permeability. This may be partly attributed to the existence of a well-developed epikarst layer as suggested by Fig. 4.16.

4.3. Proposed Model of Karstification

Field observations of caves, karst springs, swallow-holes and karrenfield clearly indicate that the three carbonate formations of the Cuddapah sedimentary basin are karstified. A specific question to be answered in semi-arid environments is to know whether observed karst has developed under present conditions or is inherited from past humid periods. Dissolution and release of calcium from minerals occurs massively during humid conditions while its accumulation and precipitation occurs relatively during dry periods. Semi-arid climates with seasonal alternations of wet and dry conditions represent such conditions. The whole process may involve the recycling and redistribution of weathering products within different cycles.

The observed cave systems, being mostly inactive or only seasonally active, have developed during the Quaternary and possibly even earlier. According to Durand et. al., (2007) more humid conditions have prevailed in southern India during part of the marine oxygen isotope stage 7 (MOIS7) which corresponds to an age of ≥ 200 ka in the Quaternary. The major phase of carbonate dissolution (calcium release) and its subsequent precipitation occurred that have probably enhanced karstification processes. Precipitation of calcium in the form of secondary calcrete in non-carbonate rocks and the soils in the study area can be linked with such weathering cycles (Durand et. al., 2006). Thus, the interglacial epoch i.e. MIS 7 or Middle Illinoian (Middle Wolstonian or Saale) in southern India may have been relatively wetter with greater moisture availability than current prevailing semi-arid conditions for the deposition of calcrete nodules and other secondary calcium deposits (Durand et. al., 2007; Pillans et. al., 1988; Shackleton, 1987; Spotl, 2002). The change of climate to the warm and humid conditions after the MIS 6 is indicated by the presence of

humid taxa in the eastern Arabian Sea (Prabhua et. al., 2004). The present moisture conditions are not sufficient for higher dissolution of bedrock (Gunnell and Bourgeon, 1997). However, it can mobilize and redistribute Ca within soil and rocks for a short-range in shallow depths. This is indicated by the presence of many secondary deposits (calcrete) in valleys, cave openings and depressions. The calcrete in the study area is mostly in the form of hardpan (hard structure of numerous calcitic nodules) or coatings on rock fragments. These secondary calcite deposits are also located in rocks other than limestones. The regional-scale increase in rainfall increased the weathering intensity but could not washout Ca to a far place rather preserved and deposited it. Other moist periods in southern India in later geological time may have also modified and evolved the karst system in the area.

However, present hydrological observations in the Narji limestone indicate active flow in conduits feeding permanent and seasonal springs. This strongly suggests ongoing karst development and dissolution processes. It is not possible to be as assertive for the two other carbonate units because of lack of field evidence, however it is likely that dissolution processes are equally active since these carbonate aquifers are located in very similar contexts than the Narji limestone aquifer.

4.3.1. Karst Evolution

Combining geological, geomorphological and cave pattern information (Fig. 4.19) it is possible to propose a tentative genetic history of karstification for the Narji limestone which is the unit having the largest accessible cave system (Fig. 4.20). It will give a global view of karst development in CB of Southern Andhra Pradesh. The carbonate rocks were deposited during Middle to Upper Proterozoic under marine conditions. The deposition was not

continuous of the same lithology, but the sequence was hindered by the change in the depositional environment. The study of cave geometry through speleology provides essential information about the type of recharge and the type of pre-solution porosity (Palmer, 1991; Palmer and Audra, 2004). The cave morphologies formed due to a combination of different processes depends essentially upon the density, penetrability and linkage of fractures/bedding planes and the hydraulic gradients involved (Ford and Ewers, 1978). Several typologies of caves could be identified in this formation:

Network Maze Caves in the upper part of the limestone near the contact with Owk shale (Nila Bilam, Yerra Zari Gabi caves),

Dendritic/Anastomotic Caves of phreatic origin (Belum cave),

Meander Caves mostly formed under vadose flow regime (Munagamanu cave).

Based on these studies, the three events of karst evolution in the area are discussed;

Stage 1: In the initial stage, it is inferred that network maze caves have developed in a confined limestone aquifer setting (e.g., Klimchouk, 2003) where diffuse infiltration takes place across quartzite and shale layers which is similar to the conceptual model suggested by Palmer (1991, 2000). Though, karstification may have started earlier, this event is believed to be Pre-Pliocene during more humid conditions prior to the onset of monsoonal conditions and Western Ghats uplifting at ~8 Ma. During this period, the sea level was more than ~100 m higher than the present level (Haq et. al., 1987).

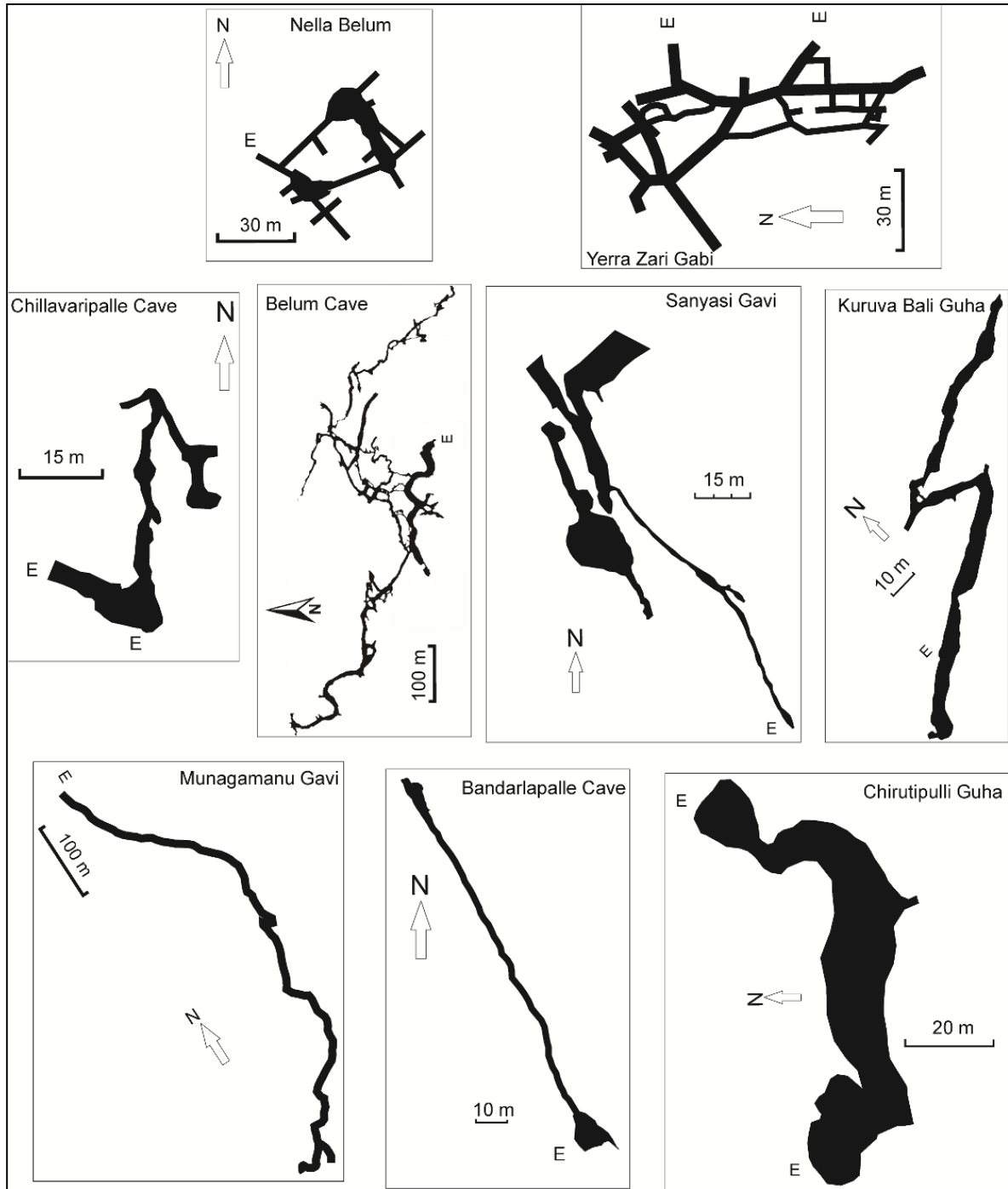


Fig. 4.19. Planimetric view of different cave patterns identified in the area (maze, dendritic and meander), which had developed in three karstified formations.

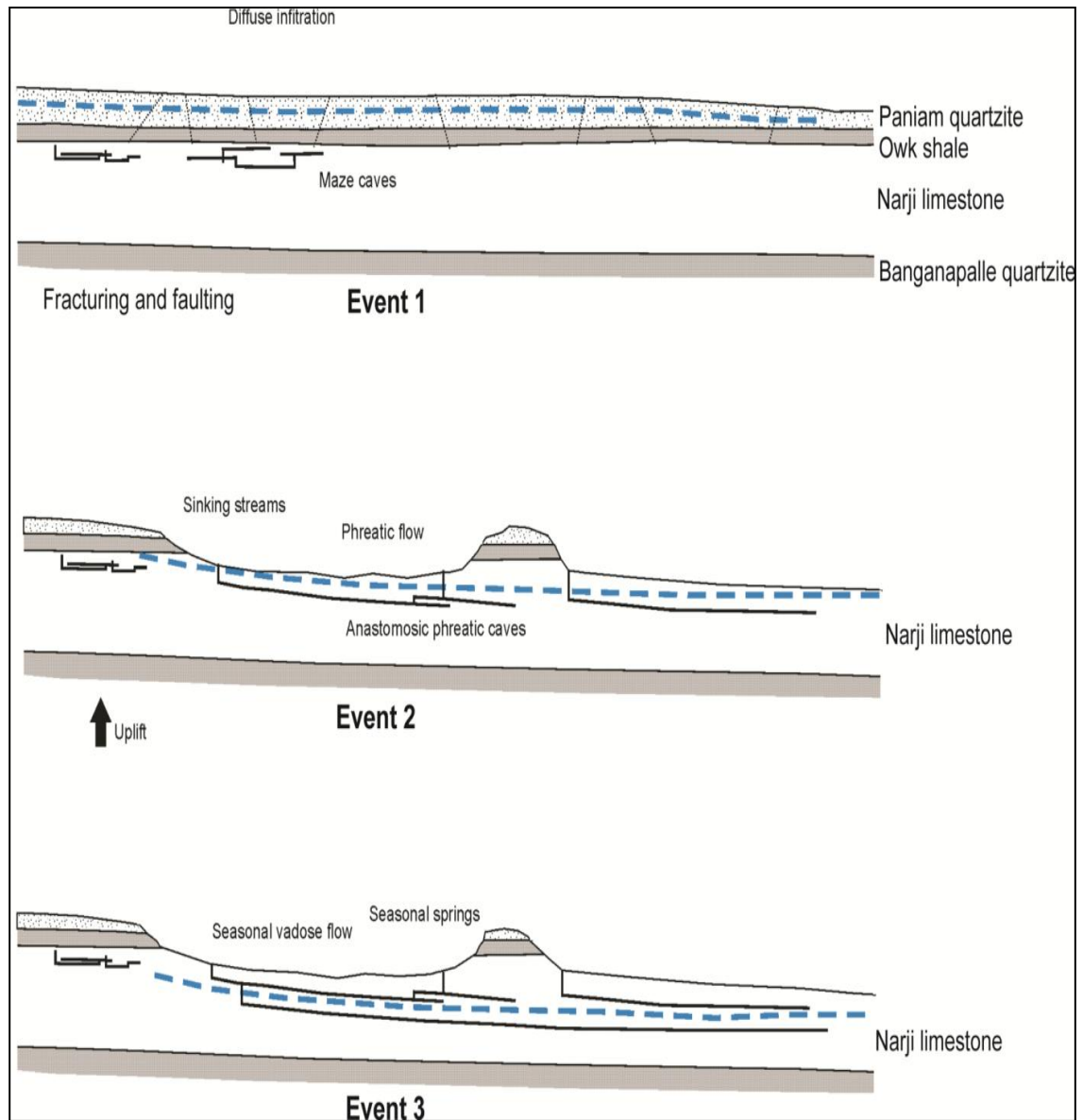


Fig. 4.20. A karstification conceptual model of the Narji limestone; 1) initial phase with development of maze cave system in a confined setting; 2) following tectonic uplift, the limestone is progressively exposed to the surface and anastomosing phreatic cave systems develop; 3) the water table gets progressively lower inducing a lower level of karstification (present state).

The fact that these relict maze caves (Nila Bilam, Yerra Zari Gabi, Fig. 4.19) are located near the top of the limestone series seems to corroborate this type of development. This model requires a significant permeability of the quartzite and shale, possibly initiated

by the pre-uplifting compressional forces, so as diffuse infiltration can take place. This long-term stability of pedo-climate coincides with the Western Ghats uplift that later acted as a barrier to the southwest monsoon.

Stage 2: After Early-Pliocene, an eustatic fall in sea-level along with the Western Ghats denudational rebound, uplift and tilting of relief to the east (Radhakrishna, 1952; Vaidyanadhan, 1964) occurred. This event is believed to cause structural compartmentalization and fragmentation that enhanced denudation rates along the Eastern Ghats margin controlled by the structural pattern of the resistant rock outcrops viz, Charnokites, Cuddapah sandstones and quartzites (Gunnell, 1998a). The entire instability event caused a ~300m surface uplift in the Western Ghats (Gunnell and Fleitout, 1998), with the harder rocks being comparatively more uplifted (Gunnell and Louchet, 1998) than their softer counterparts. Fracturing and/or block faulting and uplifting generally have contributed to the outcropping of rocks and change in the base level through geologic time. These fractures are believed to have acted as inception horizons (e.g., Rauch and White, 1970; Lowe and Gunn, 1997) for enhanced karstification. The aperture size of fractures got widened due to a change in flow kinetics from normal to turbulent plus the effects of hydraulic gradient, etc.

Karst systems develop towards water-table caves, where several cave levels develop in an uplifting landscape (e.g. Ford and Ewers, 1978; Gabrovšek and Dreybrodt, 2001; Kaufmann and Romanov, 2008). The earliest phase of cave development has an influence on the final cave morphology. The theoretical basis of this karstification indicate that significant karst systems can develop from initially fractured rock with small fracture size

within several thousand years (Dreybrodt, 1988). Given the right conditions for karstification, a mature karst system could develop within very short periods (10,000 years, White, 1988).

Stage 3: Following tectonic uplifting, a positive relief favored surface runoff and progressive erosion of the quartzite and shale which resulted in the exposure of Narji limestone at the earth surface. The uplifting of Western Ghats and the onset of monsoon (~8 Ma), caused more humidity on the west coast of India, while the entire southern India was subjected to a long lasting aridification and developed characteristics of semi-arid landscapes (Gunnell, 1998b). Due to this, the piezometric surfaces readjusted to lower base levels, maze cave systems became inactive (relict caves) and the limestone aquifer became unconfined. The bedding planes become the preferential flow paths and susceptible to dissolution. This setting supported the development of phreatic conduits (e.g. Belum cave) fed by sinking streams issued from quartzite hills and diffuse infiltration through the limestone plateau. This concept is validated by the fact that more than 70% of the analyzed phreatic conduits of the world were located along inception horizons susceptible to dissolution (Filipponi et. al., 2009). The phreatic caves in the area vary from angular and rectilinear to curved and sinuous. In Vempalle dolomite, the surveyed caves have long straight stretches with sharp angular inflections. But in most of the caves in Narji limestone curved sinuous pattern predominates (Fig. 4.19). These conduit shapes can be directly related to the influence of the dip of the rock beds; the steeper the dip, the straighter and more angular the original cave conduit pattern (Karmann and Ferrari, 2000).

However, the aridification was itself responsible for the initiation of seasonal contrasts and more intense precipitation regimes (Gunnell, 1998a). During rapid and frequent sea level fluctuating Quaternary, more humid conditions (e.g. Durand et. al., 2007) may have promoted the incision of deeper cave systems and the development of the existing ones. Further erosion of the land surface resulted in additional lowering of piezometric surfaces and the readjustment of the conduit systems (vadose conditions in the upper part of the limestone with associated development of canyon type conduits, progressive dissolution of a deeper level of phreatic conduits). This stage is still ongoing nowadays with an active inaccessible conduit network at greater depth and a seasonally active vadose flow in the explored caves. The underlying quartzites act as a regional aquitard and provide a lower limit to karst aquifer development. The deposition of sediments (lost soil from fields) on the cave floor may further prevent bottom dissolution; instead directs it to the sides and up, creating typical morphologies. This process (paragenesis, Renault, 1967) has been reported from many phreatic caves of limestone (Ford and Ewers, 1978) and other caves.

4.3.2. Regional Karstification in Southern Andhra Pradesh

From the cavern levels in different surveyed areas like, Chillavaripalle, Yadiki, etc (Gebauer, 1985; Shibasaki et. al., 1985 and this study) it can be deduced that the regional karstification in the CB has developed at different levels/stages as a result of an evolving geomorphology together with tectonics in the region. These stages could be marked at about five levels (highest one at 80 to 100m, middle three at 40 to 50m and the lowest one at 0 to 20m). The lowest level also coincides with the karst spring emergence in the area. Such types of cavern levels are also confirmed in different parts of world (Sweeting, 1950; Palmer, 1984a, b). Thus, these cavern locations represent the past (fossil/palaeo) water level

positions and possible natural discharging points that have changed during the Quaternary period were eustatic movements occurred in several parts of the world. As a result, the karst system may be vertically interconnected with superimposed successive karstification patterns. The surface streams to the east represent the current local base level.

Ford and Williams, 2007 propose a linear relationship between electrical conductivity (EC) and total hardness (TH). Using this relationship and the average EC measured at Kona springs (S2 and S3), average TH is 296 mg/l as CaCO₃. For the same spring, the specific discharge is estimated to be 0.98 l/s/km² (or 23.3 mm/a). Using Corbel formula (e.g. Ford and Williams, 2007), the denudation rate is therefore 3.7 mm/ka. Even if this data should be taken as a crude estimate, it is in the same range as denudation rates estimated in arid climatic conditions in Australia (e.g. Stone et. al., 1994) as given in Tab.1.1.

This karst region presents several characteristics of karst in arid and semi-arid regions as described by Ford and Williams, (2007). The karstic landscape is less developed than in more humid setting with a limited number of dolines, preponderance of runoff and evaporation over infiltration, which results in modest spring flow and even of a majority of springs being seasonal, predominance of point recharge over diffuse infiltration and a lower density of caves. The specific geological setting of the studied area with widespread distribution of quartzite hillocks creates favourable conditions for karstification: significant runoff generated on the hillocks provides aggressive water (i.e. dilute runoff water with low pH) which will infiltrate the karst through swallow-holes and have a good potential for active limestone dissolution. Diffuse infiltration taking place across the CO₂-rich soil zone

will also contribute to limestone dissolution within the underlying epikarst layer. However, due to the present climatic conditions combining low rainfall with high evaporation rates, diffuse infiltration and dissolution fluxes are believed to be quite limited.

Recharge of the limestone aquifers (chapter, 5) occur during the monsoon months (June to November) only after significant rainfall (average 5-7 recharge events per year): runoff on non-carbonated hilly terrains (mostly quartzite) is the main source of point recharge through swallow-holes located in the limestone plateau near the foothills. Significant runoff is also generated within the limestone areas and may recharge the aquifer through swallow-holes (as seen near the entrance of Belum cave) but also contribute to surface flow (a well developed drainage pattern can be observed on the limestone/dolomite areas indicating significant surface runoff). Finally some recharge may occur as diffuse infiltration through the soil zone and epikarst; this type of recharge seem to be quite limited as very few drip flow is observed in cave systems even after significant rain events.

In conclusion, it is proposed to consider these three carbonate formations as karstified and is undergoing active karstification processes. This has an important bearing on the hydrological functioning of these aquifers which need to be discussed in more detail. The karstic nature of these formations need to be acknowledged and considered in future development/management activities such as civil engineering work, water management, land management, etc. Dams for irrigation are being built in the region to capture runoff from quartzite hills and the impoundments are at least partly in contact with karstified rocks; in this case, important and unexpected leakage may occur due to karst permeability.

4.4. Hydrodynamics and Hydrochemistry of Narji Limestone

Discharge of the Narji limestone aquifer occurs through eight perennial and permanent karst springs located on the western side of the area. The aquifer is also highly tapped as wells for domestic use and irrigation. Groundwater flow is locally controlled by geological structures, stratigraphy and the level of karstification. The hydrodynamics and hydrochemistry of the springs indicate their karstic nature that has developed to a great degree. Certain springs respond remarkably to rainfall events- suggesting a flow similar to karst drain system.

4.4.1. Groundwater Flow

It is observed that groundwater discharge occurs within the Narji limestone and the underlying quartzites at the base of which permanent and temporary springs are located. Most springs (temporary as well as permanent) are observed in the Narji limestone at or near the contact with the Tadpatri shale (free draining springs, Ford and Williams, 2007). Groundwater from the most fluctuating zones of the aquifer (dynamic storage) discharges through local springs that drain the shallow unconfined part of the aquifer. However, towards east no spring is found and it is possible that significant flow feeds the confined limestone aquifer that develops to the east. On the eastern side, the Narji limestone is progressively buried under younger formations and this setting favours confining flow conditions: only the seasonal spring of Belum (S1) is known. Locally, the flow in springs during monsoonal months is mostly of turbulent nature. The springs (S2, S3, S13, S14 and S15) are situated only at the western foothills of the limestone plateau. No spring exists towards eastern part where human activities have significantly modified the system: a high density of paddy fields irrigated by canal water from a river/reservoir. Either pre-existing

springs are presently concealed by these modifications or a regional flow system has developed (i.e. deeper circulation in the Narji Limestone to the east) with no local discharge.

The hydrograph of Belum spring S1 (Fig. 4.21) and an observation well at Kolimigundla (Fig. 4.22, Appendix 8) shows a sharp reaction to the rainfall events and rapid recession, typical of karst aquifers with high transmissivity in conduits. The peak flow, resulting from fast recharge follows immediately after rainfall which sustains for few (3 to 4) days after rainfall. The peak flows are simultaneously indicated by a sharp decrease in the water chemistry due to quick dilution effects from fresh rain water (Fig. 4.21). This output of springs is characterized by a low or absent base flow, small basin area and flashy response to stormy rains.

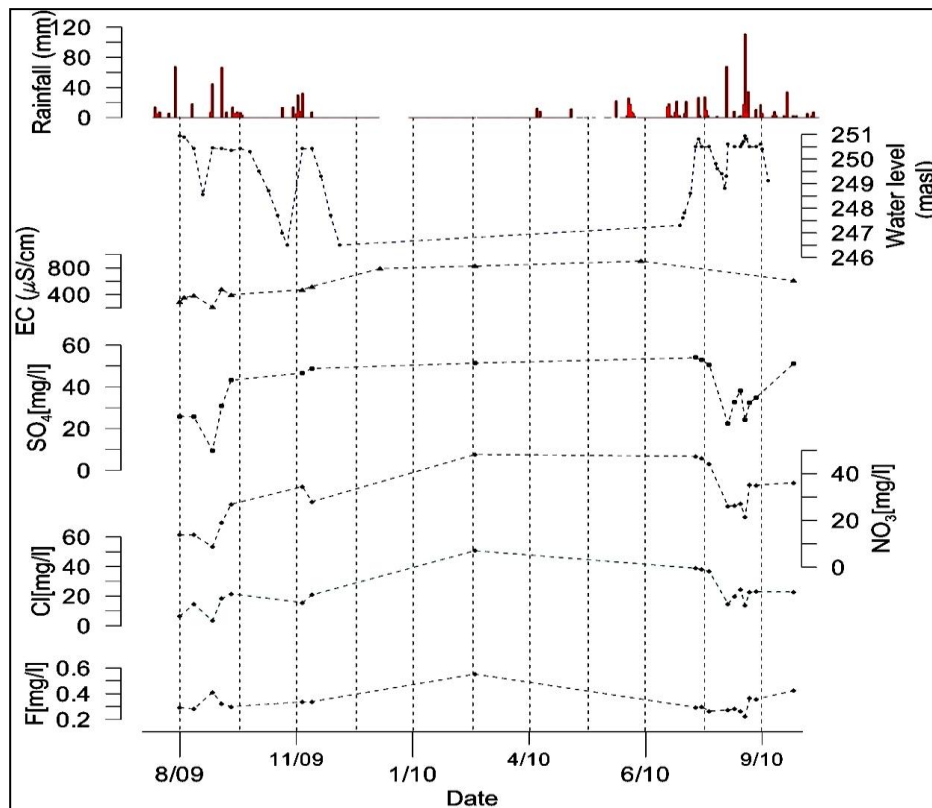


Fig. 4.21. Hydrograph and chemographs of the Belum spring (S1) showing a sharp response to the rainfall events typical of a karst aquifer.

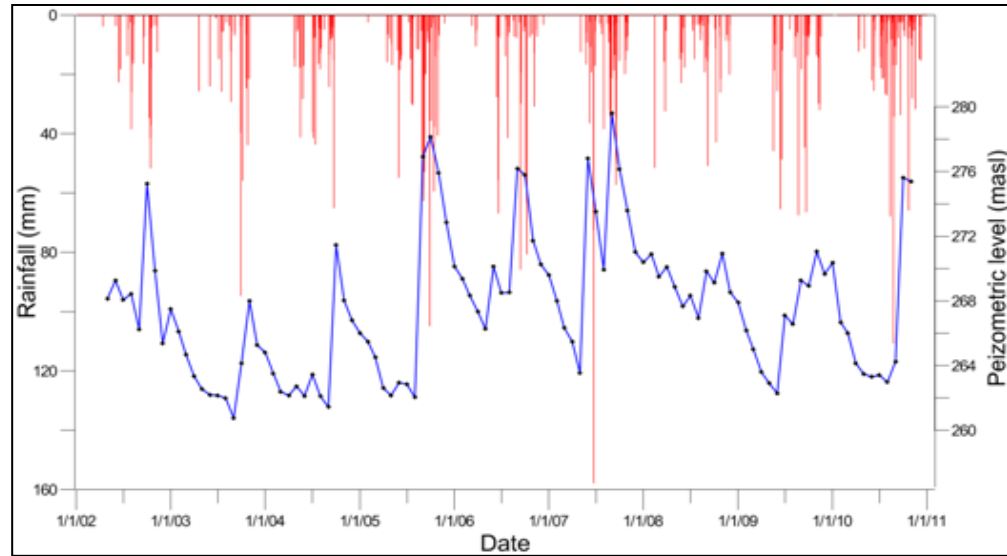


Fig. 4.22. *Hydrograph of an observation well in Narji limestone near Kolimigundla, showing a sharp response to the rainfall events typical of a karst aquifer.*

Kona spring S2, flows with a discharge that varies from less than a liter to more than 7 l/s a year (Fig. 4.23). The average discharge of Kona spring S3 remains less than a l/s throughout the year. While, the discharge of Yaganti spring (S8) varies from 3.9-8.7 l/s (Fig. 4.23). The minor springs within the limestone flow seasonally as a result of piezometric surface rise (i.e. overflow springs). At higher elevations where a very thin, sometimes absent impermeable formation covers the limestone, groundwater discharges as free draining springs. This indicates that the storage of this part of aquifer comes from the shallow subcutaneous zone. The spring S4 is located at higher level in the unsaturated zone of the Narji limestone at the floor of a surface drainage channel; in this case it may possibly drain the epikarst instead of being directly connected to the saturated zone.

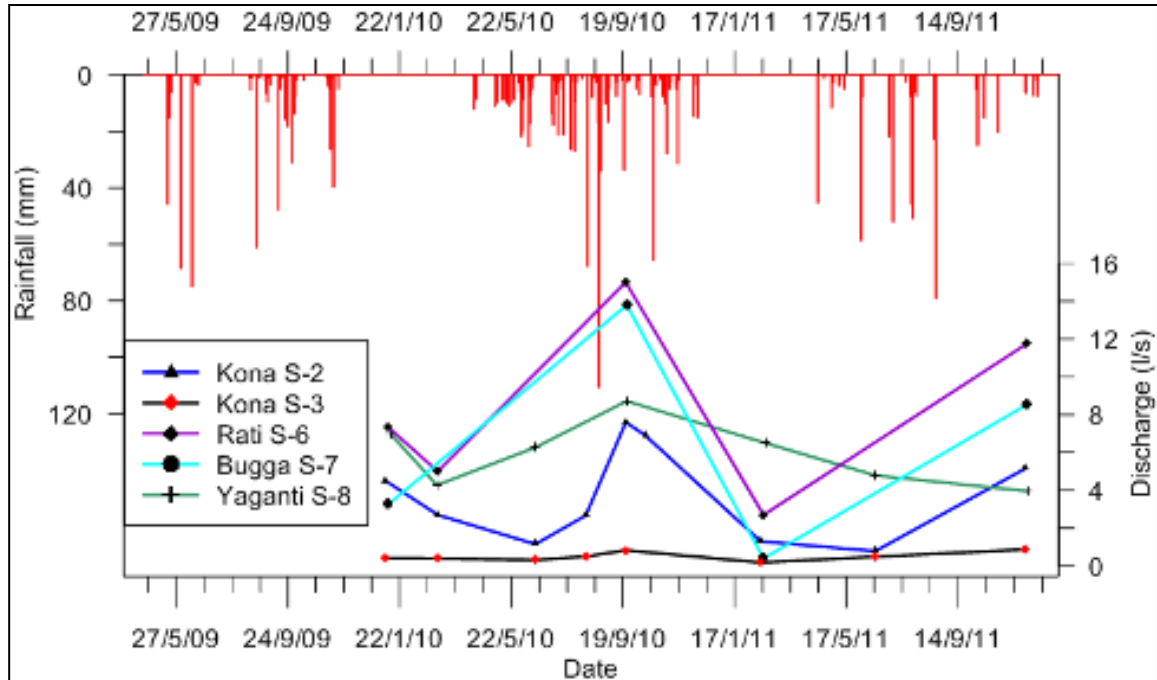


Fig. 4.23. Scatter plot showing the temporal variability of groundwater discharge from different karst springs of the Narji limestone. For location and description of springs refer to Fig. 2.1. and Appendix 6.

Springs in the area are conduit-flow as well as diffuse-flow. Conduit-flow springs discharge turbid waters during storm events (as observed in Belum); the coefficient of variation (standard deviation /mean x 100) of specific conductivity varies from 10 to more than 25 percent. While, in diffuse-flow springs water is clear to slightly turbid, the CV of specific conductivity is less than 5 percent (e.g., Quinlan and Ewers, 1985).

From the pre-monsoon and post-monsoon piezometric data (Fig. 4.24) water level during pre-monsoon and post-monsoon period varies significantly. The minimum water level during pre-monsoon was 1.2 mbgs and maximum was 21.8 mbgs, with an average value of 7 mbgs. But during post-monsoon the water level ranges from 0.6 to 19.6 mbgs with an average value of 5.9 mbgs. This showed an average decrease in depth of water level

after recharge by 1.2 m. A negative water level change was found in 18% of wells from pre- to post-monsoon. However, positive water level change was found in 82% of wells out of which 61% wells showed more than 2 m water level change. The general groundwater flow is towards SE with an inflow area situated near north and southwest. The gradient of the piezometric surface is steep in the south than in the north. Most of the pumping wells are concentrated towards south as the reservoir-canal water is available for agricultural and domestic uses in the northern parts.

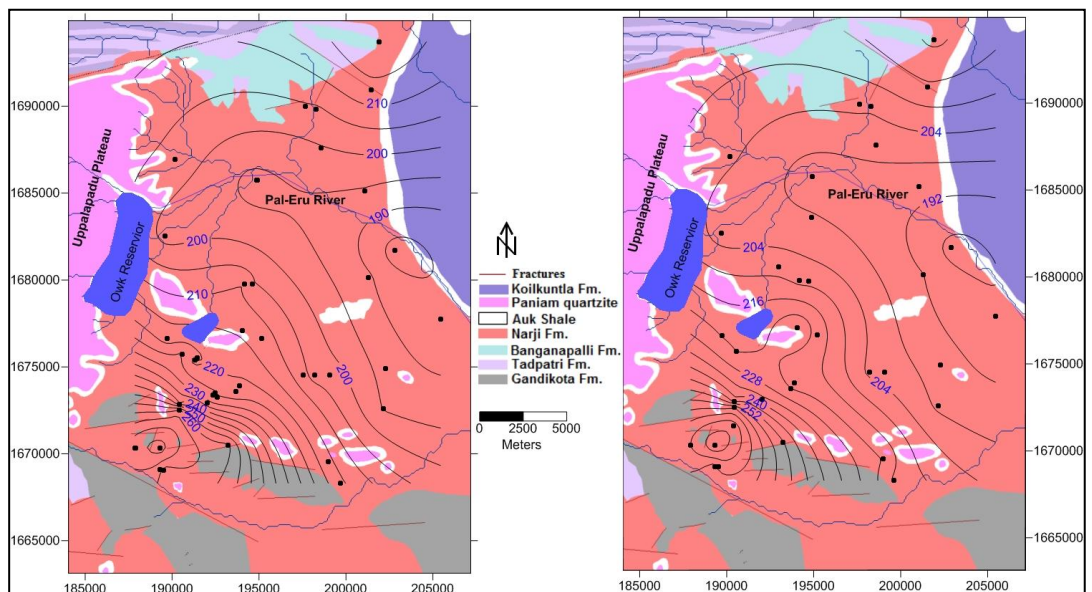


Fig. 4.24. Water level (masl) maps of the Narji limestone aquifer (left PRM and right POM) for the year 2011. Drainage and surface reservoirs are also shown.

In the Narji limestone a large part of the aquifer transmissivity occurs as conduit flow feeding karstic springs. In the massive part of the limestone, it seems that conduits provide predominant permeability as indicated by several dry wells drilled by farmers and during the touristic development of Belum cave. Boreholes drilled in the Narji limestone hit cavities (drill bit drops mentioned by the drillers). In the flaggy part and in more fractured

zones (e.g. near the contact with quartzite), additional permeability by bedding planes and joints is likely since irrigation wells with good sustained flow (average discharge 7-8 l/s) have been implemented. The productive zone seems to be between 20-65m and most boreholes produce satisfactory yields (average 10 l/s).

4.4.2. Hydrochemistry of Springs: A Means to Characterise Karst System

Fluctuation of chemical parameters in the discharging water of permanent karst springs acts a means to characterize these aquifers. Naturally, the water discharging at a karst outlet is a combination of water from the secondary porosity and relatively dilute storm-derived water. A number of studies have divided the spring water into rapid and slow components based on the variation of physico-chemical parameters (e.g., Shuster and White, 1971). Although long-term and detailed (daily) records of spring discharge and water chemistry is meagre similar behaviour is observed in all the springs with storm events.

The plot of discharge vs. EC, pH and concentration of major ions gives the best indication of the seasonal response of the karst springs. The discharge increases with monsoon rains (Fig. 4.25) with a decrease in concentration of Cl^- , HNO_3^- , SO_4^{2-} and pH values. The values vary greatly from one spring to another in spite of the fact that the springs lie in similar geologic and climatic environment.

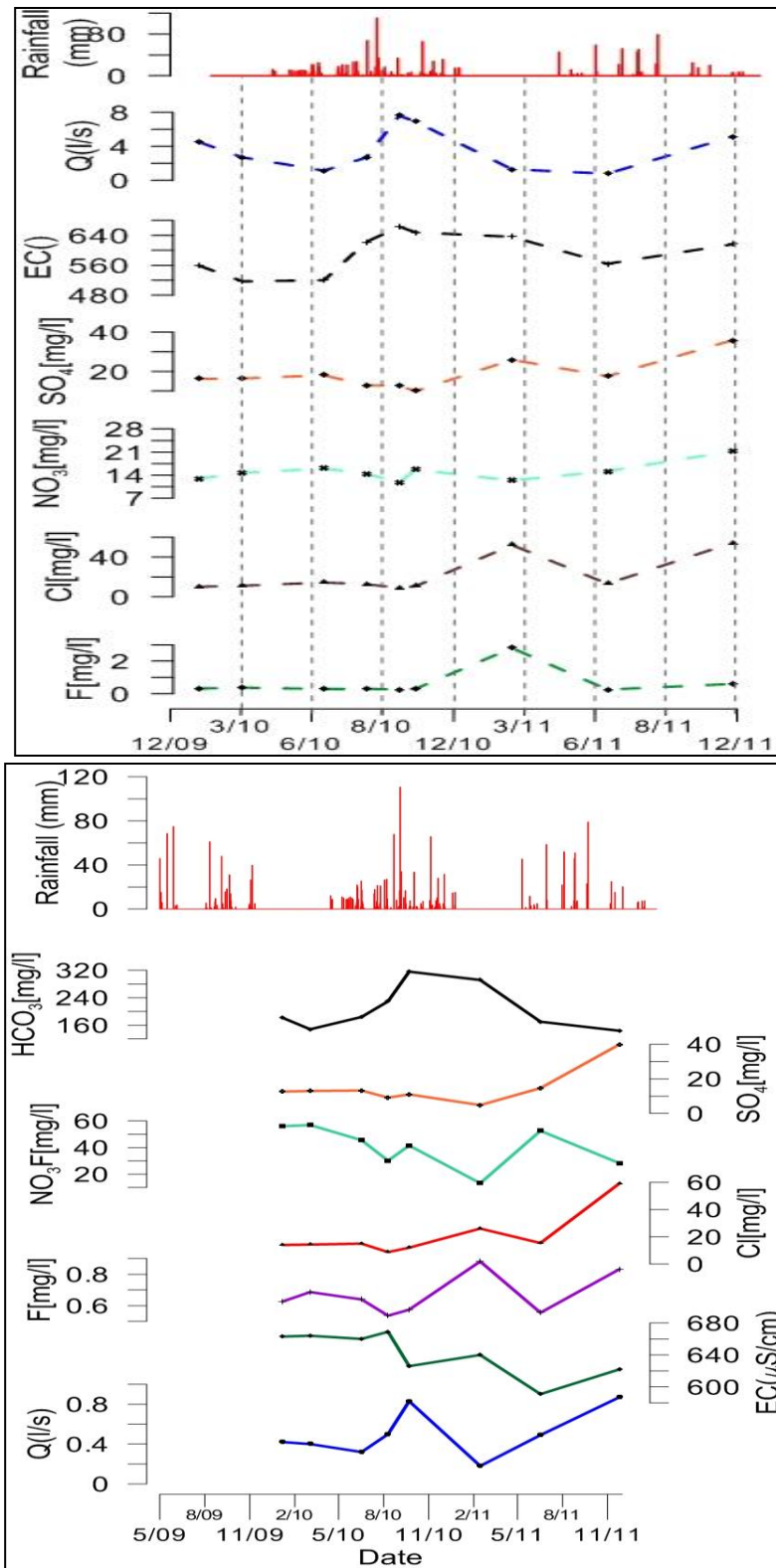


Fig. 4.25. Hydro-chemographs of Kona spring Yadiki (S2 above and S3 below). For location and description of springs refer to Fig. 2.1 and Appendix 6.

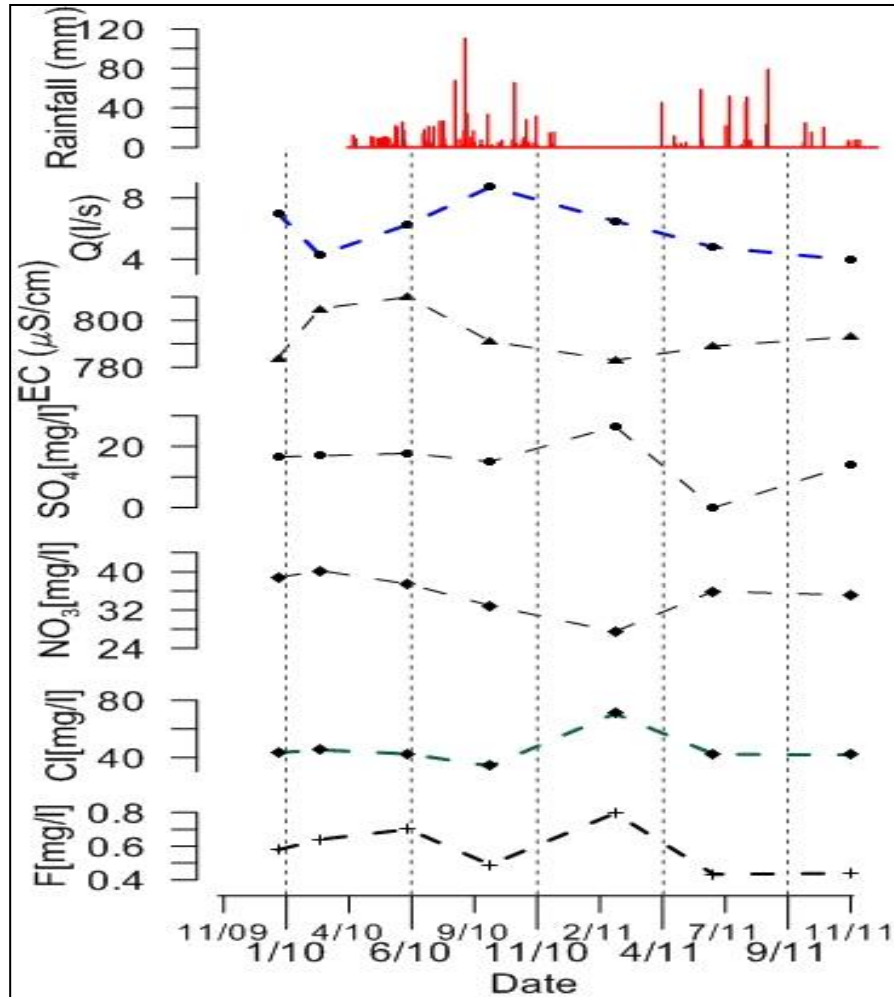


Fig. 4.26. Hydro-chemographs of Yaganti karst spring (S8). For location and description of spring refer to Fig. 2.1.

The Kona springs (S2 and S3) show a similar pattern in different parameters. S3 is a small permanent spring flowing with a mean discharge of less than a l/s. Yaganti Spring (S8) with an average discharge of 6 l/s is another permanent spring which flows from conduits at two points. The response of pH, EC and concentration of ions with discharge of Yaganti spring is shown in Fig. 4.26. These figures generally show an increase in specific conductance or an increase in concentrations during the recession of the spring flow. The comparison of spring flow and variation of their physico-chemical parameters is given in Appendix 7. The dissimilarity of the observations in springs is a widespread property in

karst terrains with well-developed conduit networks. The magnitude and temporal structure of these fluctuations vary with bedrock chemical composition, size, density and interconnectedness of the conduits and fractures, the rate and spatial distribution of groundwater recharge, the degree to which the conduit network occurs and other hydrogeological complexities.

4.5. Summary

Karst aquifers are spread in many areas of the world and supply groundwater to a large population. In semi-arid southern Andhra Pradesh these karstic zones play a vital role for the society both as a primary water supply and in economic terms (water resource for irrigated agriculture, quarrying for construction and cement production). These aquifers have not been studied adequately from the karstification point of view. A number of karst features characterise these semi-arid carbonate rocks which can pose unpredictable problems like, ground subsidence, sinkhole collapse, groundwater contamination and unpredictable water supply.

Geological, geomorphological and hydrogeological study was carried out and discussed in three formations separately. All the formations are highly karstified possessing large caves and few springs along with many surface features. Vempalle dolomite covers the western part of the basin and possesses one of the deepest caves of India. No spring flow is observed in the formation. The geology of the Narji limestone plain is highly complex and the area has been studied widely for karst development. The formation possesses one of the deepest caves of India which is famous from tourist point of view. Many temporary and permanent springs are located in the formation. Few springs flow quite variably and show

sharp responses with the rainfall events. Surface karst depressions concentrate the runoff and recharge the aquifer mostly through fast recharge. Epikarst is well developed in the limestone and shows many secondary calcite infillings on the surface. The aquifer is highly quarried for cement manufacture and building stones which is extending day-by-day in the area. Quarrying seems to have modified the hydrological characteristics of the area. Karstification is still in progress but at deeper levels and at slower pace. Speleothems of different architectural size are present in the caves. Secondary calcite deposition is also observed at many places. Koilkuntla limestone is also karstified with well developed epikarst layer as observed by the well data. No caves and springs were located in the formation. The limestone is highly pumped for agricultural purposes.

A model of karstification is discussed based on cave pattern with three main stages. Moist conditions of the past are responsible for the karst development which has minimized due to the onset of monsoon conditions and Western Ghats uplifting. Karst has developed at many elevations representing the past base levels in the Cuddapah basin. A denudation rate of 3.7 mm/ka has been proposed for this semi-arid karst area.

Groundwater level of the Narji limestone plain is shallow with average depth of 7mbgs during pre-monsoon period. During post-monsoon water level rises with an average increase of 1.2m. Most bore wells produce an average yield of 10 l/s. The karst springs of Narji limestone are both permanent and temporary. The Belum spring showed quite fast response to the rainfall while other springs flow with less variation in discharge and chemistry.

CHAPTER 5

GROUNDWATER RECHARGE IN KARST AQUIFER

5.1. Introduction

Groundwater in semi-arid regions is of fundamental importance for domestic use and economic activities (irrigated agriculture). It is often the sole water source where aquifers are vulnerable to contamination, frequent droughts and depletion. Groundwater recharge is a key component of groundwater resource estimation which maintains its yield for efficient and sustainable management (Scanlon et. al., 2002). Recharge can be described as the process by which precipitation and/or surface water reaches the phreatic zone by flowing through the unsaturated zone (e.g., Freeze and Cherry, 1979; Lerner et. al., 1990). Identification and quantification of recharge in highly heterogeneous semi-arid karst aquifers is difficult where low rainfall and high potential evapotranspiration increases the error in estimation of groundwater recharge.

As described in methodology, two main types of recharge mechanisms were identified. Point recharge is an allogenic type where surface runoff from non-carbonate areas reaches the limestone aquifer through preferential pathways. It gets concentrated through sinking streams and depressions in the limestone terrain. Diffuse recharge is autogenic water derived solely from rainfall falling on the limestone outcrop itself. It enters the aquifer through soil and epikarst layers. The conceptual model of recharge shows another type of recharge, i.e., internal runoff, which is a very small part of both allogenic and autogenic recharge and has a limited effect on groundwater. The aim of this chapter is to evaluate the relative importance of different recharge mechanisms (point and diffuse) and to validate the results with water levels. It also includes discussion on the influence of anthropogenic

changes (land clearance by quarrying and irrigation) on the groundwater. For this purpose a semi-arid limestone area, located in the western part of Cuddapah basin in the Kurnool district of Andhra Pradesh was chosen. It covers few villages of Kolimigundla, Owk and Sanjamalla mandals. The 88 km² area (Fig. 5.1) was defined on the basis of topography, geology, structure and groundwater flow. The plateau of Uppalapadu in the west and the geological contact in the east bound the study area. A major fault and a low series of hills form its southern boundary. Ground surface elevation varies from 220-370 masl. Higher elevations represent the isolated quartzite hills and plateaus. Slope is generally ~0-11 degrees. Drainage system (part of Pal-Eru tributary of Kundu River) is highly ephemeral and flows from west to east. The bedrock mainly consists in the Narji limestone with discontinuous shale and quartzite outcrops. The high runoff over shale/quartzite impacts the recharge in the limestone areas. The region is typical of karstic terrain; runoff-contributing outcrops with thin soil pockets. The aquifer is characterized by enlarged fissures and fractures acting as major infiltration pathways. This low rainfall area of Narji Limestone is the only water source available to a large population with ~8% being cultivators and is heavily utilized for domestic and irrigation water supplies. Two main soils were defined; Vertic Inceptisols (Black soils) covering 45% and Alfisols (brown to red soils) covering 12% of the total study area. The remaining 43% of the area includes rock outcrops (limestone and quartzites) and other land use classes (Fig. 5.1). The soils are described in detail in detail in chapter 2. Most part of the area supports sparse vegetation. During Kharif (monsoon season) agricultural activities take place both in rain-fed and irrigated areas. In Rabi (winter months) agricultural depends on irrigation.

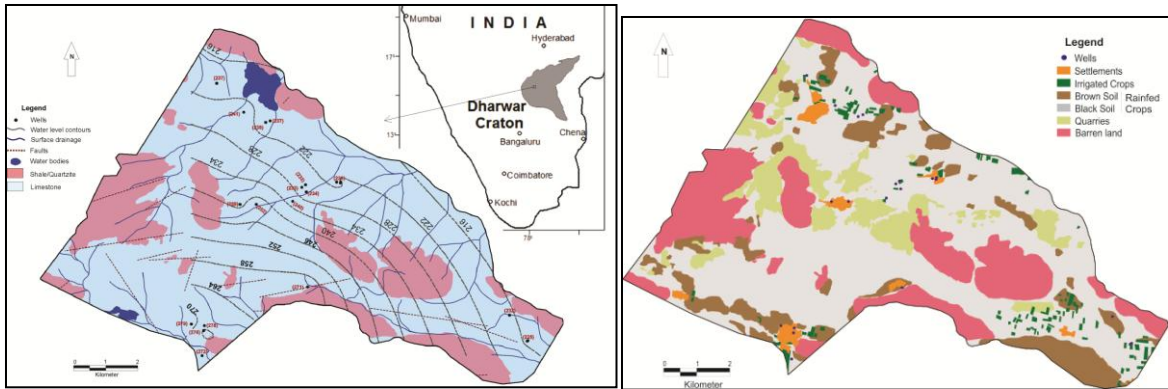


Fig. 5.1. Location of the area showing (a) geology, drainage, water level and surface elevation in masl and (b) land use of the area. The area has been selected for recharge estimation.

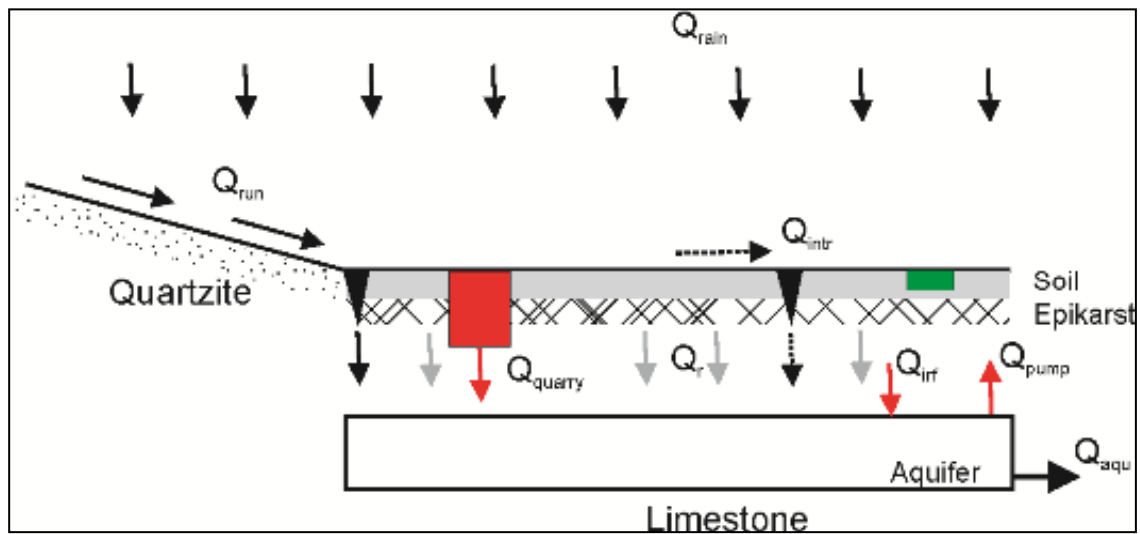


Fig. 5.2. Recharge model of the semi-arid karst aquifer; Q_{run} , Q_r and Q_{intr} are point recharge, diffuse recharge and internal runoff respectively. Q_{quarry} , Q_{irf} , Q_{pump} are the water stored in quarry depressions, irrigation return flow and pumping water that represents the impact of anthropogenic conditions in the area.

5.2. Recharge Estimation

A conceptual model of recharge in karst areas is important to develop, as it helps in defining the processes and identification of flow mechanisms. It reduces the uncertainty, time and cost of recharge quantification (Scanlon et. al., 2002; USGS, 2008). The classical recharge

methods consider a uniform condition in the aquifer and don't consider the type of recharge. Therefore, the methods need to be modified that considers the heterogeneity of karst aquifers and the semi-arid conditions. Thus, based on the field observations and geological mapping, two principle recharge components were identified (Fig. 5.2); point recharge-runoff issued from the quartzite hills and entering the groundwater (Q_{run}) and diffuse recharge enters across the soil and epikarst layers (Q_r).

In addition to the two major recharge types, internal runoff (i.e., overland flow within the limestone plateau itself) may take place after heavy rainfall and then disappear into karst groundwater (Wanfang and Beck, 2011). This generates a third type of recharge; Q_{intr} . It is the discrete autogenic recharge that enters the aquifer quickly through sinkholes in addition to diffuse recharge (Lerch et. al., 2005). It may occur in two forms; excessive runoff developed on the limestone itself and excessive saturation runoff developed over the soils. This part of recharge develops during short, high intensity, rainy events and was difficult to estimate. However, its effect on the overall groundwater balance is assumed to be very less.

5.2.1. Point Recharge (Q_{run})

The runoff from non-carbonate rocks of the area reach the limestone plateau and get localized in the depressions and dissolution fractures. This amount of rainfall directly enters the aquifer as fast recharge and causes a sharp change in water levels. This amount was calculated from daily rainfall by the versatile and well established empirical curve number (SCN) approach (SCS, 1972). The watershed coefficient, called the curve number (CN) represents the runoff potential of the land-soil complex (quartzites in this study). The curve

number is based on the hydrological soil group, land use, treatment and hydrological conditions. The soils of the area correspond to B and D hydrological groups of SCS, 1985. The major land use/land cover classes are given in Fig. 5.2 and Tab. 5.1. the runoff generated over non-permeable rocks outcrops was estimated using this method.

Land Use Class	Soils	Area (Km ²)	% Area
Dry Agriculture (Rain fed)	Black soil (5-30)*	10.88	12.36
	Other soils (60-100)*	43.02	48.89
Paddy/Irrigated crop	-	1.8	2.05
Barren (Rocky)	-	20.27	23.03
Waste land (Quarry waste)	-	10.73	12.19
Settlement	-	1.3	1.48

Tab. 5.1. Land use classes and hydrological soil groups of the study area based on soil map.

** indicates the infiltration rate in mm/hour for each soil type.*

The method assumes that for a single storm, the ratio of actual water retention after runoff begins to potential maximum retention is equal to the ratio of direct runoff to potential runoff (total rainfall), which follows equation;

$$Q_{\text{run}} = \frac{(P-0.3S)^2}{P+0.7S} \quad \text{if } P(> 0.2S), \text{ other wise } Q = 0$$

Q_{run} is runoff (mm), P is rainfall (mm), S is the potential maximum water moisture retention after runoff begins (mm). Antecedent moisture condition (AMC), an indicator of wetness index, represents the availability of moisture prior to storm event. The AMC is based on the total rainfall in the 5 day period preceding a storm. Due to the fractured nature of the quartzites the infiltration processes are complex which need a modification in the curve number adjustment (e.g., Rasmussen and Evans, 2009). Therefore, curve numbers of 75, 85 and 90 were used for the dry (AMC I), normal (AMC II) and wet condition (AMC III). The initial abstraction in mm was taken as $I_a = 0.3S$ (Vandersypen et. al., 1972). The

initial abstraction represents the accumulation of rainfall through interception, depression storage, evapotranspiration and infiltration before the start of runoff. After runoff starts, some additional rainfall is lost, mainly in the form of infiltration called actual infiltration. With increasing rainfall, the actual retention also increases up to some maximum value; the potential retention. The potential maximum retention (S) is converted to a convenient dimensionless parameter ‘curve number’ (CN) Ponce and Hawkins, (1996) as;

$$S = \frac{25400}{CN} - 254 \text{ in mm or } \frac{1000}{CN} - 10 \text{ in inches}$$

S has the limiting values of 0 and ∞ and CN is an integer ranging from 0 (no runoff potential) to 100 (all rainfall as runoff). The potential maximum storage (S) was calculated for each AMC condition to estimate the runoff amount or concentrated recharge (Q_{run}) from daily rainfall using above equations.

The average annual actual evapotranspiration in the areas is 458 mm, which represents about 70% of the annual rainfall. The highest AE rates of monsoon period match with the plant growth period in the area. Q_{run} values from this method varies from 0 to 44.3 mm/day and from 46 to 231mm/year. Average annual value is 107.3 mm (Tab. 5.2) which is about 15% of the annual rainfall. Higher values are due to thin soil cover and high karstification in the area.

5.2.2. Diffuse Recharge (Q_r)

Diffuse recharge Q_r reaches the groundwater in excess of soil moisture deficit and evapotranspiration by vertical percolation through the unsaturated zone. It was computed through soil water balance model (e.g., Rushton, 2003; Rushton et. al., 2006) that calculates the effective amount of water which ultimately reaches the aquifer due to rainfall or

irrigation through the free draining soils at their field capacity. This latter is the amount of water that a well drained soil holds against gravitational forces. The method assumes that the slope gradient should be very less so that runoff is negligible and favors infiltration (Li et. al., 2008 and 2010). The initial rainfall reduces the soil moisture deficit (SMD) leading the soil to field capacity.

Year	Rainfall	Q _{run}	Q _r	AE	(Q _{run} +Q _r)	Q _{run} %	Q _r %	(Q _{run} +Q _r)%
2002	407.6	63.7	53.7	348.6	136.1	20.2	13.2	33.4
2003	516.0	95.5	86.5	331.8	194.6	20.9	16.8	37.7
2004	542.8	50.5	74.6	413.6	128.6	9.9	13.8	23.7
2005	933.2	184.8	189.9	519.7	397.1	22.2	20.3	42.5
2006	667.2	163.0	87.9	418.8	260.4	25.8	13.2	39.0
2007	884.0	225.6	183.5	490.8	415.1	26.2	20.8	47.0
2008	525.8	26.5	8.9	467.5	54.9	8.8	1.7	10.4
2009	626.0	78.3	35.3	470.0	139.7	16.7	5.6	22.3
2010	966.6	83.5	112.2	705.7	254.7	14.7	11.6	26.4
2011	554.5	92.9	33.5	409.3	150.0	21.0	6.0	27.1
Average	662.4	107.3	86.6	457.6	213.1	15.9	13.1	32.2

Tab. 5.2. Annual rainfall and recharge in mm for the study area. The data is from Kolimigundla and Belum stations.

When the soil moisture deficit becomes zero, the extra rainfall percolates through the unsaturated zone and reaches the groundwater as diffuse recharge. The soil becomes free draining when the moisture content (θ) reaches the field capacity value (θ_{FC}). θ is the volumetric percentage of water or depth of water. It takes the average soil thickness into account. Q_r is estimated by computing the soil water content at the end of each day from the previous day from daily rainfall and evapotranspiration using an equation;

$$Q_r = \theta_D (\theta_D < 0) \text{ and } Q_r = 0 (\theta_D \geq 0)$$

θ_D is the daily soil moisture deficit required to bring the soil to water-holding capacity by taking into account the previous day moisture condition. The soils have a field capacity in the range of 0.21-0.34 which controls the overall process of groundwater recharge. An average value of wilting point and field capacity were taken as 0.17 and 0.28 respectively. To generate recharge, limiting moisture content called wetting threshold is required that depends on climate. However, percolation through macropores and desiccation cracks in black soils may induce instantaneous infiltration (Ford and Williams, 2007). The soils were assumed to be homogeneous in depth (0.5m), moisture distribution, root zone distribution, structure, organic matter, etc. This assumption holds well in the study area due to thin soil cover with no well developed soil horizons. The saturated hydraulic conductivity (Reynolds and Elrick, 1990) indicates the nature of infiltration through the soils. For black soils hydraulic conductivity is 5 mm/hr and for coarse grained soils it is 32 mm/hr. However, already wet soils showed lower value (e.g., 2 mm/hr for black soils) which indicates a little surface storage that delays recharge. Therefore, a factor of 0.5 was used in the model to represent the near surface water storage in the soils (e.g., Eilers et. al., 2007). The near surface storage is less than 1 due to high evapotranspiration, thin soil cover coupled with little vegetation (nearly bare) but not zero due to the presence of a suitable amount of clay minerals in the soils (chapter 2). However, the soils maintain saturation for much shorter periods. The unsaturated zone in this aquifer includes the soil and well developed epikarst zone. Soils are of very limited thickness where the infiltrating water may travel little bit faster. The soils also develop desiccation cracks which also cause water to reach the epikarst layer fast. The epikarst is an important zone in the upper unsaturated part of the aquifer that controls the karst aquifer hydraulic behaviour (Williams, 1983; Clemens

et. al., 1999; Trcek and Krothe, 2002; Klimchouk, 2004; Trcek, 2007). The zone is well fractured that may develop at a depth of 15-30m (Klimchouk, 2000). Epikarst mainly acts as a storage zone in karst aquifers while as saturated zone is a transmissive zone (Perrin et. al., 2003). Infiltrating water may get retained at the base of this zone some days to several months which depends on many factors (Gunn, 1983; Aquilina et. al., 2006). The detention of infiltrating water produces local saturation of the epikarst that sustains the flow in small perennial (epikarstic) springs which are also found in this area (Williams, 2008). Later this stored water also maintains seepage at some cave sites for the development of speleothems which are active at some cave sites in the area.

Diffuse recharge (Q_r) through soil cover that reaches the epikarst zone varies from 0-21mm/day. The monthly values of diffuse recharge are given in Tab. 5.3 and Fig. 5.3. Annual diffuse recharge varies from 9 to 190 mm with an average of 86mm. It comprises 13% of annual rainfall, which is comparable with the other semi-arid regions of the world. Soil water balance approach has given recharge values up to 36% of rainfall in some semi-arid regions of the world (Canton et. al., 2010). The magnitude of diffuse recharge varies with time depending on precipitation, evapotranspiration and soil conditions. It has been estimated that for clayey soils less recharge occurs than for sandy soils. The clayey soils have a higher water holding capacity and thus, allow more loss of water through evapotranspiration (Athavale et. al., 1980; Edmunds et. al., 1992).

The time required for Q_r generation considerably varies with the frequency and intensity of rainfall and with the previous moisture conditions in the soils (Fig. 5.4).

	Rainfall	AE	Q_r	Q_{run}
Jan	0.0	5.4	0.0	0.5
Feb	6.0	4.0	0.0	1.0
Mar	10.5	7.2	0.0	0.4
Apr	13.4	12.7	0.0	1.7
May	52.8	32.3	2.1	25.0
Jun	100.2	54.8	8.4	7.9
Jul	67.2	54.7	4.2	20.3
Aug	107.8	58.7	13.1	30.5
Sep	148.9	61.6	29.7	19.9
Oct	122.8	82.2	19.8	1.1
Nov	36.3	36.5	1.4	0.0
Dec	4.5	7.5	0.0	0.5

Tab. 5.3. Average monthly rainfall, Q_{run} , Q_r and AE for the study area from 2002-2011. Data is from Belum and Kolimigundla station. All values are in mm.

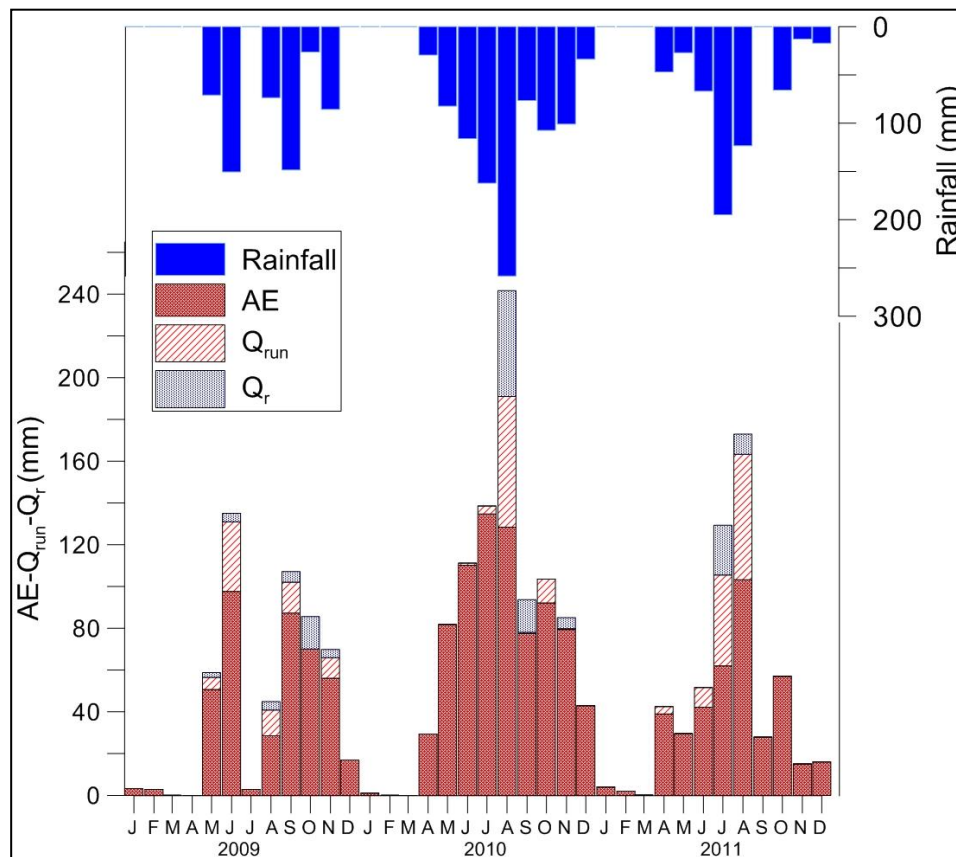


Fig. 5.3. Bar plot of the total monthly values for three years against rainfall (AE actual evapotranspiration, Q_{run} concentrated recharge and Q_r diffuse recharge). All parameters are in mm.

Commonly, 1- to 9-day rainfall events generate Q_r after a time response of 1 day to a week. The first events may not generate recharge when the soils and epikarst are relatively dry. This amount rather replenishes the soil and epikarst storage; but may produce a response to cave drips (Arbel et. al., 2010). A high rainfall amount at the beginning of the rainy season (21 mm on 03/06/10) contributed 0 to recharge as the conditions were not favorable. But a smaller rainfall amount at the end of the season (14 mm on 01/10/09) contributed 7.5 mm. Thus, Q_r is mostly influenced by daily evapotranspiration rates and soil properties. It is observed that Q_{run} generation is simultaneous with rainfall events (Fig. 5.4) which has been observed in the field. Q_{run} generation has a delay that varies from 0 to a few hours after the rainfall event. A negligible percentage of rainfall is lost to interception and evapotranspiration when it falls in high intensity events rather than smaller, temporally distributed events. The importance of continuous storm events to generate diffuse recharge is evident from these figures. The calculation is in agreement with the magnitude and lag-time measured in other semi-arid areas (e.g., Keese et. al., 2005 and Eliers et. al., 2007).

The amount of recharge from internal runoff (Q_{intr}) depends on the amount and intensity of rainfall and was difficult to estimate. It occurs after a threshold amount of recharge has reached that the soil and epikarst cannot transmit. Therefore, excess infiltrated water reaches the saturated zone through this mechanism without traveling through the unsaturated zone. This part of recharge enters the aquifer through cave entrances, shafts, etc. Its effect is attested when Belum Cave was closed for public due to internal flow in the conduits (e.g., Gebauer, 1985). The rainfall event led to the closure of cave for public on 7th Sep-2005. The highest flooding caused water to reach more than 2 m above the soil in the phreatic conduit. During this period a rainfall amount of 260mm occurred within 10 days

(30th Aug to 8th Sep-2005) that generated Q_{run} of 110mm and Q_r of 84mm. Likewise, an intense rainfall event of 170mm for 7 days (20-08-10 to 26-08-10) generated a Q_{run} of 47 mm and Q_r of 43mm that flooded the conduit.

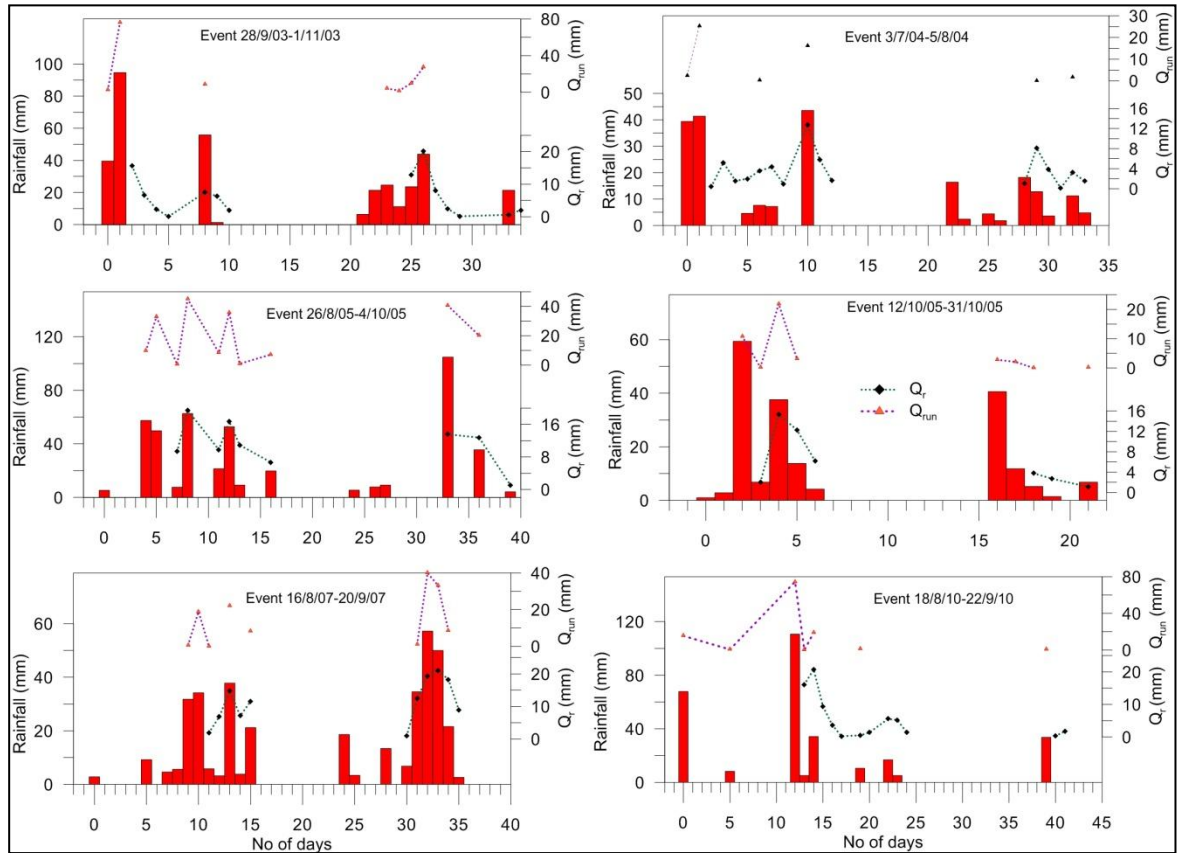


Fig. 5.4. Diagrams showing daily based recharge calculations as a function of intensity and duration of rainfall, (Q_{run} concentrated recharge and Q_r diffuse recharge).

The sum of point and diffuse recharge ($Q_{run}+Q_r$) varies from 0 to 44mm per day. Monthly ($Q_{run}+Q_r$) ranges from 0 to 87 mm (Tab. 5.2). The average data for 10 years shows that allogenic ($Q_{run}+Q_{int}$) recharge is significantly larger than the diffuse type. The average annual ($Q_{run}+Q_r$) recharge represents about 29% of rainfall and occurs during the 5-7 important events of the year. The sum of significant rainfall events (25mm/day) accounts for

430 mm/yr. The high ratio of concentrated/diffuse recharge (1.3) has an influence on the hydrodynamics and hydrochemistry of karst aquifers (e.g., Alcala et. al., 2010). The aquifer responses sharply to the rainfall and shows a large variation in water chemistry as observed in Belum spring (chapter 4). This part of recharge makes the soil to be lost in the fields and gets collected in the cave channels. The turbidity of water discharging from the conduit of Belum spring also indicates the fast recharging mechanism in the aquifer. The correlation coefficient between annual rainfall and annual recharge is high as shown in Fig. 5.5. A general equation for rainfall and recharge in the area can be written as;

$$Q_{run} = 0.25 * P - 32.56, R^2=0.61$$

$$Q_r = 0.25 * P - 76.83, R^2=0.64$$

Rainfall-recharge regression relationship has been developed for four main hydrogeological provinces (Alluvium, Sediments, Granite/Gneiss and Basalt) of India (Rangarajan and Athvale, 2000). Their results showed that these equations have a slope ranging from 0.147 to 0.174 and an intercept varying from -6 to -62 from Alluvium to Basalts areas respectively.

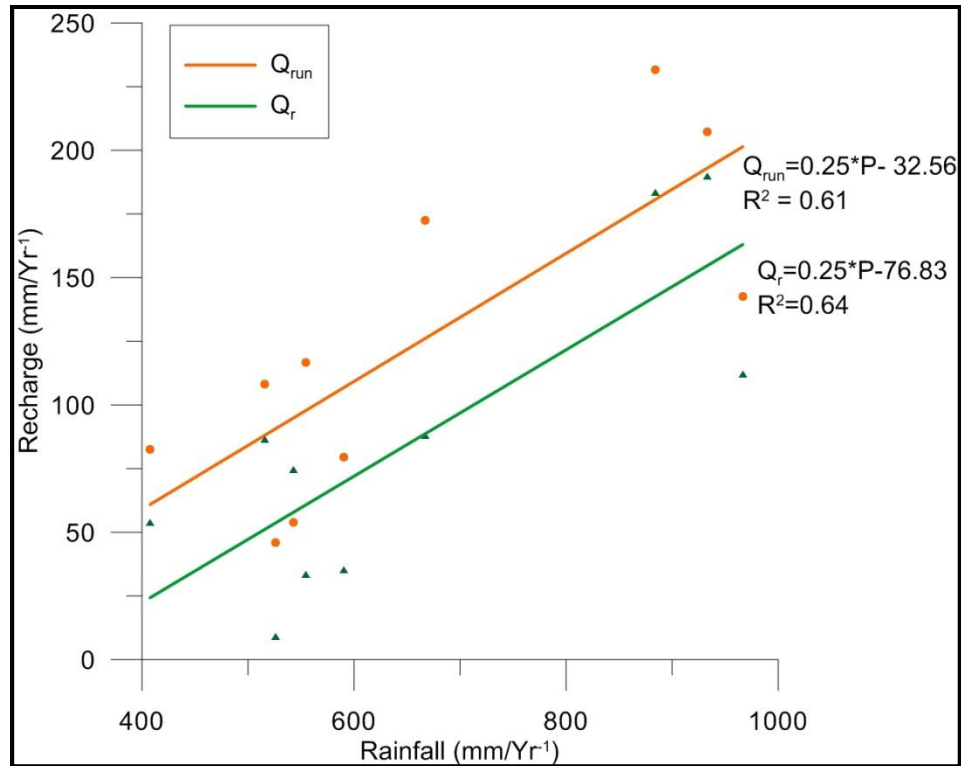


Fig. 5.5. Scatter plot showing linear correlation of different recharge types with rainfall.

5.2.3. Calibration of the Model

Monthly water level data of Kolimigundla bore well from 2002-10 (Appendix 8) was used to calibrate the recharge results. The well is located outside the Kolimigundla village and is influenced by pumping to a limited extent. The water level showed a sharp change with rainfall and recharge events (Fig. 5.6). Water level decreases sharply after month of October till December after which the decrease is less sharp. This can be related to the period of harvesting that starts for most of the crops. Change in storage was calculated using a specific yield of 0.08 for karstified limestone (e.g., GEC, 2009). Change in storage also showed good correlation with the recharge events. An average change in storage from pre- to post-monsoon is about 0.8m. For the past 10 years change in storage has not shown any significant trend except a decrease in 2008 and 2009 which record less rainfall (annual

526mm and 626mm respectively compared to average 702mm). Change in storage and water level reached highest value in 2005 when rainfall was very high and occurred in continuous rainy events than other years.

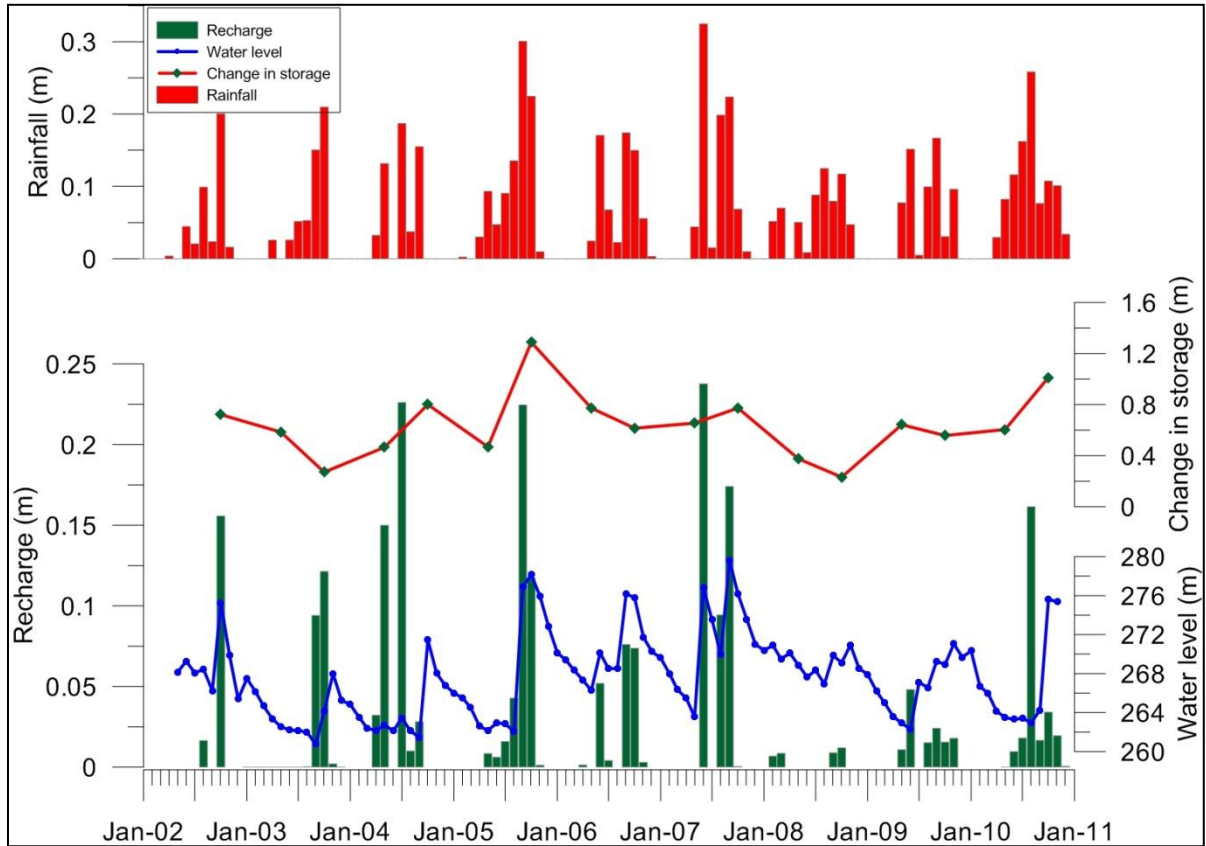


Fig. 5.6. Monthly water level, recharge ($Q_{run}+Q_r$) and change in storage of Kolimigundla bore well as shown against monthly rainfall.

Annual recharge ($Q_{run}+Q_r$) were plotted with the change in water level (Fig. 5.7). The scatter plot indicates a good correlation between the data points ($R^2=0.75$). Manual water level measurements of the Belum spring during 2009 and 2010 increased the quality of the available water level data. The time lag of recharge from rainfall was calibrated with the water level (Fig. 5.8). The aquifer reacts quickly to high precipitation events (above 30-40mm) some time 20-24 hours or even faster which causes fast recharge of the aquifer. In

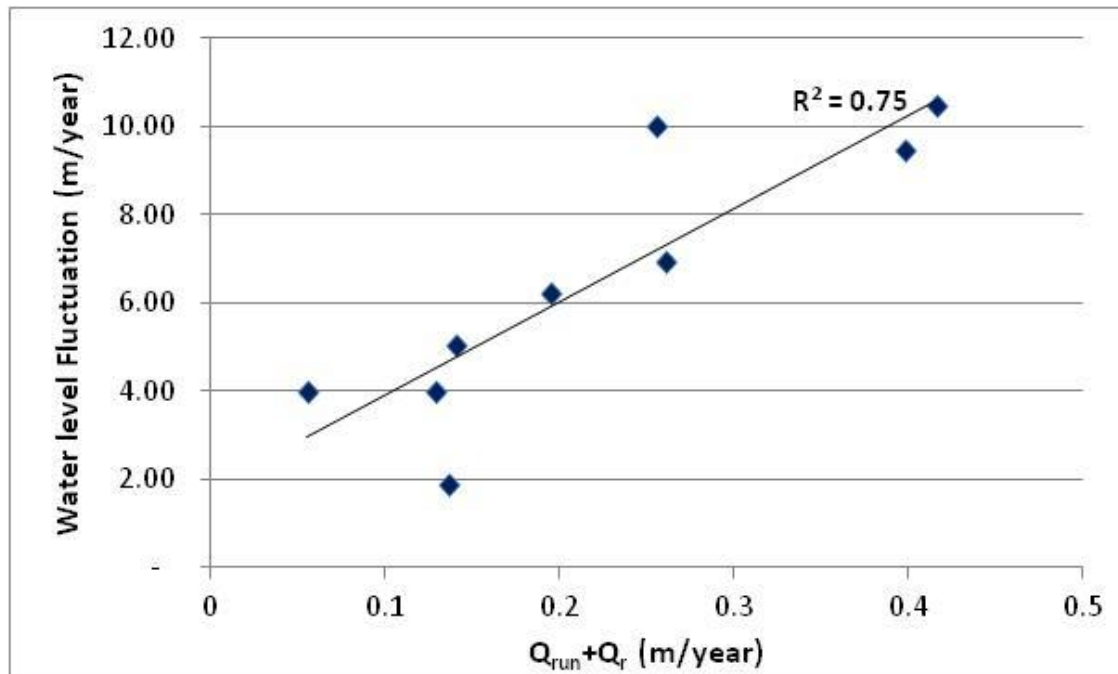


Fig. 5.7. Scatter plot of annual ($Q_{run} + Q_r$) and water level fluctuation of Kolimigundla bore well showing good correlation.

2009 a rain event of 35mm caused an increase of 4m of water level. A single rainfall event of 67mm in 2010 led to rise of 3m in water level.

It is important to compare the values with the existing results from similar geology, climate and other methods. The sum of point recharge and diffuse recharge is about 29% of rainfall which is in concordance with the results from other semi-arid karst aquifers of the world (Tab. 5.4). Recharge is less than 5% in flat homogeneous karst areas (e.g., Lerner et. al., 1990; Scanlon, et, al., 2002). It reaches as much as 30% in areas with more relief, large heterogeneity and moderate permeability. The difference in potential and actual recharge is due to spatial variation of recharge conditions (Andreua et. al., 2011).

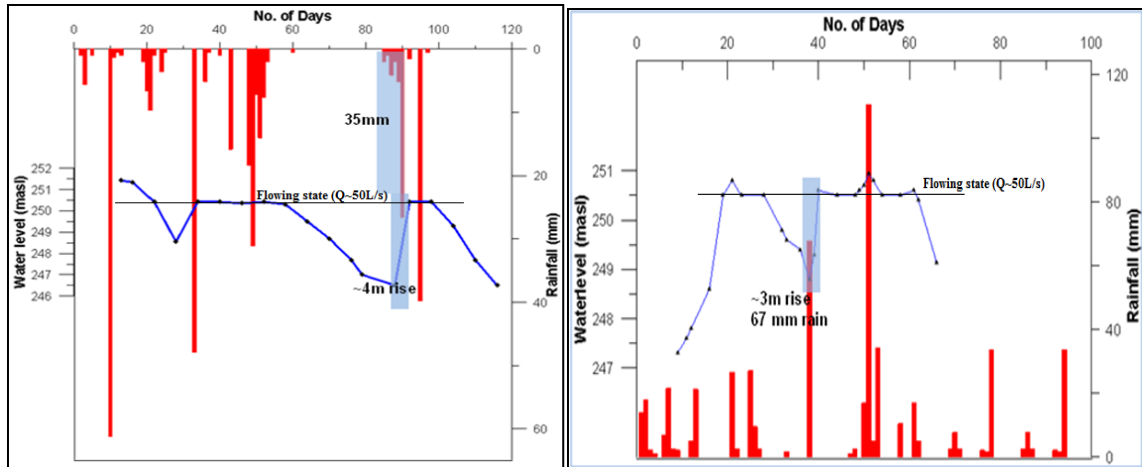


Fig. 5.8. The effect of daily rainfall on water level variation of Belum spring for two years; left 2009 and right 2010. Horizontal axis is plotted as number of days in a year to show the time lag in water level.

Location	Rainfall mm	Recharge (%)	Comments	Reference
Saudi Arabia	70	47		Hoetzi, 1995
Saudi Arabia	198	47	Sinkholes	De Vries and Simmers, 2002
Portuguese Algarve	550	27–55		De Vries and Simmers, 2002
Niger (Sahel)	600	10	Matrix	Leduc et. al., 1997
Middle East	500	29		Hughes et. al., 2008
S-E Spain	200-600	29-35		Andreu, J. M. et. al., 2011
Southern Spain		30-55		Andreu, J. M. et. al., 2008
Southern Spain	463	37	22+15*	Alcala et. al., 2010
North Central USA	400-700	10-220		Carter and Driscoll, 2006
S-E Spain	200	5		Santos and Andreu, 2010
S-E Spain	275	18		Touhami et. al., 2012
Syria	400-1300	43-67		Al-Charideh, 2012
Floridan, USA	1370	17-53	34**	Ritorto et. al., 2009
Southern India	700	29	16+13*	This study

Tab. 5.4. Annual recharge rates calculated in different semi-arid karst aquifers of the world against annual rainfall. *Concentrated+diffuse, ** Diffuse

Recharge estimation has been carried out by conventional and tracer methods in many aquifers in semi-arid India (e.g., Athavale et. al., 1992; Mohan et. al., 1996) without considering the specificities of limestone aquifers. Rangarajan and Athavale, (2000) has estimated recharge in different watershed and on varied geology (alluvium, sedimentary, granite/gneiss, basalts) of India using injection methods. According to them, the mean recharge in Kundair basin of Andhra Pradesh consisting of sandstone, shale, limestone and quartzite is about 29 mm which makes only 4.7% of annual rainfall. In Pal-Eru Peddavanka watershed (sub-basin of Kundair River in which the study area is located) the average recharge obtained from tracer injection tests was 41 mm, i.e., 5.8% of annual rainfall (Chand et. al., 2006). Ground Water Estimation Committee Methodology of 1984 has being adopted in limestone areas as well (Tab. 5.5) usually using two approaches; groundwater level fluctuation and rainfall infiltration method (GEC, 2009). The diffuse recharge estimated in this study is comparable with the other studies.

Formation	Specific Yield %	Rainfall mm	Recharge %	Reference
Bhima Limestone	<1			CGWB, 1982.
Bilara Limestone, Jodhpur	7	450	12	Ground Water Department, Rajasthan
Limestone Karnataka	<1	700	11	Central Ground Water Board
Nagaur Limestone, Rajasthan	1	400	2 (0.81*)	United Nations, 1976, cited in Sukheja, et al., 1996.
Carbonates of Cuddapah, Kurnool and Vindhyan	3	-	-	Karanth, 1987
Limestones	2 (range 1-3)		-	GEC, 1984
Karstified limestones	8 (range 5-15)		-	GEC, 1984
Narji Limestone	8		15+13**	This study

Tab. 5.5. Values of specific yield computed from pumping tests and annual recharge and rainfall of carbonate rocks in India. *Average annual groundwater level fluctuation in meters. ** is percent of point+diffuse recharge.

5.2.4. Validation of Recharge Results by Tritium Injection Method

Natural recharge rates were measured by injecting Tritium tracer into the soils north of the study area. The result indicates that an average recharge of 105.4 mm occurred for the monsoonal (effective) rainfall of 585.8 mm. This amount occurs as diffuse recharge through the soil cover in the area and comprises of 18% of the seasonal rainfall and 16% of the annual rainfall. These results also validate the diffuse recharge estimations (13% of annual rainfall) calculated by the soil water balance method. Natural recharge estimated from soil moisture and tritium concentrations is given in Tab. 5.6. Average peak concentrations reached between 1.3-1.7 meters below ground level in the soil columns (Fig. 5.9).

Site	Depth of collection m	Depth of peak conc. m	Peak dispersion m	Volume moisture %	recharge computed mm
1	2.4	1.6-1.7	1.05	12.3	128.9
2	2.8	1.4-1.5	0.84	14.1	119
3	1.6	1.3-1.4	0.75	17.3	129.7
4	2.5	1.4-1.5	0.87	8.0	69.1
5	2.0	1.5-1.6	0.95	10.6	101.0
6	3.0	1.5-1.6	0.95	12.0	114.4

Tab. 5.6. Natural recharge calculated at the injection sites in the area. The site numbers are also the serial number of scatter plots of Fig.5.9.

In semi-arid and arid carbonate areas irrigation return flow contributes a good amount to the aquifer recharge (e.g. Stigter et. al., 2006). Out of the input water (377mm at each input site) about 48-50% of water goes as irrigation return flow in semi arid areas from paddy cultivation (e.g., using a crop coefficient of 0.48-0.51 for paddy, Marechal et. al., 2003; Dewandel et. al., 2008). Therefore, 188mm of water also returns to the aquifer as

return flow from these irrigated crops particularly paddy as the area is mostly utilized for rain fed crops and scattered paddy fields.

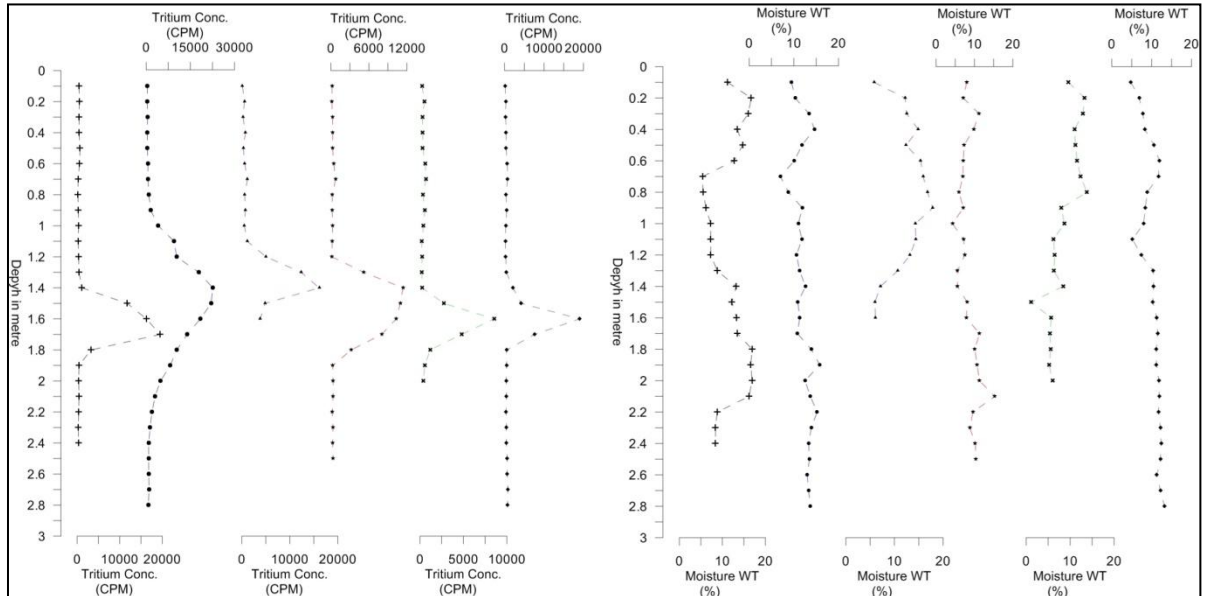


Fig. 5.9. Tritium concentration in counts per minute (CPM) and soil moisture in weight percent measured with depth from the soils cores.

5.3. Impact of Anthropogenic Activities on Groundwater and Recharge

Due to growing urbanization, the karst terrains have faced a number of modifications due to human activities across the globe (LaMoreaux et. al., 1997; Milanovic, 2002; Gao et. al., 2011). Impacts on land surface temperature (Xiao & Weng, 2007), changes in landscape and water quality (Heinz et. al., 2009; Coxon, 2011), increased soil erosion (Urich, 2002), etc have been documented in many karst areas. Construction of dams has serious impacts on karst environment (Bonacci and Rubinic, 2009; Milanovic, 2010).

The mining operations can have many impacts on the hydrogeological regime of the area. Their impact on groundwater recharge and balance needs to be assessed. The limestones of the study area are extensively quarried for extraction of construction slabs and cement manufacture. A number of cement factories are actively removing the limestone and changing the natural landscape of the area. Based on the satellite data, the area around Belum caves shows increasing trend in limestone extraction. The quarry area has increased from 9.7 km² in 1983 to 25.6 km² in 2010; a rate of 0.6 km²/year increase. Soil and weathered part is removed and dumped at other sites creating other problems. The uppermost flaggy part of the aquifer is removed which acts as an infiltration and recharging zone. Quarrying extends up to the water table. Removing of the unsaturated zone of the limestone exposes the main part of the aquifer and thus, decreases the depth to water table. This change in land-cover may have important impact on groundwater recharge and balance. The groundwater levels are shallow in this semi-arid region with high evaporations rates. The depth to water level during pre-monsoon varies from 6.56-20.2 mbgs and decrease by an average of 1.2 m after recharge. Thus, a decrease in the thickness of unsaturated zone may lead to more evaporation losses from the water table directly (e.g., Coudrain-Ribstein et. al., 1998; Maréchal et. al., 2006). Rainwater gets stored in the quarry depressions and may directly enter the aquifer without traveling through the soil and epikarst zone. This can lead to an increase in the amount of fast recharge and thus, have many consequences on the groundwater budget of the area.

Practicing agriculture in karst areas also creates number of implications (Boyer and Pasquarrel, 1996). The limestone area is also used for intensive irrigated agriculture (mainly paddy) which depends mainly on groundwater. It may cause more withdrawal of water as

more water is needed for rice production in karst areas (e.g., Ford and Williams, 2007). Dumping of domestics and other waste in the abandoned quarry depressions in the area could also have some serious implications on water quality. Restoration of the quarried areas for agriculture and other activities is very difficult in these areas as it needs lot of organic material to restore fertility of soils (e.g., Jordan et. al., 2008).

5.4. Summary

Groundwater recharge is an important process that replenishes the aquifer through surface and rainwater. It is very difficult to estimate recharge of highly heterogeneous karst aquifers in semi-arid climates. The recharge processes are complex due to climatic and karst hydrogeological peculiarities. Karst aquifer in this semi-arid area is recharged mainly by point and diffuse recharge. Point recharge is the major contributor and enters the aquifer as allogenic inputs. The surface runoff from non-karstic areas reaches the aquifer by fast mechanism ^{through} preferential pathways. Average annual point recharge of the aquifer is about 107.3mm i.e., 15% of the annual rainfall amount. This part of the recharge replenishes the groundwater very rapidly. Diffuse recharge enters the aquifer through the soil and epikarst zone. This part of infiltrating water gets stored in the epikarst and then reaches the phreatic part very late. This process depends on the soil properties and climatic conditions of the area. Diffuse recharge of 86mm i.e., 13% of annual rainfall replenishes the aquifer. The amount of diffuse recharge depends on the frequency and intensity of rainfall. Average annual recharge (sum of point and diffuse recharge) of this semi-arid limestone aquifer is 29% of the rainfall. The results of the recharge estimation were calibrated with the water levels of the borewells. The recharge estimates from nearby area covering limestone and quartzites showed that annual diffuse recharge through soils is about 105mm. Diffuse

recharge of 16% of the annual rainfall estimated by Tritium injection method validates the recharge results. The results showed that irrigation return flow also contributes to these limestone areas particularly from paddy fields. The amount of internal runoff, another type of recharge in karst areas through cave openings, etc has very less impact on the groundwater balance of the area. Annual recharge occurs during 5-7 important events in the year in which rainfall is more than 25mm a day. The high value of point recharge has a large effect on the hydrodynamics and hydrochemistry of the aquifer.

CHAPTER 6

HYDROGEOCHEMICAL CHARACTERISTICS OF KARST AQUIFER

6.1. Introduction

Groundwater dissolution of carbonate rocks creates a typical karst landscape which is characterized by the specific surface and subsurface features as described in chapter 4. The dissolutional characteristics, a different mode of subsurface water flow and a highly heterogeneous and anisotropic permeability make them different from fissured and porous aquifers. Their hydrogeochemical characteristics are quite different (Romanov et. al., 2003). The chemographs of karst springs show high-amplitude changes by the recharging water (Ryan and Meiman, 1996).

Karst aquifers are more vulnerable to pollution as the pollutants are readily conducted through unique karst structures, like swallow holes, dolines, etc (Doerfliger et. al., 1999; Kaçaroglu, 1999). There are a number of reasons for this high vulnerability (Field, 1993 and 1997; Toran and White, 2005) which include: fast recharge which bypass the filtering capability; conduit flow provides little opportunity for filtration or sorption of contaminants; pollutants are not retarded by chemical reactions or other attenuation mechanisms, such as acid-base reactions, adsorption, ion exchange, precipitation or bacteriological degradation due to fast flow velocities; pollutants are not diluted through dispersal due to flow in converging conduits, etc. The contaminants are rapidly transported to spring outlets. A comprehensive protection and control mechanism is required to consider this vulnerability to preserve the quality and quantity of groundwater (Kaçaroglu, 1999).

A number of inter-related processes govern the physical and chemical characteristics of groundwater in karst aquifers (Freeze and Cherry, 1979; Jeong, 2001; Wu et. al., 2009). These include atmospheric inputs, chemical quality of recharging water, chemical and mineral composition of the parent rocks, predominant geochemical processes, residence time and water and rock interactions during the flow processes. The proportion of calcite and dolomite in an aquifer material (Fairchild et. al., 2000) and dissolution kinetics of calcite and dolomite (White, 1988) are one of the basic factors influencing the chemical composition of waters. Calcite dissolves more quickly and is capable of reaching equilibrium in few days than dolomite. PCO_2 is also an important factor governing water chemistry variation in karst (Plummer et. al., 1978; Dreybrodt, 1981; Buhmann and Dreybrodt, 1985).

The hydrochemical behaviour is also controlled by the nature of recharge and the degree of karstification (Ford and Williams, 2007; Bakalowicz, 2005; Karimi et. al., 2005; Valdesa et. al., 2007). Contaminants easily enter the karst aquifers and transport by a variety of mechanisms depending on the physical and chemical properties of the contaminant (Vesper, et al., 2003). The concentrating and fast recharge collect a large load of sediments, pesticides, fertilizers and bacteria which adversely degrade the water quality. Land surface and anthropogenic activities provide additional chemicals from septic tanks, cesspools and agricultural practices and thus, may affect the quality of water.

In this chapter hydrochemistry is used to understand the source of major ions in karst water and also the processes modifying the groundwater chemistry in relation to space and time. For this purpose a karst area of Proterozoic sedimentary basin in southern India has

been chosen (Fig. 6.1 and 6.2). In order to check the quality of the analysis, the ionic balance was computed for each sample. The charge balance error of analysis (acceptable range 0-5%) was found to be 3.9%. The linear regression of cation sum to anion sum gives $R^2 = 0.91$ (Fig. 6.3).

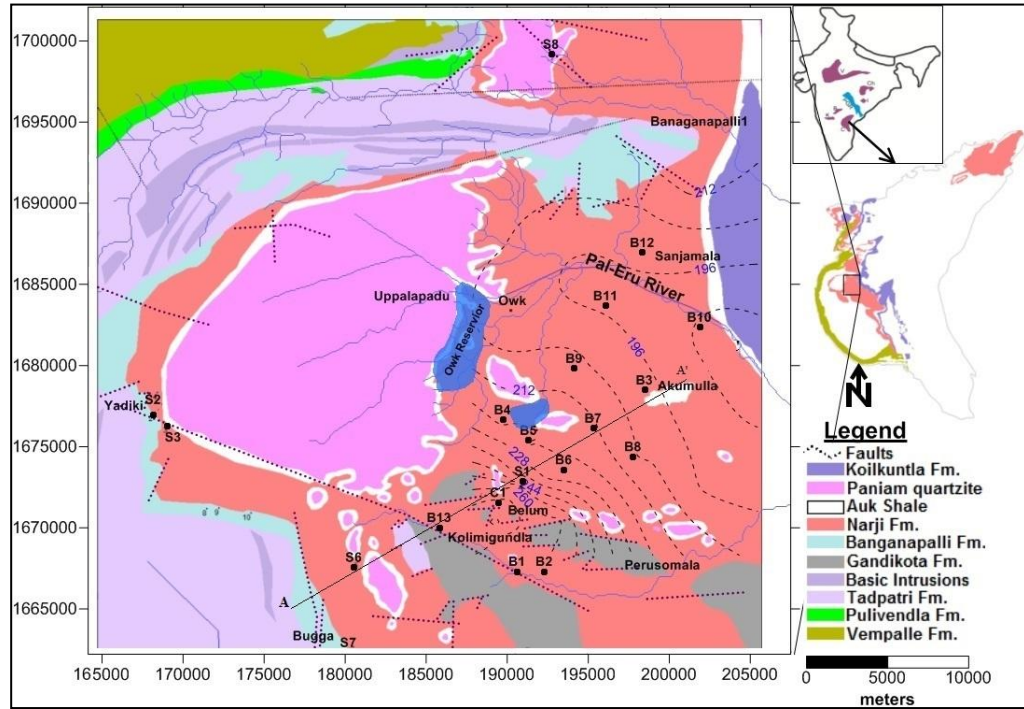


Fig. 6.1. Geological map of the karstified area. Three karstified formations of Cuddapah Basin are also shown (modified after GSI, 1997). Black dashed contours represent the water level in masl. Spring and bore well samples are represented by solid circles. Major surface drainage is shown by blue lines.

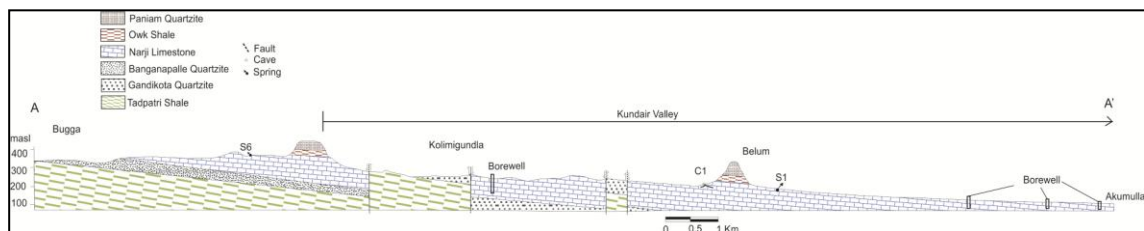


Fig. 6.2 Geological cross-section along the karstic terrain, showing the Narji limestone aquifer and location of some springs and bore wells.

6.2. Physical Parameters

The results of PRM and POM water chemistry data of 2011 (Appendix 10 and 11) were transformed into descriptive statistics (minimum, maximum, average and standard deviation) for common samples and removing the samples with large human influence as given in Tab. 6.1:

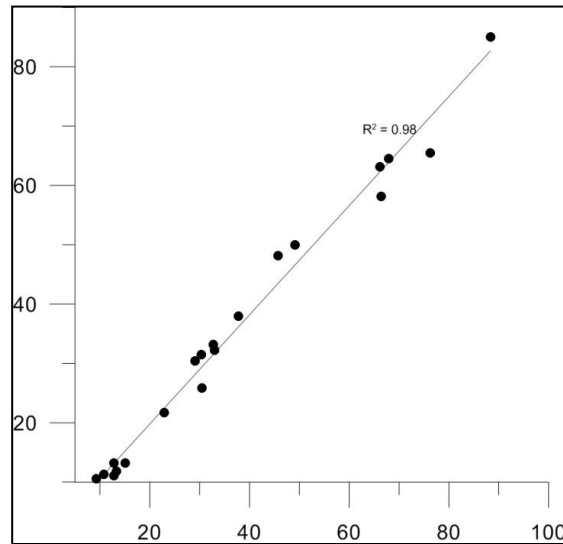


Fig.6.3. Scatter plot showing cations sum Vs anions sum for pre-monsoon (PRM) and post-monsoon (POM) samples. Good correlation indicates the quality of water chemistry analysis.

pH values were measured in-situ and range from 6.79 to 7.67 and 7.22 to 7.93 with a mean value of 7.2 and 7.48 during PRM and POM respectively (Tab. 6.1). Groundwater thus, is mildly acidic to slightly alkaline in nature. Temperature of groundwater has a mean value of 29.8 and 27.9 during PRM and POM season. A decrease in water temperature increases solubility of CO_2 , increases the equilibrium concentrations of ions (Langmuir, 1968; Palmer and Cherry, 1984) and reduces the dissolution rates of minerals (Herman and White, 1985). Specific electrical conductivity indicates the nature of groundwater since it is

related to the total concentration of charged particles in water. EC values range between 538-2013 and 422-1703 $\mu\text{S}/\text{cm}$ during PRM and POM. The mean values are 1141.7 and 942.5 $\mu\text{S}/\text{cm}$ respectively. The shift of EC values form higher to lower classes during POM

	PRM 2011 (11)				POM 2011 (11)			
	Min	Max	Mean	CV	Min	Max	Mean	CV
T	28.30	32.50	30.01	4.94	25.20	30.50	27.92	6.59
pH	6.79	7.67	7.24	3.21	7.22	7.93	7.48	3.04
EC	538.00	2013.00	1141.75	43.88	442.00	1703.00	942.55	48.55
TDS	370.95	1557.86	826.81	49.64	304.76	1317.95	677.81	54.02
Ca ²⁺	34.88	123.38	73.26	35.44	48.03	245.22	111.81	46.59
Mg ²⁺	16.82	53.81	27.60	45.43	3.70	21.12	9.96	57.03
Na ⁺	34.13	406.10	139.46	81.91	11.94	206.49	53.06	116.75
K ⁺	2.31	31.77	9.68	84.75	0.27	14.90	3.49	143.72
HCO ₃ ⁻	236.11	710.63	410.59	38.84	121.39	458.37	210.29	48.37
F ⁻	0.39	1.56	0.93	35.21	0.19	1.40	0.65	57.98
Cl ⁻	13.07	368.22	135.33	88.16	32.28	248.32	100.03	76.69
NO ₃ ⁻	4.39	120.40	27.42	113.57	28.23	119.33	51.89	47.08
SO ₄ ²⁻	2.85	131.02	54.60	82.82	22.02	160.06	53.17	72.82
Hardness	211.03	131.02	54.60	82.82	164.74	658.63	320.36	40.69
Ca ²⁺ /Mg ²⁺	0.39	4.45	1.99	59.87	1.70	21.93	8.94	64.10

Tab. 6.1. Statistical analysis of chemical parameters of groundwater for PRM and POM seasons. Number in brackets indicates the number of samples. T in °C, EC in μcm and ion concentration in mg/l except Ca²⁺/Mg²⁺ ratio. Number of samples is given in braces.

are due to the release of chemically rich water from storage which later dilutes due to monsoon recharge. The EC values of majority of the samples remain above 500 $\mu\text{S}/\text{cm}$ during both PRM and POM, which indicates that the waters remain saturated with respect to CaCO₃ (e.g, Jacobson and Langmuir, 1974b).

Total dissolved solids (TDS) consist mainly of inorganic salts (carbonates, bicarbonates, chlorides, sulphates, phosphates, nitrates, etc) together with small amount of

organic matter and dissolved gases. TDS in the groundwater varies from 370.9 to 1557.8 mg/l during PRM and 304.7 to 1317.9 mg/l during POM season. The TDS values of well waters are generally higher (mean 1373 and 484 mg/l) than spring waters (mean 1021 and 465 mg/l) during PRM and POM season respectively (Tab. 6.1).

6.3. Chemical Parameters

Ca^{2+} is higher during POM (average 111.8 mg/l, Tab. 6.1). The mean values of Mg^{2+} are respectively 27.6 and 9.9 mg/l during PRM and POM. Na^+ is higher in PRM season (average of 139.5 mg/L) than POM (average 53 mg/l). K^+ is also higher in PRM season (average 9.7 mg/L) than POM (average 3.5 mg/L). As the aquifer material contains significant quantities of clay minerals their weathering can be a cause of high values of both Na^+ and K^+ (e.g., Hem, 1985). Higher HCO_3^- was observed during PRM which varies from 236-710 (mean 410.6 mg/l). While in POM season the values range from 121.4 to 458.4 with a mean of 210.3 mg/l. This indicates the storage of more mineralized water during PRM and dilution effect due to recharging water. However, not only simple dilution but equilibrium with respect to calcite could be a likely controlling factor of calcium variation (Toran and White, 2005). F^- varies from 0.4 to 1.6 and 0.2 to 1.4 mg/l during PRM and POM respectively. The sources of fluoride in groundwater in most studies include fluoride bearing rocks, long-term irrigation practices, semi-arid climates and long residence time of groundwater along with alkaline soils (Handa, 1975). Higher concentrations of fluorine have been associated with higher TDS value in many areas (Jain et. al., 2009). Cl^- is higher in PRM season (average 135 mg/l) than POM (mean 100mg/l). Nitrate concentrations are also high in the area. In karst areas, agriculture contributes nitrate as a common groundwater

contaminant derived from leaching processes from plant nutrients, animal-waste and nitrate fertilizers (Freeze and Cherry, 1979; Peterson et. al., 2000; Kingsbury and Shelton, 2002). It is linearly correlated with the percent of agriculture (e.g., Boyer and Pasquarell, 1996). High nitrate concentration above 20 mg/l indicates influence of human activities in the area (Spalding and Exner, 1993). SO_4^{2-} is higher in PRM season (mean 54.6 mg/l) than POM. Agricultural usually contribute higher concentrations of sulfates in most groundwater of the world (Langmuir, 1971). High sulfate concentrations are found in most karst waters which affect the dissolution by removal of sulfates along with carbonates (Worthington and Ford, 1995). Chloride also shows an increase with increased sulphate concentration which implies the effect of surface contamination, especially from fertilizer application. This is also indicated by an increase of nitrate concentration. Both the seasons records higher concentration of TH (hard water >200 mg/l of CaCO_3) which is the effect of dissolution process in carbonate rocks.

6.4. Spatial Variability of Water Quality

In order to observe the spatial changes in groundwater chemistry major ion data was interpreted using Piper diagram (Piper, 1953; Freeze and Cherry, 1979). The diagram plots geochemically similar water types in defined areas and explains the mixing phenomena (Deutsch, 1997).

The Piper diagram shows a large variability in the water chemistry of the area. During PRM, 67% of the samples fall in Ca triangle and rest of samples did not show any dominant signature (Fig. 6.4a). Among anionic species, 33% of samples are Cl type, 33% bicarbonate type and rest of the samples show mixed character. During POM (Fig. 6.4b)

92% of the samples shift towards the Ca-type in case of cationic species and 33% towards HCO_3^- and 67% towards mixed nature in case of anionic species.

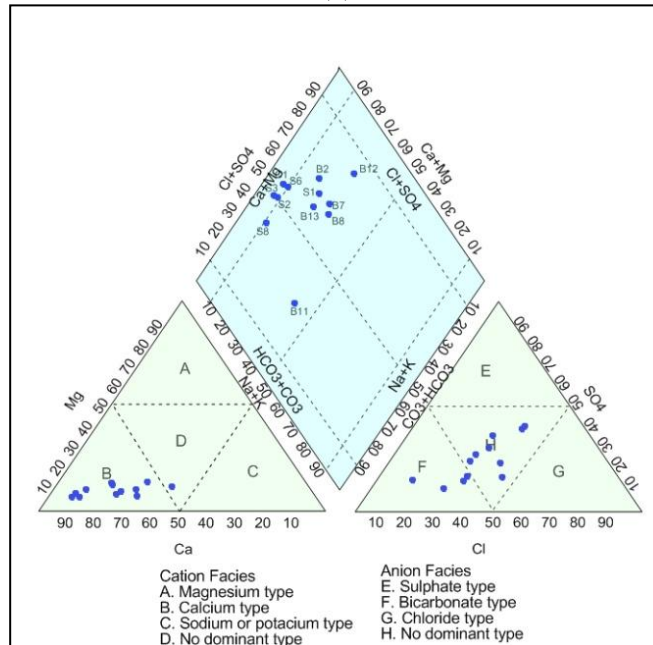
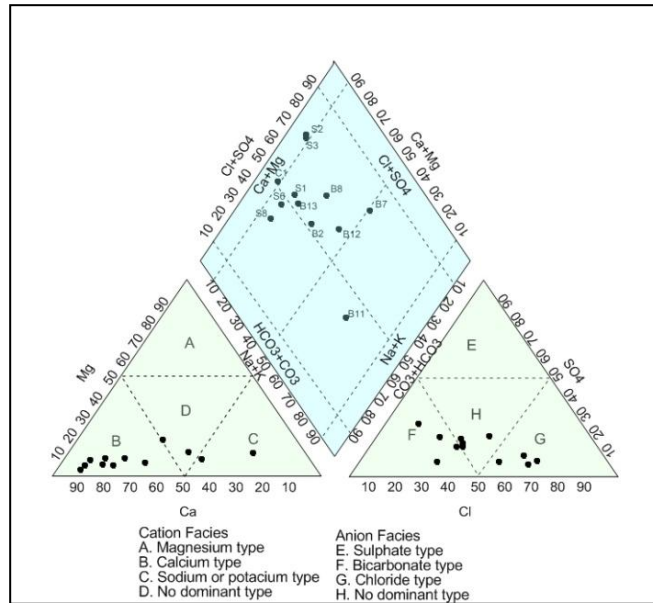


Fig. 6.4. Hydrochemical facies showing the spatial variability of spring and bore well waters on Piper Diagram (a) PRM and (b) POM samples.

The karst waters showed no major water types (Tab. 6.2). Ca-HCO₃-Cl waters are represented by 42% of samples and include S1, S6, B2, B8 and B13 samples. S8 is of Ca-HCO₃ type, S2 and S3 are of Ca-Cl type in which average Ca²⁺+Mg²⁺+HCO₃⁻ constitutes 83% of total ions. B7 is Ca-Na-Cl type, B13 is of Ca-Na-HCO₃-Cl type and B11 of Na-HCO₃ type.

ID	Name	Water Type	
		PRM	POM
S1	Belum Spring	Ca-HCO3-Cl	Ca-Na-HCO3-Cl-SO4
S2	Yadiki Spring 1	Ca-Cl-HCO3	Ca-HCO3-Cl
S3	Yadiki Spring 2	Ca-Cl-HCO3	Ca-HCO3-Cl
S6	Rati Spring	Ca-HCO3	Ca-HCO3-Cl
S8	Yaganti Spring	Ca-HCO3-Cl	Ca-HCO3-Cl
B2	BW	Ca-Na-HCO3-Cl	Ca-SO4-HCO3-Cl
B7	HP	Na-Ca-Cl-HCO3	Ca-Na-Cl-HCO3-SO4
B8	HP	Ca-Na-Cl-HCO3	Ca-Na-Cl-HCO3
B11	HP	Na-Ca-HCO3-SO4	Ca-Na-HCO3
B12	BW	Ca-Na-Cl-HCO3	Ca-Na-Cl-SO4
B13	HP	Ca-Na-HCO3-Cl	Ca-Na-HCO3-Cl-SO4

Tab. 6.2. Water types as observed in the spring and bore well waters for the two seasons.

From the Piper diagram, no major water grouping was distinguished for the samples. However, spring waters from Belum S1, Kona S2, Kona S3, Rati S6 and bore well B13 can be separated into a major group. The Kona springs S2, S3 are less affected by the human activities and are hydrogeologically separated from the rest of the samples. The discharge of spring S2 (Fig. 5) do not show any marked variation. Diffuse recharge and diffuse flow in these springs develops less change in chemistry after recharge. The reason for very high

concentration of certain ions in B7 is not known however; the sample was collected from a village hand pump which could have large human influence. B11 and B12 are located in agriculturally cultivated area. C1 has a large human impact and is fed by sewage from the cave area. All springs lie in the field of $\text{Ca}^{2+} + \text{Mg}^{2+} > 70\%$. Bore well samples B11 and B12 have a large influence from agriculture as they were collected from paddy fields. Average concentration of agriculture related parameters in these samples is very high (Na^+ 355, Cl^- 299, NO_3^- 113, SO_4^{2-} 183 mg/l) compared with other samples. C1 has a large human influence caused by sewage effluent (near Belum Cave entrance). It showed very high concentration of Cl^- , NO_3^- and SO_4^{2-} which is comparable with the B11 and B12 and hence, was not used for statistical analysis. S6 shows very high concentration of Ca^{2+} which may be due to more dissolution in the rock as the spring flows from the epikarst zone of the aquifer. A very large increase in the $\text{Ca}^{2+}/\text{Mg}^{2+}$ ratio of S2, S3 and S8 during POM indicates more dissolution of the rock.

During POM majority of samples shift towards the Ca-HCO₃-Cl type (Fig. 4b). S8 fall in the pure Ca-HCO₃ type field and do not show any change in water type during POM. In case of samples B2 and B13, HCO₃ ions gets exchanged and water becomes Ca-Cl type during POM season.

Thus, spatial variations in groundwater chemistry are mainly due to chemical processes and land use. Dissolution is the most important chemical process in the generation of high Ca^{2+} and HCO_3^- ions. It is observed that groundwater and surface reservoir water is utilized for irrigation purposes. Fertilizers along with liquid sprays and manure could cause an increase in concentration of nitrogen, phosphate and potassium. Agricultural usually

contributes higher concentrations of sulfates in groundwater (e.g., Langmuir, 1971). High sulfate values are frequently found in carbonate aquifers. However, the carbonate rock rarely contains measurable concentrations of sulfur minerals (few beds possess pyrite crystals, Kumar, 1983). Fertilizers along with liquid sprays and manure could cause an increase in concentration of nitrogen, phosphate and potassium. Thus, land use is the main cause of spatial variability for such parameters particularly in the northern part. Both the seasons records higher concentration of TH (hard water >200 mg/l of CaCO_3) which is the effect of dissolution process in carbonate rocks. In semi-arid climates, the return flow particularly from paddy can contribute concentrated amount of ions. The high evaporation process in semi-arid areas causes enrichment of ions in groundwater as observed by high TDS values.

6.5. Seasonal (PRM-POM) Variability of Water Quality

Major ion data was used to understand the spatial, seasonal and temporal changes in groundwater chemistry. The chemical variation from PRM to POM is quite clear in most of the samples. The difference in concentration of chemical parameters from PRM to POM (expressed as percent) for springs and wells is shown in Tab. 6.2.

The slight decrease in temperature, EC and TDS during POM is due to the fresh recharging water that dilutes the more mineralized water from storage. EC of all samples remain above $500 \mu\text{S}/\text{cm}$ (average $1319 \mu\text{S}/\text{cm}$) during PRM and slightly below in POM (average $1060 \mu\text{S}/\text{cm}$). The higher TDS values in the area could be attributed to semi-arid conditions; less rainfall, more evaporation (Tizro and Voudouris, 2008).

Spring/ Bore well	Dissolution related			Agriculture and land use related									
	Ca ²⁺	Mg ²⁺	HCO ₃ ⁻	Na ⁺	K ⁺	Cl ⁻	NO ₃ ⁻	SO ₄ ²⁻	TH	Ca ²⁺ /Mg ²⁺	EC	TDS	T
Belum	-68	69	55	56	73	-79	-247	-526	-21	-438	15	15	7
Kona 1	-93	78	65	63	92	-968	-612	-1118	-44	-789	3	3	0
Kona 2	-196	-28	-14	10	-15	-1097	-1435	88	-147	-125	23	23	0
Rati	29	78	40	83	81	82	-148	70	39	-220	-7	-7	15
Yaganti	-79	67	35	61	79	9	-130	7	-20	-438	0	0	7
B2	35	69	80	79	-70	35	16	7	49	-109	56	56	12
B7	-117	48	-20	41	-33	-3	81	46	-34	-320	23	23	2
B8	-4	41	33	19	18	-16	-53	9	4	-78	0	0	-1
B11	2	57	20	19	72	76	57	-83	33	-125	21	28	12
B12	-245	61	53	67	97	37	-133	56	-26	-780	15	15	12
B13	-24	81	72	78	97	67	-402	-85	25	-549	45	45	0

Tab. 6.2. Difference in ionic concentration in percent from PRM to POM (Pre minus Post/Pre*100). Positive values indicate a decrease in concentration and negative values indicate an increase in concentration during POM season.

The dilution effect is also found by the decrease of Mg²⁺, HCO₃⁻ during POM season. An increase of Ca²⁺ in majority of samples does not indicate dilution. Thus, not only simple dilution but equilibrium with respect to calcite could be a likely controlling factor of chemical variation (Toran and White, 2005).

In karst areas, where agriculture is a dominant practice, nitrate is a common groundwater contaminant (Kingsbury and Shelton, 2002) and linearly correlated with the percent of agriculture (e.g., Boyer and Pasquarell, 1996). The high concentration of nitrates in POM can be due to warm and moist soil conditions that are suitable for nitrification of soil organic-N (Kingsbury, 2008) and decreased N uptake as a result of crop harvest in the area.

The springs are hydrogeologically separated from the rest of the samples except B8. S2 is a permanent spring showing less variability in discharge and chemistry (Fig. 5) whereas S3 and S6 flow with less than a 1/s discharge round the year. Spring waters except S1 and S6 are colorless, odorless throughout the year. S1 flows with a high turbidity during monsoon months. It carries a lot of sediments collected from the highly karstified areas through sink holes. S6 discharges from the epikarst layer of the aquifer. In case of S1, B2 and B13 the area is hydrogeologically more complex than the other area. The area possesses a number of surface and sub-surface karst features. Concentrated recharge is the main contributor of the groundwater along with diffuse recharge through the soil cover. The area is mostly used for rain fed agriculture along with some isolated paddy and vegetable fields. S1 has a large human influence as the spring is located within a village and possibly connected underground through conduits with the Belum cave stream (C1 sample). S8 is also a permanent spring from the same limestone but has no hydrological connectivity with the rest of the sampled points. Borehole samples from the northern area show higher concentration in agriculture related parameters compared to the ones located in the southern area. The reason for this high concentration is that the northern area is highly cultivated for the paddy crop round the year.

Chemical parameters were divided into dissolution-related and agriculture and land use related parameters. For springs and bore wells during PRM and POM the mean and CV is given in Tab. 6.4. Agriculture related parameters, like K^+ , Na^+ , Cl^- , Mg^{2+} , NO_3^- and SO_4^{2-} show more variability during both seasons. However, springs show less variability in dissolution related parameters.

			Dissolution-related			Agriculture, land use-related					
			Ca ²⁺	Mg ²⁺	HCO ₃ ⁻	Na ⁺	K ⁺	Cl ⁻	NO ₃ ⁻	SO ₄ ²⁻	EC
Springs (5)	PRM	Mean	73.6	20	320	64.8	6.34	62.3	14.2	36.1	702
		CV	33.9	16.6	19.1	41.8	48.1	96.5	47.2	134	20.8
	POM	Mean	137	6.81	176	21.7	1.81	107	63.9	36.7	675
		CV	46	45.9	26.5	28.6	58.9	82.4	49	26.8	14.4
Bore wells (6)	PRM	Mean	87.2	28.6	437	135	13.2	121	67.7	55	1526
		CV	25.1	30	36.9	56	62.6	84.9	111	80.7	30.6
	POM	Mean	96.7	14.8	252	106	9.76	143	44.5	71	1381
		CV	39.7	40.8	49.7	72.1	120	87.6	22.7	67	65.9

Tab. 6.4. Mean and coefficient of variation of different ions in spring and bore well samples during PRM and POM. Mean is expressed in mg/l and CV as percentage. Number of samples is given in parenthesis.

Correlation matrix of the parameters for PRM and POM samples is shown in Tab. 6.5. A statistically good correlation with R² more than 0.6, was observed between different parameters (shaded cells). TDS shows positive correlation with Ca²⁺, Mg²⁺, Cl⁻, and SO₄²⁻, Br⁻ and TH is correlated with EC and TDS during both seasons. Cl⁻ shows good correlation with SO₄²⁻ and TH. NO₃⁻ is correlated with SO₄²⁻ and TH. The positive relation of TDS and nitrate during POM and no such relation in PRM indicate the agricultural source of nitrate.

6.6. Temporal Variability of Water Quality

The intra-site variability of chemical parameters for S1, S2 and S8 is shown in Fig. 6.5. Belum spring S1 shows sharp change in flow and chemistry during monsoon months. Most of the time spring remains in non-flowing condition and gets large influence from human activities. During high rainy events the discharge reaches up to 50 l/s which sharply decrease after rainfall. During periods of high recharge, ionic concentrations decreased to the lowest for S1 but increased sharply to a maximum during non-flowing conditions. Dilution effect is

the main reason for sharp decrease in chemistry during monsoon months in the springs. The catchment area of the spring gets faster recharge than other springs. Fast recharge is the main cause of large temporal variations in groundwater chemistry. The rapid change in chemistry in S1 reflects dilution and rapid flow-through time, which result in low ionic concentrations during high recharge periods. This also reflects the short residence time of groundwater.

	pH	EC	TDS	Ca ²⁺	Mg ²⁺	Na ⁺	K ⁻	HCO ₃ ⁻	F ⁻	Cl ⁻	NO ₃ ⁻	SO ₄ ²⁻	Br ⁻	TH
pH	1.00 1.00													
EC	-0.35 -0.47	1.00 1.00												
TDS	-0.35 -0.47	1.00 1.00	1.00 1.00											
Ca ²⁺	-0.05 -0.42	0.83 0.80	0.82 0.79	1.00 1.00										
Mg ²⁺	-0.32 -0.45	0.78 0.67	0.78 0.67	0.67 0.43	1.00 1.00									
Na ⁺	-0.24 -0.44	0.37 0.67	0.38 0.65	0.10 0.47	0.73 0.83	1.00 1.00								
K ⁻	-0.01 -0.34	0.71 0.17	0.72 0.17	0.39 -0.1	0.52 0.02	0.57 0.08	1.00 1.00							
HCO ₃ ⁻	-0.12 -0.09	-0.0 0.43	-0.0 0.39	-0.1 0.33	0.41 0.56	0.73 0.67	0.24 -0.1	1.00 1.00						
F ⁻	0.08 0.46	0.19 -0.3	0.21 -0.3	0.12 -0.1	0.60 -0.19	0.86 0.14	0.38 -0.2	0.64 0.39	1.00 1.00					
Cl ⁻	-0.14 -0.54	0.64 0.81	0.64 0.82	0.39 0.71	0.86 0.50	0.92 0.51	0.75 0.45	0.58 -0.02	0.79 -0.5	1.00 1.00				
NO ₃ ⁻	-0.65 -0.60	0.56 0.90	0.56 0.90	0.52 0.80	0.74 0.65	0.49 0.67	0.15 0.02	0.39 0.29	0.36 -0.2	0.46 0.75	1.00 1.00			
SO ₄ ²⁻	-0.47 -0.40	0.77 0.61	0.79 0.63	0.51 0.28	0.86 0.73	0.79 0.57	0.66 0.29	0.34 -0.06	0.59 -0.5	0.84 0.72	0.73 0.63	1.00 1.00		
Br ⁻	0.16 -0.70	0.37 0.80	0.38 0.79	0.18 0.63	0.50 0.77	0.50 0.86	0.55 0.31	0.20 0.32	0.52 -0.2	0.59 0.81	0.22 0.86	0.44 0.76	1.00 1.00	
TH	-0.24 -0.50	0.86 0.88	0.86 0.87	0.85 0.93	0.96 0.73	0.56 0.70	0.51 -0.0	0.24 0.48	0.47 -0.1	0.76 0.74	0.72 0.87	0.80 0.51	0.42 0.79	1.00 1.00

Tab. 6.5. Correlation matrix between different groundwater chemical parameters. The top value in each row represents PRM season and bottom values POM season. TH is total hardness as CaCO₃.

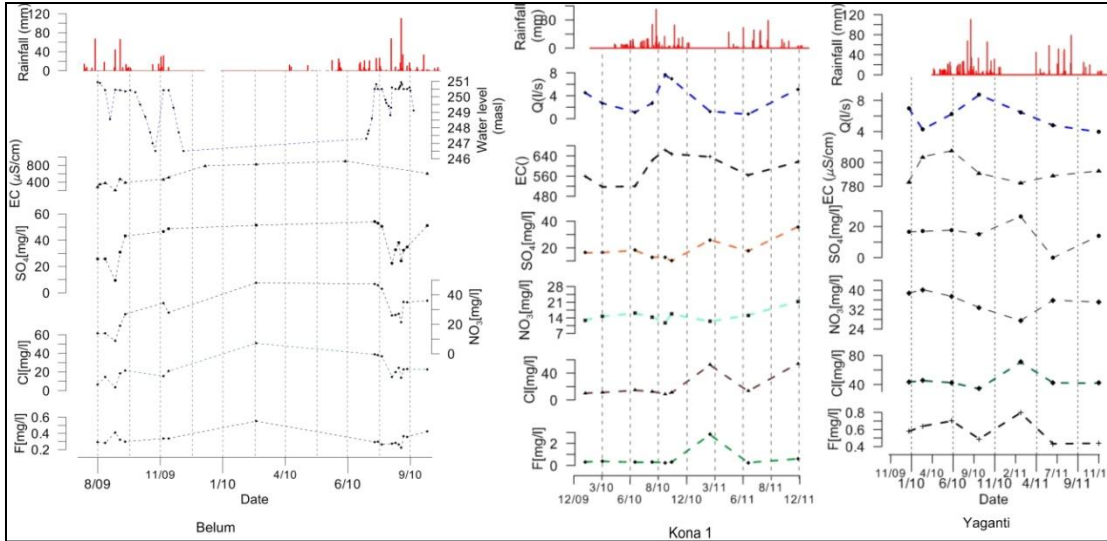


Fig. 6.5. Intra-site temporal variability of physico-chemical parameters in springs (S1, S2, S8). Water level was used for Belum spring (S1) whereas discharge was compared for others springs.

The intra-site temporal variability of different constituents was observed by comparing the coefficient of variation (CV) in percentage (Tab. 6.6. and Fig. 6.6). The most sensitive springs are S1, S2 and S6. S1 shows high variability in discharge and chemistry than other springs. The less seasonal fluctuations in chemistry of other springs indicate a longer residence time. The mineralogical controls and longer residence time may be responsible for the production of Ca-Mg-HCO₃ type water from calcite and dolomite dissolution in S2 and S2 springs. S1 and S6 are more sensitive to EC, NO₃⁻ and SO₄²⁻ ions.

	S1		S2		S3		S6		S8	
	Mean	CV	Mean	CV	Mean	CV	Mean	CV	Mean	CV
Q	-	-	3.6	69.4	0.5	47.5	8.4	59.8	6.1	27.3
EC	615.8	56.9	593.9	9.3	641.9	4.3	568.8	11.8	792.6	1.2
Cl ⁻	28.9	63.9	20.8	88.9	20.6	79.5	39.3	110.7	45.7	25.4
NO ₃ ⁻	31.4	42.3	14.9	18.6	40.5	38.3	18.9	60.1	35.4	11.9
SO ₄ ²⁻	42	33.2	18.4	43.2	14.8	71.5	62.5	36.1	17.8	25.2
HCO ₃ ⁻	255.4	69.2	266.6	56.7	208	31.3	189.7	28.4	342.6	8.9
pH	7.5	4.4	7.3	9.5	7.3	3.6	7.6	2.7	6.9	7.5
T	29.2	4.5	30.2	3.9	30.5	5.4	28.4	7.4	32	2.6

Tab. 6.6. Mean and coefficient of variation CV (%) of different physico-chemical parameters showing intra-site temporal variability in karst springs. Q in (l/s, T in °C, EC in µS/cm and ion concentration in mg/l.

6.7. Hydrochemical Evolution

To assess the chemical evolution of groundwater from PRM to POM season LL-diagram (Langelier and Ludwig, 1941) was plotted for equivalent ratios of ions (Fig. 6.7). The diagram shows a broader scatter and samples fall in all the major fields during PRM.

The central part of the diagram is occupied by majority of the samples which depicts mixed chemical characteristics. The scatter plot (Fig. 6.7) shows that groundwater is influenced by dissolution of gypsum/anhydrite (indicated by I), carbonate dissolution (II) and silicate dissolution (III). Most of the samples are dominated by the carbonate and silicate dissolution. About 58% of samples are of bicarbonate alkali type. Two samples (B7, C1) are dominated by gypsum dissolution. B11 lies close to the typical meteoric water character.

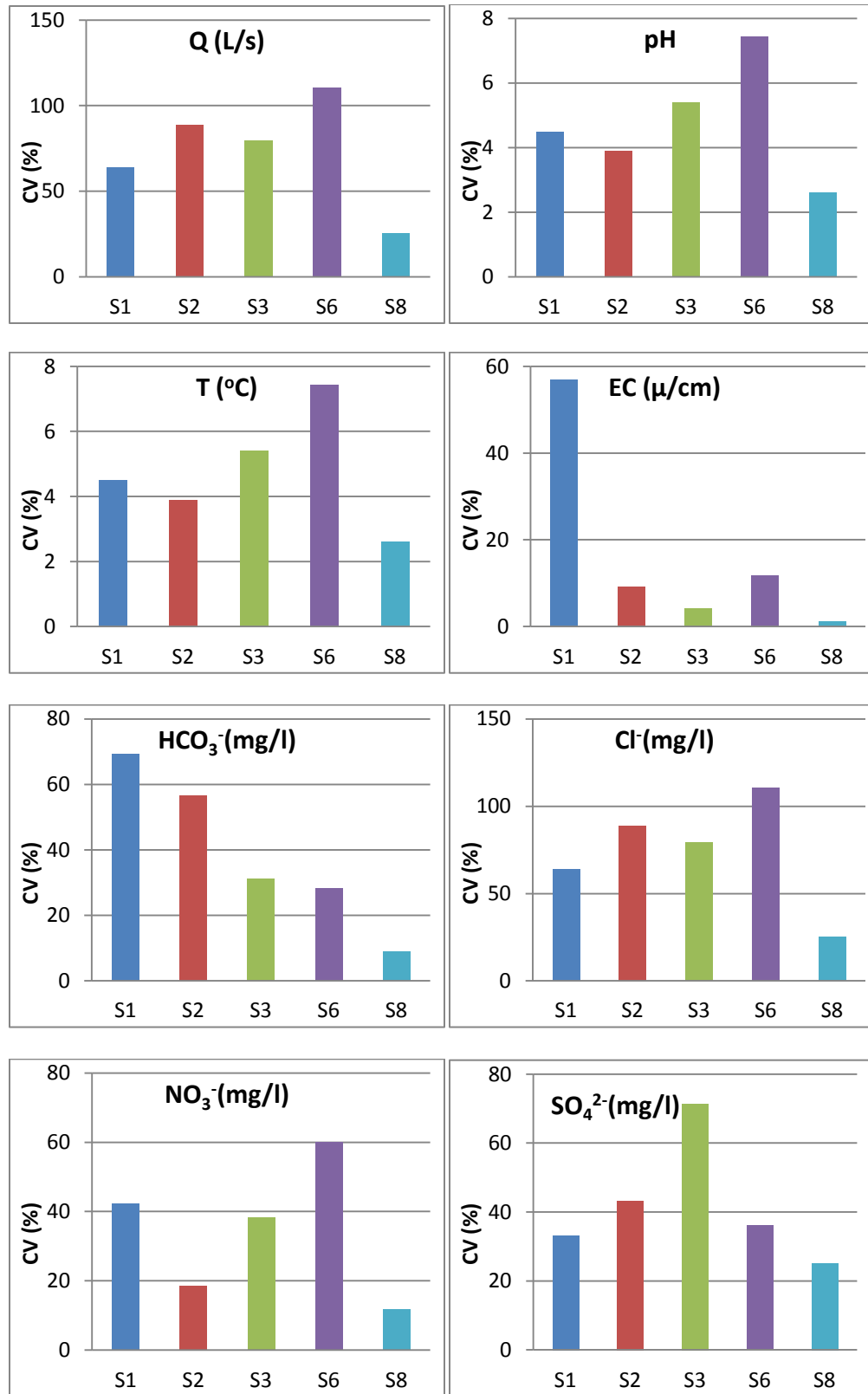


Fig. 6.6. Temporal variability as indicated by the CV (%) of physico-chemical parameters in karst springs.

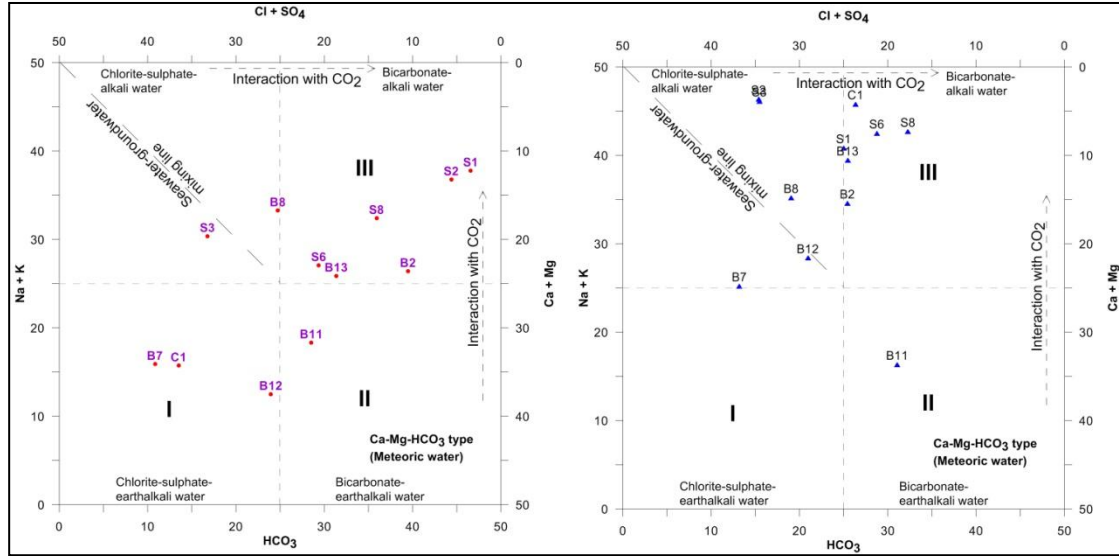


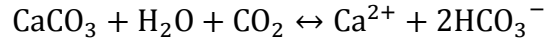
Fig. 6.7. Hydrogeochemical evolution of groundwater during PRM and POM using LL-Diagram. The pink lines indicate the possible shift of chemistry from mixed character to Ca-Mg dominated field.

During POM, a completely different scenario is observed with a significant diagonal shift towards the upper half of the diagram in which bicarbonates and major alkali are the dominant ions. Interaction with CO₂ causes more dissolution and release of bicarbonates. S1, S6, B2 and B13 samples are located in highly karstified area. During POM season B7, B12, B8, S2 and S3 shift towards the chlorite-sulphate-alkali water type and showed an increase in Cl⁻+SO₄²⁻ and Na⁺+K⁺ concentration. B8 and B12 are affected by agricultural practices of the area and B7 is influenced by humans as the sample was collected from village hand pump.

6.8. Water–rock Interaction in Karst Aquifer

The source of Ca²⁺ and Mg²⁺ in carbonate waters is generally the dissolution of calcite and dolomite minerals of the rocks. Thus, chemical composition of water is used to infer the processes of mineral dissolution and water-rock interaction. The general equilibrium

reaction of limestone dissolution, if dolomite part is negligible is expressed by the following reaction,



According to the equation the dissolution of calcite releases equivalent charge ratio 1:1 of Ca^{2+} and HCO_3^- . The large scatter of samples about 1:1 line indicate that Mg is also added to the groundwater system in suitable amounts (Fig. 6.8). Hence, another source should contribute extra calcium and magnesium (e.g. Wu, 2009).

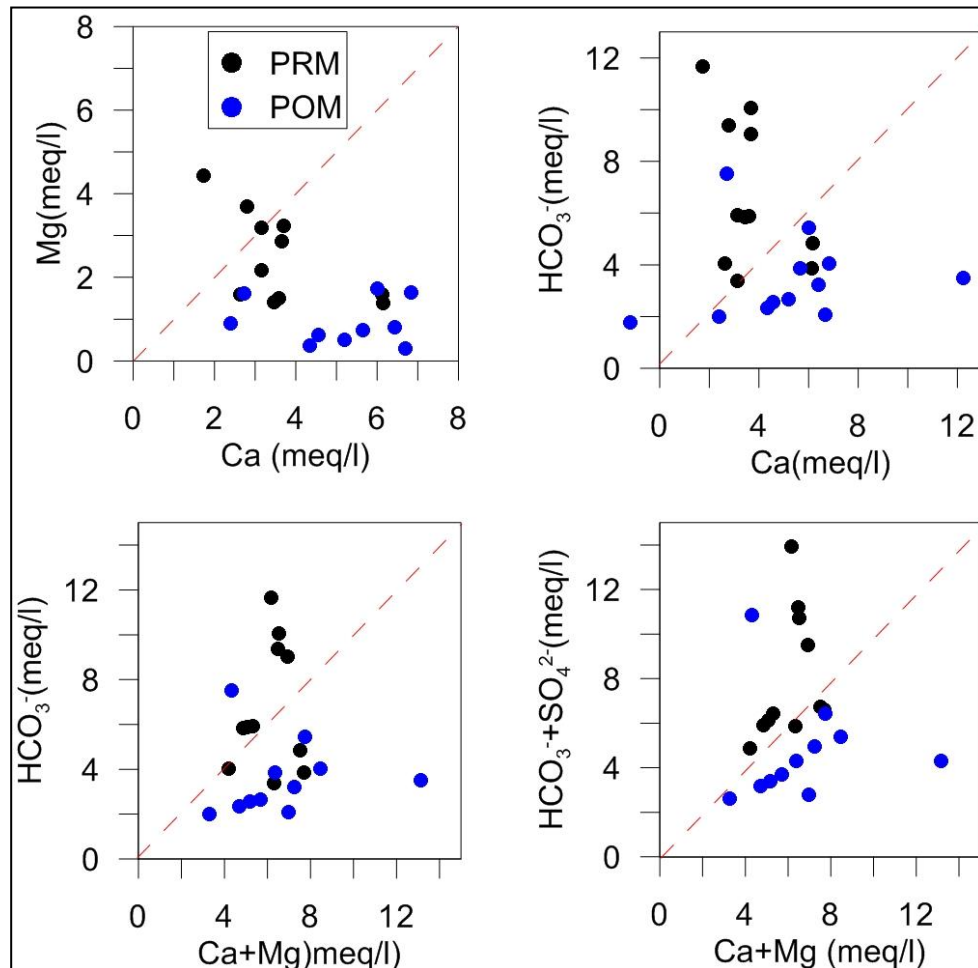
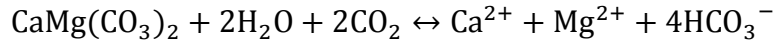


Fig. 6.8. Scatter plots between various cations and anions that can indicate the possible nature of equilibrium reactions between rock and water in the area during PRM (black dots) and POM (blue dots). Less scatter is observed between $\text{Ca}^{2+} + \text{Mg}^{2+}$ Vs $\text{HCO}_3^- + \text{SO}_4^{2-}$.

Narji limestone contains significant concentration of dolomite (average carbonates ~60.5% as $\text{CaCO}_3 + \text{MgCO}_3$ and average CaO and MgO ~34.6% and ~0.5% respectively (Kumar, 1983). The chemical reactions that control the water quality could be expressed as;



Thus, dissolution of this impure carbonate rock results in the increase in Ca^{2+} and Mg^{2+} content in groundwater. A plot of molar ratio of $\text{Ca}^{2+} + \text{Mg}^{2+}$ to the $\text{HCO}_3^{2-} + \text{SO}_4^{2-}$ showed that 70% of samples lie close to 1:1 line during PRM and 66% during POM season which reflects that $\text{Ca}^{2+} + \text{Mg}^{2+}$ equilibrates the $\text{HCO}_3^- + \text{SO}_4^{2-}$ concentration. From the above plots, it is clear that dissolution of carbonate rocks plays major role in the acquisition of calcium and magnesium ions. During POM the samples showed a good correlation but fall below 1:1 equiline which shows the increased concentration of Ca^{2+} and Mg^{2+} ions.

The $\text{Ca}/(\text{Ca} + \text{Mg})$ Vs. $\text{SO}_4/(\text{SO}_4 + \text{HCO}_3)$ scatter plot (Fig. 6.9) shows also a wider scatter. All spring waters and bore wells located in highly karstified area are represented by high $\text{Ca}/(\text{Ca} + \text{Mg})$ molar ratio indicating calcite is mainly related with water interaction. The bore wells (B7, B11, B12) located in agriculture dominated areas shows high ratio of $\text{SO}_4/(\text{SO}_4 + \text{HCO}_3)$. This behaviour is almost same in POM samples. However, majority of samples fall in the middle of the diagram indicating dolomitic interactions. A value of 0.5 and 1 for $\text{Ca}/(\text{Ca} + \text{Mg})$ molar ratio are related to the dissolution of dolomite and pure calcite respectively (Fron dini, 2008).

It is observed that the highest Ca^{2+} and Mg^{2+} are associated with high SO_4^{2-} . Sulfate plotted against Ca^{2+} and Mg^{2+} (Fig. 6.10) shows that samples plot above 1:1 line which

reflects continued dissolution of carbonate material with little addition of SO_4^{2-} . Oxidation of pyrite in the rock may increase sulphate concentration that enhances carbonate dissolution (e.g., Spence and Telmer, 2005; Li et. al., 2008).

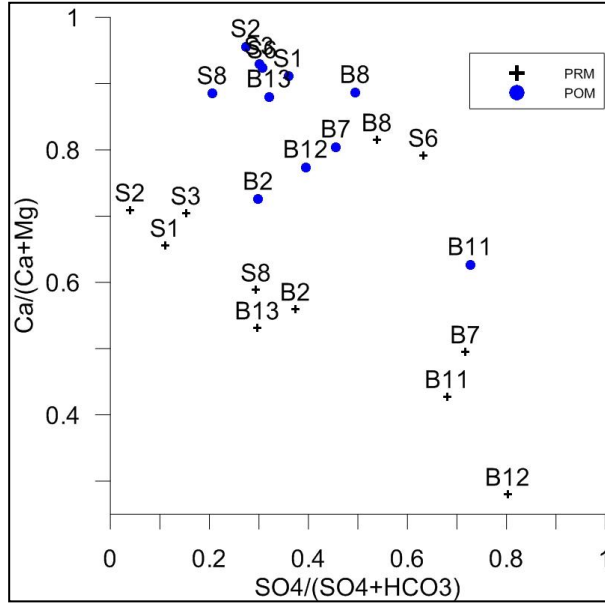


Fig. 6.9. Plot of $\text{SO}_4/\text{SO}_4+\text{HCO}_3$ vs. $\text{Ca}/\text{Ca}+\text{MG}$ for the PRM and POM samples of the area.

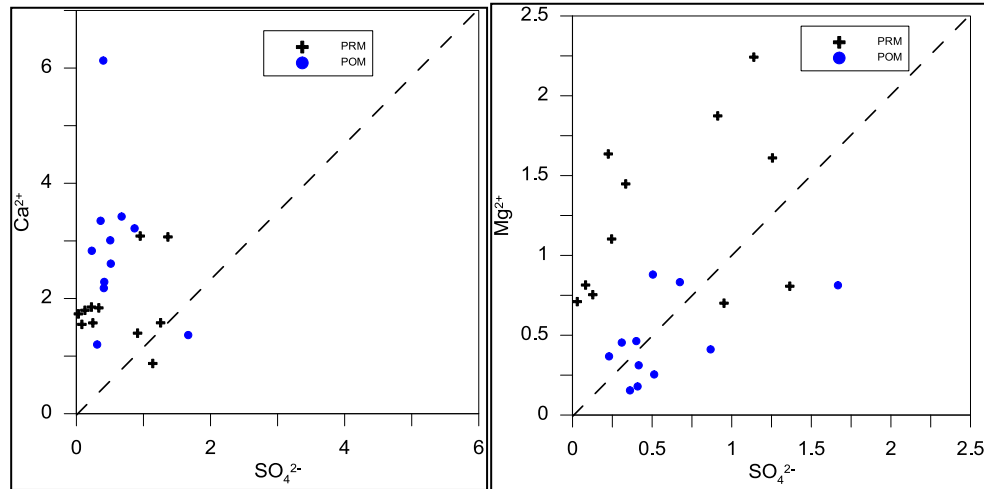


Fig. 6.10. Plot of SO_4^{2-} vs. Ca^{2+} and SO_4^{2-} vs. Mg^{2+} for the PRM and POM samples of the area.

Gibbs' ratio (Gibbs, 1970) were plotted separately for major cations ($\text{Na}^+/\text{Na}^++\text{Ca}^{2+}$) and major anions ($\text{Cl}^-/\text{Cl}^-+\text{HCO}_3^-$) vs. log TDS for PRM and POM (Fig. 6.11a and b). The

plots indicate that the chemistry of water is controlled predominantly by the chemical interaction between rock and groundwater. Few samples lying close to evaporation end indicate that it also has a significant effect on groundwater chemistry during both seasons. The nature of such interactions also depends upon many factors (e.g., reaction time, irrigation and anthropogenic influences).

Temperature as plotted against the concentrations of TDS, SO_4^{2-} , Ca^{2+} , Mg^{2+} , F which showed a large scatter. However a general increase of ion concentration was observed with increase in temperature during PRM season. This indicates that temperature also contributes to the water–rock interaction during PRM when average temperature is high. The nature of such interactions also depends upon many factors, (e.g., reaction time, irrigation and anthropogenic influences).

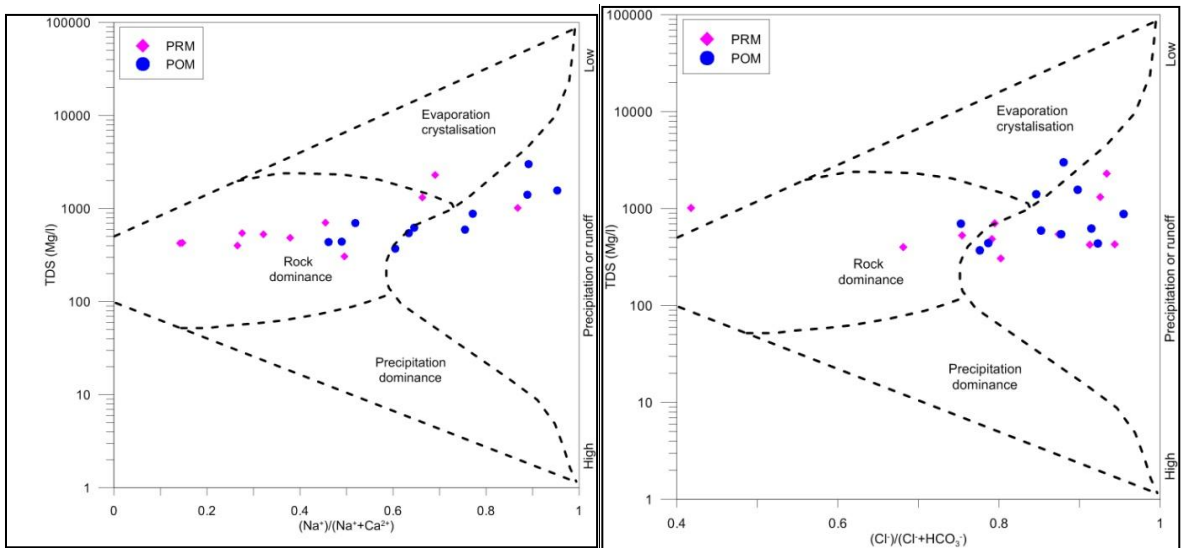


Fig. 6.11. Gibbs plot showing the mechanism that controls the chemistry of groundwater (a) cations and (b) anions.

$\text{Ca}^{2+}/\text{Mg}^{2+}$ molar ratio in spring and well waters is highly variable and is generally high during POM season. $\text{Ca}^{2+}/\text{Mg}^{2+}$ molar ratios vary from 0.39-4.45 during PRM with an average value of 1.99. During POM the value increases to an average of 8.9. High ratio is usually attributed to the calcite weathering and a decrease in ratio from POM to PRM seasons can indicate the release of more Mg ions from the rock or increase in silicate weathering. Thus, the newer water will have a high $\text{Ca}^{2+}/\text{Mg}^{2+}$ ratio while, older water will show lower $\text{Ca}^{2+}/\text{Mg}^{2+}$ ratio as it will dissolve more Mg with time. High temperature during PRM also favors the release of more Mg from the rock. Thus, the variation in $\text{Ca}^{2+}/\text{Mg}^{2+}$ molar ratio seems to be related to the rock weathering. A decrease of $\text{Ca}^{2+}/\text{Mg}^{2+}$ with increase of Mg^{2+} also indicates the release of Mg^{2+} ions from the source rock.

$\text{Ca}^{2+}/\text{Mg}^{2+}$ molar ratio equal to one indicates dissolution of dolomite but a higher indicates more calcite contribution (Zhu et. al., 2007). A more than 2 ratio also indicates the weathering of silicate minerals. The molar ratio is generally less than 2 in this karst area during PRM and an increase in ratio during POM indicates that the dissolution of dolomite and calcite are the dominant geochemical processes with little dissolution from silicate minerals.

Na^+/Cl^- ratio is widely used indicator in many groundwater studies (Magaritz et. al., 1989; Maa et. al., 2011). The plot shows a large scatter however, majority of the samples fall below 1:1 line during PRM (Fig. 6.12) which indicates that dissolution, though not halite is the main source of these ions. During POM majority of samples fall along 1:1 line. Since the ratio Na^+/Cl^- is less than unity the excess of Cl^- over Na^+ suggests additional contributions of Cl^- from other sources. Three samples (B7, B11, B12) fall above 1:1 aquiline in which extra

Na^+ is contributed from other sources. These three samples have large human influences particularly through agriculture sources as explained above. A greater ratio indicates that Na^+ may get released from silicate weathering (e.g., Mayback, 1987).

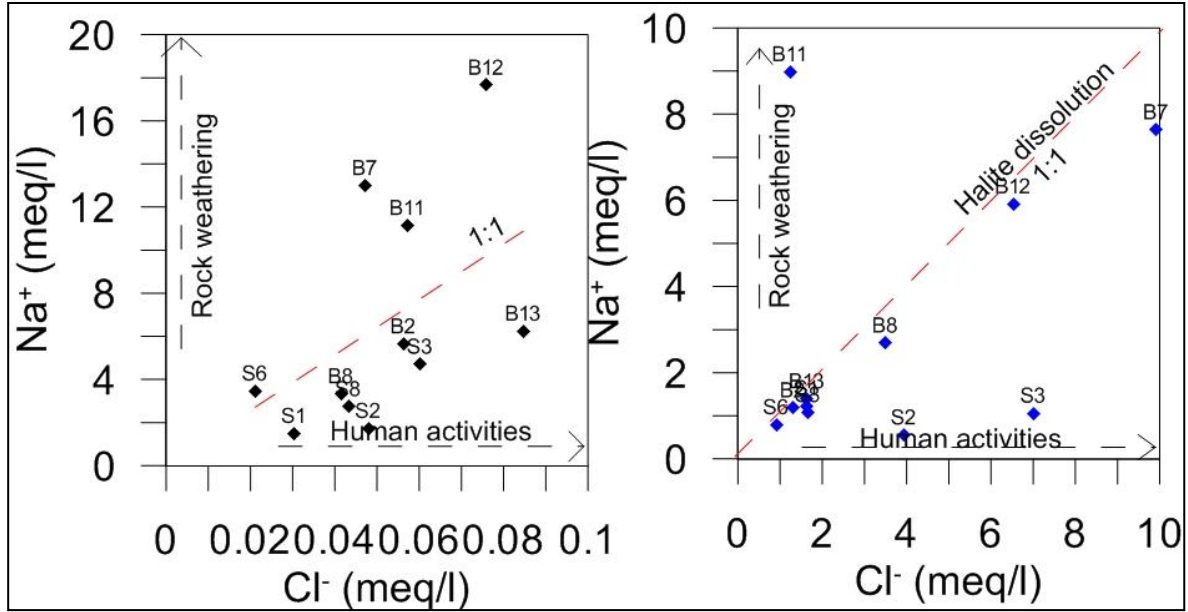


Fig. 6.12. Na^+ Vs Cl^- plots for PRM and POM showing the processes of water rock interaction.

Higher concentrations of chloride in the area indicate a source from evaporation process. Na^+/Cl^- ratio would be unchanged if evaporation is a dominant process and no other mineral releases the ions. However, average value of ratio is 2.2 during PRM and 1.3 during POM. EC vs. Na^+/Cl^- plot shows large scatter with majority of samples showing an inclined trend (increase in Na^+/Cl^- ratio with increase in EC). This indicates that ions get concentrated by evaporation also (e.g., Rajmohan and Elango, 2004). Ion exchange does not seem to remove sodium and therefore, has very less effect on groundwater chemistry. Thus, evapotranspiration is an effective indicator of concentration of ions (e.g., Guo et. al., 2007) that dominates over ion-exchange processes. This evaporative effect is also indicated by the Gibbs diagrams as the samples fall towards evaporation side.

6.9. Summary

The hydrogeochemical characteristic of karst aquifers is quite different from other aquifers. The results from physico-chemical analysis of water samples have been discussed. The physico-chemical variables showed a significant statistical difference between PRM and POM seasons. The spatial variability in water chemistry is clearly observed. Ca^{2+} , Mg^{2+} and HCO_3^- are directly related to the natural water-rock interaction. These ions are derived from limestone dissolution possessing little MgCO_3 content. High concentrations of SO_4^{2-} , Cl^- , NO_3^- suggests the anthropogenic source particularly from the areas dominated by agricultural practices. Land use has a major role in changing pollution-related constituents. Agriculture is the main source of nitrates and sulfate. However, weathering of clastic rocks may contribute little sodium and potassium ions. The less contaminated springs are hydrogeologically separated from the rest of the area and have less human influence.

On the basis of water chemistry and physicochemical results it is obvious that groundwater has encompassed many hydrogeochemical processes. The original chemical signature of groundwater gets modified to a great degree during post-monsoon season by monsoon recharge water. Water seems to have acquired majority of the ions dominantly through water-rock interaction and mixing processes mainly dilution. The different types of recharge water (concentrated and diffuse) get mixed and lead to final groundwater chemistry.

The groundwater is the sole source for domestic and agricultural activities in the region. Cultivation is the main source of income for a major population. Thus, cultivation of paddy, grams and other rain fed crops are economically important and is carried over many

areas. It is therefore, important to consider the contamination of groundwater by irrigation return flow, application of fertilizers and farm manure, leaching of soil minerals and contaminant release from domestic sewage, etc. The high concentrations of nitrates, sulfates and chloride indicate these sources. Due to seasonal changes in agricultural activities and vegetation growth, possible variations in $p\text{CO}_2$ are likely. Physical process, like evapotranspiration also led to the concentration of certain ions particularly in agriculture dominated areas. Dumping of domestic waste directly in karst depressions (common practice in the area) could also be the cause of anthropogenic sources.

Hence, it can be recommended that future detailed chemical investigations of water, rock and soil is needed to understand the hydrochemical processes. Frequent sampling, particularly during monsoon months will be helpful in understanding the interaction of different processes. Such investigations will be useful for the characterization of the aquifer flow systems and the control of karst heterogeneities on groundwater flow.

CHAPTER 7

CHARACTERIZATION OF KARST AQUIFER USING ISOTOPES AND TRACERS

7.1. Introduction

Environmental isotopes of ^{18}O and ^2H are found in abundance in biosphere and participate virtually in all hydrological, geological, chemical and biological systems (Clark and Fritz, 1997; Faure and Mensing, 2005). Due to small differences in physico-chemical properties, isotopes undergo a mass-dependent fractionation during many processes (Gat, 1996). The isotope fractionation takes in two ways;

- The heavier isotopic molecules have a lower mobility (diffusion determined by temperature) and thus, have a lower velocity and a smaller collision frequency-the primary condition for chemical reactions. They react slowly than the lighter isotopes (e.g., $\text{Ca}^{12}\text{CO}_3$ dissolves faster in an acid solution than $\text{Ca}^{13}\text{CO}_3$). This is called Kinetic isotopic fractionation.

- The heavier molecules generally have higher binding energies and thus, escape less easily. They have lower vapor pressures and also evaporate less easily. Such difference lead to equilibrium isotope fractionation, which varies with temperature (largest at lower temperatures and disappears at high temperatures).

The processes involved and the application of the fractionation of ^{18}O and ^2H have been studied by many authors (Hoefs, 1997; Clark and Fritz, 1997; Taylor et. al., 2002). According to Craig, (1961a) the isotopic composition of meteoric water changes and the

$\delta^2\text{H}/\delta^{18}\text{O}$ ratio remains constant that falls on a straight line- Meteoric Water Line or Global Meteoric Water Line (GMWL) defined by an equation Craig, (1961b);

$$\delta\text{D} = 8 * \delta^{18}\text{O} + 10$$

The slope 8 of GMWL depends on the enrichment factor of ^2H and ^{18}O (8.2 at 25°C) where the ^2H enrichment in water is roughly 8 times greater than ^{18}O (Clark and Fritz, 1997). The factor varies with temperature and therefore, an increase in temperature results in a decrease in slope. The intercept 10 is a function of the meteorological conditions of the ocean water where the precipitation originates.

As the vapors travel, the lighter isotopes (^1H and ^{16}O) preferentially move in the vapour phase. The resulting vapour mass gets depleted in heavier isotopes (Clark and Fritz, 1997). When vapour condense, the heavier isotopes get enriched in rain compared to the remaining vapour (Dansgaard, 1964) because of Rayleigh rainout effect- the process of rainout distillation of heavy isotopes from the vapour along the trajectory of an air mass (Mook, 2006 Fig. 7.1). The kinetic fractionation of ^{18}O is more than ^2H depending on temperature and relative humidity (Shivanna et. al., 2008).

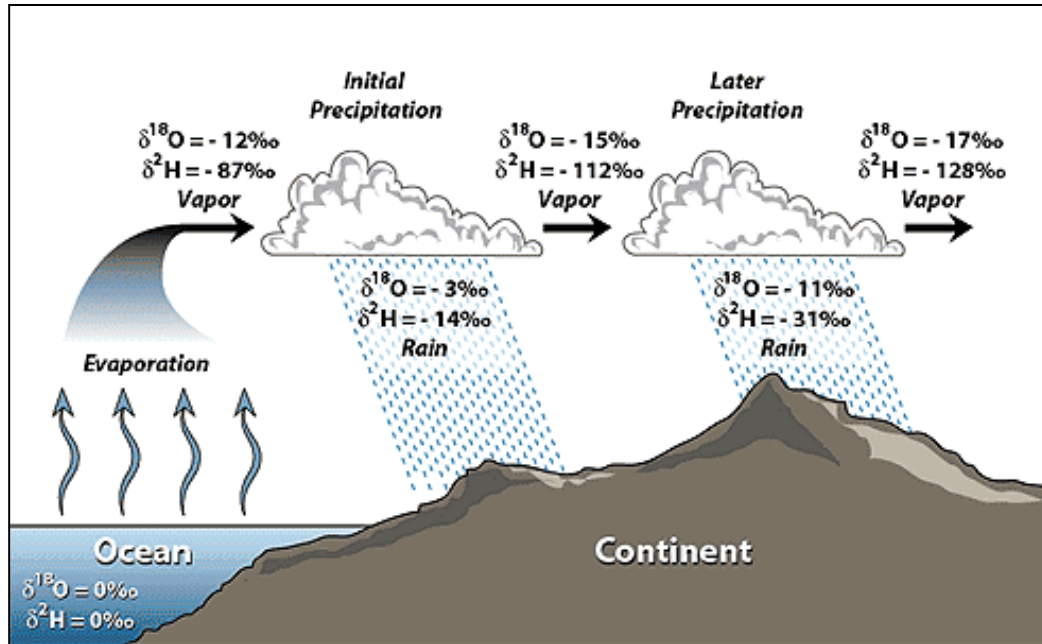


Fig. 7.1. Rainout effect on $\delta^2\text{H}$ and $\delta^{18}\text{O}$ values (based on Hoefs, 1997 and Coplen et. al., 2000).

According to Craig, (1961b) isotopically depleted water is associated with cold regions and enriched (evaporated) waters are found in warm regions (Fig. 7.2). This is recognized as a tool for characterizing groundwater recharge and is the basis of groundwater provenance studies (Clark and Fritz, 1997).

The isotopic composition of precipitation is also effected by seasons (Clark and Fritz, 1997) and latitude (Rozanski et. al., 1993; Bowen and Revenaugh, 2003). The seasonal variation in temperature produce more depleted values during colder months than during summers. The distance from coasts to inland causes progressive $\delta^{18}\text{O}$ depletion in precipitation (Clark and Fritz, 1997) due to rainout and temperature effect. Higher altitudes are isotopically depleted than lower altitudes.

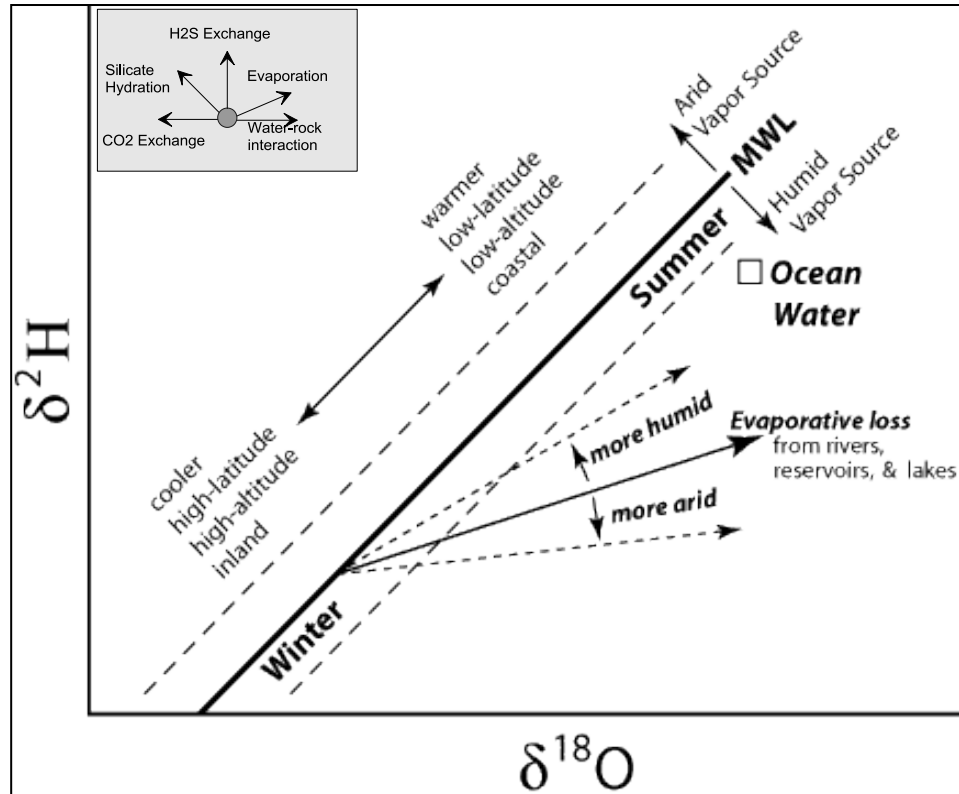


Fig. 7.2. Generalized diagram showing how common hydrologic processes affect oxygen and hydrogen isotopic composition of water (source: <http://cierzo.sahra.arizona.edu/programs/isotopes/oxygen.html> and insert from Toran, 2006).

A large number of studies have used stable isotope in different terrains of India as useful tools for many hydrological investigations (e.g., Kumar et. al., 1982; Gupta, 1983; Sukhija et. al., 1998; Navada and Rao, 1991; Datta et. al., 1994; Datta et. al., 1996; Sinha et. al., 2002; Gupta and Deshpande, 2003; Shivanna et. al., 2004). Bhattacharya et. al., (1985) analyzed oxygen and hydrogen isotopes in groundwater, rivers, lakes, hot springs etc. from many locations in India.

High d excess values are largely from Deccan plateau area which is surrounded by Western and Eastern Ghats (Deshpande et. al., 2003). It has also been noted that seasonal or

inter-annual variability in isotopic signature of groundwater is small (<1‰ in the $\delta^{18}\text{O}$) over whole of the India which is due to the result from processes of selection, mixing and dispersion during groundwater recharge (Gupta and Deshpande, 2005b). Rao, (2003) located an old lost channel that flowed during 7000-3000 BP and got disappeared in the sands of the Rajasthan desert.

No such study using stable isotopes has been carried out for the quantification of groundwater in this semi-arid carbonate area. This chapter presented the first account of the environmental isotope compositions of local groundwater and its relation with rainfall to investigate the source of air mass responsible for the storm and its contribution to the groundwater recharge. The objective is to understand groundwater composition and aquifer characteristics.

7.2. ^2H and ^{18}O Isotopes

7.2.1. Rainwater and Local Meteoric Water Line

The isotopic signature of 16 rain water samples during a period of ten months (July-2010 to November-2011 Appendix 12) were plotted to determine the $\delta^2\text{H}$ Vs $\delta^{18}\text{O}$ relationship with least-square regression equation. The isotope data of the groundwater samples for PRM and POM season are given in Appendix 13 and 14. The positive delta values indicate that sample has more heavy isotope than the standard, negative delta values indicates that sample has less heavy isotopes than the standard.

The $\delta^{18}\text{O}$ and $\delta^2\text{H}$ of the rain samples range between -5.81 to 2.98‰ and -56.34 to 9‰, with average values of -19.17 and -1.19‰, respectively. The values are depleted in heavy isotopes than the average west coast rainfall data (e.g., Deshpande et. al., 2003) which indicates the rainout effect of incoming moisture from the Arabian Sea. A local meteoric water line (LMWL) was obtained by a best-fit line during both SW- and NE-monsoon season (Fig. 7.3) which is defined by an equation;

$$\delta^2\text{H} = 7.02 \delta^{18}\text{O} - 10.79, R^2 = 0.7$$

This line was compared with the literature from nearest stations (Tab. 7.1 & Fig. 7.3). The slope of LMWL (7.02) is nearly the same as that of global meteoric water line (GMWL), but the Y-intercept is lower. The slight deviation of the LMWL is caused by the effect of local evaporation on raindrops (Kumar et. al., 1982).

Station	LMWL ($(\delta\text{D} = a * \delta^{18}\text{O} + b)$)	Reference
Mumbai	$\delta\text{D} = (8 \pm 0.3) * \delta^{18}\text{O} + (8.4 \pm 0.8)[R^2 = 0.94]$	GNIP
Kozikode	$\delta\text{D} = (7.2 \pm 0.2) * \delta^{18}\text{O} + (7.6 \pm 0.8)[R^2 = 0.99]$	GNIP
Lower Maner Basin	$\delta\text{D} = (7.3 \pm 0.1) * \delta^{18}\text{O} + (4 \pm 1.1)[R^2 = 0.98]$	Kumar, et. al., 1982
Kurnool (AP)*	$\delta\text{D} = (7.02 \pm 0.3) * \delta^{18}\text{O} - (10.79 \pm 0.2)[R^2 = 0.7]$	This study

Tab. 7.1. LMWL equations for different station of India based on various studies.

LMWL helps in groundwater investigations in any region (Warrier et. al., 2010). Based on the direct relation between rainfall and the hydrological response of the system rainfall contribution to the groundwater can be quantified by applying the stable isotopes ^2H or ^{18}O (Shivanna et. al., 2004). In order to use isotopes in hydrological studies the isotopic composition of rainfall should be known which causes recharge. In Indian context, the

rainfall during southwest and northeast monsoons shows two distinct isotopic signatures (Fig. 7.3) which can be ascribed to the difference in vapour sources.

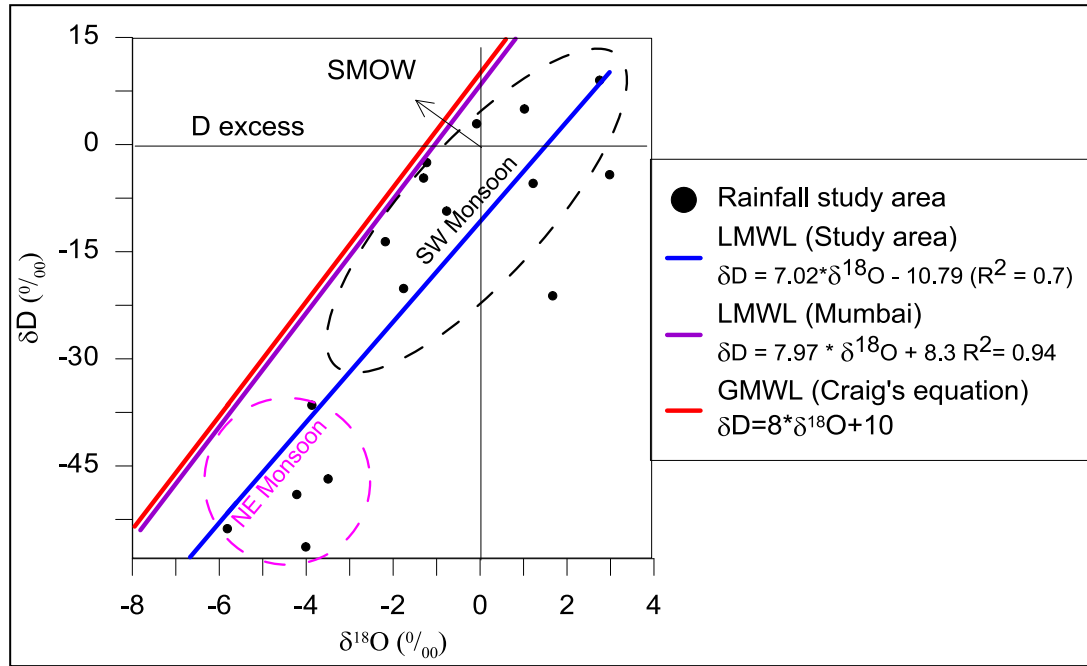


Fig. 7.3. Plot of $\delta^2\text{H}$ versus $\delta^{18}\text{O}$ for rainwater samples. GMWL and LMWL (Mumbai) represent the global meteoric line of Craig (1961) and the local meteoric water line from Mumbai, respectively.

In Southern India, the Western Ghats have large affect on the pluviometric character of the south-west monsoon. The areas west of Ghats are humid with heavy rain while the area to the east is comparatively dry, semi-arid and depleted due to rain out effect except the east coast (Deshpande et. al., 2003). Gupta and Deshpande, (2005a) have divided India into four zones based on the isotopic signature of groundwater. The study area lies in the intermediate zone which has a mixed character. According to them, the isotopic signature of rain gets also modified by the soil properties.

The relatively enriched isotopic values ($\delta^{18}\text{O} > -5\text{‰}$) of southwest monsoon reveals their moisture from the Arabian Sea (e.g., Warrier et. al., 2010). The depleted nature of NE-Monsoon rainfall is due to the fact that these winds originated from the depleted continental vapors of Central Asia as well from the Bay of Bengal and South China Sea (Deshpande et. al., 2003). The two sources of moisture seasons have different isotopic characteristics whose imprints may be identifiable in the geographic distribution of isotopes in groundwater.

Monthly data of the isotopic signature of rainfall is shown in Fig. 7.4. It is clear that the rainfall isotope content is enriched in monsoon months as compared to non-monsoon months and due to more evaporation under high relative humidity. This is because of more contribution from southwest monsoon to the local atmospheric moisture (Kumar et. al., 1982). On the other hand, in retreating monsoon months the winds blow over more continental areas before reaching the study area whose isotope values get depleted.

7.2.2. Groundwater

The isotopic values of the groundwater (springs, wells and rain water) during PRM and POM are given in Appendix 13 and 14 and the statistical analysis is given in Tab. 7.2. The average values are -18.5‰ for $\delta^2\text{H}$ and -2.4‰ for $\delta^{18}\text{O}$ during PRM. During POM the samples become enriched in heavy isotopes indicated by higher values. The trend is almost same for the springs and wells of the area.

Compared with the rainfall, the groundwater is depleted in the area. As the western sided rains are heavy and therefore, the groundwater is expected to be depleted in the central and eastern part of the Indian Peninsula than the west (Deshpande et. al., 2003).

A plot of $\delta^2\text{H}$ vs. $\delta^{18}\text{O}$ for groundwater samples is shown in Fig. 7.5 for pre- and post-monsoon. The distribution of $\delta^2\text{H}$ and $\delta^{18}\text{O}$ has a similar range and lie on or close to the LMWL, indicating that water is of meteoric origin. The $\delta^2\text{H}$ – $\delta^{18}\text{O}$ relationship of groundwater samples fits a least-squares regression line of the type equations as shown in Fig. 7.5.

$$\delta^2\text{H} = 4 * \delta^{18}\text{O} - 9.4, R^2 = 0.83 \quad \text{PRM season}$$

$$\delta^2\text{H} = 3.1 * \delta^{18}\text{O} - 11.1, R^2 = 0.87 \quad \text{POM season}$$

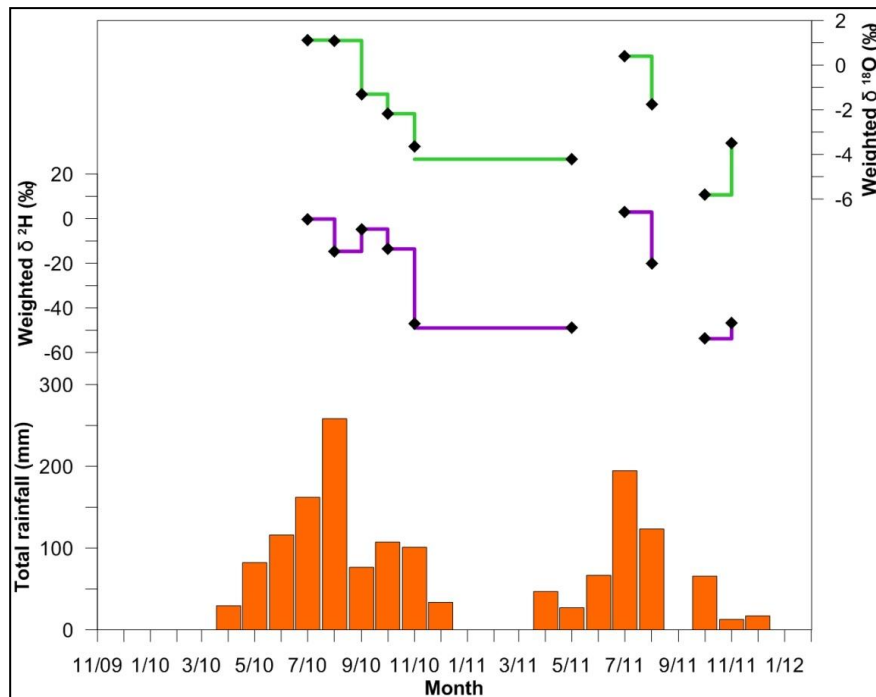


Fig. 7.4. Step plot showing the weighted monthly isotopic signature as a function of total monthly rainfall for the study period.

The $\delta^{18}\text{O}$ and $\delta^2\text{H}$ plots define an array with a slope of ~ 4 and 3.1 respectively that reflects isotope fractionation during evaporation, with the slope implying humidity (Clark and Fritz, 1997).

	Statistics	PRM			POM		
		δ^2H (‰)	$\delta^{18}O$ (‰)	d-excess	δ^2H (‰)	$\delta^{18}O$ (‰)	d-excess
<i>Springs</i>	Min	-24.3	-3.7	-4.4	-24.2	-4.0	-14.7
	Max	-13.0	-1.6	6.2	-6.9	1.0	7.6
	Mean	-18.5	-2.4	0.4	-17.1	-1.9	-1.8
	CV	-0.2	-0.4	11.1	-0.5	-1.1	-5.4
<i>Wells</i>	Min	-19.1	-1.9	-12.9	-19.8	-2.3	-32.9
	Max	-6.5	0.7	-1.5	-2.1	3.9	1.0
	Mean	-11.8	-0.6	-7.2	-11.4	-0.1	-10.5
	CV	-0.4	-1.4	-0.5	-0.6	-20.8	-1.3
<i>Rainfall</i>	Min	-56.3	-5.8	-24.3	-21.2	-2.2	-34.5
	Max	-36.5	-3.5	-5.5	9.0	3.0	7.3
	Mean	-48.5	-4.3	-14.2	-5.8	0.2	-7.5
	CV	-0.2	-0.2	-0.6	-1.7	8.6	-1.8

Tab. 7.2. Statistical parameters of isotopic composition of springs, bore well and rain water collected during PRM and POM 2011 period.

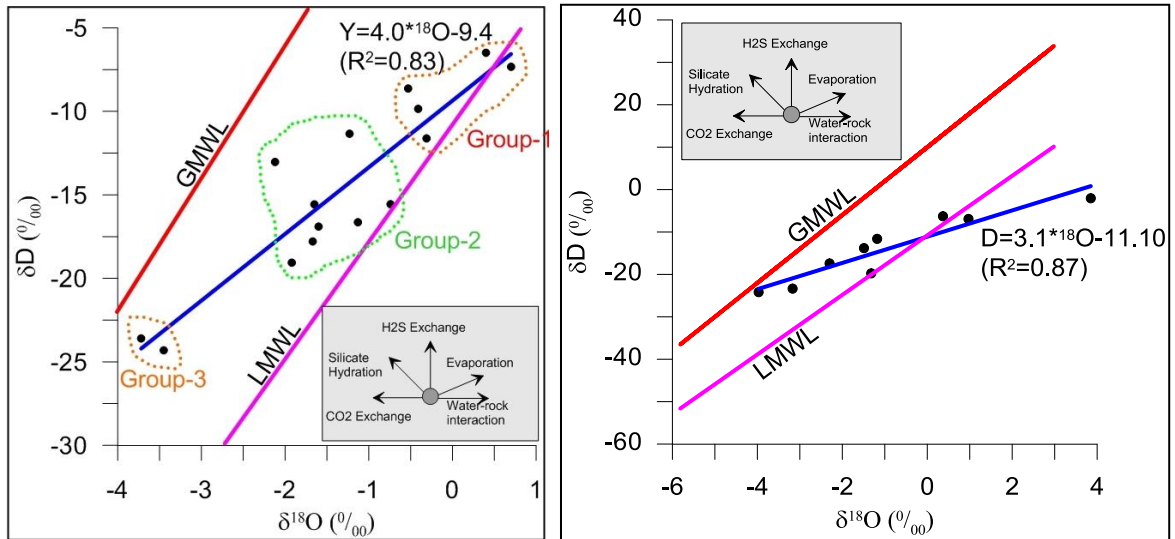


Fig. 7.5. Plot of δ^2H Vs $\delta^{18}O$ for groundwater samples for PRM (left) and POM 2011 (right). GMWL and LMWL represent the global meteoric line of Craig (1961) and the local meteoric water line, respectively. Blue line is a trend line through water sample data.

During POM, the samples show less scattering than PRM which is due to amount effect of the rainfall. The scattering of samples suggested that these waters were strongly affected by evaporation which is more prominent in PRM and less affected in POM season. In case of PRM samples the slope of the regression line is higher than the POM data. The low slope indicates a secondary evaporation effect. The groundwater trend line (evaporation line) obtained by the least square fit has a lower slope than both GMWL and LMWL of the study area.

The original isotope composition of the groundwater prior to evaporation (primordial signature) was determined at the intersection with the LMWL. The values for $\delta^{18}\text{O}$ and $\delta^2\text{H}$ were $\sim 0.5\text{‰}$ and -8‰ for PRM and $\sim 0\text{‰}$ and -12‰ for POM respectively. The range of rainwater is however, 3 to -6 for $\delta^{18}\text{O}$ and 10 to -50 for $\delta^2\text{H}$. This indicates that primordial value of POM is close to the rainwater while in PRM it shows much deviation from the rainwater range. Thus, during PRM more fractionation effect has occurred due to high temperature and less rainfall. The evaporation line for different water types (springs, wells) is an indication of the effect of isotopic enrichment before recharge (Wu, et. al., 2009). The results also indicate a more recharge contribution from monsoon rainfall than non-monsoon months.

During PRM, the samples were grouped into three groups having different isotopic signatures. Group-1 samples have enriched values in heavy isotopes. The reason for such enrichment is that these samples fall in the thick soil cover area which is dominated by the agricultural, particularly paddy throughout the year. The irrigation is dominated by canal

type from surface reservoir water. This group certainly points to the irrigation return flow where water is exposed to atmospheric conditions for a prolonged period of time that later enters the groundwater system as evaporated irrigation return flow. Group-3 samples are depleted in heavy isotopes. The samples indicate least effected water as the isotopic values are close to the signature of rainwater. Moreover, these samples are hydrogeologically isolated from rest of the samples. The diffuse recharge to these springs is less due to the absence of soil cover as observed from field investigations and thus, they get recharged by fast type, which is also indicated by their isotopic signature. Group-2 samples have a mixed character and fall within the two groups. This could indicate that these samples and the area in which they fall have both fast and diffuse recharge type as observed in the field investigations. Group-2 samples mostly fall in the high water level area and group-1 samples in the low water level area which indicates that a significant isotopic enrichment has taken place along groundwater flow direction. It has been documented that stable isotope ratios of groundwater become more homogeneous along groundwater flow paths (e.g., Clark and Fritz, 1997; McGuire et. al., 2002). If the mean $\delta^2\text{H}$ and $\delta^{18}\text{O}$ values in rain water are similar to groundwater, it indicates high hydraulic conductivities of the aquifer material which causes rapid recharge of the groundwater (Marfia et. al., 2004).

It has been estimated that the evaporation from a fresh water surface results in an evaporation line with a slope of 3.5-6 in the normal range of relative humidity of 75-10. However, in arid environments this slope may reach less than 3 (Allison et. al., 1983). The isotopic values are similar to the SW-monsoon signature which is enriched than the other rains. Thus, indicating that the major source of recharging water is the SW monsoons.

During PRM water including the irrigated water becomes more enriched in stable isotopes due to more evaporation. This phenomenon is clearly depicted by the enhanced deviation of sizable samples from the LMWL (large scatter). In PRM there is usually no rain and the groundwater becomes the main source for irrigation and part of the water goes back into the aquifer as an evaporated return flow.

7.2.3. Deuterium Excess and Groundwater Recharge

Deuterium excess (d) is the excess deuterium that cannot be accounted by equilibrium fractionation between water and vapour. Deuterium excess is defined by an equation of the type (Dansgaard, 1964);

$$d = \delta^2\text{H} - \delta^{18}\text{O}$$

d-excess is an indicator of kinetic fractionation during evaporation, governed by molecular diffusivity of isotopic species (Clark and Fritz, 1997). Although temperature and wind speed can influence its value, the relative humidity is the most important factor. In the Global Meteoric Water line d-excess has a value of ~10 representing evaporation at ~85% relative humidity. However, the d-excess value in the regional precipitation can be greater if the evaporation occurs under lower humidity (Gat and Carmi, 1970). Alternatively, significant re-evaporation of local surface waters under low humidity creates vapours with high d-excess. If such a vapour mixes with atmospheric reservoir and re-condenses, the resultant precipitation will have high d-excess (Clark and Fritz, 1997). The vice-versa can happen under high humidity in the area.

The d-excess value of rainfall in the study area varies from -34.54 to 7.32 with an average value of -9.6 which is quite different from the rainfall of western areas. The lower

d-excess values than the western coast indicate that the rainfall undergoes more evaporation during its travel from Arabian Sea. The d-excess for groundwater samples (Fig. 7.9 & Tab. 7.2) ranges between -12.93 to 6.16‰ with an average of -4.18‰ in PRM samples and from -32.85 to 7.57‰ with an average value of -6.61‰ during POM. The relative humidity in the study area varies from 50% in March (non-monsoon months) and a highest of 75% in the monsoon months. The high humidity in monsoon months corresponds to the low d-excess, while as in non-monsoon the d-excess increases from -6.6‰ to -4.2‰. The lesser d- value (<10.5) indicates a marine origin of the southwest monsoon, but a continental contribution to the northeast monsoon as it has a higher d-excess (Warrier et. al., 2010).

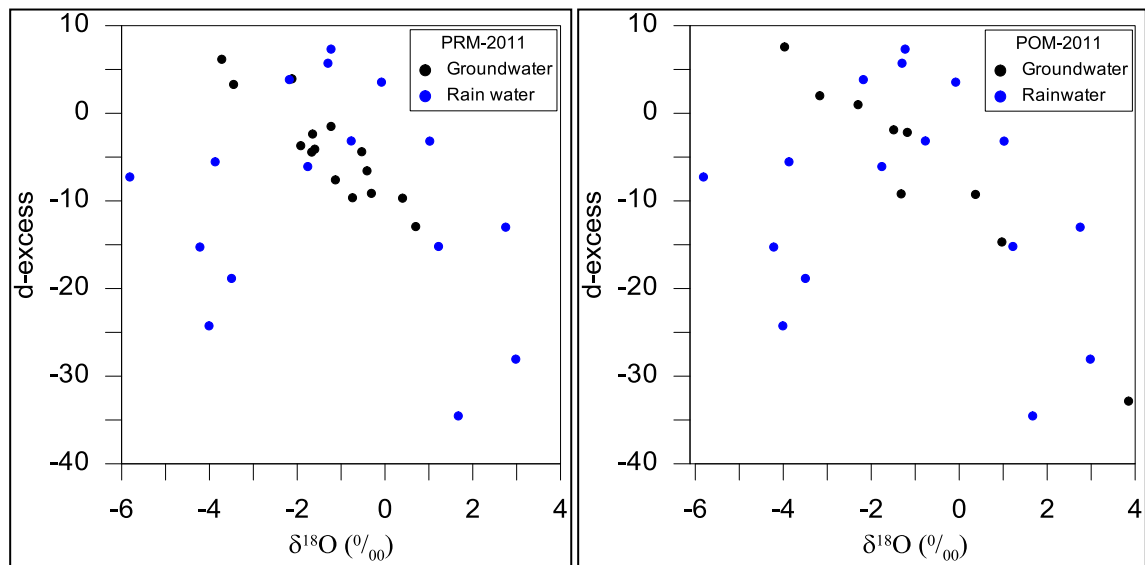


Fig. 7.9. A scatter plot of $\delta^{18}O$ Vs d-excess for PRM (left) and POM (right) samples of 2011.

The low d-excess values indicate that significant evaporation of rainwater makes the residual groundwater with lower values of d-excess. The slope of the regression line in groundwater, which is lower than rainfall, also indicates it. The d-excess could be more

useful parameter, instead of slope of regression line in deciphering the effect of evaporation in modifying the isotopic character of rainwater prior to recharge (Deshpande et. al., 2003).

7.2.4. Isotopic Time Series of Karst Springs

Groundwater discharging from some temporary and permanent springs of the area were monitored for isotopic signature from 2010-11 (Appendix 15) along with other parameters as described in previous chapters. The statistical analysis of the isotopic data for this time period is given in Tab. 7.3.

Spring	Elevation (masl)	δ^2H (‰)				$\delta^{18}O$ (‰)			
		Min	Max	Mean	C.V	Min	Max	Mean	C.V
S-1*	254	-22	0.3	-12	-49	-5.8	4.5	-1.3	-179
S-2*	381	-30	-20	-23	-13	-4.5	1.3	-2.3	-97
S-3*	412	-21	-11	-17	-19	-3.3	-1	-2.4	-36
S-6*	351	-23	-6.9	-15	-37	-3.7	1	-1.5	-120
S-7*	314	-18	-11	-14	-25	-2.8	0.5	-1.5	-115
S-8*	308	-29	-16	-22	-19	-4.4	-3.2	-3.8	-11
Rain		-56	9	-19	-116	-5.8	3	-1.2	-222
PRM-2011		-24	-6.5	-15	-38	-3.7	0.7	-1.3	-96
POM-2011		-24	-2.1	-14	-56	-4	3.9	-0.9	-259

Tab. 7.3. Statistical analysis of isotopic composition of spring and rain water collected during 2009 to 2011 period. Water samples were collected three to four times a year.

The isotopic values show a relatively similar distribution with time and space. However, the high variation in $\delta^{18}O$ of S-1 with large outliers in the data (Fig. 7.6a, red symbols) is observed in S-1. All the springs show their isotopic values lying within the range of rainwater isotope values. The Box-Whisker plots easily defines the range of data

sets and indicates the nature of data scattering by plotting minimum, maximum, first quartile, second quartile (median) and third quartile.

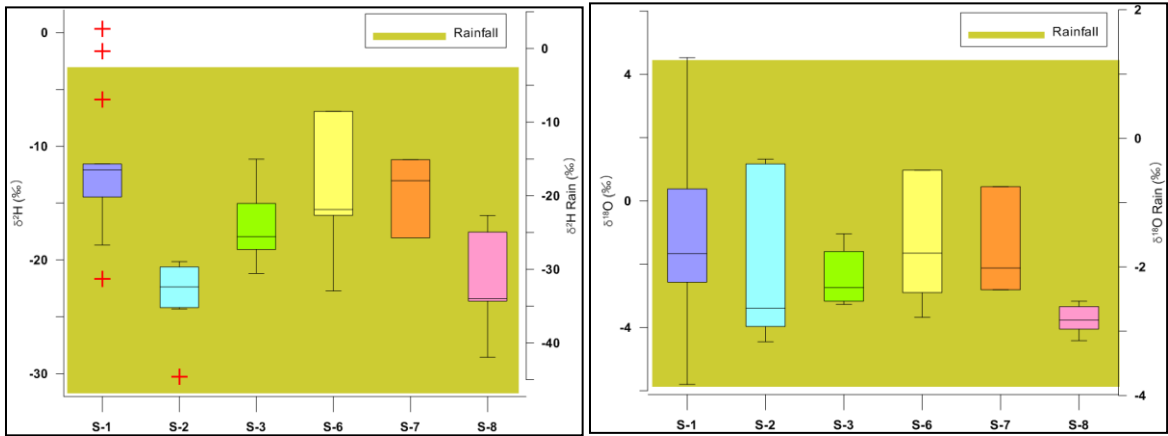


Fig. 7.6. Box-Whisker plot showing the variability of $\delta^2\text{H}$ (a) and $\delta^{18}\text{O}$ (b) isotopic composition of spring compared with rainwater during 2010 to 2011.

Fig. 7.6b shows the box-whisker plot of $\delta^{18}\text{O}$ of spring waters during the study period. All the springs fall within the range of the rainfall values, except the S1 in which minimum and maximum values have a larger range. It is observed that most of the data lies within the range of the third quartile of the plot.

The temporal evolution of isotopic composition of Belum springs (S1) is shown to vary markedly with the water level variation (Fig. 7.7). The spring responds sharply to any significant recharge event (as described in chapter 4) which is clearly indicated by the isotope signature of its discharging water. The isotope composition of the peak flow period of the spring (average -12.803 and -0.688 for $\delta^2\text{H}$ and $\delta^{18}\text{O}$ respectively) is usually identical

with the average rain water isotope composition (-9.83 and -0.29 for $\delta^2\text{H}$ and $\delta^{18}\text{O}$ respectively) during these months.

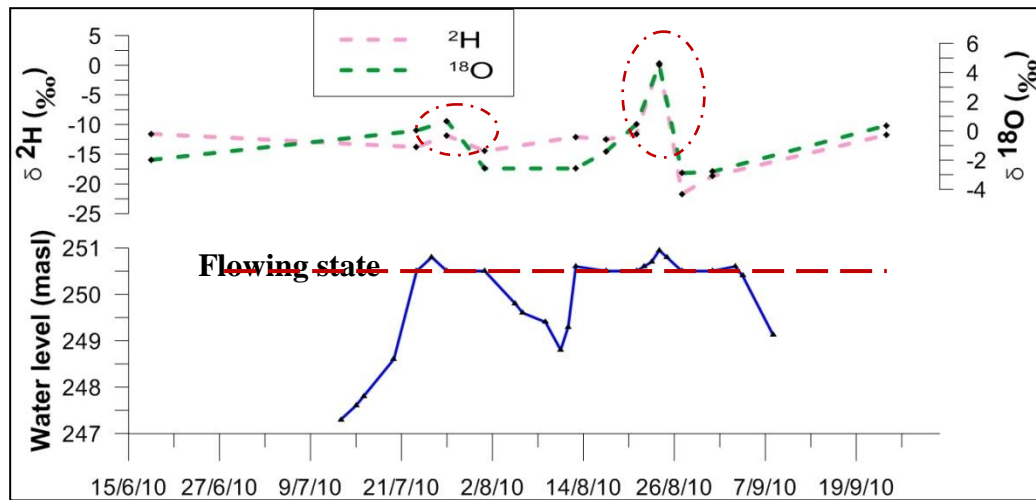


Fig. 7.7. Temporal evolution of $\delta^2\text{H}$ and $\delta^{18}\text{O}$ of groundwater collected from Belum spring (S1). For spring location, refer to Fig. 2.1.

The relation of the peak flow isotope composition with rainwater composition indicates that fresh water gets added to the system during monsoon months and the aquifer gets recharged by fast infiltration through preferential flow and less by diffuse flow. Thus, groundwater flow in this spring is a conduit type. The impermeable shales and quartzites form high elevation hills and plateaus that give a topographic control of the area. This also provides fast recharge water to the area.

The discharge hydrographs along with isotopic variation of the other springs (S2, 3, 6, 7, & 8) during the period 2010 to 2011 are given in Fig. 7.8. The hydrograph-isotope relation is not similar to S1. The figures reflect a mixed isotopic signature possibly from diffuse and concentrated flow in these springs.

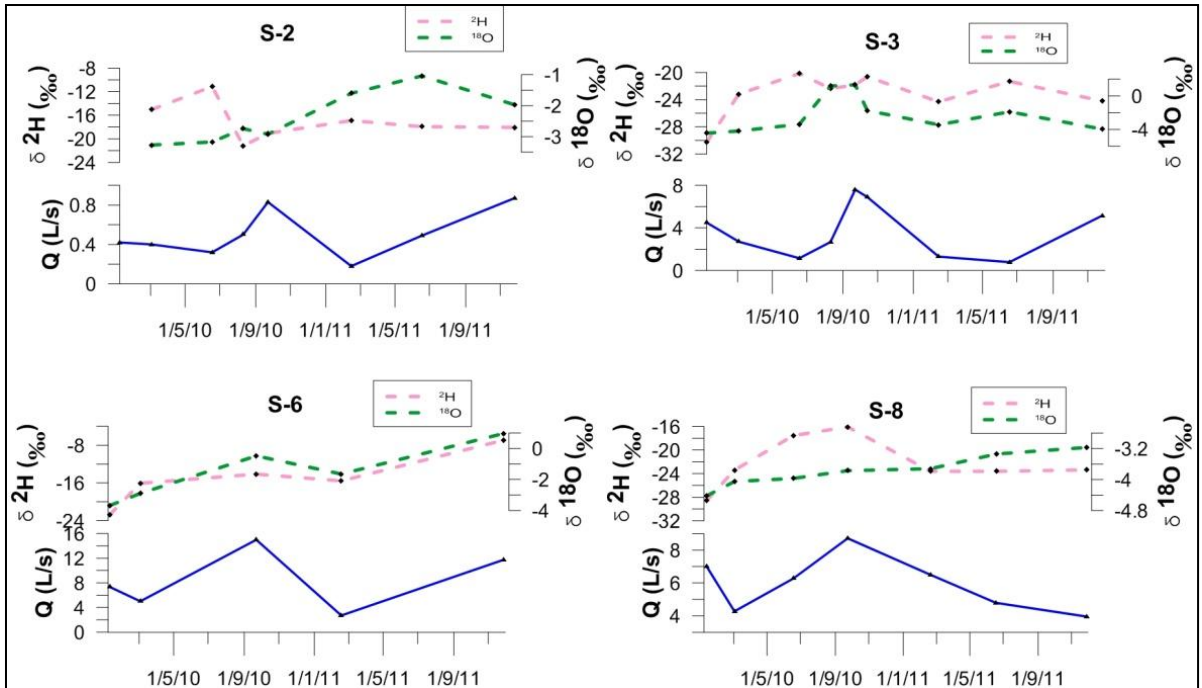


Fig. 7.8. Temporal evolution of $\delta^{2}\text{H}$ and $\delta^{18}\text{O}$ of groundwater collected from different springs (Kona1, S2; Kona2, S3; Rati, S6 & Yaganti, S8). For spring location and characteristics refer to Fig.2.1 and Appendix 6.

7.3. Karst Aquifer Characteristics Inferred from Tracer Study

In karst, a tracer is injected into a karst feature (e.g., sink hole, cave stream) and flushed with a large volume of water when needed. The water samples from wells and springs in the vicinity of the injection point are analyzed for the dye concentrations in time and space. The tracer can be directly observed at springs or indirectly detected at levels different from natural background levels by water analysis.

Quantitative analysis gives a concentration-time series data called breakthrough curves (Fig. 7.10) which need computer codes to interpret. The structure of the curve is influenced by structure of conduits (Field, 1999). The tailing effect of breakthrough curve

may occur due to many reasons like, diffusion of tracer into matrix or fissures (Maloszewski et. al., 1999), tracer movement under low flow velocity or hydraulic gradient, tracer mixing with an underground lake (Zhengxing, 1988), tracer transport in the layered subsurface geology (Iqbal, 2000), diffusive tracer exchange in matrix (Maloszewski and Zuber, 1993), hydrodynamic-controlled rather than matrix- or fissure-diffusion (Massei et. al., 2006).

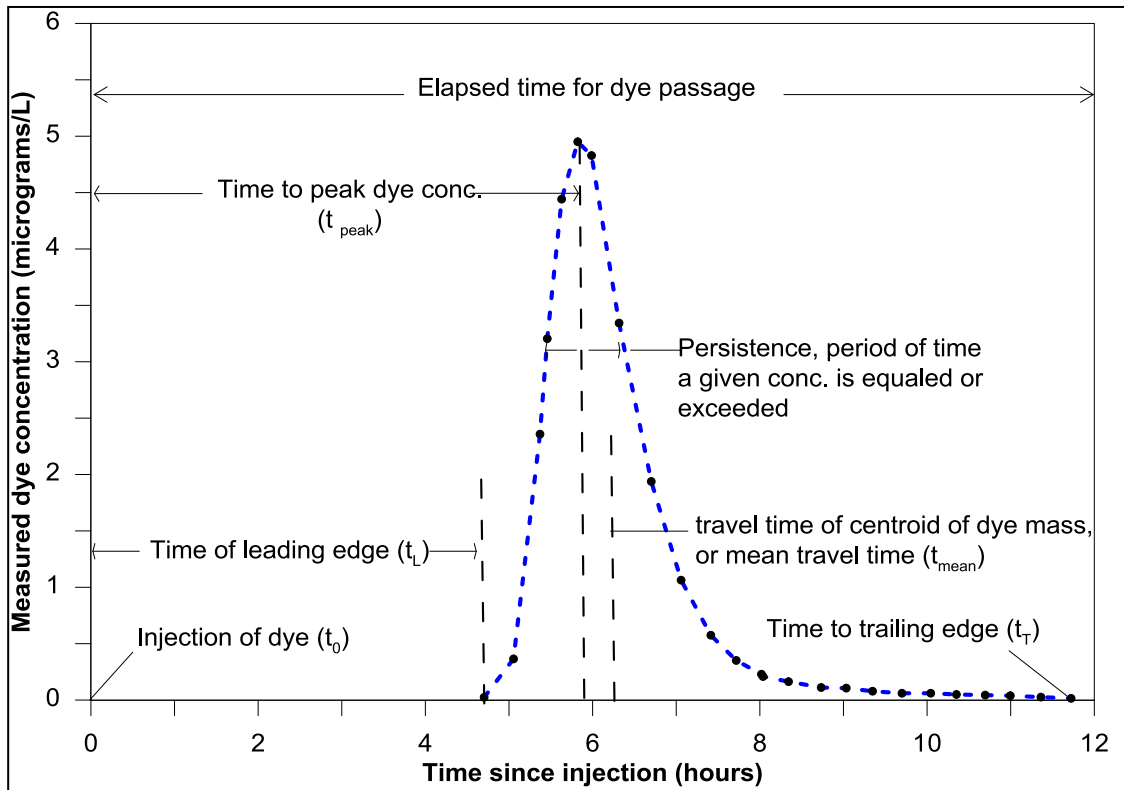


Fig. 7.10. Figure shows a hypothetical single-peaked tracer breakthrough curve with its different parts and interpretation.

A tracer test may fail in certain cases due to a number of reasons. Lack of understanding of the hydrologic system, incorrect choice of tracers and use of insufficient concentration are the major cause. Incorrect assumption of flow direction, very slow

groundwater velocity and a large distance of sampling point may lead to failure. Dilution of tracer through dispersion and mixing causes the loss of tracer quantity (e.g., Hauns et. al., 2001). Strong sorptive properties of most dyes limit their application largely in karst with conduit flow.

The Munagamanu cave (C8) in Narji limestone opens to the surface on the slopes of the Uppalapadu plateau of Dhone mandal. The conduit travels for a distance of 444.5m (inset in Fig. 7.11) with a small stream at the bottom. Tracers were injected in to the cave stream. The horizontal distance of the injection and sampling points is about 1.4 km. The cave stream was flowing with 1-2 l/s) with EC= 453, pH=7.30 $\mu\text{S}/\text{cm}$. Water dripping was active during the period and the total discharge of the drips was about 1-2 l/min. The drip water had EC 1393 $\mu\text{S}/\text{cm}$ and pH 7.28.

Spring S2 was sampled frequently. Other springs in the area flow through the upper most karstified epikarst only for monsoon months. Observed discharge rate of such spring remain below 1 l/s for the year and were not sampled during the test period.

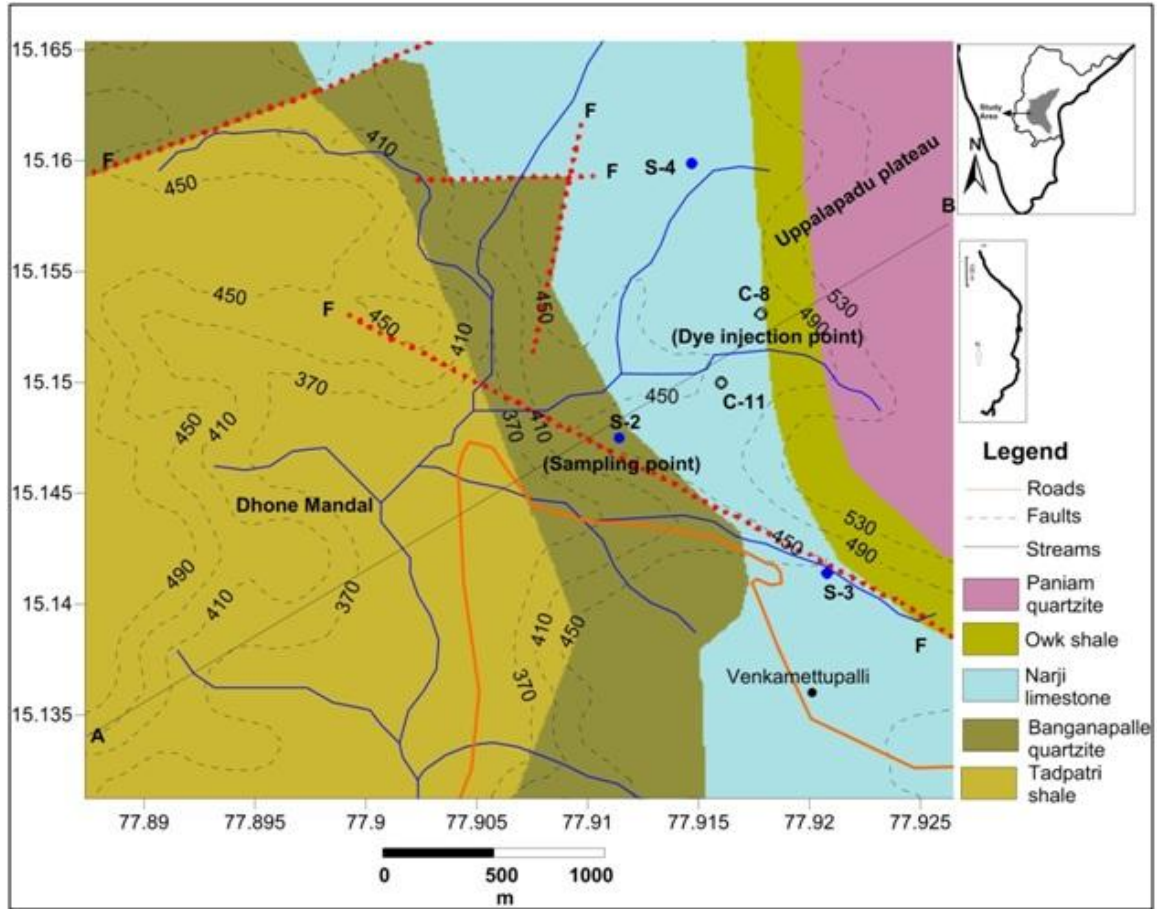


Fig. 7.11. Geological map of Yadiki area showing the dye injection point and sampling locations. Dashed contours are surface elevations in meters above sea level. (For Cave and spring locations refer to Fig. 2.1). Inset shows the subsurface profile of Munagamani Gavi (C8) for more details refer to chapter 4.

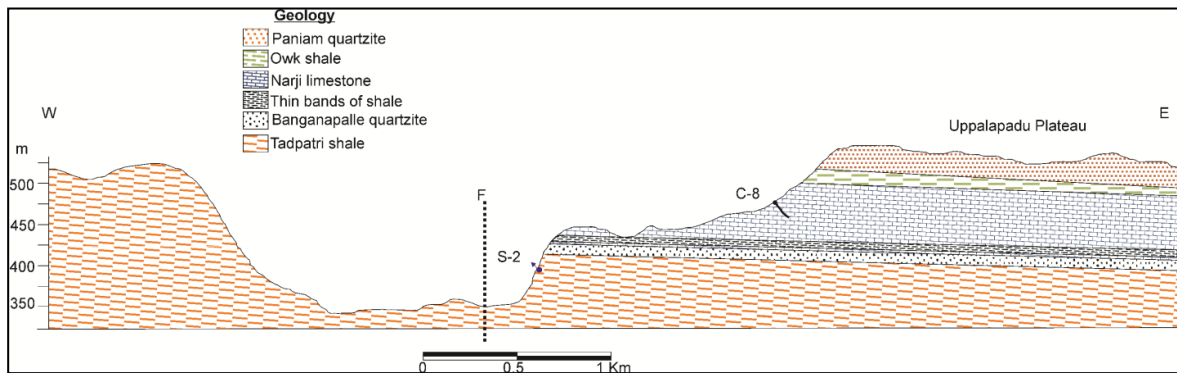


Fig. 7.12. Geological cross-section of Yadiki area showing the cave and spring location.

In spite of less distance (1.4km) from the injection point, there was no change in the color of the water due to tracer. However, it was not possible to analyze the water samples for tracer concentration. From EC, temperature, Cl and bicarbonate concentration measurements at the spring water it was observed that no such fast variation was observed in measured concentration. It may be possible that the tracer reached the spring very late due to more mixing in the flow route. The possible reason is that the dye got diffused into small pores and fissure volume as the dye disappeared under the barrier into small swallets from injection point. The results indicate that the dye was pushed into small pores and fissures near the injection site and captured by small dead-end pores, where diffusion processes caused more mixing (e.g., Mohammadi et. al., 2007). Hence, the dye could have moved out from matrix and fissures as diffusive process which generated a long tailing that was not observed in the samples.

It has been documented that different karst structures contribute differently to the flow between the injections and sampling point. In this case, the spring emerges out of the quartzite bedding that underlies the limestone. This indicates that the water after getting lost in the pool flows towards the base of the karstified limestone with more diffusive flow characteristics. The water finally emerges at the contact between limestone and quartzite or through the upper most part of the underlying quartzite.

Tracer results indicated that the Kona spring (S2) is mostly a diffuse or a mixed type of spring and not purely a conduit spring (e.g., Quinlan and Ewers, 1985). This also indicates that the tracer output at the sampling location purely depends on the

hydrogeological setup and the nature and degree of karstification. The dye got lost in the stream after short duration and there of possibility that it was captured in the rock dominated by matrix porosity. This can also be correlated with the fact that the cave gets closed or narrowed from the distance where the stream gets lost after a barrier. The results also indicate that the spring flow and chemistry depends on the conduit length and nature of discharge.

7.4. Summary

Environmental isotopes are of particular importance in karst hydrogeological studies which has been carried in many karst areas of world. $\delta^2\text{H}$ and $\delta^{18}\text{O}$ isotopes of rain and groundwater were analyses for the semi-arid karst area. Local Meteoric Water Line of rainfall data shows a slope of 7.02. The rainfall is depleted in heavy isotopes than the west coast rainfall. Rainfall isotope data indicates two sources of vapour-SW and NE monsoon. The samples collected after SW monsoon season are more depleted which indicates their origin from continental areas. The low deuterium excess values of rainfall than west coast indicate more evaporation effect during its travel towards inland. Groundwater isotope data shows more depletion in heavy isotopes than rainfall -a result of high evaporation of the area. Groundwater samples fall close to the LMWL with a slope of 4 and 3.1 for $\delta^2\text{H}$ and $\delta^{18}\text{O}$ respectively. This slope is lower than LMWL which indicates the effect of isotope fractionation due to more evaporation. During POM groundwater data is less scattered that is related to the amount effect of rainfall. The primordial signature of groundwater in POM samples is close to the range of rainwater while, the PRM data shows more deviation. Thus, groundwater during PRM gets more fractionated due to higher temperature and little rainfall.

The lower d-excess values of groundwater during monsoon months are related to the effect of more humidity in these months. Groundwater samples were grouped into three classes based on isotope data. The more enriched samples fall in the area with thick soil cover and having effect from agriculture. This indicates that the irrigated water becomes more enriched and then recharges the aquifer as depleted irrigation return flow. The least depleted samples are less affected during hydrological processes and fall in highly karstified areas with fast recharge conditions. Other samples were of mixed character and were affected by both diffuse and fast recharge. The isotopic signature of spring water time series clearly indicates their hydrological behaviour. The relation with water level and discharge indicates more isotope variation during peak flow periods in Belum spring.

Tracer results helped to infer the connectivity between the cave stream and the spring in the Kona karst area. The short duration tracer test helped to characterize the karstic nature of the Narji limestone. Results indicate that the Kona spring (S2) is mostly diffuse or mixed type and not purely a conduit type spring. This also indicates that the tracer output at the sampling location depends on the hydrogeological setup and the nature of karstification. The dye got lost in the stream after short distance and there is possibility that it was captured in the rock dominated by matrix porosity.

CHAPTER 8

CONCLUSION AND RECOMMENDATIONS

8.1. CONCLUSION

Karst is a distinctive landscape developed mostly in carbonate rocks (limestone, dolomite and gypsum) by the dissolutional action of groundwater. It develops both on surface and underground with characteristics karst geomorphological landforms. The overall mechanism of dissolution called karstification is a dependent process influenced by a variety of factors like, climate, $p\text{CO}_2$, nature of rock, presence of weak zones in rocks, etc.

Karst hydrogeology is an important subject because the aquifers are characterized by a rapid flow in highly conductive conduits and channels and slow flow in primary porosity zones. The aquifers are characterized by triple porosity, duality of recharge, storage and groundwater flow with high velocity of groundwater in highly organized channels and conduits and low velocity in fractures and matrix porosity. This large variability in conductivity and other properties makes the prediction and modeling of flow and transport very cumbersome in such aquifers. In general, the conductivity of limestone rock is small however; the dissolution creates large pathways for flow in which the conductivity increases by a large magnitude. Due to their specific geomorphological and hydrogeological peculiarities, these aquifers are most complex to study as they are not represented by elementary volume. Vertical zonation of the aquifer includes epikarst layer which acts as an important infiltration and storage unit in the aquifer. The presence of cavities and hierarchically organised flow between them make any modelling technique difficult. Karst

areas have no permanent surface drainage; runoff lost through sinking streams, swallow holes and other depressions.

Karst aquifers act as a large reservoir for groundwater resources particularly in semi-arid areas where groundwater is the sole source of water supply for the population. These karstified areas are highly fragile characterized by low and irregular rainfall, high temperatures and evaporation rates and is prone to drought periods. Along with the semi-arid climate of the area, there is a rapid social and economic demand for the resources from these aquifers. These activities increase the demand for water, building stones and cement material from the area.

Karst aquifers are widespread across globe in many climatic regimes and supply groundwater to a large population but the nature of karst and the processes in semi-arid areas are still less understood particularly in terms of hydrogeology. These rocks form potential groundwater aquifers in many areas of Indian sub-continent as well. For the hydrogeological characterization of karst aquifers of the semi-arid India the carbonate formations of the Proterozoic Cuddapah Basin, southern Andhra Pradesh have been selected. The karstified rocks cover about 17% of the basin area and form important groundwater reservoirs in many drought prone areas of southern Andhra Pradesh. In semi-arid southern Andhra Pradesh these karstic zones play a vital role for the society both as a primary water supply and in economic terms (water resource for irrigated agriculture, quarrying for construction and cement production). The aquifers are not properly studied from the karstification point of view for their water resources and need to be characterized by including their heterogeneities

developed from rock solubility. Karst features can pose unpredictable problems like, ground subsidence, sinkhole collapse, groundwater contamination and unpredictable water supply. This thesis therefore, focuses on the hydrogeological characterization of these karst aquifers and using the approaches applied in other karst areas of the world.

The area is geologically, stratigraphically and economically very important. Hydrogeologically the carbonate rocks are the major source of groundwater in many drought prone areas. The area is characterized by low rainfall-evapotranspiration ratio (aridity index of 0.38) with a large temporal and seasonal variability in rainfall. Rainfall occurs mainly in monsoon months (June-September). Average annual rainfall of the studied area is 709mm in which 63% of rainfall is contributed by monsoons. Temperature in non-monsoon months reaches as high as 45°C. The area is characterized by rolling topography with a large variation in elevation from west to east in the basin. The carbonate massif in the centre of the basin is nearly flat plain bounded by flat topped quartzitic plateaus and hills. This plain area is drained by the tributaries of Kundu River with majority of streams being ephemeral. The soils of the basin vary from place to place but the most part of this central plain is overlain by thin, less developed black and red soils. Vegetation is mostly in the form of scattered open scrub type plants in the plain areas. The chief economic activities include agriculture, mineral exploitation (cement, construction slabs), rearing of domestic animals and sericulture. Limestone quarrying for building stones and cement construction spreads over a large area.

Geologically the karstified areas are complex where tectonics has played a vital role in karstification. Major fractures and faults coincide with the tectonic history of the southern India. The karstified units vary in thickness and other properties from place to place. The units represent major aquifer systems of the area. Geological, geomorphological and hydrogeological study was carried out and discussed in three formations separately. All the formations are highly karstified possessing large caves and few springs along with many surface features. Vempalle dolomite covers the western part of the basin and posses one of the deepest caves of India. No spring flow is observed in the formation. The geology of the Narji limestone plain is highly complex and the area has been studied widely for karst development. The formation possesses one of the longest caves of India which is famous from tourist point of view. Many temporary and permanent springs are located in the formation. Few springs flow quite variably and show sharp responses with the rainfall events. Surface karst depressions concentrate the runoff and recharge the aquifer mostly through fast recharge. Epikarst is well developed in the limestone and shows many secondary calcite infillings on the surface. The aquifer is highly quarried for cement manufacture and building stones which is extending day-by-day in the area. Quarrying seems to have modified the hydrological characteristics of the area. Karstification is still in progress but at deeper levels and at slower pace. Speleothems of different architectural size are present in the caves. Secondary calcite deposition is also observed at many places. Koilkuntla limestone is also karstified with well developed epikarst layer as observed by the well data. No caves and springs were located in the formation. The limestone is highly pumped for agricultural purposes.

A model of karstification is discussed based on cave pattern within three main stages. The area displays a set of peculiar karst landforms modified by tectonic activities and change in base level during their formation. The primary porosity and smaller fractures develop into more enlarged ones that develop into a well developed and hierarchally organized cave patterns. The uplift of Western Ghats and lowering of base level of erosion resulted in the (dissolution) caving of deeper parts of the limestone which is represented by a number of paleo-phreatic conduits in the region. Climatic changes during the past geological time periods have greatly modified the hydrogeological development of karst groundwater. Moist conditions of the past are responsible for the karst development which has minimized due to the onset of monsoon conditions and Western Ghats uplifting. Karst has developed at many elevations representing the past base levels in the Cuddapah basin. A denudation rate of 3.7 mm/ka has been proposed for this semi-arid karst area.

Groundwater levels of the Narji limestone plain are shallow with average depth of 7mgl during pre-monsoon period. During post-monsoon water level rises with an average increase of 1.2m. Most bore wells produce an average yield of 10 l/s. The karst springs of Narji limestone are both permanent and temporary. The Belum spring shows quite fast response to the rainfall while other springs flow with less variation in discharge and chemistry.

Groundwater recharge is an important process that replenishes the aquifer through surface and rainwater. It is very difficult to estimate recharge of highly heterogeneous karst aquifers in semi-arid climates. The recharge processes are complex due to climatic and karst

hydrogeological peculiarities. Karst aquifer in this semi-arid area is recharged mainly by two mechanisms- point recharge and diffuse recharge. Point recharge is the major contributor and enters the aquifer as allogenic inputs. The surface runoff from non-karstic areas reaches the aquifer by fast mechanism through preferential pathways. Average point recharge of the aquifer is about 107.3mm i.e., 15% of the annual rainfall amount. This part of the recharge replenishes the groundwater very rapidly and has number of effects on overall groundwater balance of the area. Diffuse recharge enters the aquifer through the soil zone. This part of infiltrating water gets stored in the epikarst zone and the reaches the phreatic part very late. Soil properties and climatic conditions affect the overall process of diffuse recharge. Diffuse recharge of 86mm i.e., 13% of annual rainfall replenishes the aquifer. The amount of diffuse recharge depends on the frequency and intensity of rainfall. Average annual recharge of this semi-arid limestone aquifer is 29% of the rainfall. The results of the recharge estimation were calibrated with the water levels of the borewells. The recharge estimates from nearby area covering limestone and quartzites showed that annual diffuse recharge through soils is about 105mm. Diffuse recharge of 16% of the annual rainfall estimated by Tritium injection method validates the recharge results. The results also showed that irrigation return flow also contributes to the recharge in these limestone areas. The amount of internal runoff, another type of recharge in karst areas through cave openings, etc has very less impact on the groundwater balance of the area. Annual recharge occurs during 5-7 important events in the year in which rainfall is more than 25mm a day. The high value of point recharge has a large effect on the hydrodynamics and hydrochemistry of the aquifer.

The hydrogeochemical characteristic of karst aquifers is quite different from other aquifers. The results from physico-chemical analysis of water samples have been discussed and showed a significant statistical difference between PRM (Pre-Monsoon) and POM (Post-Monsoon) seasons. The spatial variability in water chemistry is clearly observed. Ca^{2+} , Mg^{2+} and HCO_3^- are directly related to the natural water-rock interaction. These ions are derived from limestone dissolution possessing little MgCO_3 content. High concentrations of SO_4^{2-} , Cl^- , NO_3^- suggests the anthropogenic source particularly from the areas dominated by agricultural area. Land use has a major role in changing pollution-related constituents. Agriculture is the main source of nitrates and sulfate. Weathering of clastic rocks may contribute little sodium and potassium ions. The less contaminated springs are hydrogeologically separated from the rest of the area and have less human influence. On the basis of water chemistry and physicochemical results it is obvious that groundwater has encompassed many hydrogeochemical processes. The original chemical signature of groundwater gets modified to a great degree during post-monsoon season by recharging water. Water seems to have acquired majority of the ions dominantly through water-rock interaction and mixing processes mainly dilution. The different types of recharging waters (concentrated and diffuse) get mixed and lead to final groundwater chemistry.

The groundwater is the sole source for domestic and agricultural activities in the region. Cultivation is the main source of income for a major population. Thus, cultivation of paddy, grams and other rain fed crops are economically important and is carried over many areas. It is therefore, important to consider the contamination of groundwater by irrigation return flow, application of fertilizers and farm manure, leaching of soil minerals and

contaminant release from domestic sewage, etc. The high concentrations of nitrates, sulfates and chloride indicate these sources. Due to seasonal changes in agricultural activities and vegetation growth, possible variations in $p\text{CO}_2$ are likely. Physical process, like evapotranspiration also led to the concentration of certain ions particularly in agriculture dominated areas. Dumping of domestic waste directly in karst depressions (common practice in the area) could also be the cause of anthropogenic sources.

Another highlight of this work is the use of isotopic data of rainfall and groundwater in this semi-arid karst. Environmental isotopes are of particular importance in karst hydrogeological studies which has been carried in many karst areas of the world. $\delta^2\text{H}$ and $\delta^{18}\text{O}$ isotopes of rain and groundwater were analysed from this semi-arid karst area. Local Meteoric Water Line of rainfall data shows a slope of 7.02. The rainfall is depleted in heavy isotopes than the west coast rainfall. Rainfall isotope data indicates two sources of vapour-SW and NE monsoon. The samples collected after SW monsoon season are more depleted which indicates their origin from continental areas. The low deuterium excess values of rainfall than west coast indicate more evaporation effect during its travel towards inland. Groundwater isotope data shows more depletion in heavy isotopes than rainfall -a result of high evaporation of the area. Groundwater samples fall close to the LMWL with a slope of 4 and 3.1 for $\delta^2\text{H}$ and $\delta^{18}\text{O}$ respectively. This slope is lower than LMWL which indicates the effect of isotope fractionation due to more evaporation. During POM groundwater data is less scattered that is related to the amount effect of rainfall. The primordial signature of groundwater in POM samples is close to the range of rainwater while, the PRM data shows more deviation. Thus, groundwater during PRM gets more fractionated due to higher

temperature and little rainfall. The lower d-excess values of groundwater during monsoon months are related to the effect of more humidity in these months. Groundwater samples were grouped into three classes based on isotope data. The more enriched samples fall in the area with thick soil cover and having effect from agriculture. This indicates that the irrigated water becomes more enriched and then recharges the aquifer as depleted irrigation return flow. The least depleted samples are less affected during hydrological processes and fall in highly karstified areas with fast recharge conditions. Other samples were of mixed character and were affected by both diffuse and fast recharge. The isotopic signature of spring water time series clearly indicates their hydrological behaviour. The relation with water level and discharge indicates more isotope variation during peak flow periods in Belum spring. The relation with water level and discharge indicates more enrichment of isotopes during peak flow periods.

Tracer results helped to infer the connectivity between the cave stream and the spring in the Kona karst area. The short duration tracer test helped to characterize the karstic nature of the Narji limestone. Results indicate that the Kona spring (S2) is generally a diffuse or mixed type and not purely a conduit type spring. The dye got lost in the stream after short distance and there is possibility that it was captured in the rock dominated by matrix porosity. This also indicates that the tracer output at the sampling location depends on the hydrogeological setup and the nature of karstification.

8.2. Recommendations

- A major concern in semi-arid regions is the scarcity of water resources and the need to have adequate water resource management tools. There is a lack of proper hydrogeological knowledge on karst groundwater in many regions. It is therefore, important to study the karst landscapes of the country more effectively. Appropriate studies will help to understand aquifer structure, functioning and evolution, etc for their sustainable exploitation and implementation of management policies for protecting the quantity and quality of the resource. This demands the use of state-of-the-art research of karst aquifers in Indian context.
- The present conceptual model of the karst aquifer in this area needs improvement incorporating the detailed studies on soils and epikarst as they represent the main storage zone in karst aquifers. Modeling can help to simulate the nature of the low permeability volumes in such aquifers. Recharge estimation and assessment of groundwater balance on a regional scale should be carried out using well established and new approaches applicable to karst environments.
- The present flow of groundwater in karst aquifers is guided by the past long-term dissolution and flow mechanism. Therefore, it is important to study their short-term characteristics in order to understand the long-term hydrodynamics of the groundwater system. Detailed applications of spring hydrographs and chemographs, tracer studies and isotopes will enhance the further knowledge of karst studies in India.

- Another important problem in karst areas is the geomorphological and hydrogeological circumstances that make these aquifers highly vulnerable to contamination from human activities. The aquifers once polluted are very difficult to renew in terms of groundwater quality and quantity. Dumping of domestic and other waste on limestone directly in the area will have some serious implications on water quality. Hence, it is recommended that future detailed chemical investigations of water, rock and soil is needed to understand the hydrochemical processes. Frequent sampling, particularly during monsoon months will be helpful in understanding the interaction of different processes. Such investigations will be useful for the characterization of the aquifer flow systems and the control of karst heterogeneities on groundwater.
- Due to growing urbanization, the karst terrains have faced a number of modifications due to human activities across the globe. Practicing agriculture, construction of dams has serious impacts on karst environments. The limestones of the study area are extensively quarried for extraction of construction slabs and cement manufacture. A number of cement factories are actively removing the limestone and changing the natural landscape of the area. The quarry area is increasing at a rate of $0.6 \text{ km}^2/\text{year}$. These changes will create a number of ecological implications which need to be studied and discussed for the management of these aquifers and their resources. Restoration of the quarried areas for agriculture and other activities is very difficult and should be discussed in detail in further exploitation of the resources. This will provide a scientific basis for protection and utilization of resources in karst areas of the country particularly groundwater.

REFERENCES

- Aguilera, H. and Murillo, J. M. (2009). The effect of possible climate change on natural groundwater recharge based on a simple model: a study of four karstic aquifers in SE Spain. *Environ. Geology*, 57(5), 963-974.
- Ahmed, S. and De Marsily, G. (1987). Comparison of Geostatistical methods for estimating transmissivity using data on transmissivity and specific capacity. *Water Res. Res.*, 23(9), 1717-1737.
- Alcala, F. J. and Custodio, E. (2008a). Atmospheric chloride deposition in continental Spain. *Hydrol. Process.*, 22(18), 3636-3650.
- Alcalá, F. J. and Custodio, E. (2008b). Using the Cl/Br ratio as a tracer to identify the origin of salinity in aquifers in Spain and Portugal. *J. Hydrol.*, 359, 189-207.
- Alcala, F. J., Canton, Y., Contreras, S., Were, A., Serrano-Ortiz, P., and et. al., (2010). Diffuse and concentrated recharge evaluation using physical and tracer techniques: results from a semiarid carbonate massif aquifer in south-eastern Spain. *Environ Earth Sci.* DOI 10.1007/s12665-010-0546-y.
- Al-Charideh, A. (2011). Recharge rate estimation in the Mountain karst aquifer system of Fige spring, Syria. *Environ Earth Sci.*, DOI 10.1007/s12665-011-1365-5.
- Allison, G. B. and Barnes, C. J. (1983). Estimation of evaporation from non-vegetated surfaces using natural deuterium. *Nature*, 301, 143-145.
- Allison, G. B. and Hughes, M. W. (1983). The use of natural tracers as indicators of soil-water movement in a temperate semi-arid region. *J. Hydrol.*, 60, 157-173.
- Allison, G. B. and Hughes, M. W. (1983). The use of natural tracers as indicators of soil-water movement in a temperate semi-arid region. *J. Hydrol.*, 60, 157-173.
- Allison, G. B., Barnes, C. J. and Hughes, M.W. (1983a). The distribution of deuterium and oxygen-18 in dry soils: II. Experimental. *J. Hydrol.*, 64, 377-397.
- Allison, G. B., Barnes, C. J., Hughes, M. W. and Leaney, F. W. J. (1983b). The effect of climate and vegetation on oxygen-18 and deuterium profiles in soils. *Proc. Of Int. Symposium on Isotope Hydrology. Water Res. Dev., IAEA, Vienna, No. IAEA-SM-270/20.*
- Allison, G. B., Stone, W. J. and Hughes, M. W. (1985). Recharge in karst and dune elements of a semi-arid landscape as indicated by natural isotopes and chloride. *J. Hydrol.*, 76, 1-25.
- Andreo, B., Carrasco, F., Bakalowicz, M., Mudry, J. and Vadillo, I. (2002). Use of the hydrodynamic and hydrochemistry to characterise carbonate aquifers. Case study of the Blanca-Mijas unit (Malaga, southern Spain). *Environ. Geol.*, 43, 108-119.
- Andreo, B., Carrasco, F., Durán, J. J. and LaMoreaux, J. W. (2010). *Advances in Research in Karst Media.* Springer Heidelberg Dordrecht, London, New York.

- Andreo, B., Vías, J., Durán, J. J., Jiménez, P., López-Geta, J. A. and Carrasco, F. (2008). Methodologies for groundwater recharge assessment in carbonate aquifers: application to pilot sites in southern Spain. *Hydro. J.*, 16, 911-925.
- Andreu, J. M., Alcalá, F. J., Vallejos, A., Pulido-Bosch, A. (2011). Recharge to mountainous carbonated aquifers in SE Spain: Different approaches and new challenges. *J. Arid Environ.*, 75(12), 1262-1270.
- Angulo-Jaramillo, R., Vandervaere, J. P., Roulier, S., Thony, J. L., Gaudet, J. P. and Vauclin, M. (2000). Field measurement of soil surface hydraulic properties by disc and ring infiltrometer: A review and recent developments. *Soil Tillage Res.*, 55, 1-29.
- Ankeny, M. D., Kaspar, T. C. and Horton, R. E. (1988). Design for an automated tension infiltrometer. *Soil Sci. Soc. Am. J.*, 52, 893-896.
- Aquilina A., Ladouche, B. and Dorfliger, N. (2005). Recharge processes in karstic systems investigated through the correlation of chemical and isotopic composition of rain and spring-waters. *App. Geochemistry*, 20, 2189-2206.
- Aquilina, L., Ladouche, B. and Dorfliger, N. (2006). Water storage and transfer in the epikarst of karstic systems during high flow periods. *J. Hydro.*, 327, 472-485.
- Aquilina, L., Ladouche, B., Dorfliger, N. and Bakalowicz, M. (2004). Water circulation, residence time and water-rock interaction in a complex karst hydrosystem (Thau lagoon, S-France). *Ground Water*, 41, 6, 790-805.
- Arbel, Y., Greenbaum, N., Lange, J. and Inbar, M. (2010). Infiltration processes and flow rates in developed karst vadose zone using tracers in cave drips. *Earth Surf. Process. Landforms*, 35, 1682-1693.
- ASTER GDEM. 30m land surface Digital Elevation Model data available through <http://gdem.ersdac.jspacesystems.or.jp>.
- Aswathanarayana, U. (1962a). Age of the Cuddapahs, India. *Nature, Lond.*, 193, 470.
- Aswathanarayana, U. (1964). Isotopic ages from the Eastern Ghats and Cuddapahs of India. *J. Geophys. Res.*, 69, 3479-3486.
- Athavale, R. N., Murthi, C. S. and Chand, R., (1980). Estimation of recharge to the phreatic aquifers of the Lower Maner Basin, India, by using the tritium injection method. *J. Hydrol.*, 45, 185-202.
- Athavale, R. N., Rangarajan, R. and Muralidharan, D., (1992). Measurement of natural recharge in India. *J. Geol. Soc. India*, 39, 235-244.
- Athavale, R.N., Murthi, C. S. and Chand, R. (1980). Estimation of recharge to the phreatic aquifers of the Lower Maner Basin, India, by using the tritium injection method. *J. Hydrol.*, 45, 185-202.

- Atkinson, T. C. (1977a). Carbon dioxide in the atmosphere of the unsaturated zone: An important control of groundwater hardness in limestones. *J. Hydrol.*, 35, 111-123.
- Atkinson, T. C. (1977b). Diffuse flow and conduit flow in limestone terrain in the Mendip Hills, Somerset (Great Britain), *J. Hydrol.*, 35, 93-110.
- Atkinson, T. C., Smith, D. I., Lavis, J. J. and Whitaker, R. J. (1973). Experiments in tracing underground waters in limestones. *J. Hydrol.*, 19, 323-349.
- Azzaz, H., Cherchali, M., Meddi, M., Houha, B., Puig, J. M. and Achachi, A. (2008). The use of environmental isotopic and hydrochemical tracers to characterize the functioning of karst systems in the Tlemcen Mountains, northwest Algeria. *Hydro. J.*, 16, 531-546.
- Bagarello, V., Iovino, M. and Elrick, D. (2004). A simplified falling-head technique for rapid determination of field-saturated hydraulic conductivity. *Soil Sci. Soc. Am. J.*, 68, 66-73.
- Bakalowicz, M. (2003). Epikarst, the skin of karst. Conference on Epikarst. The Karst Water Institute, Shepherdstown, West Virginia.
- Bakalowicz, M. (2005). Karst groundwater: a challenge for new resources. *Hydro. J.*, 13(1), 148-160.
- Balakrishna, S. and B. E. Vijayam. (1968). Sedimentation of non-clastics in the western part of the Cuddapah basin. *Bull. Nat. Geophys. Res. Inst.*, 6, 2, 51-67.
- Baltas, E. A., Dervos, N. A. and Mimikou, M. A. (2007). Technical Note: Determination of the SCS initial abstraction ratio in an experimental watershed in Greece. *Hydrol. Earth Syst. Sci.*, 11, 1825-1829.
- Barbieri, M., Boschetti, T., Petitta, M. and Tallini, M. (2005). Stable isotope (^2H , ^{18}O and $^{87}\text{Sr}/^{86}\text{Sr}$) and hydrochemistry monitoring for groundwater hydrodynamics analysis in a karst aquifer (Gran Sasso, central Italy). *App. Geochem.*, 20, 2063-2081.
- Basu, H., Gangadhran, G. R., Kumar, S., Sharma, U. P., Rai, A. K. and Chaki, A. (2007). Sedimentary facies of Gulcheru Quartzite in the southwestern part of the Cuddapah Basin and their implication in deciphering the depositional environment. *J. Geol. Soc. India*, 69, 347-358.
- Beekman, H. E., Gieske, A. and Selaolo, E. T. (1996). GRES: Groundwater recharge studies in Botswana 1987-1996 Botswana. *J. Earth Sci.*, III, 1-17.
- Bhagavan, K. V. B. and Rao, R. K. L. (1985). Geomorphic Features of a part of Cuddapah and Nellore District, Andhra Pradesh-using Remote Sensing Techniques. *Photonirvachak, J.*, Indian Soc. Photo-Int. and Remote Sensing, 13, 2.
- Bhaskar Rao, Y. J., Pantulu, G. V. C., Damodar Reddy, V. and Gopalan, K. (1995). Time of Early Sedimentation and Volcanism in the Proterozoic Cuddapah Basin, South India. Evidence from Rb-Sr Age of Pulivendla Mafic Sill. *Geol. Soc. India Mem.*, 33, 329-338.

- Bhattacharya, S. K., Gupta, S. K. and Krishnamurthy, R. V. (1985). Oxygen and hydrogen isotopic ratios in groundwater and river waters from India. *Proc. Indian Acad. Sciences. Earth Planet. Sci.*, 94(3), 283-295.
- Blasch, K. W., and Bryson, J. R. (2007). Distinguishing Sources of Ground Water Recharge by Using d^2H and $d^{18}O$. *Groundwater*, 45(3), 294-308.
- Blavoux, B, and Mudry, J. (1983). Use of the physico-chemical variations of karst waters to understand how an aquifer works: example from the fontaine de vaucluse system (Southeastern France). *Hydrogeological Processes in Karst Terranes (Proceedings of the Antalya Symposium and Field Seminar, October 1990)*. IAHS Publ. 207, 327.
- Bonacci, O. (1993). Karst spring hydrographs as indicators of karst aquifers. *J. Hydrol. Sci.*, 38, 51-62.
- Bonacci, O. (1995). Ground water behaviour in karst: example of the Ombla Spring (Croatia). *J. Hydrol.*, 165, 113-134.
- Bonacci, O. and Rubinic, J. (2009). Water losses from a reservoir built in karst: the example of the Boljunčica reservoir (Istria, Croatia). *Environ. Geology*, 58(2), 339-345.
- Bosák, P. (2003). Karst processes from the beginning to the end: How can they be dated? *Speleogenesis and Evolution of Karst Aquifers*, 1, 3, 2.
- Boughton, W. C. (1989). A review of the USDA SCS curve number method. *Aus. J. of Soil Research*, 27(3), 511-523.
- Bouwer, H. (1961). A double tube method for measuring hydraulic conductivity of soil in situ above a water table. *Soil Sci. Soc. Am. Proc.*, 25, 334-342.
- Bouwer, H. (1966). Rapid field measurement of air entry value and hydraulic conductivity of soil as significant parameters in flow system analysis. *Water Res. Res.*, 2, 729-738.
- Bowen, G. J. and Revenaugh, J. (2003). Interpolating the isotopic composition of modern meteoric precipitation. *Water Res. Res.*, 39(10).
- Boyer, D. G. and Pasquarell, G. C., (1996). Agricultural land use effects on nitrate concentrations in a mature karst aquifer. *J. Am. Water Res. Ass.*, 32, 565-573.
- Buhmann, D. and Dreybrodt, W. (1985). The kinetics of calcite dissolution and precipitation in geologically relevant situations of karst areas. *Chem. Geol.*, 48, 189-211.
- Canton, Y., Villagarcía, L., Moro, M. J., Serrano-Ortíz, P., Were, A., Alcalá, F. J., Kowalski, A. S., Solé-Benet, A., Lázaro, R. and Domingo, F. (2010). Temporal dynamics of soil water balance components in a karst range in southeastern Spain: estimation of potential recharge, *Hydro. Sci. J.*, 55(5), 737-753.
- Carter, J. M. and Driscoll, D. G. (2006). Estimating recharge using relations between precipitation and yield in a mountainous area with large variability in precipitation. *J. Hydrol.*, 316, 71-83.

- Cartwright, I., Tamie, R., Weaver, L. and Fifield, K. (2006). Cl/Br ratios and environmental isotopes as indicators of recharge variability and groundwater flow: An example from the southeast Murray Basin, Australia. *Chemical Geology*, 231, 38-56.
- CGWB, (2007). Ground Water Information Kurnool District, Andhra Pradesh. Central Groundwater Board, Ministry of Water Resources, Government of India.
- CGWB, (2012). Aquifer systems of India. Central Ground Water Board. Government of India.
- Chand, R., Mondal, N. C., Singh, V. S., and Prasanti, A. (2006). Groundwater Recharge Evaluation in a River Basin, Andhra Pradesh, India. *Advances in Geosciences*, 4.
- Chandra, P.C., Satyanarayana, T. and Raju, K. C. B. (1987). Geoelectrical response of cavities in limestones: An experimental field study from Kurnool District, Andhra Pradesh, India. *Geoexploration*, 24(6), 483-502.
- Clark, I. and P. Fritz. (1997). *Environmental Isotopes in Hydrogeology*, Lewis Publishers, Boca Raton.
- Clemens, T., Hückinghaus, D., Liedl, R. and Sauter, M., (1999). Simulation of the development of karst aquifers: role of the epikarst. *Int J. Earth Sciences*, 88, 157-162.
- Contreras, S., Boer, M. M., Alcalá, F. J., Domingo, F., García, M., Pulido-Bosch, A., Puigdefábregas, J. (2008). An ecohydrological modelling approach for assessing longterm recharge rates in semiarid karstic landscapes. *J. Hydrol.*, 351, 42-57.
- Coplen, T. B., Herczeg, A. L. and Barnes, C. (2000). Isotope engineering: using stable isotopes of the water molecule to solve practical problems, in *Environmental Tracers in Subsurface Hydrology*, ed. by P.G. Cook and A. L. Herczeg, Kluwer Academic Publishers, Boston, 2000.
- COST Action 65, (1995). *Hydrogeological Aspects of Groundwater Protection in Karstic Areas*. Published by the European Commission Directorate-General XII Science, Research and Development, Luxembourg.
- Coudrain-Ribstein, A., Prats, B., Talbi, A., Jusserand, C. (1998). Is the evaporation from phreatic aquifers in arid zones independent of the soil characteristics? *CR Acad Sci Paris, Sci Terre Planèt*, 326,159-165.
- Coward, J. M. H., Waltham, A. C. and Bowser, R. J. (1972). Karst springs in the Vale of Kashmir. *J. Hydrol.*, 16, 213-223.
- Coxon, C. (2011). Agriculture and Karst. In van Beynen, P.E. (ed.) *Karst Management*, Springer, Dordrecht, 103-138.
- Craig, H. (1961a). Standard for reporting concentrations of deuterium and oxygen-18 in natural waters. *Science*, 133, 1833-1934.
- Craig, H. (1961b). Isotopic variations in meteoric waters. *Science*, 133, 1702-1703.

- Crandall, C. A., Katz, B. G. and Hirten, J. J. (1999). Hydrochemical evidence for mixing between the Suwannee River and Upper Floridan aquifer. *Hydro. J.*, 7, 454-467.
- Crawford, A. R. and Compston, W. (1973). The Age of the Cuddapah and Kurnool Systems, Southern India. *J. Geolo. Soc. of Australia*, 19(4), 453-464.
- CWC, (2009). Drought Prone Areas Programme (DPAP), Department of Land Resources. Govt. of India, Ministry of Rural development.
- Dansgaard, W. (1964). Stable isotopes in precipitation. *Tellus*, 16, 436-468.
- Daoxian, (1981). Mentioned in Short, N. M. and Blair, R. W. (1986). Karst landforms and lakes. *Geomorphology from Space: a global overview of regional landforms*. NASA publication.
- Dar, F. A., Perrin, J., Riotte, J., Gebauer, H. D., Narayana, A. C. and Ahmed, S. (2011). Karstification in the Cuddapah Sedimentary Basin, Southern India. Implications for Groundwater Resources. *Acta Carsologica*, 40(3), 457-472.
- Datta, P. S., Bhattacharya, S. K. and Tyagi, S. K. (1996). ^{18}O Studies on recharge of phreatic aquifers and groundwater flow-paths of mixing. *J. Hydrol.*, 176, 25-36.
- Datta, P. S., Bhattacharya, S. K., Mookerjee, P. and Tyagi, S. K. (1994). Study of groundwater occurrence and mixing in Pushkar (Ajmer) valley, Rajasthan, with $\delta^{18}\text{O}$ and hydrochemical data. *J. Geol. Soc. India*, 43, 449-456.
- Davis, S. N., Thompson, G. M., Bentley, H. W., Stiles, G. (1980). Groundwater tracers-a short review. *Ground Water*, 18(1), 14-23.
- De Vries, J. J. and Simmers, I. (2002). Groundwater recharge: an overview of processes and challenges. *Hydro. J.*, 10(1), 5-17.
- Deshpande, R. D., Bhattacharya, S. K., Jani, R. A., Gupta, S. K. (2003). Distribution of oxygen and hydrogen isotopes in shallow groundwater from Southern India: influence of a dual monsoon system. *J. Hydrol.*, 271, 226-239.
- Dettinger, M. D. (1989). Reconnaissance estimates of natural recharge to desert basins in Nevada, U.S.A., by using chloride-balance calculations. *J. Hydrol.*, 106, 55-78.
- Deutsch, W. J. (1997). *Groundwater chemistry-fundamentals and applications to contamination*. CRC Press; 1 edition.
- Dewandel, B., Gandolfi, J. C., de Condappa, D. and Ahmed, S. (2008). An efficient methodology for estimating irrigation return flow coefficients of irrigated crops at watershed and seasonal scale. *Hydrol. Process.*, 22, 1700-1712.
- Doerfliger, N., Jeannin, P. Y., Zwahlen, F. (1999). Water vulnerability assessment in karst environments: a new method of defining protection areas using a multi-attribute approach and GIS tools (EPIK method). *Environ. Geol.* 39(2), 165-176.
- Drever, J. I. (1997). *The Geochemistry of Natural Waters*. Prentice Hall, New Jersey, p. 436.

- Dreybrodt W. and Gabrovsek, F. (2002). Basic processes and mechanisms governing the evolution of karst. *J. Speleogenesis and Evolution of Karst Aquifers*, 1(1).
- Dreybrodt, W. (1981). Kinetics of the dissolution of calcite and its application to karstification. *Chem. Geol.*, 31, 245-269.
- Dreybrodt, W. (1988) Processes in karst systems. Physics, chemistry and geology. Springer series in physical environment 4. Springer, Berlin Heidelberg New York, p. 88.
- Dreybrodt, W. (1990). The role of dissolution kinetics in the development of karst aquifers in limestone: a model simulation of karst evolution. *J. Geology*, 98, 639-655.
- Droque, C. (1971). Coefficient d'infiltration ou infiltration efficace, sur les roches calcaires, Actescolloque d'hydrologie en pays calcaire. Besançon, 121-131.
- Droque, C. (1980). Essai d'identification d'un type de structure de magasins carbonates fissurées. Application à l'interprétation de certains aspects du fonctionnement hydrogéologique. (Test for identifying the type of structure of fractured carbonate aquifers. Application to the interpretation of certain hydrogeological aspects). Mémoires hors série Société Géologique de la France, 11, 101-108.
- Dubey, D. P., Tiwari, R. N. and Dwivedi, U. (2006). Evaluation of Pollution Susceptibility of Karst Aquifers of Rewa Town (Madhya Pradesh), Using DRASTIC Approach. *J. Environ. Sci. and Eng.*, 48(2), 113-118.
- Dufresne, D. P. Drake, C. W. (1999). Regional groundwater flow model construction and well field site selection in a karst area, Lake City, Florida. *Eng. Geology*, 52, 129-139.
- Durand, N., Ahmad, S. M., Hamelin, B. and Curmi, P. (2006). Origin of Ca in South Indian calcretes developed on metamorphic rocks. *J. Geochemical Exploration*, 88, 275-278.
- Durand, N., Gunnell, Y., Curmi, P. and Ahmad, M. (2007). Pedogenic carbonates on Precambrian silicate rocks in South India: Origin and palaeoclimate significance. *Quat. Intern.*, 162-163, 35-49.
- Dutt, N. V. B. S. (1962). Geology of Kurnool System of rocks in Cuddapah and the Southern part of Kurnool District. *Rec. Geol. Surv. India*, 87, 549-694
- Dutt, N. V. B. S. (1975). Middle and Later Proterozoic Sedimentary basins; Geology and Mineral Resources of Andhra Pradesh. Ramesh Publ., Hyderabad, 205.
- Dutta, N. P., Bose R. N. and Saikia, B. C. (1970). Detection of solution channels in limestone by electrical resistivity method. *Geophysical Prospecting*, 18(3), 335-465.
- Dutton, A. R. (1995). Groundwater isotopic evidence for paleo-recharge in U. S. High Plains aquifers. *Quat. Res.*, 43, 221-231.
- Eagon, H. B. and Johe, D. E. (1972b). Practical solutions for pumping tests in carbonate-rock aquifers. *Ground Water*, 10(4), 6-13.

- Ebrahimian, M., See, L. F., Ismail, M. H. and Malek, I. A. (2009). Application of Natural Resources Conservation Service–Curve Number Method for Runoff Estimation with GIS in the Kardeh Watershed, Iran. *European J. Sci. Res.*, 34(4), 575-590.
- Edmunds, W. M., Darling, W. G., Kinniburgh, D. G., Kotoub, S. and Mahgoub S. (1992). Sources of recharge at Abu Delaig, Sudan. *J. Hydrol.*, 131, 1-24.
- Edmunds, W. M., Smedley, P. L. (2000). Residence time indicators in groundwater: the East Midlands Triassic sandstone aquifer. *Appl. Geochem.*, 15, 737-752.
- Eisenlohr, L. Bouzelboudjen, M. Kiraly, L. Rossier Y. (1997). Numerical versus statistical modeling of natural response of a karst hydrogeological system. *J. Hydrol.*, 202, 244-262
- El Kashouty, M. (2010). Modeling of the limestone aquifer using isotopes, major and trace elements in the western river Nile between Beni Suef and El Minia. Fourteenth International Water Technology Conference, IWTC14 2010 Cairo, Egypt.
- El Ouali, A., Mudry, J., Mania, J., Chauve, P., Elyamine, N., Marzouk, M. (1999). Present recharge of an aquifer in a semi-arid region: an example from the Turonian limestones of the Errachidia basin, Morocco. *Environ. Geol.*, 38, 2.
- Eliers, V. H. M. Carter R. C. Rushton K. R. (2007). A single layer soil water balance model for estimating deep drainage (potential recharge): An application to cropped land in semi-arid North-east Nigeria. *Geoderma*, 140, 119-131.
- Ellins, K. K. (1992). Stable isotopic study of the groundwater of the Martha Brae River basin, Jamaica. *Water Res. Res.*, 28(6), 1597-1604.
- El-Naqa, A. (1994). Estimation of transmissivity from specific capacity data in fractured carbonate rock aquifer, central Jordan. *Environ. Geol.*, 23, 73-80.
- Elrick, D. E., Reynolds, W. D. and Tan, K. A. (1989). Hydraulic conductivity measurements in the unsaturated zone using improved well analyses. *Ground Water Monit. Rev.*, 9, 184-193.
- EPA. (1999). The QTRACER Program for Tracer-Breakthrough Curve Analysis for Karst and Fractured-Rock Aquifers. National Center for Environmental Assessment–Research. U.S. Environmental Protection Agency, Washington, DC 20460.
- Fairchild, I. J., Borsato, A., Tooth, A. F., Frisia, S., Hawkesworth, C. J., Huang, Y. M., McDermott, F. and Spiro, B. (2000). Controls on trace element (Sr-Mg) compositions of carbonate cave waters: implications for speleothem climatic records. *Chem. Geol.*, 166, 255-269.
- Falcone, R. A., Falgiani, A., Parisse, B., Petitta, M., Spizzico, M., Tallini, M. (2008). Chemical and isotopic ($d^{18}O$ and, d^2 and, $d^{13}C$ and, ^{222}Rn) multi-tracing for groundwater conceptual model of carbonate aquifer (Gran Sasso INFN underground laboratory-central Italy). *J. Hydrol.*, 357, 368-388.

- Faure, G. and Mensing, T. M. (2005). *Isotopes-Principles and Applications*. Third edition. John Wiley and Sons.
- Fetter, C. W. (1980). *Applied Hydrogeology*. Merrill Publishing International, Charles E., 488.
- Field, M. S. (1993). Karst hydrology and chemical contamination. *J. Environ. Systems*, 22, 1-26.
- Field, M. S. (1988). The vulnerability of karst aquifers to chemical contamination: EPA, 600/D-89/008, 13.
- Field, M. S. (1997). Risk assessment methodology for karst aquifers: solute-transport modelling. *Environ. Mon. and Assess.*, 47(1), 23-37.
- Field, M. S., (1999). The QTRACER Program for Tracer-Breakthrough Curve Analysis for Karst and Fractured-Rock Aquifers. National Center for Environmental Assessment, U.S. Environmental Protection Agency, Washington, D.C.
- Filipponi, M., Jeannin, P. Y. and Tacher, L. (2009). Evidence of inception horizons in karst conduit networks. *Geomorphology*, 106, 86-99.
- Fleury, P., Plagnes, V. and Bakalowicz, M. (2007). Modelling of the functioning of karst aquifers with a reservoir model: Application to Fontaine de Vaucluse (South of France). *J. Hydrol.*, 345(1-2), 38-49.
- Ford D. C. and Williams, P. W. (2007). *Karst Geomorphology and Hydrology*, John Wiley and Sons, 2007, 562
- Ford, D. (2006). Jovan Cvijic and the founding of karst geomorphology. *Environ. Geol.*, 51, 675-684.
- Ford, D. C. and Ewers, R. O. (1978). The development of limestone cave systems in the dimensions of length and depth. *Canadian J. Earth Sciences*, 15, 1783-1798.
- Freeze, R. A. and Cherry, J. A. (1979). *Groundwater*. Prentice Hall, New Jersey, 604.
- Fron dini, F. (2008). Geochemistry of regional aquifer systems hosted by carbonate-evaporite formations in Umbria and southern Tuscany (central Italy). *App. Geochemistry*, 23(8), 2091-2104.
- Frot, E., van Wesemael, B. (2009). Predicting runoff from semi-arid hill slopes as source areas for water harvesting in the Sierra de Gador, southeast Spain. *Catena*, 79, 83-92.
- Gabrovsek, F. and Dreybrodt, W. (2001). A comprehensive model of the early evolution of karst aquifers in limestone in the dimensions of length and depth. *J. Hydrol.*, 240(3-4), 206-224.
- Gabrovšek, F., and Dreybrodt, W. (2001). A model of the early evolution of karst aquifers in limestone in the dimensions of length and depth. *J. Hydrol.*, 240, 27-34.

- Gao, X., Wang, Y., **Ma, T. and et. al. (2011)**. Anthropogenic impact assessment of Niangziguan karst water. *Water Management*, 164, WM10.
- Gardner, W. R. (1958). Some steady-state solutions of the unsaturated moisture flow equation with application to evaporation from a water table. *Soil Sci.*, 85, 228-232.
- Gat, J. R. (1996). Oxygen and hydrogen isotopes in the hydrologic cycle. *Annual Review of Earth and Planetary Sciences*, 24, 225-262.
- Gat, J. R. and Carmi, I. (1970). Evolution of the isotopic composition of atmospheric waters in the Mediterranean Sea area. *J. Geophys. Res.*, 75, 3039-3048.
- Gebauer, H. D. (1985). Kurnool 1984: Report of the speleological expedition to the district of Kurnool, Andhra Pradesh, India.-*Abhandlungen zur Karst und Höhlenkunde*, 21, 77. Munchen.
- Gebauer, H. D. (1986). Preliminary report of the first German speleological expedition to the Himalaya. *Int. J. Speleo.*, 15, 53-56.
- Gebauer, H. D. (1997). **Indien 1996/97**: Kurnool, Jaypur-Jagdulpur und Meghalaya.-*Mitt. Verb. dt. Höhlen- u. Karstforsch.*, 43(4), 104-111.
- GEC, (2009). Report of the ground water resource estimation committee. Ground water resource estimation methodology, New Delhi, 2009. Ministry of Water Resources Government of India.
- Gee, G. W. and Hillel, D. (1988). Groundwater recharge in arid regions: review and critique of estimation methods. *Hydrol. Processes*, 2, 255-266.
- Gee, G. W., Zhang, Z. F., Tyler, S. W., Albright, W. H. and Singleton, M. J. (2004). Chloride-mass balance for predicting increased recharge after land-use change. University of California. Available via DIALOG. <http://www.repositories.cdlib.org/lbnl/LBNL-55584>.
- Geyer, T., Birk, S., Liedl, R. and Sauter, M. (2008). Quantification of temporal distribution of recharge in karst systems from spring hydrographs. *J. Hydrol.*, 348, 452-463.
- Gibbs, R. J. (1970). Mechanisms controlling World's water chemistry, *Science*, 170, 1088-1090.
- Gillieson, D. (2009). *Caves: processes, development and management*. John Wiley and Sons, p. 336.
- GNIP/ISOHIS. (2001). Isotope Hydrology Information System of International Atomic Energy Agency, (IAEA), Vienna, Austria. The ISOHIS Database. <http://isohis.iaea.org>.
- Goldscheider, N. and Drew, D. (2007). *Methods in Karst Hydrogeology*. Taylor and Francis Group, London, UK.
- Goldscheider, N., Hotzl, H., Kass W. and Ufrecht, W. (2003). Combined tracer tests in the karst aquifer of the artesian mineral springs of Stuttgart, Germany. *Environ. Geol.*, 43, 922-929.

- Goldscheider, N., Meiman, J., Pronk, M. and Smart, C. (2008). Tracer tests in karst hydrogeology and speleology. *Int. J. Speleology*, 37(1), 27-40.
- Green, W. H. and Ampt, G. A. (1911). Studies on soil physics: the flow of air and water through soils. *J. Agric. Sci.*, 4, 1-24.
- GSI, (1997). Cuddapah Geological Quadrangle Map Series, (1:250,000). Geological Survey of India, Kolkata.
- Gunn, J. (1983). Points recharge of limestone aquifers- A model from Newzealand Karst. *J. Hydrol.*, 61, 19-29.
- Gunnell, Y. and Fleitout, L. (1998). Morphotectonic evolution of the Western Ghats, India. In: *Geomorphology and Global Tectonics* (Ed. by M. Summerfield). John Wiley and Sons, Chichester.
- Gunnell, Y. (1998a). The interaction between geological structure and global tectonics in multistoreyed landscape development: a denudation chronology of the South Indian shield. *Basin Research*, 10, 281-310.
- Gunnell, Y. (1998b). Passive margin uplifts and their influence on climatic change and weathering patterns of tropical shield regions. *Glob. Planet. Change* 18, 47-57.
- Gunnell, Y. and Louchet, A. (1998). The influence of rock hardness and divergent weathering on the inter-pretation of apatite fission track denudation rates: evidence from charnockites in South India and Sri Lanka. *Zeitschrift für. Geomorphologie*, 44(4), 481-504.
- Gunnell, Y. and Bourgeon, G. (1997). Soils and climatic geomorphology on the Karnataka Plateau, Peninsular India. *Catena*, 29, 239-262.
- Guo, Q., Wang, Y., Ma, T. and Ma, R. (2007). Geochemical processes controlling the elevated fluoride concentrations in groundwater of the Taiyuan Basin, Northern China. *J. Geochemical Exploration*, 93(1), 1-12.
- Gupta, S. K. (1983). An Isotopic investigation of a near-surface groundwater system. *Hydrol. Sci. J.*, 28, 2, 261-272.
- Gupta, S. K. and Deshpande, R. D. (2003). Synoptic hydrology of India from the data of isotopes in precipitation. *Curr. Sci.*, 85, 1591-1595.
- Gupta, S. K. and Deshpande, R. D. (2005a). The need and potential applications of a network for monitoring of isotopes in waters of India. *Curr. Sci.*, 88, 1, 10.
- Gupta, S. K. and Deshpande, R. D. (2005b). Groundwater isotopic investigations in India: What has been learned? *Curr. Sci.*, 89, 5, 10.
- Gupta, S., Dandele, P. S., Verma M. B. and Maithani, P. B. (2009). Geochemical assessment of groundwater around Macherla-Karempudi area, Guntur District, Andhra Pradesh. *J. Geol. Soc. India*, 73, 202-212.

- Gururaja, M. N. and Chandra, A. (1987). Stromatolites from Vempalle and Tadpatri Formations of Cuddapah Supergroup, Andhra Pradesh and their Significance. *Memoir of Geological Society of India*, 6, 399-437.
- Handa, B. K. (1975). Geochemistry and genesis of fluoride contaminating groundwater in India. *Groundwater*, 13, 275-281.
- Haq, B. H., Hardenbol, J. and Vail, P. R. (1987). The chronology of fluctuating sea level since the Triassic. *Science*, 235, 1156-1167.
- Hauns, M., Jeannin, P. Y., Atteia, O. (2001). Dispersion, retardation and scale effect in tracer breakthrough curves in karst conduits. *J. Hydrol.*, 241,177-193.
- Häuselmann, P., Jeannin, P. Y., Bitterli, T. (1999). Relationships between karst and tectonics: case-study of the cave system north of Lake Thun (Bern, Switzerland). *Geodinamica Acta*, 12(6), 377-388.
- Hawkins, R. H. (1975). Importance of Accurate Curve Number in the Estimation of Storm Runoff. *J. Am. Water Res. Ass.*, 11(5).
- Healy, R. W. and Cook, P. G. (2002). Using groundwater levels to estimate recharge. *Hydrog. J*, 10, 91-109.
- Heinz, B., Birk, S., Liedl, R., Geyer, T., Straub, K. L. and **et. al.**, (2009). Water quality deterioration at a karst spring (Gallusquelle, Germany) due to combined sewer overflow: evidence of bacterial and micro-pollutant contamination. *Environ. Geol.* 57(4), 797-808.
- Hem, J. D. (1985). Study and Interpretation of the Chemical Characteristics of Natural Water. United States Geol. Survey, Water Supply, Paper 2254, 1-263.
- Herczeg, A. L., Leane, F. W., Stadter, M. F., Allan, G. L. and Field, L. K. (1997). Chemical and isotopic indicators of point-source recharge to a karst aquifer, South Australia. *J. Hydrol.*, 192, 271-299.
- Herman, J. S. and White, W. B. (1985). Dissolution kinetics of dolomite: effects of lithology and fluid flow velocity. *Geoch. Cosmoch Acta* 49, 2017-2026.
- Hess, J. W. and White, W. B. (1988). Storm response of the karstic carbonate aquifer of southcentral Kentucky. *J. Hydrol.*, 99, 235-252.
- Hills, R. C. (1971). Lateral flow under cylinder infiltrometer- a graphical correction procedure. *J. Hydrol.*, 13, 153-162.
- Hobbs, S. L. and Smart, P. L. (1986). Characterisation of carbonate aquifers: a conceptual base, 9th International Congress of Speleology, Barcelona.
- Hoefs, J. (1997). Stable Isotope Geochemistry, 4th ed., Springer-Verlag, Berlin. IAEA www.isohis.iaea.org
- Hoetzi, H. (1995). Groundwater recharge in an arid karst area (Saudi Arabia). *IAHS Publ* 232, 195-207.

- Hughes, G., Mansour, M. M. and Robins, N. S. (2008). Evaluation of distributed recharge in an upland semi-arid karst system: the West Bank Mountain Aquifer, Middle East. *Hydrog. J.*, 16, 845-854.
- Huntley, D., Nommensen, R. and Steffey, D. (1992). The Use of Specific Capacity to Assess Transmissivity in Fractured-Rock Aquifers. *Ground Water*, 30, 3.
- Ingram, R. G. S., Stone, N., Carey, M. and Smart, P. (2012). Catchment-scale water balance modelling in a Carboniferous Limestone aquifer. *Geol. Soci. London, Special Publication*, 364, 249-267. <http://sp.lyellcollection.org>
- Iqbal, M. Z. (2000). Effects of layered heterogeneity in subsurface geologic materials on solute transport under field conditions: a case study from north-eastern Iowa, USA. *Hydrog. J.*, 8, 257-270.
- Jacobson, R. L. and Langmuir, D. (1974a). Controls on the quality variations of some carbonate spring waters. *J. Hydrol.*, 23, 247-265.
- Jacobson, R., L. and Langmuir, D. (1974b). Dissociation constants of calcite and CaHCO_3^+ from 0 to 50°C. *Geoch. Cosmoch. Acta*, 38(2), 301-318.
- Jain, A. K., Rao, M. B. M., Mohan Rao, M. S. R. and Swamy, M. V. (2009). Groundwater Scenario in Andhra Pradesh. WASHCost (India), Centre for Economic and Social Studies. Hyderabad. www.cess.ac.in
- Jeelani, G. (2008). Aquifer response to regional climate variability in a part of Kashmir Himalaya in India. *Hydrog. J.*, 16, 1625-1633
- Jennings, J. N. (1971). *Karst (An Introduction to Systematic Geomorphology)*, 7. MIT Press: London, 2, 3.
- Jennings, J. N. (1983). The disregarded karst of the arid and semiarid domain. *Karstologia*, 1, 61-73.
- Jeong, C. H. (2001). Effect of land use and urbanization on hydrochemistry and contamination of groundwater from Taejon area, Korea. *J. Hydrol.*, 253, 194-210.
- Jhanwar, M. L., Rajurkar, S. T. and Phadtere, P. N. (1964). Stratigraphy of the Vempalle formation of Cuddapah basin. *J. Indian Geosc. Ass.*, 4, 43-62.
- Johnston, C. D. (1987). Distribution of environmental chloride in relation to subsurface hydrology. *J. Hydrol.* 94, 67-88.
- Jones, I. C., Banner, J. L. and Humphrey, J. D. (2000). Estimating recharge in a tropical karst aquifer. *Water Res. Res.*, 36(5), 1289-1299.
- Jordan, M. M., Pina, S., Garcia-Orenes, F., Almendro-Candel, M. B., Garcia-Sanchez, E., (2008). Environmental risk evaluation of the use of mine spoils and treated sewage sludge in the ecological restoration of limestone quarries. *Environ. Geol.*, 55, 453-462.

- Jukic, D. and Denic-Jukic, V. (2009). Groundwater balance estimation in karst by using a conceptual rainfall–runoff model. *J. Hydrol.*, 373, 302-315.
- Jukic, D. and Denic-Jukic, V. D. (2004). A frequency domain approach to groundwater recharge estimation in karst. *J. Hydrol.*, 289, 95-110.
- Kaçaroglu, F. (1999). Review of Groundwater Pollution and Protection in Karst Areas. *Water, Air and Soil Pollution*, 113(1-4), 337-356.
- Kaila, K. L. and Tewari, H. C. (1985). Structural trends in the Cuddapah basin from deep seismic soundings (DSS) and their tectonic implications. *Tectonophysics*, 115, 69-86.
- Kale, V. S. (1991). Constraints on the evolution of the Purana basins of peninsular India. *J. Geol. Soci. India*, 38, 231-252.
- Kamal, M. Y. (1974). Sedimentology and Sedimentary tectonics of the Kurnool system, near Kurnool. Unpublished thesis, Osmania University, Hyderabad.
- Kamal, M. Y. and Vijayam, B. E. (1981). Sedimentary tectonics of the Kurnool basin, near Kurnool. Fourth workshop on status, problems and programmes in Cuddapah basin. Indian Inst. Peninsular Geol., Hyderabad.
- Karanth, K R. (1987). Ground Water Assessment: Development and Management. Tata McGraw-Hill Education, Ground-water management, 720.
- Karimi, H., Raeisi, E. and Bakalowicz, M. (2005). Characterising the main karst aquifers of the Alvand basin, northwest of Zagros, Iran, by a hydrogeochemical approach. *Hydro. J.*, 13(5-6), 787-799.
- Karmann, I. and Ferrari, J. A. (2000). Karst and caves of the Upper Ribeira State Park (PETAR), southern São Paulo State. In: Schobbenhaus, C.; Campos, D. A.; Queiroz, E. T.; Winge, M.; Berbert-Born, M. (Edit.) *Sítios Geológicos e Paleontológicos do Brasil*. Published on Internet at the address; <http://www.unb.br/ig/sigep/sitio043/sitio043english.htm>.
- Kasipathi, C., Arjunudu, K., Rao, K. S. and Rao, M. S. (2008). Cuddapah Formations of Andhra Pradesh, India. A New Report of Prospects for Rich Banded Iron Ore Formation. *Canadian J. Pure and App. Sci.*, 2(1), 227-233.
- Kattan, Z. (1997). Environmental isotope study of the major karst springs in Damascus limestone aquifer systems: case of the Fiegh and Barada springs. *J. Hydrol.*, 193, 161-182.
- Kattan, Z. (2001). Use of hydrochemistry and environmental isotopes for evaluation of groundwater in the Paleogene limestone aquifer of the Ras Al-Ain area (Syrian Jezireh). *Environ. Geo.*, 41(1-2), 128-144.
- Katz, B. G. (2002). Demystifying Ground-water Flow and Contaminant Movement in Karst Systems Using Chemical and Isotopic Tracers. U.S. Geological Survey Karst Interest Group Proceedings, Shepherdstown, West Virginia, August, 20-22, 2002.

- Katz, B. G., Chelette, A. R. and Pratt, T. R. (2004). Use of chemical and isotopic tracers to assess nitrate contamination and ground-water age, Woodville Karst Plain, USA. *J. Hydrol.*, 289(1-4), 36-61.
- Kaufmann, G. and Romanov, D. (2008). Cave development in the Swabian Alb, south-west Germany: A numerical perspective. *J. Hydrol.*, 349, 302-317.
- Keese, K. E., Scanlon, B. R. and Reedy, R. C. (2005). Assessing controls on diffuse groundwater recharge using unsaturated flow modelling. *Water Res. Res.*, 41(6).
- Kher, S. V. and Peshwa, V. V. (1989). The Geology and Structure of the Area south of Gani, Kurnool District, Andhra Pradesh- A Study Based on Remotely Sensing Data. *J. Indian Soci. Remote Sensing*, 17(4).
- King, W., 1872. Kadapah and Kurnool formations in the Madras presidency. *Geol. Surv. Ind. Mem.*, 8.
- Kingsbury, J. A. (2008). Relation between Flow and Temporal Variations of Nitrate and Pesticides in Two Karst Springs in Northern Alabama. *J. Am. Water Res. Ass.*, 44, 478-488.
- Kingsbury, J. A. and Shelton, J. M. (2002). Water Quality of the Mississippian Carbonate Aquifer in Parts of Middle Tennessee and Northern Alabama, USGS Water-Resources Investigations Report, 02-4083, 36, Nashville, Tennessee. <http://pubs.usgs.gov/wri/wri024083>.
- Király, L. (1975). Rapport sur l'état actuel des connaissances dans le domaine des caractères physiques des roches karstiques. In: *Hydrogeology of Karstic Terrains* (eds. Burger et Dubertret). Union of Geological Sciences, Series B, 3, 53-67.
- Kiraly, L. (1998). Modelling karst aquifers by the combined discrete channel and continuum approach. *Bulletin d'Hydrogeologie*, 16, 77-98. Centre d'Hydrogeologie, Universite de Neuchâtel.
- Kiraly, L. (1998). Modelling karst aquifers by the combines discrete channel and continuum approach. *Bulletin d'Hydrogéologie*, 16, 77-98. Centre d'Hydrogeologie, Universite de Neuchâtel.
- Kiraly, L. (2003). Karstification and groundwater flow, *Speleogenesis Evol. Karst Aquifers*, 1, 1-26.
- Klimchouk, A. B. (2000). The formation of epikarst and its role in vadose speleogenesis. In: *Speleogenesis, evolution of karst aquifers*. National Speleological Society, 91-99.
- Klimchouk, A. B. (2003). Unconfined versus confined speleogenetic settings: variations of solution porosity. *Speleogenesis and Evolution of Karst Aquifers*, 1(2), 2.
- Klimchouk, A. B. (2004). Towards defining, delimiting and classifying epikarst: Its origin, processes and variants of geomorphic evolution. *Speleogenesis and Evolution of Karst Aquifers*, 2(1), 2.

- Klute, A. and Dirksen, C., 1986. Hydraulic conductivity and diffusivity, laboratory methods. p. 687-732. In A. Klute (ed.) *Methods of soil analysis. Part 1.* SSSA, Madison, WI.
- Korkmaz, N. (1990). The estimation of groundwater recharge from spring hydrographs. *Hydro. Sci. J.*, 35.
- Kovács, A. (2003). *Geometry and hydraulic parameters of karst aquifers: A hydrodynamic modeling approach.* Thèse, Université De Neuchâtel.
- Kranjc, A. (2010). Arid Karst or Karst in Arid Countries? 2nd Symposium on Living with Landscapes. *Egyptian J. Envir. Change*, 2, 1.
- Krawczyk, W. E. and Ford, D. C. (2006). Correlating Specific Conductivity with Total Hardness in Limestone and Dolomite Karst Waters. *Earth Surface Processes and Landforms*, 31, 221-234.
- Kumar, B., Athavale, R. N. and Sahay, K. S. N. (1982). Stable-isotope geohydrology of the lower Maner basin, Andhra Pradesh, India. *J. Hydrol.*, 59, 315-330.
- Kumar, J. V. (1983). *Geological and hydrogeological studies of part of Cuddapah basin.* Unpublished Ph.D thesis, Osmania University, Hyderabad.
- Kumar, P. S., Babu, M. J. R. K., Praveen, T. V. and Vagolu, V. K. (2010). Analysis of the Runoff for Watershed Using SCS-CN Method and Geographic Information Systems. *Int. J. Eng. Sci. and Tech.*, 2(8), 3947-3654.
- Labat, D., Ababou, R., Mangin, A. (2000). Rainfall-runoff relations for karstic springs. Part I. Convolution and spectral analyses. *J. Hydrol.*, 238, 123-148.
- Lai, J. and Ren, L. (2007). Assessing the size dependency of measured hydraulic conductivity using double-ring infiltrometers and numerical simulation. *Soil Sci. Soc. Am. J.*, 71, 1667-1675.
- Lakey, B., Krothe, N. C. (1996). Stable isotopic variation of storm discharge from a perennial karst spring, Indiana. *Water Res. Res.*, 32(3), 721-731.
- Lambs, L., Balakrishna, K., Brunet, F. and Probst, J. L. (2005). Oxygen and hydrogen isotopic composition of major Indian rivers: a first global assessment. *Curr. Sci.* 89(5), 10.
- LaMoreaux, P. E. Powell, W. J., LeGrand, H. E. (1997). Environmental and legal aspects of karst areas. *Environ. Geology*, 29, 1-2.
- Lang, Y. C., Liu, C. Q., Zhao, Z. Q., Li, S. L. and Han, G. L. (2006). Geochemistry of surface and ground water in Guiyang, China: Water/rock interaction and pollution in a karst hydrological system. *Appl. Geochemistry*, 21(6), 887-903.
- Langelier, W. F. and Ludwig, H. F. (1941). Graphical method for indicating of the mineral character of natural waters. *J. Am. W.W. Asso.*, 34, 335-352.
- Langmuir, M. (1968). Stability of calcite based on aqueous solubility measurements. *Geoch. Cosmoch. Acta*, 32, 835-851.

- Langmuir, M. (1971). The geochemistry of some carbonates ground waters in central Pennsylvania. *Geoch. Cosmoch. Acta*, 35, 1023-1045.
- Langston, A L., Sreaton, E J., Martin, J B and Bailly-Comte, V. (2012). Interactions of diffuse and focused allogenic recharge in an eogenetic karst aquifer (Florida, USA). *Hydrog. J.*, 20, 767-781.
- Larsen, D., Swihart, G. H. and Xiao, Y. (2001). Hydrochemistry and isotope composition of springs in the Tecopa basin, southeastern California, USA. *Chemical Geol.*, 179, 17-35.
- Lastennet, R., Puig, J. M., Emblanch, C. and Blavoux, B. (1995). Influence of the non saturated zone on the functioning of karst systems. Demonstration from springs in northern Vaucluse, France. *Hydrogologie* 4, 57-66.
- Leaney, F. W. and Herczeg, A. L. (1995). Regional recharge to a karst aquifer estimated from chemical and isotopic composition of diffuse and localized recharge, South Australia. *J. Hydrol.*, 164, 363-387.
- Leaney, F. W., Smettem, K. R. J. and Chittleborough, D. J. (1993). Estimating the contribution of preferential flow to subsurface runoff from a hillslope using deuterium and chloride. *J. Hydrol.*, 147, 83-103.
- Leduc, C., Bromley, J. and Schroeter, P. (1997). Water table fluctuation and recharge in semi-arid climate: some results of the HAPEX-Sahel hydrodynamic survey (Niger). *J. Hydrol.*, 189(1-4),123-138.
- Lee, E. S. and Krother, N. C. (2001). A four-component mixing model for water in a karst terrain in southcentral Indiana; USA. Using solute concentration and stable isotopes as tracers. *Chemical Geology*, 179, 129-143.
- Legrand, H. E. And Stringfield., V. T. (1971). Development and Distribution of Permeability in Carbonate Aquifers. *Water Res. Res.*, 7(5), 1284-1294.
- Lerch, R. N., Wicks, C. M. and Moss, P.L. (2005). Hydrologic characterization of two karst recharge areas in Boone County, Missouri. *J. Cave Karst Stud.*, 67(3), 158-173.
- Lerner, D. N., Issar, A. S. and Simmers, I. (1990). Groundwater recharge: a guide to understanding and estimating natural recharge. International Association of Hydrogeologists, International Contributions to Hydrogeology, 8, IAH, Wallingford, UK.
- Li, S., Calmels, D., Han, G., Gaillardet, J. and Liu, C. (2008). Sulphuric acid as an agent of carbonate weathering constrained by $\delta^{13}\text{C}_{\text{DIC}}$: Examples from Southwest China. *Earth and Planetary Science Letters*, 270(3-4), 30, 189-199.
- Li, X. Y., Contreras, S. and Solé-Benet, A. (2008). Unsaturated hydraulic conductivity in limestone dolines: influence of vegetation and rock fragments. *Geoderma*, 145, 288-294.
- Li, X. Y., Contreras, S., Solé-Benet, A., Cantón, Y. and Domingo, D. and et. al. (2011). Controls of infiltration-runoff processes in Mediterranean karst rangelands in SE Spain. *Catena*, 86(2), 98-109.

- Liedl, R., Sauter, M., Huckinghaus, D., Clemens, T. and Teutsch, G. (2003). Simulation of the development of karst aquifers using a coupled continuum pipe model. *Water Res. Res.*, 39.
- Lloyd, J. W. (1986). A review of aridity and groundwater. *Hydrol. Process*, 1, 63-78.
- Lowe, D. J. and Gunn, J. (1997). Carbonate Speleogenesis: an inception horizon hypothesis. *Acta Carsologica*, 26, 457-488.
- Lowe, D. J. (2000). Role of stratigraphic elements in speleogenesis; the speleoinception concept. In: Klimchouk, A., Ford, D.C., Palmer, A. N., Dreybrodt, W. (editors) *Speleogenesis evolution of karst aquifers*. National Speleological Society, 65-76.
- Ma, J., He, J., Qi, S., Zhu, G., Zhao, W., Edmunds, W. M. and Zhao, Y. (2011). Groundwater recharge and evolution in the Dunham Basin, northwestern China. *Appl. Geochemistry*, 28, 19-31.
- Mace, R. E. (1997). Determination of Transmissivity from Specific Capacity Tests in a Karst Aquifer. *Ground Water*, 35(5).
- Magaritz, M., Aravena, R., Peaia, H., Suzuki, O. and Grill, A. (1989). Water chemistry and isotope study of streams and springs in Northern Chile. *J. Hydrol.*, 108, 323-341.
- Maloszewski, P. and Zuber, A. (1993). Tracer experiments in fractured rocks: Matrix diffusion and the validity of models. *Water Res. Res.* 29, 2723-2735.
- Maloszewski, P., Herrmann, A. and Zuber, Z. (1999). Interpretation of tracer tests performed in fractured rock of the Lange Bramke basin, Germany. *Hydro. J.*, 7, 209-218.
- Maloszewski, P., Stichler, W., Zuber, A. and Rank, D. (2002). Identifying the flow systems in a karstic-fissured-porous aquifer, the Schnealpe, Austria, by modelling of environmental ^{18}O and ^3H isotopes. *J. Hydrol.*, 256(1/2), 48-59.
- Manghi, F., Mortazavi, B., Crother, C. and Hamdi, M. R. (2009). Estimating Regional Groundwater Recharge Using a Hydrological Budget Method. *Water Res. Man.*, 23, 2475-2489.
- Mangin, A. (1975). Contribution a l'étude hydrodynamique des aquifers karstiques. Troisieme partie. Constitution et fonctionnement des aquifers karstiques. *Annales de Speleologie*, 30(1), 21-124
- Mangin, A. (1994). Karst hydrogeology. In: *Groundwater Ecology* (J. Gibert, D.L. Danielopol and J. A. Stanford, eds), 43-67. Academic Press, San Diego, CA, USA.
- Marechal J. C., Varma, M. R.R., Riotte, J., Vouillamoz, J.M. and et. al. (2009a). Indirect and direct recharges in a tropical forested watershed: Mule Hole, India. *J. Hydrol.*, 364(3-4), 272-284.

- Maréchal, J. C., Dewandel, B., Ahmed, S., Galeazzi, L. and Zaidi, F. K. (2006). Combining the groundwater budget and water table fluctuation methods to estimate specific yield and natural recharge. *J. Hydrol.*, 329, 281-293.
- Marechal, J. C., Galeazzi, L., Dewandel, B. and Ahmed, S. (2003). Hydrology of the Mediterranean and Semiarid Regions. Proceedings of an international symposium held at Montpellier. April 2003. IAHS Publ 278.
- Maréchal, J. C., Ladouche, B., and Dörfliger, N. (2009b). Hydrogeological analysis of groundwater contribution to the 6-8 September 2005 flash floods in Nîmes. Bureau de Recherches Géologiques et Minières (brgm)-Service Eau. DOI 10.1051/lhb: 2009019.
- Marei, A., Khayat, S., Weise, S., Ghannam, S., Sbaih M. and Geyer, S. (2010). Estimating groundwater recharge using the chloride mass-balance method in the West Bank, Palestine, *Hydrol. Sci. J.*, 55(5), 780-791.
- Marfia, A., M., Krishnamurthy, R. V., Atekwana, E. V. and Panton, W. F. (2004). Isotopic and geochemical evolution of ground and surface waters in a karst dominated geological setting: a case study from Belize, Central America. *App. Geochemistry*, 19, 937-946.
- Martin J. B. and White, W. B. (2007). *Frontiers of Karst Research. Proceedings and recommendations of the workshop held on May 3-5, San Antonio, Texas, USA.* Karst Waters Institute, Inc. P.O. Box 4142, Leesburg, Virginia 20177. http://www.karstwaters.org/publications/sp13_wholebook.pdf
- Martínez-Santos, P. and Andreu, J.M. (2010). Lumped and distributed approaches to model natural recharge in semiarid karst aquifers. *J. Hydrol.*, 388(3-4), 389-398.
- Massei, N., Wang, H. Q., Field, M. S., Dupont, J. P., Bakalowicz and M., Rodet, J. (2006). Interpreting tracer breakthrough tailing in a conduit-dominated karstic aquifer. *Hydro. J.*, 14, 849-858.
- Mayback, M. (1987). Global chemical weathering of surficial rocks estimated from river dissolved loads. *Am. J. Sci.*, 287, 401-428.
- Mayer, J. (1999). Spatial and Temporal Variation of Groundwater Chemistry in Pettyjohns Cave, Northwest Georgia, USA. *J. Cave and Karst Studies*, 61(3), 131-138.
- McCoy, K. J. and Kozar, M. D. (2008). Use of sinkhole and specific capacity distributions to assess vertical gradients in a karst aquifer. *Environ. Geol.*, 54, 921-935. DOI [10.1007/s00254-007-0889-1](https://doi.org/10.1007/s00254-007-0889-1).
- McDermott, F., Schwarcz, H. and Rowe, P. J. (2005). Isotopes in speleothems. *Developments in Paleoenvironmental Research*, 10, 185-225.
- McGuire, K. J., DeWalle, D. R. and Gburek, W. J. (2002). Evaluation of mean residence time in subsurface waters using oxygen-18 fluctuations during drought conditions in the mid-Appalachians. *J. Hydrol.*, 261(1-4), 132-149.

- McKenzie, D. P., Nisbet, E. and Sclater, J. G. (1980). Sedimentary basin development in the Archean. *Earth and Planetary Science Letters*, 48, 35-41.
- Meigs, L. C., Beauheim, R. L. (2001). Tracer tests in a fractured dolomite. Experimental design and observed tracer recoveries. *Water Res. Res.*, 37(5), 1113-1128.
- Meijerink, A. M. J., Rao, D. P. and Rupke, J. (1984). Stratigraphic and structural development of the Precambrian Cuddapah Basin, SE India. *Precambrian Res.*, 26, 57-104.
- Milanovic, P. (2002). The environmental impacts of human activities and engineering constructions in karst regions. *Episodes*, 25(1).
- Milanovic, S., Stevanovic, Z. and Jemcov, I. (2010). Water losses risk assessment: an example from Carpathian karst. *Environ. Earth Sci.*, 60(4), 817-827.
- Mohammadi, Z., Raeisi, A., and Zare, M. (2007). A dye-tracing test as an aid to studying karst development at an artesian limestone sub-aquifer: Zagros Zone, Iran. *Environ. Geol.* 52, 587-594.
- Mohan Rao, M. S. R., Adhikari, R. N., Chittaranjan, S. and Chandrappa, M. (1996). Influence of conservation measures on groundwater regime in a semi-arid tract of South India. *Agricultural Water Management*, 30, 301-312.
- Mook, W. G. (2006). Introduction to Isotope Hydrology. Stable and Radioactive Isotopes of Hydrogen, Oxygen and Carbon. IAH publication, Taylor and Francis.
- Mouli, P. C., Mohanb, S. V. S. and Reddy, J. (2003). A study on major inorganic ion composition of atmospheric aerosols at Tirupati. *J. Hazardous Materials*, 96, 217-228.
- Mudry, J., 1990. Chemical mass flow vs. discharge and the functioning of karst aquifers. *J. Hydrol.*, 120(1-4), 283-294.
- Munnich, K. O. (1968). Moisture movement measured by isotope tagging. In: Guide book on nuclear technique in Hydrology. International Atomic Energy Agency, Vienna, 112-117
- Murthy, P. B. (1950). Genesis of asbestos and barite, Cuddapah district, Rayalseema, South India. *Econ. Geol.*, 45, 681-696.
- Murthy, Y. G. K. (1981). The Cuddapah Basin- A Review of Basin Development and Basement Framework Relations. *Fourth workshop on status, problems and programs in Cuddapah Basin*. Inst. Of Indian Peninsular Geology, Hyderabad, 51-73.
- Murthy, Y. G. K., Setti, T. L. N., Rajurkar, S. T., Meoloi, S. H. and et. al. (1979). Salient features of the revised geological map of the Cuddapah basin. *Third workshop on status and problems in Indian Peninsular shield*. Inst. Of Indian Peninsular Geology, Hyderabad.
- Murty, K.S. (1988). Karst Hydrogeology: India. In: Karst Hydrogeology and Karst Environment Protection. IAH, 21st Congress, 10-15 October, 446-450, Guilin, China.
- Nagaraja Rao, B. K., Rajaurkar, S. T. and Ramalingaswamy, G. (1987). Stratigraphy, Structure and Evolution of the Cuddapah Basin. *Mem. Geol. Soc. India* 6, 33-86.

- Narayanaswami, S. (1966). Tectonics of Cuddapah Basin. *J. Geol. Soc. Ind.*, 7, 33-50.
- Navada, S. V. and Rao, S. M. (1991). Study of Ganga River-Groundwater Interaction Using Environmental Oxygen-18. *Isotopenpraxis, Isotopes in Environmental and Health Studies*, 27, 8.
- NBSS and LUP (2000). Soils of Andhra Pradesh. National Bureau of Soil Survey and Land Use Planning. Indian Council of Agr. Res. (ICAR), Nagpur.
- Newton, J. G. (1987). Development of sinkholes resulting from man's activities in the Eastern United States. US GPO, IV, 54 <http://pubs.er.usgs.gov/publication/cir968>.
- NIH, (1997). Determination of SCS Runoff curve Number and Land Use Change for Hamidnagar Sub-basin of Punpun basin. CS (AR), 14, 96/97, Roorkee.
- Nimmo, J. R., Perkins, K. S., Schmidt, K. M., Stock, J. D., Miller, D. M. and Singha, K. (2009). Hydrologic characterization of desert soils with varying degrees of pedogenesis: Field experiments evaluating plant-relevant soil-water behavior. *Vadose Zone J.*, 8(2), 480-495.
- Nimmo, J. R., Schmidt, K. M., Perkins, K. S. and Rapid, J. D. S. (2009). Measurement of Field-Saturated Hydraulic Conductivity for Areal Characterization. *Vadose Zone J.*, 8, 142-149.
- NRLD, (2009). National register of large dams. Government of India, New Delhi.
- Padilla, A. and Pulido-Bosch, A. (2008). A simple procedure to simulate karstic aquifers. *Hydrological Processes*, 22(12), 1876-1884.
- Pal, D. K. and Deshpande, S. B. (1987), Genesis of clay minerals in a red and black soil complex of Southern India. *Clay Research*, 6(1), 6-13.
- Palmer A. N. (2000). Maze origin by diffuse recharge through overlying formations. In: Klimchouk A., Ford D., Palmer A. and Dreybrodt W. (Eds.), *Speleogenesis: Evolution of Karst Aquifers*. Huntsville, Ala., National Speleological Society, 387-390.
- Palmer, A. N. (1984a). Recent trends in karst geomorphology. *J. Geol. Education*, 32, 247-253.
- Palmer, A. N. (1984b). Geomorphic interpretation of karst features, in LaFleur, R.G., ed., *Groundwater as a geomorphic agent: Boston, Massachusetts*, Allen and Unwin, p. 173-209.
- Palmer, A. N. (1991). Origin and morphology of limestone caves. *Geological Society of America Bulletin*, 103, 1-21. doi: [10.1130/0016-7606\(1991\)103<0001:OAMOLC>2.3.CO;2](https://doi.org/10.1130/0016-7606(1991)103<0001:OAMOLC>2.3.CO;2).
- Palmer, A. N. and Audra, P. H. (2004). Patterns of Caves. *Encyclopedia of Caves and Karst Science*, 573-575

- Palmer, A.N. (2000). Digital modelling of individual solution conduits. In: Klimchouk, A.B., Ford, D.C., Palmer, A., Dreybrodt, W. (Eds.), *Speleogenesis: Evolution of Karst Aquifers*. National Speleological Society, Huntsville, 194-200.
- Palmer, C. D., and Cherry, J. A. (1984). Geochemical evolution of groundwater in sequence of sedimentary rocks: *J. Hydrol.*, 75 27-65.
- Palmer, C. D., Cherry, J. A. (1984). Geochemical evolution of groundwater in sequences of sedimentary rocks. *J. Hydrol.*, 75, 27-65.
- Perrin, J. (2003). A conceptual model of flow and transport in a karst aquifer based on spatial and temporal variations of natural tracers, Thesis, University of Neuchâtel, Switzerland, 227.
- Perrin, J., Jeannin, P. Y. and Zwahlen, F. (2003). Epikarst storage in a karst aquifer: a conceptual model based on isotopic data, Milandre test site, Switzerland. *J. Hydrol.*, 279, 106-124.
- Perrin, J., Jeannin, P. Y., Cornaton, F. (2006). The role of tributary mixing in chemical variations at a karst spring. *J. Hydrol.*, 332, 158-173.
- Perrin, J., Jeannin, P. Y., Zwahlen, F. (2003). Implications of the spatial variability of the infiltration water chemistry for the investigation of a karst aquifer. *Hydrog. J.*, 11(6), 673-687.
- Perrin, J., P.Y. Jeannin, F. Zwahlen, (2003a). Epikarst storage in a karst aquifer: a conceptual model based on isotopic data, Milandre test site, Switzerland *J. Hydrol.*, 279, 106-124
- Perroux, K. M. and White, I. (1988). Designs for disc permeameters. *Soil Sci. Soc. Am. J.* 52, 1205-1215.
- Peterson, E. W., Davis, R. K., Brahana, J. V. and Orndorff, H. A. (2000). Movement of nitrate through regolith covered karst terrain, Northwest Arkansas. *J. Hydrol.*, 256(1-2), 35-47.
- Pettijohn, F. J. (1975). *Sedimentary Rocks*. Longman Higher Education. ISBN, 9780060451912, 628.
- Peyraube, N. Lastennet, R., and Denis, A. (2012). Geochemical evolution of groundwater in the unsaturated zone of a karstic massif, using the pCO₂-SIc relationship. *J. Hydrol.*, 430-431, 13-24.
- Philip, J. R. (1992). Falling head ponded infiltration. *Water Res. Res.*, 28, 2147-2148.
- Phillips, F. M. (1994). Environmental tracers for water movement in desert soils of the American Southwest. *Soil Sci. Soci. America J.*, 58, 14-24.
- Pillans, B., Holgate, G., and Mcglone, M. (1988). Climate and Sea Level during Oxygen Isotope Stage 7b: On-Land Evidence from New Zealand. *Quaternary Research*, 29, 176-185.

- Piper, A. M. A. (1953). Graphic procedure in the geochemical interpretation of water analysis. Groundwater Note 12. United State Geological Survey.
- Planning commission, (1990). Report of the Inter Ministry task group on efficient utilisation of water resources planning commission.
- Plummer, L. N., Wigley, T. M. L. and Parkhurst, D. L. (1978). The kinetics of calcite dissolution in CO₂ water systems at 5-6⁰C and 0.0-1.0 atm CO₂. *Am. J. Sci.* 278, 179-216.
- Ponce, V. M. and Hawkins, R. H. (1996). Runoff curve number: Has it reached maturity? *J. Hydro. Eng.*, 1(1).
- Prabhua, C. N. Shankara, R. Anupamab, K. Taiebc, M. Bonnefillec, R. Vidalc, L. and Prasadb, S. (2004). A 200 ka pollen and oxygen-isotopic record from two sediment cores from the eastern Arabian Sea. *Palaeogeography, Palaeoclimatology, Palaeoecology*, 214, 309-321.
- Prasad, K. N. (1996). Pleistocene Cave Fauna from Peninsular India. *J. Caves and Karst Studies*, 58(1), 30-34.
- Pujari P. R. and Soni, A. K. (2009). Sea water intrusion studies near Kovaya limestone mine, Saurashtra coast, India. *Environ. Monit. Assess.* 154(1-4), 93-109.
- Quinlan, J. F. and Ewers, R. O. (1985). Ground water flow in limestone terranes: Strategy rationale and procedure for reliable, efficient monitoring of ground water quality in karst areas, in National symposium and exposition on aquifer restoration and ground water monitoring, 5th, Columbus Ohio, 1985, Proceedings: Dublin, Ohio, 197-234.
- Quinlan, J. F. and Alexander, E. C. (1987). How often should samples be taken at relevant locations for reliable monitoring of pollutants from an agricultural, waste-disposal, or spill site in a karst terrane? A first approximation. *Proceedings of the 2nd Conference on Sinkholes and the Environmental Impacts of Karst*, 277-293.
- Quinn, J. J., Tomasko, D. and Kuiper, J. A. (2006). Modeling complex flow in a karst aquifer. *Sedimentary Geology*, 184, 343-351.
- Radhakrishna, B. P. (1952). The Mysore Plateau, its structural and physiographical evolution. *Bull. Mysore Geologists Assoc*, 3.
- Raeisi, E., Zare, M. and Eftekhari, P. (1999). Application of dye tracing for determining the characteristics of Sheshpeer karst spring, Iran. *Theor. Appl. Karstol*, 11-12, 109-118.
- Rajmohan, N. and Elango, L. (2004). Identification and evolution of hydrogeochemical processes in the groundwater environment in an area of the Palar and Cheyyar River Basins, Southern India. *Environ. Geol.*, 46, 47-61.
- Raju, R. D. (2009). Cuddapah Basin: India's Emerging Uranium-Hub. *J. Indian Ass. Sedimentologists*, 28(2), 15-24.

- Ramam, P. K. and Murthy, V. N., 1997. Purana basins: Cuddapah, Pakhal, Bhima. *In Geology of Andhra Pradesh*. Geological Society of India, Bangalore, 245.
- Rande, P. (2007). Environmental impact assessment of land use planning around the leased limestone mine using remote sensing techniques. *Iran J. Environ. Health. Sci. Eng.*, 4, 1.
- Rangarajan, R. and Athavale, R. N. (2000). Annual replenishable groundwater potential of India: an estimate based on injected tritium studies. *J Hydrol.*, 234, 38-53.
- Rao, S. M. (2003). Use of isotopes in search of Lost River. *Journal of Radioanalytical and Nuclear Chemistry*, 257(1), 5-9.
- Rasmussen, T. C. and Evans, D. D. (1993). Water infiltration into exposed fractured rock surfaces. *Soil Science Soc. Am. J.*, 57, 324-329.
- Rauch, H. W. and White, W. B. (1970). Lithological controls on the development of solution porosity in carbonate aquifers. *Water Res. Res.*, 6, 1175-1192.
- Reddy, M. R., Reddy, N. J., Reddy, Y. V. And Reddy, T. V. K. (2000). Water resources development and management in the Cuddapah district, India. *Environ. Geology*, 39, 3-4.
- Reddy, P. R., Chandrakala, K., Prasad, A. S. S. S. R. S. and Rama Rao, Ch. (2004). Lateral and vertical crustal velocity and density variations in the Southwestern Cuddapah Basin and adjoining Eastern Dharwar Craton. *Curr. Sci.*, 87, 1607-1614.
- Renault, P. (1967). Contribution a l'étude des cations mécaniques et sédimentologiques dans la spéléogenèse. *Annales de Spéléologie*, 22:5-21 and 209-67; 23:259-307 and 529-96; 24:317-37. *Encyclopedia of Caves and Karst Science*.
- Renner, S. and Sauter, M. (1997). Heat as a natural tracer: Characterisation of a conduit network in a karst aquifer using temperature measurements of the spring water. In: Gunay, G., Johnson, A. I. (Eds.), *Karst Waters and Environmental Impacts*, 319-326.
- Reynolds, W. D. and Elrick D. E. (1990). Ponded infiltration from a single ring. I. Analysis of steady flow. *Soil Sci. Soc. Am. J.*, 54, 1233-1241.
- Reynolds, W. D., Elrick, D. E. and Topp, G. C. (1983). A re-examination of the constant head well permeameter method for measuring saturated hydraulic conductivity above the water table. *Soil Sci.*, 136, 250-268.
- Riding, R. and Sharma, M. (1998). Late Palaeoproterozoic (~1800-1600 Ma) stromatolites, Cuddapah Basin, southern India. Cyanobacterial or other bacterial Microfabrics? *Precambrian Res.*, 92, 21-35.
- Ritorto, M., Sreaton, E J., Martin, J B and Moore, P J. (2009). Relative importance and chemical effects of diffuse and focused recharge in an eogenetic karst aquifer: an example from the unconfined upper Floridan aquifer, USA. *Hydrog. J.*, 17, 687-1698.
- Romanov, D., Gabrovsek, F. and Dreybrodt, W. (2003). The impact of hydrochemical boundary conditions on the evolution of limestone karst aquifers. *J. Hydrol.*, 276, 240-253.

- Rossiter, D. G. (2002). Description of Soil Moisture Regimes according to USDA Soil Taxonomy 8th edition of Keys. http://www.itc.nl/personal/rossiter/research/nsm/nsm_SMR.html.
- Rotzoll, K. and El-Kadi, A. I. (2008). Estimating hydraulic conductivity from specific capacity for Hawaii aquifers, USA. *Hydrog. J.*, 16, 969-979.
- Roy, A. K. (1947). Geology of the Dhone taluk and neighbouring parts, Kurnool districts. Unpublished Geological Survey of India Progress Report.
- Rozanski, K., Araguás-Araguás, L. and Gonfiantini, R. (1993). Isotopic patters in modern global precipitation, in *Climate Change in Continental Isotopic Records*, Geophys. Monogr. Ser., 78, 1-36, AGU, Washington, DC.
- Ruggieri, R., Galletti, L. and Biswas, J. (2011). The karst Mandhip Khol-Python cave complex in the lenticular limestone intercalations of the metamorphic Chhatrela Formation (Chhattisgarh, India). *Carsologica*, 40(1).
- Rushton, K R, Eilers, V H M and Carter, R C. (2006). Improved soil moisture balance methodology for recharge estimation. *J. Hydrol.*, 318, 379-399.
- Rushton, K. R. (2003). *Groundwater Hydrology: Conceptual and Computational Models*. 416, Wiley, Chichester.
- Ryan, M. T. and Meiman, J. (1996). An examination of short-term variations in water quality at a karst spring in Kentucky: *Ground Water*, 34(1), 23-30.
- Sami, K. and Hughes, D. A. (1996). A comparison of recharge estimates to a fractured sedimentary aquifer in South Africa from a chloride mass balance and an integrated surface-subsurface model. *J. Hydrol.*, 179, 111-136.
- Sandor, C. C. (1967). The hydraulic properties and yield of dolomite and limestone aquifers, in *Hydrology of Fractured Rocks*, Proceedings of Dubrovnik Symposium (October 1965), International Association of Scientific Hydrology, Publication, 73, 120-138.
- Sankar, G. J., Rao, M. J., Rao, P. B. S. and Jugran, D. K. (2001). Hydromorphogeology and Remote Sensing Applications for Groundwater Exploration in Agnigundala Mineralised Belt, Andhra Pradesh, India. *Photonirvachak, Journal of the Indian Society of Remote Sensing*, 29, 3. *Shield. J. Fac. Mar. Sci. Technol., Tokai Univ.*, 21, 31-45.
- Santos, P. M. and Andreu, J. M. (2001). Lumped and distributed approaches to model natural recharge in semiarid karst aquifers. *J. Hydrol.*, 388, 389-398.
- Sanza, E. and Lopeza, J. J. (2000). Infiltration Measured by the Drip of Stalactites. *Ground Water*, 389(2), 247-253.
- Sauro, F., Zampier, D. and Filipponi, M., (2013). Development of a deep karst system within a transpressional structure of the Dolomites in north-east Italy. *Geomorphology*, 184, 51-63.

- Sauro, F., Zampieri, D. and Filipponi, M. (2013). Development of a deep karst system within a transpressional structure of the Dolomites in north-east Italy. *Geomorphology*, 184, 51-63.
- Sauter, M. (1992). Quantification and Forecasting of Regional Groundwater Flow and Transport in a Karst Aquifer (Gallusquelle, Malm, SW. Germany). Universität Tübingen, 16 Geowissenschaftliche Fakultät. Bereich 16 Geowissenschaftliche Fakultät (ohne Institutszuordnung). <http://tobias-lib.uni-tuebingen.de/volltexte/2005/2039/>.
- Scanlon, B. R. (1990). Relationships between groundwater contamination and major-ion chemistry in a karst aquifer. *J. Hydrol.*, 119(1-4), 271-291.
- Scanlon, B. R. and Thrailkill, J. (1987). Chemical similarities among physically distinct spring types in a karst terrain. *J. Hydrol.*, 89, 259-279.
- Scanlon, B. R. Mace, R. E. Barrett, M. E. and Smith, B. (2003). Can we simulate regional groundwater flow in a karst system using equivalent porous media models? Case study, Barton Springs Edwards aquifer, USA. *J. Hydrol.*, 276, 137-158.
- Scanlon, B. R., Healy, R. W. and Cook, P. G. (2002). Choosing appropriate techniques for quantifying groundwater recharge. *Hydro. J.*, 10, 18-39.
- Scanlon, B. R., Keese, K. E., Flint, A. L., Flint, L. E. and et. al. (2006). Global synthesis of groundwater recharge in semiarid and arid regions. *Hydrol. Process.*, 20, 3335-3370.
- SCS, (1985). SCS National Engineering Handbook, Section 4, Hydrology. Soil Conservation Service, Washington, D.C, USA.
- Sen, S. N. and Narsimha, R. (1968). Igneous activity in Cuddapah Basin and adjacent areas and suggestions on the palaeogeography of the Basin. *Proc. Symp. Upper Mantle Project*, January 1967, Hyderabad (India).
- Sequeirai, R and Kelkar, R. (1978). Geochemical Implications of Summer Monsoonal Rainwater Composition over India. *J. App. Meteorology*, 17.
- Shackleton, N. J. (1987). Oxygen Isotopes, Ice Volume and Sea Level. *Quat. Sci. Reviews*, 6, 183-190.
- Sharma, M. L. and Hughes, M. W. (1985). Groundwater recharges estimation using chloride, deuterium and oxygen-18 profiles in the deep coastal sands of Western Australia. *J. Hydrol.*, 81, 93-109.
- Sharma, M., and Shukla, M. (1999). Carbonaceous megaremaines from the Neoproterozoic Owk Shales Formations of the Kurnool Group. Andhra Pradesh, India. *Curr. Sci.* 76, 1247-1251.
- Sharma, P. and Gupta, S. K. (1987). Isotopic investigation of soil water movement: a case study in the Thar Desert, western Rajasthan. *Hydro. Sci. J.*, 32(4).
- Shi, J. A., Wang, Q., Chen, G. J. Wang, G. Y. and Zhang, Z. N. (2001). Isotopic geochemistry of the groundwater system in arid and semiarid areas and its significance: a

case study in Shiyang River basin, Gansu province, northwest China. *Environ. Geology* 40, 4-5.

Shibasaki, T., Balakrishna, S., Yoshimura, T., Venkatanarayana, B., Furukama, H., Venkateswara, R. T., Chuman, N., Ramanohan, R. Y. and Venkateswaralu, K. (1985). Karstification process of carbonate rocks in the Cuddapah sedimentary Basin, Indian Peninsular Shield. *J. Fac. Mar. Sci. Technol., Tokai Univ.*, 21, 31-45.

Shivanna, K., Tirumalesh, K., Noble, J., Joseph, T. B., Gursharan, S., Joshi, A. P. and Khati, V. S. (2008). Isotope techniques to identify recharge areas of springs for rainwater harvesting in the mountainous region of Gaucher area, Chamoli District, Uttarakhand. *Curr. Sci.*, 94, 1003-1011.

Shivanna, K., Kulkarni, U. P., Joseph, T. B. and Navada, S. V. (2004). Contribution of storms to groundwater recharge in the semi-arid region of Karnataka, India. *Hydro. Process.* 18, 473-485.

Short, N. M., and Blair, R. W. (1998). Karst Landforms and Lakes. *Geomorphology from Space: A Global Overview of Landforms.*
http://geoinfo.amu.edu.pl/wpk/geos/geo_home_page.html

Shouse, P. J., Ellsworth, T. R. and Jobes, J. A. (1994). Steady-state infiltration as a function of measurement scale. *Soil Sci.*, 157, 129-136.

Shuster, E. T., and White, W. B. (1971). Seasonal fluctuations in the chemistry of limestone spring: A possible means for characterizing carbonate aquifers, *J. Hydrol.*, 14, 93-128.

Shuster, E. T., and White, W. B. (1972). Source areas and climatic effects in carbonate groundwaters determined by saturation indices and carbon dioxide pressures, *Water Res. Res.*, 8(4), 1067-1073.

Sidle, W. C. (1998). Environmental Isotopes for Resolution of Hydrology Problems. *Environ. Mon. and Assess.*, 52(3), 389-410.

Simmers, I. and De Vries, J. (2002). Groundwater recharge: an overview of processes and challenges. *Hydro. J.*, 10, 5-17.

Singh, A. P. and Mishra, D. C. (2002). Tectonosedimentary evolution of Cuddapah basin and Eastern Ghats mobile belt (India) as Proterozoic collision: gravity, seismic and geodynamic constraints. *J. Geodynamics*, 33, 249-267.

Singh, D. K. and Singh, A. K. (2002). Groundwater Situation in India: Problems and Perspective. *Int. J. Water Res. Development*, 18, 4.

Singh, T., N. (1985). Kuteshwar limestone deposit studies for protection against bansagar dam. *Karst Water Resources (Proceedings of the Ankara-Antalya Symposium, July 1985).* IAHS Publ., 161.

Singh, Y. (1985). Hydrogeology of the karstic area around Rewa, M. P., India. *Karst Water Resources (Proceedings of the Ankara-Antalya Symposium, July 1985).* IAHS Publ., 161.

- Sinha, B. P. and Sharma, S. K. (1988). Natural groundwater recharges estimation methodologies in India. *In: Estimation of Natural Groundwater Recharge (ed. by I. Simmers), 301-311. NATO, ASI Series. Dordrecht: Reidel.*
- Sinha, K., Kulkarni, K., Sharma, S., Ray, A. and Bodhankar, N. (2002). Assessment of aquifer system using isotope techniques in urban centres Raipur, Calcutta and Jodhpur, India. *The Application of Isotope Techniques to the Assessment of Aquifer Systems in Major Urban Areas. IAEA-TECDOC-1298, IAEA, Vienna, 95-108.*
- Smare, C. C. (1988). Artificial Tracer Techniques for the Determination of the Structure of Conduit Aquifers. *Ground Water, 26, 4.*
- Smart, C. C. and Karunaratne, K. C. (2002). Characterization of fluorescence background in dye tracing. *Environ. Geology, 42, 492-498.*
- Smart, P. L. and Laidlaw, I. M. S. (1977). An evaluation of some fluorescent dyes for water tracing. *Water Res. Res., 13, 15-33.*
- Smith, D. I., and Atkinson, T. C. (1976), Process, landforms, and climate in limestone regions, in Derbyshire, E., ed., *Geomorphology and climate: New York, John Wiley, 367-409.*
- Smith, M. J., Paron, P. and Griffiths, J. S. (2011). *Geomorphological mapping; Developments in Earth Surface Processes, 15.*
- Sophocleous, M. A. (1992). Groundwater recharges estimation and regionalization: the Great Bend Prairie of central Kansas and its recharge statistics. *J. Hydrol. 137, 113-140.*
- Soumya, B S., Sekhar, M., Riotte, J. and Braun, J. J. (2009). Non-linear regression model for spatial variation in precipitation chemistry for South India. *Atmospheric Environ., 43, 1147-1152.*
- Spalding, R. F., Exner, M. E., Martin, G. E. and Snow, D. D. (1993). Effects of sludge disposal on groundwater nitrate concentrations. *J. Hydrol., 142, 213-228.*
- Spence, J. and Telmer, T. (2005). The role of sulphur in chemical weathering and atmospheric CO₂ fluxes: Evidence from major ions, $\delta^{13}\text{CDIC}$, and $\delta^{34}\text{SSO}_4$ in rivers of the Canadian Cordillera. *Geoch. Cosm. Acta, 69(23), 5441-5458.*
- Spötl, C., Mangini, A., Frank, N., Eichstädter, R. and Burns, S. J. (2002). Start of the last interglacial period at 135 ka: Evidence from a high Alpine speleothem. *Geology, 30(9), 815-818.*
- Stigter, T. Y. Ribeiro, L. and Carvalho Dill, A. M. M. (2006). Evaluation of an intrinsic and a specific vulnerability assessment method in comparison with groundwater salinisation and nitrate contamination levels in two agricultural regions in the south of Portugal. *Hydro. J., 14, 79-99.*

- Stone, J., Allan, G. L. and Fifield, L. K. (1994). Limestone erosion measurements with cosmogenic chlorine-36 in calcite - preliminary results from Australia. *Nuclear Instruments and Methods in Physics Research, Series B*, 92, 311-316.
- Stone, W. J. (1992). Paleohydrologic implications of some deep soil water chloride profiles, Murray Basin, South Australia. *J. Hydrol.* 132, 201-223.
- Subba Rao, N. and Devadas, D. (2005). Quality criteria for groundwater use for development of an area, *J. Appl. Geochem.*, 7(1), 9-23.
- Subyani, A. and Sen, Z. (2006). Refined chloride mass-balance method and its application in Saudi Arabia. *Hydrol. Process.* 20, 4373-4380.
- Sukhija B S. and Rama, (1973). Evaluation of groundwater recharge in the semi-arid region of India using the environmental tritium. *Proc Ind Acad Sci*, 77(6), 279-292.
- Sukhija B. S., Reddy, D. V., Nagabhushanam, P. and Hussain, S. (2003). Recharge processes: piston flow vs preferential flow in semi-arid aquifers of India. *Hydro. J.*, 11, 387-395.
- Sukhija, B. S., Nagabhushanam, P. and Reddy, D. V. (1996). Groundwater recharge in semi-arid regions of India: an overview of results obtained using tracers. *Hydro. J.*, 4, 3.
- Sukhija, B. S., Reddy, D. V. and Nagabhushanam, P.(1998). Isotopic fingerprint of palaeoclimates during the last 30,000 years in deep confined groundwaters of Southern India: *Quaternary Res.*, 20, 252-260.
- Sweeting, M. M. (1950). Erosion cycle and limestone caverns in Ingleborough District. *Geogr. J.*, 115, 63-78.
- Taylor, S., Feng, X., Williams, M. and McNamara, J. (2002). How isotopic fractionation of snowmelt affects hydrograph separation. *Hydrol. Process.*, 16, 3683-3690.
- Thraillkill, J. (1968). Chemical and hydrologic factors in the excavation of limestone caves. *Geol. Soc. Am. Bull.*, 79, 19-46.
- Ting, C. S., Kerh, T. and Liao, C, J. (1998). Estimation of groundwater recharge using the chloride-mass balance method, Pingtung Plain, Taiwan. *Hydro. J.*, 6, 282-292.
- Tîrlă, L. and Vijulie, I. (2013). Structural-tectonic controls and geomorphology of the karst corridors in alpine limestone ridges: Southern Carpathians, Romania. *Geomorphology*, accepted, available online May 2013.
- Tizro and Voudouris, (2008). Groundwater quality in the semi-arid region of the Chahardouly basin, West Iran. *Hydrol. Process.*, 22, 3066-3078.
- Toran, L. and White, W. B. (2005). Variation in nitrate and calcium as indicators of recharge pathways in Nolte Spring, PA. *Environ Geol*, 48, 854-860.
- Toran, L., 2006. Isotopes in groundwater investigation. *Groundwater*, 20, 6.

- Touhami, T., Andreu, J. M., Chirino, E., Sánchez, J. R. and et. al. (2012). Recharge estimation of a small karstic aquifer in a semiarid Mediterranean region (ES Spain) using a hydrological model. *Hydro. Process.* 27(2), 165-174.
- Trcek, B. (2007). How can the epikarst zone influence the karst aquifer hydraulic behaviour? *Environ. Geol.*, 51, 761–765.
- Trcek, B. and Krothe, N. C. (2002). The role of the epikarst zone in karst aquifer recharge processes. *Geologica*, 45(2), 579-584.
- Tricker, A. S. (197). The infiltration Cylinder: some Comments on its use. *J. Hydrol.*, 36, 383-391.
- Uliana, M. M., John, M. and Sharp, Jr. (2001). Tracing regional flow paths to major springs in Trans-Pecos Texas using geochemical data and geochemical models. *Chemical Geology*, 179, 53-72.
- UNEP, (1999). UNEP, World Atlas of Desertification, Edward Arnold, London, UK.
- Urich, P. B. (2002). Land use in karst terrain: review of impacts of primary activities on temperate karst ecosystems. Science for conservation. Department of Conservation, Wellington, New Zealand. ISBN 0-478-22262-9
- USGS, United States Geological Survey, 2008. Groundwater recharge. Available via DIALOG. http://www.water.usgs.gov/ogw/gwrp/activities/gw_recharge.html.
- Vaidyanadhan, R. (1964). Geomorphology of Cuddapah Basin. *J. Ind. Geosci. Assn.*, 4, 29-36.
- Vaidyanathan, R. (1961). Stromatolites in lower Cuddapah limestones (Precambrian) in Cuddapah basin. *Curr. Sci.*, 30, 221.
- Valdesa, D., Duponta, J. P., Laignela, B., Ogiera, S., Leboulanger, T. and Mahlera, B. J. (2007). A spatial analysis of structural controls on Karst groundwater geochemistry at a regional scale. *J. Hydrol.*, 340(3-4), 244-255.
- Vallejos, A., Pulido-Bosch, A., Martin-Rosales, W. and Calvache, M. L. (1997). Contribution of environmental isotopes to the understanding of complex hydrologi systems. A case study: Sierra de Gador, SE Spain. *Earth Surface Processes and Landforms* 22, 1157-1168.
- Vandenschrack, G., Van Wesemael, B., Frot, E., Pulido-Bosch, A., Molina, L., Stie´venard, M. and Souchez, R. (2002). Using stable isotope analysis (d D–d 18O) to characterise the regional hydrology of the Sierra de Gador, south east Spain. *J. Hydrol.*, 265, 43-55.
- Vandersypen, D. R., Bali, J. S. and Yadav, Y. P. (1972). Hand Book of Hydrology. Soil Conservation Division, Ministry of Agriculture, Govt. of India.
- Venkatanarayana, B. and T. V. Rao, (1989). Geological and geophysical investigations for delineating karstic structures of the southwestern portion of Cuddapah basin, Andhra

- Pradesh, India. In Berry, B.F. (ed.) *Proc. of 3rd Multidisciplinary Conference on Sinkholes and the Engineering and Environmental Impacts of Karst*, Oct. 1989, USA, 59-64, AA Balkema publishers.
- Venkatarayana, B., Ahmed, S., and Agnihotri, V. (1999). The hydrogeology of the Kuteshwar limestone deposits, Madhya Pradesh, India. *J. Environ. Hydro.*, 7.
- Verbist, K., Torfs, S., Cornelis, W. M., Oyarzún, R., Soto, G. and Gabriels, D. (2010). Comparison of Single and Double-Ring Infiltrometer Methods on Stony Soils. *Vadose Zone J.*, 8, 462-475.
- Verbovsek, T. (2008). Estimation of Transmissivity and Hydraulic Conductivity from Specific Capacity and Specific Capacity Index in Dolomite Aquifers. *Hydrologic Eng.*, 13, 9. [ISSN 1084-0699/2008/9-817-823](https://doi.org/10.1061/(ASCE)1084-0699(2008)9:817-823).
- Vervier, P. (1990). Hydrochemical characterization of the water dynamics of a karstic system. *J. Hydrol.*, 121, 103-117.
- Vesper, D. J., Loop, C. M. and White, W. B. (2003). Contaminant transport in karst aquifers. *Speleogenesis and Evolution of Karst Aquifers*, 1(2), 2.
- Vijayam, B. E., Kamal, M. Y. and Veeriah, K., (1981). Sedimentation in the Kurnool group. *Fourth workshop on status, problems and programmes in Cuddapah basin*. Indian Inst. Peninsular Geol., Hyderabad.
- Wadia, (1939). *Geology of India*. Macmillan and co., limited, St. Martin's Street, London.
- Walker, G. R., Jolly, I. D. and Cook, P. G. (1991). A new chloride leaching approach to the estimation of diffuse recharge following a change in land use. *J. Hydrol.*, 128, 49-67.
- Wanfang and Beck, (2011). Zhou, W., Beck, B. F., 2011. Engineering Issues on Karst. *Karst Management*, 9-45.
- Warrier, C. U., Babu, M. P., Manjula, P., Velayudhan, K. T., Hameed, A. S. and Vasu, K. (2010). Isotopic characterization of dual monsoon precipitation-evidence from Kerala, India. *Curr. Sci.*, 98(11), 10.
- Werner, A., Hotzl, H., Maloszewski, P. and Kâss, K. (1977). Interpretation of tracer tests in karst systems with unsteady flow conditions. *Karst Hydrology (Proceedings of Workshop W2 held at Rabat, Morocco, April-May 1997)*. IAHS Publ. no. 247.
- White, I. and Sully, M. J. (1987). Macroscopic and microscopic capillary length and time scales from field infiltration. *Water Res. Res.*, 23, 1514-1522.
- White, W. B. (1988). *Geomorphology and Hydrology of Karst Terrains*. Oxford University Press, New York, New York, 464.
- White, W. B. (2002). Karst hydrology: recent developments and open questions. *Eng. Geology*, 65, 85-105.

- White, W. B. (2003). Conceptual models for karstic aquifers. *Speleogenesis and Evolution of Karst Aquifers*, 1(1). 2.
- White, W. B., Culver, D. C., Herman, J. S., Kane, T. C. and Mylroie, J. E. (1997). Karst lands: the dissolution of carbonate rock produces unique landscapes and poses significant hydrological and environmental concerns. *American Sci.*, 83(5), 450-459.
- Wicks, C. M. and Engeln, J. F.(1997). Geochemical evolution of a karst stream in Devils Icebox Cave, Missouri, USA. *J. Hydrol.*, 198(1-4), 30-41.
- Williams, P. W. (1972). Morphometric analysis of polygonal karst in New Guinea. *Geol. Soc. Am. Bull.*, 83, 761-796.
- Williams, P. W. (1983). The role of the subcutaneous zone in karst hydrology. *J. Hydrol.*, 61, 45-67.
- Williams, P. W. (2008). The role of the epikarst in karst and cave hydrogeology: a review. *International Journal of Speleology*, 37(1), 1-10.
- Wood, W. W. (1999). Use and misuse of the chloride-mass balance method in estimating ground water recharge. *Groundwater*, 37, 2-3.
- Wood, W. W. and Sanford, W. E. (1995). Chemical and isotopic methods for quantifying ground-water recharge in a regional, semi-arid environment. *Ground Water*, 33(3), 458-468.
- Wood, W. W., Rainwater, K. A. and Thompson, D. B. (1997). Quantifying macropore recharge: examples from a semi-arid area. *Ground Water*, 35(6), 1097-1106.
- Wooding, R. A. (1968). Steady infiltration from a shallow circular pond. *Water Res. Res.*, 4, 1259-1273.
- Worthington S. R. H. and Ford D. C. (1995). High sulfate concentrations in limestone springs: An important factor in conduit initiation? *Environ. Geology*, 25, 9-15.
- Wright V. P. and Smart, P. L. (1994). Paleokarst (dissolution diagenesis): its occurrence and hydrocarbon exploration significance. In: Wolf, K.H., Chilingarian, G.V. (Eds.), *Diagenesis IV. Developments in Sedimentology* 51. Elsevier, Amsterdam, 477-517.
- Wu, P., Tang, C., Zhu, L., Liu, C., Cha, X. and Tao, X. (2009). Hydrogeochemical characteristics of surface water and groundwater in the karst basin, southwest China. *Hydrol. Process.*, 23, 2012-2022.
- Xiao, H. and Weng, Q. (2007). The impact of land use and land cover changes on land surface temperature in a karst area of China. *J. Environ. Management*, 85, 245-257.
- Yehdegho, B. and Reichl, P. (2002). Recharge areas and hydrochemistry of carbonate springs issuing from Semmering Massif, Austria, based on long-term oxygen-18 and hydrochemical data evidence. *Hydro. J.*, 10, 628-642.
- Yonge, C. J., Ford, D. C., Gray, J. and Schwarcz, H. P. (1985). Stable isotope studies of cave seepage water. *Chemical Geology: Isotope Geoscience section*, 58(1-2), 97-105.

- Youngs, E. G. (1987). Estimating hydraulic conductivity values from ring infiltrometer measurements. *J. Soil Sci.*, 38, 623-632.
- Zare, M. (2007). Zargham Mohammadi, Ezzatollah Raeisi, A dye-tracing test as an aid to studying karst development at an artesian limestone sub-aquifer: Zagros Zone, Iran. *Environ. Geol.*, 52, 587-594.
- Zhengxing, M. (1988). An outline of the underground water tracing in karst regions of China. In: *Proc IAH Congr Karst Hydrol Karst Environ Protection*, Guilin, China, 894-901.
- Zhou, W. and Beck, B. F. (2011). Engineering issues in karst. In *karst management* (Philip E Van Beynen). Nature, P. 41.
- Zhu, G. F., Li Z.Z. Su, Y. H., Ma, J. Z. and Zhang, Y. Y. (2007). Hydrogeochemical and isotope evidence of groundwater evolution and recharge in Minqin Basin, Northwest China. *J. Hydrol.*, 333, 239-251.

Appendix 1. Stratigraphic record of Indian Geology showing the major carbonate units in the country. (Compiled from Wadia, 1919; Murty, 1981; GSI, 1997; Kumar, 2006). Three karstified units of Cuddapah basin are highlighted.

Age		Major Rock Unit	Formation	Description
Cenozoic	Eocene	Kirthar series	Subathu series Sylhet LS Nummulitic Ls.	Marine nummulitic limestone and shales Foramiferal limestone. Impure limestone.
	Jurassic		Kalhan LS., Lilang group, Daonella Ls. Jaisalmer LS. Kioto Ls.	Limestone. Limestones. -Do- Unfossiliferous limestone.
Palaeozoic	Triassic		Patcham Fm.	Shelly Limestone.
	Permian		Zewan Fm. Productus limestone	Limestone, shale. Fossiliferous limestone.
	Carboniferous		Syringothyris Ls.	Grey Limestone.
	Silurian		Hapathnar group	Limestone, shale
Proterozoic	Ordovician		Dhaulagiri Ls./Nilgiri Ls.	Limestone.
	Upper Purana	U. Vindhyan Kurnool G	Bhandar Ls. Koilkuntla Ls. Narji Ls.	Micritic, oolitic and stromatolitic Lst. Massive and flaggy limestones. Massive and flaggy limestones.
		Bhima G Indravati G	Shahabad Ls. Kanger Ls Jagdapur Ls	Limestone. Stromatolitic Ls, flaggy with -dolomite.
		Chhattisgarh G	Raipur Ls. Charmuria Ls	-Do- Limestone, stromatolitic with dolomite bands/flaggy
	Lower Purana	L. Vindhyan	Rohtasgarh Ls. Nimbahara Ls. Fawn Ls.	Limestone, locally intraclastic, rippled. Limestone. Dolomitized Lst with stromatolitic and dessication features towards top.
Cuddapah SG Penganga (P-G basin) Pakhal G. (P-G basin) Kaladgi G		Kajrahat Limestone Vempalle Formation Chanda Lst Rajaram Lst (735 m) Pandikunta Lst (340m) Kaladgi series	Limestone and shale. Dolomite. Tidal shoal bar within dolomitic Limestone. Calcareous sandstone with lenses of limestone and dolomite. Flat bedded, dolomitic-limestone, stromatolitic. Limestone with shales and clays	
	Gangpur Group	Birmitrapur Fm. Jammu Ls./Riassi Ls Raiola Ls.	Limestone, dolomite, quartzite Limestone Limestone and dolomite	
ARCHAEAN				

Appendix 2. Data of monthly rainfall from 1999-2011 at Kolimigundla from Mandal Revenue Office, Kurnool District, A.P.

Year	Jan	Feb	Mar	Apr	May	June	July	Aug	Sep	Oct	Nov	Dec	Annual
1999	0	14.2	0	0	45.6	163.2	46	283.3	72	78.2	3.8	0	706.3
2000	0	0	0	18	82	190.2	120	397.4	76.6	148	9.6	0	1041.8
2001	0	0	0	132	16.8	6.8	25.8	115.2	163.4	281.6	16.4	0	758
2002	0	0	0	3.8	0	44.4	20.6	99	23.6	200.2	16	0	407.6
2003	0	0	0	25.6	0	26	51.6	52.8	150.4	209.6	0	0	516
2004	0	0	0	32.4	131.6	0	187	37.2	154.8	0	0	0	543
2005	0	2.4	0	30	93.2	47.2	90.4	135.4	300.6	224.4	9.6	0	933.2
2006	0	0	0	0	24.4	170.4	67.6	22.4	174	149.8	55.4	3.2	667.2
2007	0	0	0	0	44	324.6	15.2	198.4	223.6	68.4	9.8	0	884
2008	0	51.4	70	0	50.2	8.4	88	124.8	79.4	117	47.2	0	636.4
2009	0	0	0	0	77.4	151.4	4.8	99.4	166.6	30.4	96	0	626
2010	0	0	0	29.4	82.22	116.1	162	258.3	76.49	107.3	101	33.7	966.62
2011	0	0	0	46.9	27.03	66.81	195	123.4	0	65.79	12.7	17	554.55
Mean	0	5.23	5.38	24.5	51.88	101.2	82.6	149.8	127.8	129.3	29	4.15	701.77

Appendix 3. Rainfall and Pan Evaporation data collected at Belum Cave station from 2009-2011.

Month	Total Monthly Rainfall (mm)	Total monthly Pan EVP (mm)	Average Pan EVP (mm/day)	No. of Rainy days a month (>2.5mm/day)
Apr-09	0.0	158.1	8.8	0
May-09	70.9	295.5	9.5	5
Jun-09	150.4	219.0	7.3	4
Jul-09	0.0	274.8	8.9	0
Aug-09	73.7	146.3	4.7	8
Sep-09	148.4	162.5	5.4	13
Oct-09	26.3	186.2	6.0	5
Nov-09	85.7	122.6	4.1	9
Dec-09	0.0	146.8	4.7	0
Jan-10	0.0	176.6	5.7	0
Feb-10	0.0	208.3	7.4	0
Mar-10	0.0	311.1	10.0	0
Apr-10	29.4	328.5	10.9	2
May-10	82.2	357.0	11.5	1
Jun-10	116.1	339.7	11.3	7
Jul-10	162.2	257.8	8.3	15
Aug-10	258.3	216.4	7.0	10
Sep-10	76.5	132.1	4.4	10
Oct-10	107.3	193.1	6.2	12
Nov-10	101.0	136.2	4.5	10
Dec-10	33.7	75.2	2.4	3
Jan-11	0.0	76.0	2.5	0
Feb-11	0.0	163.6	5.8	0
Mar-11	0.0	297.3	9.6	0
Apr-11	46.9	277.2	9.2	2
May-11	27.0	165.1	5.3	6
Jun-11	66.8	152.2	5.1	2
Jul-11	194.8	134.7	4.3	8
Aug-11	123.4	249.0	8.0	3
Sep-11	0.0	221.1	7.4	0
Oct-11	65.8	254.6	8.2	4
Nov-11	12.7	173.4	6.7	2
Dec-11	17.0	132.7	4.3	3

Appendix 4. Stratigraphic classification of Cuddapah Basin after GSI, 1997. Three karstified units are shown in color.

Gr.	Formation	Lithology	Thickness	Age
Kurnool	Nandyal Fm.	Shale, Limestone	50-100	Upper Proterozoic
	Koilkuntla Fm.	Limestone with shale	15-50	
	Paniam Fm.	Quartzite	10-30	
	Owk Fm.	Shale	10-15	
	Narji Fm.	Massive limestone, Flaggy limestone	100-200	
	Banganapalle Fm.	Quartzite with conglomerate	10-50	
Nallamalai	Cumbum Fm.	Dolomite/limestone, shale with phyllites, quartzite	2000	Middle Proterozoic
	Bairenkonda Fm.	Quartzite	1500-4000	
Chitravati	Gandikota Fm.	Quartzite, shale	300	
	Tadpatri Fm.	Shale and tuff, Dolomite/limestone, Quartzite, Basic sill	4600	
	Pulivendla Fm.	Quartzite with shale /limestone/dolomite intercalations, Basic flow.	1-75	
Papaghni	Vempalle Fm.	Dolomite/chert/mudstone, quartzite.	1900	
	Gulcheru Fm.	Quartzite/arkose with conglomerate.	28-210	
Basement		Granite–g�nisses, basic dykes, amphibolites and mica schist	Lower Proterozoic and Archaean	

Appendix 5. Description of the caves located in the different carbonate rocks of the CB. (N.L., Narji Limestone; V.D., Vempalle Dolomite.

Sector	ID	Name	X	Y	Length [m]	Depth [m]	Geology	Alt. masl	Reference
Kolimi-gundla	C1	Belum Guhalu	78.22	15.12	3225	-29	N.L.	287	Gebauer 1983, 1985
	C2	Belum Spring	78.20	15.23	65	10	N.L.	251	Gebauer 1983
	C3	Chirutipuli Guha	78.12	15.15	92	-9	N.L.	289	Gebauer 1983, 1985
	C4	Bugga Guhalu	78.10	15.10	>10		N.L.	308	This Study
	C5	Nela Bilam	78.14	15.33	>100	-14	N.L.	231	Gebauer 1985
	C6	Bandarlapalle Guha	78.10	15.09	117	-18	N.L.	324	This Study
Dhone	C7	Kuruva Bali Guha	77.83	15.15	318	-77	V.D.	427	Gebauer 1985
	C8	Munagamanu Gavi	77.94	15.18	444.5	-16.4	N.L.	475	Gebauer 1985, 1997
	C9	Panchalingala swami Guha	77.81	15.25	58	-10	V.D.	364	Gebauer 1985
	C10	Langu Gavi	77.94	15.29	65	2-3.	N.L.	422	Gebauer 1997
	C11	Udagamanu Gavi	78.06	15.15	100		N.L.	458	Gebauer 1997
Yaganti	C12	Yaganti caves	78.14	15.36	139		N.L.	337	Gebauer 1983
	C13	Yerra Zari Gabbi	77.17	15.47	684	-48	N.L.	358	Gebauer 1983
	C14	Bila Sorgam	78.20	15.47	700	-40	N.L.	337	Gebauer 1983
	C15	Sanyasula Gavi	78.31	15.58	234	-18	N.L.	390	Gebauer 1983, 1985
	C16	Kottala Guhalu	78.25	15.42	65	5	N.L.	251	Gebauer 1983

contd.....

Betam-cherla	C17	Nemmalasilla Gavi	78.16	15.46	35		N.L.	403	Gebauer 1997
	C18	Muchchatles-wara Gavi	78.22	15.50	50		N.L.	396	Gebauer 1997
	C19	Boya Dari Gavi	78.26	15.51	40		N.L.	405	Gebauer 1997
	C20	Chintamanu Gavi	78.15	15.55	100		N.L.	407	Gebauer 1997
	C21	Errabadde Caves	78.17	15.50	60		N.L.	334	Gebauer 1997
	C22	Road Cave	78.25	15.45	20		N.L.	370	This Study
	C23	Jan Galu Gavi	78.29	15.47	40	-17	N.L.	364	Gebauer 1997
	C24	Krishnamma kona	78.25	15.52	140		N.L.	370	Gebauer 1997
Other	C25	Edurla Gavi	?	?	62	-9	?		Gebauer 1985
	C26	Chillavaripalle Cave	77.85	14.72	86	-7	V.D.	375	Shibasaki 1985

Appendix 6. Description of the springs of the carbonates and quartzites of the CB. (N.L., Narji Limestone; V.D., Vempalle Dolomite; Q. Quartzite). (*) Gebauer 1984; () Shibasaki, 1985; (#) Gowd, 2005; (TS) This study; (\$) Toposheets.**

ID	Spring name	X	Y	Alt.	Geology	Q [l/s]		EC	pH	Comments
				masl		Min.	Max.	[μ S/cm]		
S1	Belum	78.20	15.23	254	N.L.(*)	-	50	674.63	6.34	Temporary spring with rapid and turbid flow during rains
S2	Kona1	77.97	15.29	381	N.L. (*)	1.15	6.3	576.2	7.01	Permanent spring, diffuse flow, basin area, 15.05 km ² . Specific discharge 0.74l/s/km ²
S3	Kona2	78.04	15.25	412	N.L. (TS)	0.31	0.83	628.4	6.78	Permanent, diffuse flow
S4	Kona3	78.05	15.27	405	N.L. (TS)	0	2	676	7.25	Over flow spring
S5	Kona4	77.97	15.24	452	N.L. (TS)	0	5	708	7.27	Over flow spring
S6	Rati	78.14	15.19	351	N.L. (TS)	0	15	594	6.88	Perennial to annual
S7	Bugga	78.12	15.03	314	N.L. (TS)	0	13.8	1105	7.03	Over flow spring
S8	Yaganti	78.20	15.35	308	N.L. (*)	4.2	8.72	789.2	6.65	Permanent, conduit flow
S9	Chillavari palle	77.94	14.70	331	Q/V.D. (**)	-	-	-	-	Over flow spring
S10	Rayala cheruvu	77.92	15.14	290	V.D. (\$)	-	-	-	-	Over flow spring
S11	Rayala cheruvu	77.97	15.17	282	V.D. (\$)	-	-	-	-	Over flow spring
S12	Pyapali	77.84	15.31	410	V.D. (\$)	-	-	-	-	Over flow spring

contd.....

S13	Chintalay a-palli	78.04	15.20	397	Q. (#)	0	5.5	485	7.52	Over flow spring, flows along bedding planes
S14	Kundana- kota	77.96	16.35	423	Q. (#)	0	11.5	431	8.14	Over flow spring, along bedding planes
S15	Masanu- palli	77.99	15.19	397	Q. (#)	0	9.4	545	7.57	Over flow spring
S16	Q1	78.10	15.11	371	Q. (TS)	-	-	-	-	Over flow spring
S17	Q2	78.05	15.09	329	Q. (TS)	-	-	-	-	Over flow spring
S18	Q3	78.08	15.20	377	Q. (TS)	-	-	-	-	Over flow spring
S19	Q4	78.02	15.12	331	Q. (TS)	-	-	-	-	Over flow spring
S20	Q5	78.12	15.05	322	Q. (TS)	-	-	-	-	Over flow spring

Appendix 7. Statistical analysis of the spring flow and their physico-chemical parameters as measured during the study period (2009-2011).

	Parameter	Discharge (l/s)	EC ($\mu\text{S}/\text{cm}$)	Cl ⁻	NO ₃ ⁻	SO ₄ ²⁻	HCO ₃ ⁻	pH	T ($^{\circ}\text{C}$)
				(mg/l)					
Belum (S1)	Min	-	213	3.5	8.8	9.5	88.5	6.7	27.4
	Max	50	1801	71.6	57.2	69.4	440.4	7.9	31.6
	Mean	-	615.8	28.9	31.4	42	255.4	7.5	29.2
	SD	-	350.5	18.5	13.3	13.9	176.7	0.3	1.3
	CV (%)	-	56.9	63.9	42.3	33.2	69.2	4.4	4.5
Kona 1 (S2)	Min	0.8	517	8.7	11.8	10	113.6	6.3	28.2
	Max	7.6	663	54.5	21.3	35.9	472.7	8.1	31.4
	Mean	3.6	593.9	20.8	14.9	18.4	266.6	7.3	30.2
	SD	2.5	55	18.5	2.8	7.9	151.2	0.7	1.2
	CV (%)	69.4	9.3	88.9	18.6	43.2	56.7	9.5	3.9
Kona 2 (S3)	Min	0.2	591	8.7	13.2	4.8	143.6	7	28.3
	Max	0.8	669	59.2	56.9	39.9	315.9	7.7	33.1
	Mean	0.5	641.9	20.6	40.5	14.8	208	7.3	30.5
	SD	0.2	27.3	16.4	15.5	10.6	65	0.3	1.6
	CV (%)	47.5	4.3	79.5	38.3	71.5	31.3	3.6	5.4
Rati (S6)	Min	2.7	508.0	15.3	8.1	48.4	132.6	7.4	25.4
	Max	15.0	680.0	116.7	37.1	96.1	254.1	7.9	30.8
	Mean	8.4	568.8	39.3	18.9	62.5	189.7	7.6	28.4
	SD	5.0	66.9	43.5	11.4	22.6	53.9	0.2	2.1
	CV (%)	59.8	11.8	110.7	60.1	36.1	28.4	2.7	7.4
Bugga (S7)	Min	0.4	1093.0	117.8	11.2	118.4	209.6	6.8	30.4
	Max	13.8	1272.0	165.8	31.4	226.5	273.3	7.3	32.8
	Mean	6.5	1160.3	142.2	22.6	172.5	242.0	7.1	31.7
	SD	5.9	79.3	24.0	10.4	76.4	33.5	0.2	1.0
	CV (%)	91.1	6.8	16.9	45.8	44.3	13.9	3.3	3.1
Yaganti (S8)	Min	3.9	783	34	27.5	14.1	321	6.1	30
	Max	8.7	810	70.8	40.2	26.5	364.1	7.5	32.6
	Mean	6.1	792.6	45.7	35.4	17.8	342.6	6.9	32
	SD	1.7	9.9	11.6	4.2	4.5	30.5	0.5	0.8
	CV (%)	27.3	1.2	25.4	11.9	25.2	8.9	7.5	2.6

Appendix 8. Monthly water level (masl) of an observation bore well in Narji Limestone at Kolimigundla village (data source GWD, 2010).

Date	WL	Date	WL	Date	WL	Date	WL
01-05-02	268.14	01-07-04	263.45	01-09-06	276.19	01-11-08	270.94
01-06-02	269.27	01-08-04	262.11	01-10-06	275.79	01-12-08	268.55
01-07-02	268.07	01-09-04	261.44	01-11-06	271.73	01-01-09	267.9
01-08-02	268.44	01-10-04	271.445	01-12-06	270.25	01-02-09	266.19
01-09-02	266.24	01-11-04	268.02	01-01-07	269.6	01-03-09	265.01
01-10-02	275.26	01-12-04	266.805	01-02-07	268	01-04-09	263.6
01-11-02	269.86	01-01-05	266.01	01-03-07	266.35	01-05-09	262.91
01-12-02	265.38	01-02-05	265.48	01-04-07	265.48	01-06-09	262.3
01-01-03	267.49	01-03-05	264.51	01-05-07	263.54	01-07-09	267.11
01-02-03	266.115	01-04-05	262.61	01-06-07	276.81	01-08-09	266.56
01-03-03	264.67	01-05-05	262.16	01-07-07	273.53	01-09-09	269.27
01-04-03	263.35	01-06-05	262.94	01-08-07	269.94	01-10-09	268.93
01-05-03	262.55	01-07-05	262.85	01-09-07	279.6	01-11-09	271.05
01-06-03	262.196	01-08-05	262.04	01-10-07	276.16	01-12-09	269.67
01-07-03	262.16	01-09-05	276.92	01-11-07	273.574	01-01-10	270.35
01-08-03	261.99	01-10-05	278.15	01-12-07	271.021	01-02-10	266.68
01-09-03	260.755	01-11-05	275.92	01-01-08	270.381	01-03-10	266.01
01-10-03	264.14	01-12-05	272.85	01-02-08	270.9	01-04-10	264.14
01-11-03	267.991	01-01-06	270.14	01-03-08	269.5	01-05-10	263.49
01-12-03	265.262	01-02-06	269.37	01-04-08	270.11	01-06-10	263.3
01-01-04	264.82	01-03-06	268.34	01-05-08	268.88	01-07-10	263.42
01-02-04	263.53	01-04-06	267.35	01-06-08	267.66	01-08-10	262.97
01-03-04	262.385	01-05-06	266.26	01-07-08	268.324	01-09-10	264.25
01-04-04	262.165	01-06-06	270.12	01-08-08	266.94	01-10-10	275.63
01-05-04	262.721	01-07-06	268.5	01-09-08	269.84	01-11-10	275.37
01-06-04	262.13	01-08-06	268.52	01-10-08	269.12		
Contd...		Contd...		Contd...			

Appendix 9. Analyzed chemical data of rainwater during the study period. All concentrations in mg/l.

ID	Date	F⁻	Cl⁻	NO₃⁻	SO₄⁻	Na⁺	K⁺	Mg²⁺	Ca²⁺
R1	13-09-09	0.014	0.344	0.809	1.257				
R2	29-09-09	0.019	0.270	0.091	2.998				
R3	09-11-09	0.003	0.212	0.087	0.261				
R4	12-11-09	0.00	0.24	0.08	1.17				
R5	25-07-10	0.01	0.68	0.72	1.43				
R6	29-07-10	0.00	0.64	0.72	2.00				
R7	12-08-10	0.01	1.28	1.76	1.59				
R8	24-08-10	0.01	1.17	0.71	0.87				
R9	26-08-10	0.02	0.39	0.70	4.71				
R10	20-09-10	0.01	0.75	1.03	1.38				
R11	22-10-10	0.27	0.43	0.98	3.56	0.31	0.23	0.63	21.48
R12	05-11-10	0.00	0.20	0.12	0.39				
R13	17-11-10	0.28	2.41	6.92	5.17	2.39	2.44	0.85	10.61
R14	06-07-11	0.01	0.87	1.84	0.00	0.14	0.76	0.00	1.33
R15	26-07-11	0.01	1.59	1.57	0.00	0.70	0.46	0.16	3.89
R16	27-07-11	0.02	0.80	0.67	0.21	0.13	0.68	1.39	46.95
R17	21-08-11	0.01	0.22	0.00	0.18	0.00	0.22	0.00	0.88

Appendix 10. Results of the Pre-monsoon (PRM) water chemistry analysis in mg/l for representative samples of the study area. Temp. in °C, EC in µS/cm and ionic conc. in mg/l.

Pre-Monsoon (PRM) N=20																		
ID	Name	X	Y	T	pH	EC	TDS	Ca ²⁺	Mg ²⁺	HCO ₃ ⁻	Na ⁺	K ⁺	F ⁻	Cl ⁻	NO ₃ ⁻	SO ₄ ²⁻	Br ⁻	Hardness
B1	BW	78.123	15.063	32.30	7.08	860	592.97	67.82	31.88	592.17	110.54	8.43	0.61	75.55	8.19	9.88	0.32	300.29
B2	BW	78.138	15.063	32.50	7.02	1008	695.02	73.48	34.75	612.90	129.79	6.97	1.04	71.19	42.65	32.07	0.63	326.16
B3	BW	78.194	15.165	30.05	7.32	812	559.87	72.51	37.44	666.88	131.82	4.14	1.26	75.98	20.45	15.21	0.64	334.79
B4	BW	78.113	15.147	30.20	6.97	863	595.04	98.59	18.16	327.04	91.02	1.56	0.92	61.58	32.38	86.10	0.23	320.90
B5	BW	78.128	15.136	29.60	6.74	891	614.34	71.30	31.70	597.75	132.61	8.79	0.76	52.18	54.42	18.27	0.37	308.21
B6	BW	78.149	15.12	28.80	7.08	926	638.48	102.56	27.61	537.49	89.64	23.32	0.78	66.19	56.37	9.61	0.35	369.60
B7	HP	78.165	15.143	29.10	7.06	3890	3010.47	63.11	38.66	205.00	298.65	22.46	0.87	341.52	233.40	120.56	2.16	316.27
B8	HP	78.188	15.128	28.70	6.98	1013	698.46	123.38	16.82	294.10	76.43	18.18	0.76	106.96	32.61	91.35	0.52	377.43
B9	HP	78.154	15.176	27.90	6.80	3052	2361.94	233.04	98.05	698.08	358.34	2.71	2.29	294.47	255.82	463.17	3.82	984.62
B10	HP	78.225	15.2	28.00	7.37	2004	1550.90	31.19	20.93	536.72	402.23	4.08	2.01	194.37	143.86	167.96	1.85	163.78
B11	HP	78.171	15.211	28.70	6.79	1812	1402.31	55.95	44.97	572.64	256.17	2.31	1.05	185.52	120.40	87.56	1.37	324.26
B12	BW	78.192	15.241	28.80	7.29	2013	1557.86	34.88	53.81	710.63	406.10	31.77	1.40	368.22	12.78	109.33	2.39	307.82
B13	HP	78.078	15.087	30.50	7.45	1270	875.67	74.08	39.25	551.32	143.53	8.01	1.56	174.54	11.24	21.56	1.03	346.12
S1	Belum	78.125	15.113	30.20	7.20	907	625.38	62.05	19.55	362.42	65.03	9.06	0.56	32.45	16.24	7.86	1.24	235.27
S2	Yadiki	77.968	15.29	28.30	7.22	636	438.52	69.30	17.05	356.00	34.13	3.38	0.88	13.07	7.21	2.85	0.39	243.16
S3	Yadiki 2	78.036	15.246	28.40	7.20	640	441.28	71.83	18.09	358.58	39.66	3.84	1.11	17.34	4.39	12.22	0.42	253.76
S6	Rati	78.139	15.19	30.00	7.67	538	370.95	122.75	19.37	236.11	108.13	10.97	0.39	174.81	18.18	131.02	1.53	386.30
S7	Bugga	78.121	15.032	30.40	7.33	1272	877.04	52.65	19.37	246.28	79.34	4.71	0.80	71.57	18.61	39.22	0.23	211.03
S8	Yaganti	78.198	15.359	32.40	7.30	791	545.39	63.05	26.47	361.21	62.81	6.06	0.80	64.82	20.50	23.58	4.18	266.13
BC	BC	78.111	15.101	31.20	7.41	1801	1393.79	75.77	21.73	264.82	272.40	10.83	0.82	343.47	24.23	96.64	0.71	278.50

Appendix 11. Results of the Post-monsoon (POM) water chemistry analysis in mg/l for representative samples of the study area. Temp. in °C, EC in µS/cm and ionic conc. in mg/l.

Post-Monsoon (POM) N=11																		
ID	Name	Name	X	Y	T	pH	EC	TDS	Ca ²⁺	Mg ²⁺	HCO ₃ ⁻	Na ⁺	K ⁺	F ⁻	Cl ⁻	NO ₃ ⁻	SO ₄ ²⁻	Br ⁻
B1	BW	78.157	15.021	28.7	7.5	442	304.76	48.03	10.89	121.39	27.09	11.87	0.19	46.29	35.87	29.70	0.19	164.74
B2	HP	78.165	15.143	28.4	7.25	2980	2306.22	136.90	19.98	246.20	175.55	29.81	0.33	351.57	43.87	64.73	2.57	424.16
B3	HP	78.195	15.13	29	7.31	1018	701.91	128.69	9.87	196.39	61.78	14.90	0.76	123.93	49.94	83.27	1.46	362.20
B4	HP	78.164	15.209	25.2	7.55	1438	1012.21	54.60	19.51	458.37	206.49	0.66	1.40	44.25	51.41	160.06	0.41	216.47
B5	BW	78.161	15.248	25.3	7.33	1703	1317.95	120.39	21.12	331.44	135.95	1.09	0.32	231.44	29.71	48.45	0.88	387.55
B6	BW	78.101	15.08	30.5	7.34	702	484.03	91.50	7.48	156.29	32.06	0.27	0.91	58.18	56.38	39.89	0.26	259.39
B7	Belum	78.125	15.113	28.2	7.4	769	530.23	104.17	6.10	162.45	28.38	2.44	0.63	58.09	56.39	49.23	0.04	285.45
B8	Yadiki 1	77.968	15.29	28.2	7.74	616	424.73	133.94	3.70	126.10	12.75	0.28	0.26	139.53	51.30	34.65	0.44	350.03
B9	Yadiki 2	78.036	15.246	28.3	7.72	622	428.87	245.22	11.12	212.91	24.37	3.02	0.23	248.32	119.33	38.46	0.32	658.63
B10	Rati	78.139	15.19	25.4	7.93	578	398.53	87.21	4.30	142.61	18.16	2.04	0.65	32.28	45.14	39.24	0.12	235.66
B11	Yaganti	78.198	15.359	30	7.22	789	544.02	113.12	8.82	235.26	24.69	1.27	0.92	58.84	47.10	22.02	1.22	318.96
B12	BC	78.111	15.101	28.3	7.28	1691	1308.66	103.08	6.62	169.98	11.94	0.58	0.83	59.22	28.23	39.94	0.05	284.84

Appendix 12. Stable isotope data of rainfall samples collected at Belum station during the study period.

ID	Sampling date	δ^2H (‰)	$\delta^{18}O$ (‰)	d-excess
R1	25-07-10	-5.44	1.22	-15.2
R2	29-07-10	4.98	1.02	-3.18
R3	12-08-10	-9.32	-0.77	-3.16
R4	24-08-10	-21.18	1.67	-34.54
R5	26-08-10	-4.22	2.98	-28.06
R6	20-09-10	-4.69	-1.3	5.71
R7	22-10-10	-13.6	-2.18	3.84
R8	05-11-10	-36.5	-3.87	-5.54
R9	17-11-10	-56.34	-4.01	-24.26
R14	02-05-11	-49.00	-4.22	-15.26
R10	06-07-11	2.91	-0.08	3.55
R11	26-07-11	9	2.75	-13
R12	27-07-11	-2.52	-1.23	7.32
R13	21-08-11	-20.16	-1.76	-6.08
R15	27-10-11	-53.79	-5.81	-7.27
R16	25-11-11	-46.82	-3.50	-18.85

Appendix 13. Stable isotope data of bore wells and springs of the area during pre-monsoon (PRM) season, 2011.

Sample		x	y	Elevation masl	H2	O18	d excess
B1	BW	190632	1667292	262	-15.56	-0.74	-9.64
B3	BW	198489	1678481	211	-9.85	-0.41	-6.57
B5	BW	191334	1675379	238	-16.64	-1.13	-7.6
B8	HP	197788	1674372	210	-11.34	-1.23	-1.5
B9	HP	194160	1679812	212	-8.63	-0.53	-4.39
B10	HP	201883	1682345	190	-6.49	0.4	-9.69
B11	HP	196092	1683674	202	-7.33	0.7	-12.93
B12	BW	198358	1686944	199	-11.62	-0.31	-9.14
B13	HP	185826	1670000	300	-19.06	-1.92	-3.7
S1	Belum	190966	1672861	254	-17.79	-1.67	-4.43
S2	Yadiki	812405	1676881	381	-24.31	-3.45	3.29
S3	Yadiki	813140	1676393	412	-16.9	-1.6	-4.1
S6	Rati	180554	1667552	351	-15.57	-1.65	-2.37
S7	Bugga	180224	1662307	314	-13.03	-2.12	3.93
S8	Yaganti	192726	1699167	308	-23.6	-3.72	6.16

Appendix 14. Stable isotope data of bore wells and springs of the area during post-monsoon (POM season), 2011.

Sample	Place	X	Y	Elevation masl	H2	O18	d excess
B1	HP	190632	1667292	255	-19.76	-1.32	-9.2
B8	HP	197788	1674372	209	-11.62	-1.18	-2.18
B11	HP	196092	1683674	198	-6.3	0.37	-9.26
B12	BW	195066	1687690	200	-2.05	3.85	-32.85
B13	BW	185826	1670000	281	-17.42	-2.3	0.98
S1	Belum	190966	1672861	381	-13.81	-1.49	-1.89
S2	Yadiki	812405	1676881	381	-24.19	-3.97	7.57
S6	Rati	180554	1667552	314	-6.93	0.97	-14.69
S8	Yaganti	192725	1699167	308	-23.36	-3.17	2

Appendix 15. Time series of stable isotope data of springs of the Narji Limestone aquifer analyzed during the study period.

Spring	Date	$\delta^2\text{H}$ (‰)	$\delta^{18}\text{O}$ (‰)
S2	07-01-10	-30.26	-4.45
	04-03-10	-23.17	-4.19
	17-06-10	-20.15	-3.39
	10-08-10	-22.37	1.17
	22-09-10	-21.84	1.32
	13-10-10	-20.62	-1.75
	14-02-11	-24.31	-3.45
	17-06-11	-21.31	-1.9
	25-11-11	-24.19	-3.97
S3	04-03-10	-15.03	-3.27
	17-06-10	-11.13	-3.17
	10-08-10	-21.19	-2.74
	22-09-10	-19.08	-2.92
	14-02-11	-16.9	-1.6
	17-06-11	-17.94	-1.04
	25-11-11	-18.06	-1.97
S6	10-01-10	-22.72	-3.68
	04-03-10	-16.07	-2.9
	22-09-10	-14.13	-0.48
	17-02-11	-15.57	-1.65
	27-11-11	-6.93	0.97
S7	10-01-10	-18.05	-2.81
	23-09-10	-11.18	0.45
	17-02-11	-13.03	-2.12
S8	12-01-10	-28.56	-4.42
	03-03-10	-23.41	-4.05
	17-06-10	-17.55	-3.97
	23-09-10	-16.08	-3.77
	19-02-11	-23.6	-3.72
	18-06-11	-23.61	-3.34
	28-11-11	-23.36	-3.17

KARSTIFICATION IN THE CUDDAPAH SEDIMENTARY BASIN, SOUTHERN INDIA: IMPLICATIONS FOR GROUNDWATER RESOURCES

ZAKRASEVANJE V SEDIMENTACIJSKEM BAZENU CUDDAPAH, JUŽNA INDIJA: POSLEDICE ZA ZALOGE PODZEMNE VODE

Farooq Ahmad DAR¹, Jerome PERRIN², Jean RIOTTE³, Herbert Daniel GEBAUER⁴, Allu Chinna NARAYANA⁵
& Shakeel AHMED¹

Abstract

UDC 551.435.8:556.33(540)

Farooq Ahmad Dar, Jerome Perrin, Jean Riotte, Herbert Daniel Gebauer, Allu Chinna Narayana & Shakeel Ahmed: Karstification in the Cuddapah Sedimentary Basin, Southern India: Implications for Groundwater Resources

The Cuddapah sedimentary basin extends over a significant part of the southern part of Andhra Pradesh State, Southern India. Proterozoic carbonate rocks in the basin are constituted by as three main units- the Vempalle dolomite, the Narji and Koilkuntla limestones. These carbonate rocks are of strategic importance for local communities as they provide the main water source for irrigation and domestic use and they are also intensively quarried for cement production and building stones. It is therefore, of primary importance to assess to which extent these carbonate units are karstified so as to provide recommendations for appropriate land and water resource management. The field investigations carried out indicate that these carbonate units are significantly karstified and karstification has been an ongoing process with several phases under variable climatic conditions. As a result, a significant part of aquifer recharge occurs as point-recharge through swallow-holes and groundwater flow is channelized by conduit networks which emerge at karst springs. Karst development was possibly more active during past humid conditions; however karstification is still an ongoing process under the present semi-arid climate especially in the favorable case where karst drains the runoff issued from upstream quartzitic hills. The karstic nature of these carbonate units need to be integrated in future research and development programmes to avoid practices that may lead to unexpected collapses, reservoir leaks, inaccurate groundwater budgeting, etc.

Keywords: karst, karst aquifer, cave, semi-arid, groundwater resource, India.

Izvleček

UDK 551.435.8:556.33(540)

Farooq Ahmad Dar, Jerome Perrin, Jean Riotte, Herbert Daniel Gebauer, Allu Chinna Narayana & Shakeel Ahmed: Zakrasevanje v sedimentacijskem bazenu Cuddapah, južna Indija: Posledice za zaloge podzemne vode

Sedimentacijski bazen Cuddapah obsega pomemben del južnega dela indijske države Andhra Pradesh. Proterozoj-ske karbonate sestavljajo tri glavne enote, Vempalle dolomit ter Narji in Koilkuntla apnenici. Ti karbonati so lokalno pomembni, saj predstavljajo glavni vodni vir za namakanje in gospodinjstva ter pomemben vir gradbenih materialov. Poznavanje stopnje zakraselosti karbonatov je lahko pomembno pri upravljanju vodnih virov in inženirskih posegih na območju. Terenske raziskave so pokazale veliko zakraselost omenjenih karbonatov; pomemben del napajanja vodonosnikov poteka točkovno, skozi ponore, pretakanje pa se vrši v dobro razviti mreži kraških kanalov. Glavna faza razvoja krasa je verjetno potekala v preteklih, bolj vlažnih obdobjih. Proces zakrasevanja v današnji polsušni klimi so posebej intenzivni na območju, kjer se na kras steka voda iz kvarcitnega zaledja. Zakraselost karbonatov bo treba upoštevati pri upravljanju območja in bodočih razvojnih projektih. Le na ta način se bomo lahko izognili težavam, kot so puščanje iz jezov, udiranje, napačna ocena vodnih zalog in podobno.

Ključne besede: kras, kraški vodonosnik, jama, polsušno, zaloge podzemne vode, Indija.

¹ Indo-French Centre for Groundwater Research, CSIR-National Geophysical Research Institute (NGRI), Hyderabad, India, e-mail: farooq.dar1@gmail.com

² Indo-French Centre for Groundwater Research (IFCGR), Hyderabad, India

³ Indo-French Cell for Water Sciences (IFCWS), IRD, Bangalore, India

⁴ German Karst and Cave Research Association, Munich, Germany

⁵ Centre for Earth & Space Sciences, University of Hyderabad

Received/Prejeto: 8.3.2011

INTRODUCTION

Karst regions, representing about 15% of the continental landmass are widespread across the globe and present unique geomorphological characteristics which have specific consequences on land and water resources management (e.g. Ford & Williams 2007). In India, karstified carbonate rocks are distributed across the country in different geomorphological, geological and climatic contexts (Himalayan region, North-eastern hills, and sedimentary basins in peninsular India, etc.). Regionally, these karstic zones play a vital role for the society both as a primary water supply and in economic terms (water resource for irrigated agriculture, quarrying for construction and cement production).

There are only a few studies on the characteristics and the role of karst in Indian carbonate terrains, and these publications mostly focus on groundwater resour-

ces (e.g. Coward *et al.* 1972; Murty 1981; Shibasaki *et al.* 1985; Sing 1985; Chandra *et al.* 1987; Venkatanarayana & Rao 1989; Venkatanarayana *et al.* 1999; Singh & Dubey 2001; Dubey *et al.* 2006; Jeelani 2008).

The description of karst features and the understanding of karstification processes are important for an adequate land and water resource management because specific problems are known to occur in karst regions such as ground subsidence, sinkhole collapse, groundwater contamination and unpredictable water supply.

The present study aims at characterising the karstification of the main carbonate units situated within the Cuddapah sedimentary basin, southern Andhra Pradesh (Fig. 1), proposing a model of karstification, and evaluating the role of karstification on the groundwater resource.

STUDY AREA

The study area (Fig. 1) forms a part of the Cuddapah Basin of Proterozoic age. It lies in a semi-arid region with long hot dry summers with day temperature reaching 45 °C and a well-defined monsoon season where most rainfall occurs as high intensity events. This study therefore, complements other karst studies in similar climatic realms which are still outnumbered (Jennings 1983).

GEOLOGICAL SETTING

The crescent shaped Cuddapah sedimentary basin is situated in the eastern part of the Dharwar Craton in the southern Andhra Pradesh, India (Fig. 1). Spreading over an area of about 44,500 km², it is one of the extensive sedimentary basins of southern India (Narayanaswami 1966; Qureshi *et al.* 1968; King 1872; Crawford *et al.* 1973; Dutt 1975; Kailasam 1976; Murthy 1981; Kaila *et al.* 1985; Kale 1991; Ramam *et al.* 1997; Kasipathi *et al.* 2008; Raju 2009). The basin convexes towards west and extends for a length of about 400 km in north–south direction with a maximum width of 145 km in the middle.

The centre of the Cuddapah basin between Atmakur and Cuddapah is a broad flat plain drained by the Kundair and Pennar Rivers with a few scattered hills (e.g. mesa, butte) (Fig. 1). The plain descends from an elevation of 260 m at Atmakur to 130 m near Cuddapah. The plain is bounded on the west by flat topped Erramala Hills and the plateaus of Uppalapadu and Gandikota which slope gently easterly towards the plain. In the east,

the Nallamala range defines steep N–S trending rugged parallel ridges.

Sedimentary units of different rock assemblage are divided into two groups: Cuddapah and Kurnool groups of Proterozoic age separated by an unconformity (Meijerink *et al.* 1984) (Fig. 2).

The Archean aged peninsular gneissic complex constitutes the basement. The Cuddapah Supergroup is composed predominantly of arenaceous and argillaceous sequences with subordinate calcareous sediments, while the Kurnool Group has a more carbonate-rich geology. The lower Cuddapahs represents a cyclic repetition of quartzite-shale sequence while the Kurnool group shows two quartzite-limestone-shale sequences (Ramam *et al.* 1997). There was contemporaneous igneous activity manifested as sills, flows and other intrusive rocks in older sequences (Crawford *et al.* 1973; Ramam *et al.* 1997; Anand *et al.* 2003). The provenance of sediments was west and southwest (Pascoe 1950; King 1872). The shallow sub-marine shelf environment prevailed during the sedimentation of the basin (Shibasaki *et al.* 1985), whose depocenter was successively migrating towards east (Singh & Mishra 2002).

The stratigraphy of the basin has been discussed by various geologists (Narayanaswami 1966; Sen & Narsimha 1968; King 1872; Kaila *et al.* 1979; Ramam *et al.* 1997; Geological Survey of India (GSI) 1997). The younger Kurnool Group was deposited unconformably over the older Cuddapah Supergroup (Fig. 2). The Cud-

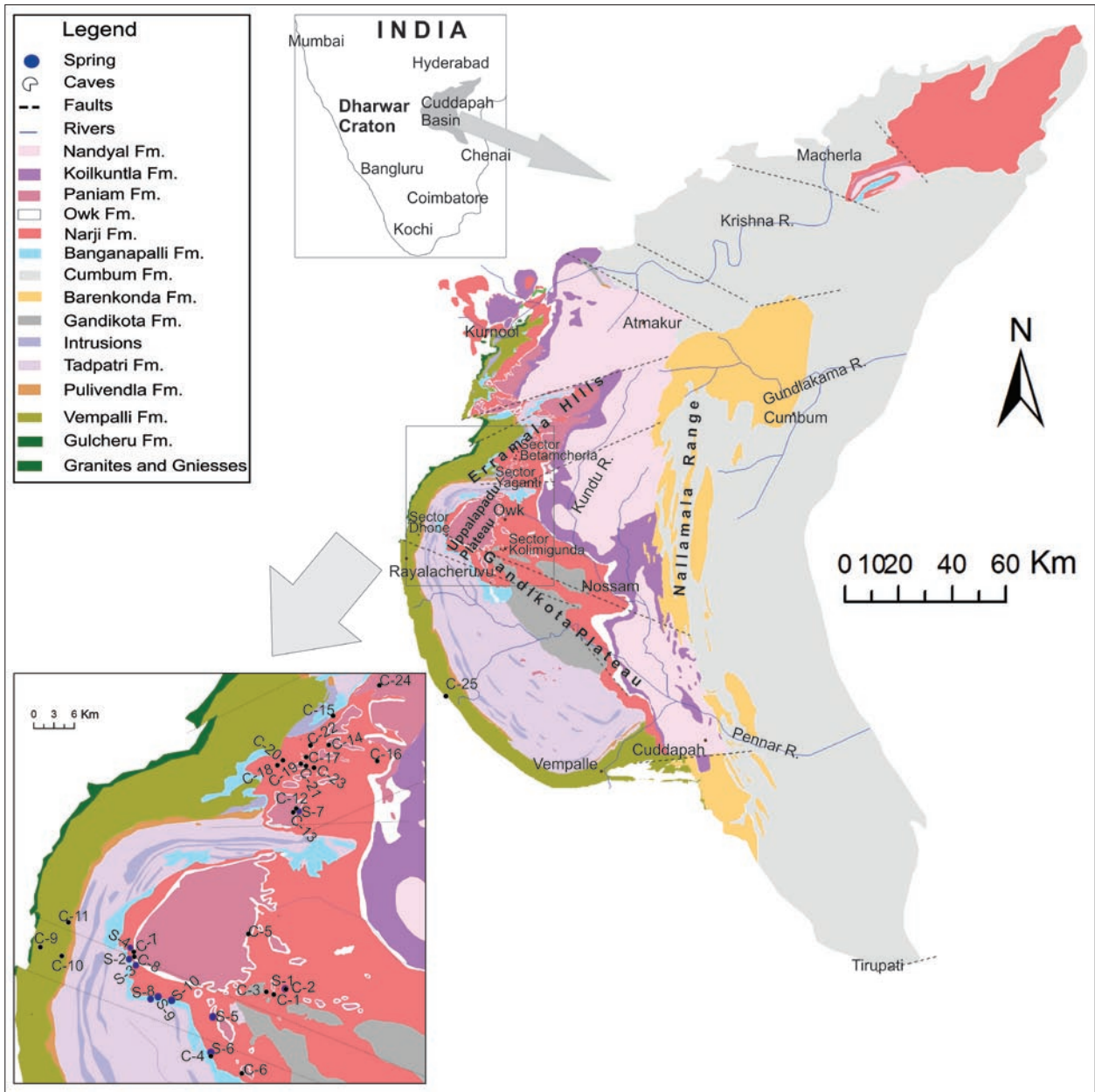


Fig. 1: Geological map of the Cuddapah sedimentary basin (modified from GSI 1997) and its location in the southern Indian peninsula. The location of caves (C) and springs (S) is also given.

dapah Supergroup has comparatively steeper dips than the easterly dipping Kurnool Group (Fig. 3). The general thickness of the whole sedimentary sequence is of the order of 6,000–12,000 m. The Kurnool System is thin, with maximum thickness of 370 m but it is superficially very extensive (Fig. 1).

The main carbonate rocks of the basin are the Vempalle Formation of the Cuddapah Supergroup and the Narji and Koilkuntla Formations of the Kurnool Group. Of the total area of the basin (44,500 km²), 17%

(i.e. 7,690 km²) shows the exposure of these potentially-karstified rocks. The areal extent of Vempalle, Narji and Koilkuntla Formations is 1,830, 4,333 and 1527 km² respectively.

Vempalle Formation

The conglomeratic quartzite of Gulcheru Formation is conformably overlain by the thick Vempalle Formation constituted predominantly of dolomite (Fig. 2). The contact is gradational from quartzite to flaggy quartzite

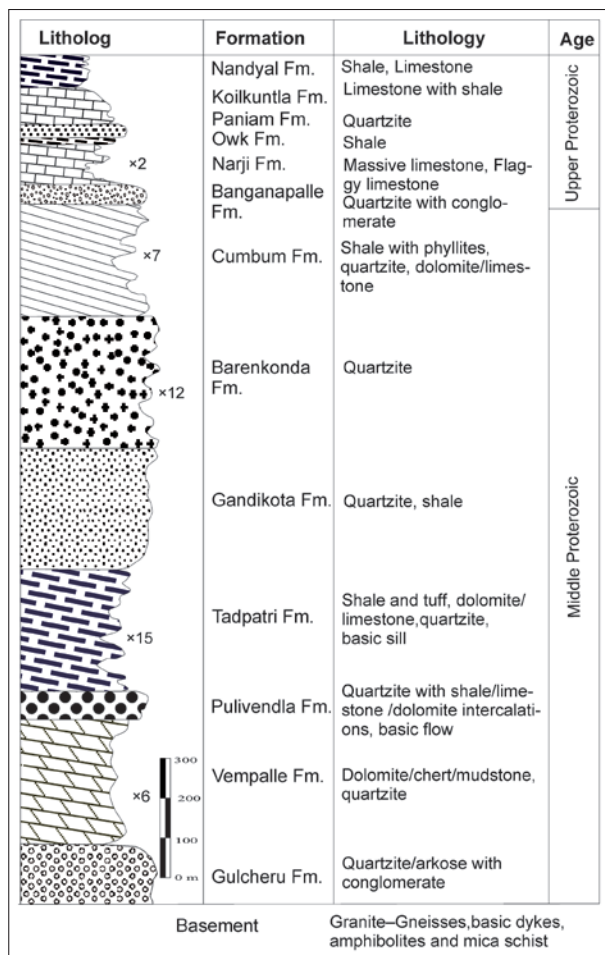


Fig. 2: Litholog showing the succession of rock formations encountered in the Cuddapah sedimentary basin.

to dolomite, with minor argillaceous sediments (Roy 1947; Anand *et al.* 2003). The lower part of the Vempalle sequence comprises of purple shale with interbedded layers of dolomite, succeeded by grey, greenish or brown dolomite with interbedded laminae of purple shale and beds of chert and intraformational conglomerates, which

in turn is overlain by a purple and buff shale with thin dolomite layers and chert beds (Dutt 1962). The thickness of the Vempalle Formation varies from 1,250 to 1,900 m (Roy 1947; Jhanwar *et al.* 1964). It is the only stratigraphic unit in the Cuddapah sequence that contains a sequence of intrusive trap sills and pillow type lava flows. These rocks show some stromatolitic features (Vaidyanathan 1961; Riding & Sharma 1998). This formation is well exposed in the western part of the Cuddapah Basin. The rocks generally strike NNE-SSW and dip 15-25° towards east.

Narji Formation

The base of the Narji Formation starts with a highly siliceous pink and purple shale/shaly limestone with thin lenticular lenses of gritty ferruginous sandstone at some places. It grades into bluish-grey, high-grade massive limestone. The upper part of the limestone is flaggy (very regular 5-10 cm beds) that is mined for flooring and roofing material. At places where the formation rests over the Cuddapahs, the basal Banganapalle conglomerate of boulders and pebbles mark the transition between them. The lower part of the limestone shows interbedded shale, quartzite and intraformational conglomerates in several places (Dutt 1962).

The massive limestone is extremely fine grained, compact and gives a metallic sound. Narji limestone shows a dip of 0-10° towards NE with a strike varying from NNW-SSE to NW-SE. The thickness of the Narji Limestone is quite variable: 0-192 m (Dutt 1962), 100-200 m (Murthy *et al.* 1979; Murthy 1981; Nagaraja Rao *et al.* 1987) up to 100 m thick around Kurnool (Kamal 1974; Kamal & Vijayam 1981; Vijayam *et al.* 1981). A litholog from Kolimigundla area showed 1 m of black soil, 30 m of flaggy limestone, 50 m of massive limestone, and a tectonic contact with Gandikota quartzite below. Some micro- and macro-stylolitic structures are also present. The rocks are overlain by the buff colored shale of the Owk Formation. These rocks extensively

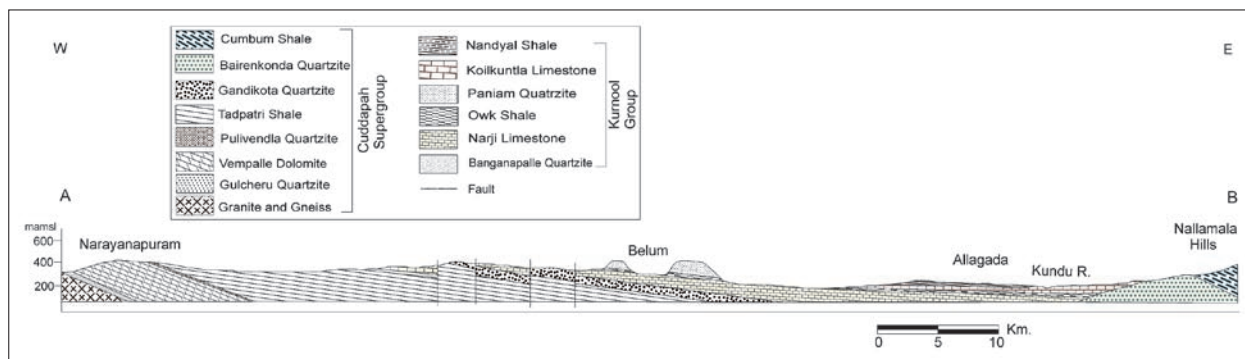


Fig. 3: Geological cross-section across the Cuddapah sedimentary basin showing the location of the three karstified formations (Vempalle, Narji, and Koilkuntla) (the trace of the cross-section is indicated in Fig. 1).

outcrop in the western part of the Kundair valley, where the remnants of the overlying shale and quartzite occur in the form of small hillocks (mesas).

Koilkuntla Formation

The Koilkuntla Limestone is light to dark grey-colored, massive and flaggy in nature, overlying the Paniam quartzite. Extensively exposed in the Kundair valley, the formation spreads to the east up to the foot of the Nallamala range. The flaggy beds differ from Narji by possessing imperfect, wavy planes of bedding. The lower part of the formation includes the intercalation of shale and weathers to buff platy bits. The middle part of the formation is more calcareous, well bedded and tough. Towards the top the color of the limestone changes to purple and pass into Nandyal shale. The thickness ranges from 0–90 m (Dutt 1962). The purple Nandyal Shale with earthy calcareous intercalations, 50–100 m thick, overlies the Koilkuntla limestone.

CLIMATE AND VEGETATION

The Cuddapah basin climate is semi-arid with a dry season from December to May and a monsoon season from June to November. Mean annual temperature is 28.0 °C (minimum 17 °C and maximum 44 °C) and average annual rainfall is 670 mm. The monthly evaporation varies from 72–263 mm, with an annual total of 1,840 mm (Vittal *et al.* 2004). The aridity index is 0.36 which corresponds to the semi-arid class of UNEP (1992).

The main vegetation in the form of open scrub type jungles is scattered. Dense forests cover the Nallamala range. Other vegetation includes the rain-fed and irrigated crops that are mainly grown in the plains of Kundair valley. Major crops grown include paddy, oats, cotton, sunflower, groundnut and chilly. The chief economic activities include agriculture and mineral exploitation (cement, construction slabs).

FIELD OBSERVATIONS

KARST FEATURES IN THE VEMPALLE DOLOMITE

In this formation a typical landscape of hills dissected by valleys has developed; the hills have an asymmetric geometry with a gentle slope that follows the dip of the beds (5–18°) and a steeper slope on the opposite side. The origin of this morphology is not clear. In the area north of Rayala Cheruvu, these hills are elongated along a W–E axis. Hill width is between 400–800 m and length between 1,000–2,000 m. Slopes on the western side is >25°,



Fig. 4: Picture taken at the bottom of Kuruva Bali Guha (Vempalle dolomite) showing the phreatic shaped conduit and sediment accumulation on the floor.

whereas on the eastern flank it is <10° (dip-slope). The hill height is between 100–150 m.

The dolomite is karstified with existence of a few caves of limited extension (Tab. 1). The longest cave is “Kuruva Bali Guha” C11 (318 m in length, 77 m in depth) which is also the deepest known cave in southern India (Gebauer 1985). This cave shows presence of infiltration water during the monsoon (from observations on the soil of the deepest part, it seems that a stream is meandering through the clay/silt deposits and possibly some water filling occurs after intense recharge, Fig. 4). The geological cross-section of the area (Fig. 5) shows that the cave ends near the bottom of the valley which constitutes the base level. Recharge occurs seasonally on the hills and feeds the fissured-karstified dolomite aquifer with a water table close to the valley bottom. In the valleys, irrigation wells exhibit quite variable discharge and some wells are dry. This is typical of a highly heterogeneous aquifer. No karst springs are known and it is possible that natural discharge occurs within the alluvial deposits of the main valleys.

KARST FEATURES IN THE NARJI LIMESTONE

The Narji limestone occupies a vast planar region surrounded by smooth topped hills of Gandikota quartzite (mostly in the Western part) and from place to place, by mesas of Owk shale and Paniam quartzite (Figs. 6 & 7).

Tab. 1: List of the natural caves developed in two of the three karstified formations of the Cuddapah basin (compilation of original data and data published in Gebauer 1985, 1997, and Gebauer & Abele 1983). The caves are located either on Fig. 1 or Fig. 6.

	ID	Cave name	Longitude	Latitude	Length [m]	Depth [m]	Geology	Reference
Sector Kolimigundla	C1	Belum Guhalu	78°06'41.4"	15°06'7.6"	3225	-29	Narji lim.	Gebauer 1983, 1985
	C2	Belum Karst Spring	78°07'30.0"	15°06'47.2"	65		Narji lim.	Gebauer 1983
	C3	Chirutipuli Guha	78°06'06.7"	15°06'19.5"	92	-9	Narji lim.	Gebauer 1983, 1985
	C4	Bugga Guhalu	78°01'30.3"	15°00'34.8"	>10		Narji lim.	
	C5	Nela Bilam	78°04'27.12"	15°10'59.04"	>100	-14	Narji lim.	Gebauer 1985
	C6	Bandarlapalle Guha	78°04'12.2"	14°59'37.3"	117	-18	Narji lim.	
Sector Dhone	C7	Munagamanu Gavi	77°55'9"	15°09'11.2"	864	-16	Narji lim.	Gebauer 1985, 1997
	C8	Udagamanu Gavi	77°54'57.9"	15°09'0"	100		Narji lim.	Gebauer 1997
	C9	Panchalingaswami Guha	77°47'10.0"	15°09'35.0"	58	-10	Vempalle dol.	Gebauer 1985
	C10	Langu Gavi	77°49'43.0"	15°11'39.0"	65		Narji lim.	Gebauer 1997
	C11	Kuruva Bali Guha	77°49'04.8"	15°09'00.2"	318	-77	Vempalle dol.	Gebauer 1985
Sector Yaganti	C12	Yaganti caves	78°8'23.7"	15°21'3.1"	139		Narji lim.	Gebauer 1983
	C13	Yerra Zari Gabbi	77°08'11.5"	15°20'49.9"	684	-48	Narji lim.	Gebauer 1983
Sector Betamcherla	C14	Bila Sorgam	78°11'7.1"	15°26'13.1"	700	-40	Narji lim.	Gebauer 1983
	C15	Sanyasula Gavi	78°10'50"	15°28'40"	234	-18	Narji lim.	Gebauer 1983, 1985
	C16	Kottala Guhalu	78°15'	15°25'	65	5	Narji lim.	Gebauer 1983
	C17	Nemmalasilla Gavi	78°09'02"	15°25'15"	35		Narji lim.	Gebauer 1997
	C18	Muchchatleswara Gavi	78°06'43"	15°24'35"	50		Narji lim.	Gebauer 1997
	C19	Boya Dari Gavi	78°08'45"	15°24'40"	40		Narji lim.	Gebauer 1997
	C20	Chintamanu Gavi	78°07'12"	15°24'55"	100		Narji lim.	Gebauer 1997
	C21	Errabadde Caves	78°09'06"	15°24'35"	60		Narji lim.	Gebauer 1997
	C22	Road cave	78°09'34.7"	15°26'06.7"	20		Narji lim.	
	C23	Jan Galu Gavi	78°09'50"	15°24'25"	40	-17	Narji lim.	Gebauer 1997
	C24	Krishnammakona 5	78°15'	15°31'	140		Narji lim.	Gebauer 1997
Other area	C25	Chillavaripalle cave	77°50'06.4"	14°36'43.7"	86	-7	Vempalle dol.	Shibasaki 1985

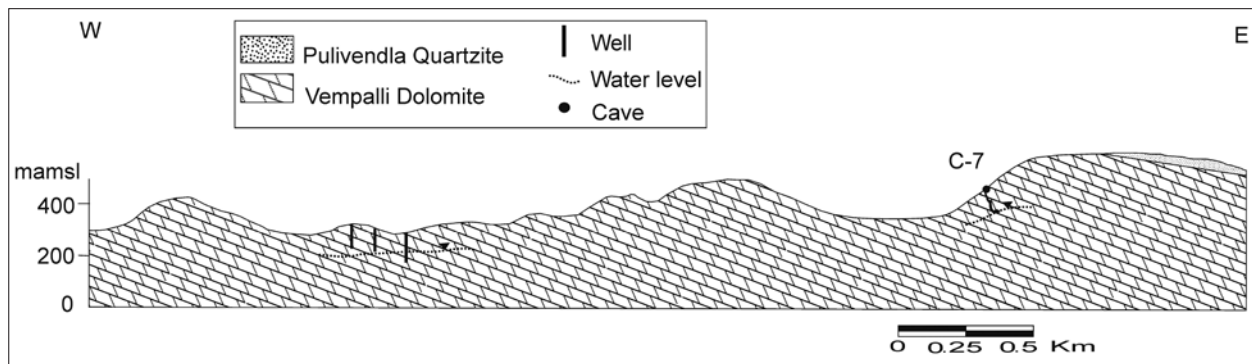


Fig. 5: Geological cross-section across the Vempalle dolomite with representation of the main known cave and inferred piezometric surface based on observations in the cave and existing borewells in the surroundings.

The massive limestone is well karstified and contains the major caves of southern India (Tab. 1). Several typologies of caves could be identified: 1) network maze caves in the upper part of the limestone near the contact with Owk shale (Nila Bilam, Yerra Zari Gabi caves), 2) dendritic/anastomotic cave patterns of phreatic origin (Belum cave), 3) meander cave mostly formed under vadose flow regime (Munagamanu cave) (Fig. 8). At the

foot of quartzite hills, a significant number of swallow-holes are observed and during the monsoon streams issued from the hills will infiltrate within a few hundred meters after reaching the limestone plain (Fig. 6). These recharge events generates significant water level rise in the karstic network and activate seasonal springs. The hydrograph of one of these springs (Fig. 6: S1, Belum spring) shows a sharp reaction to the rainfall events and

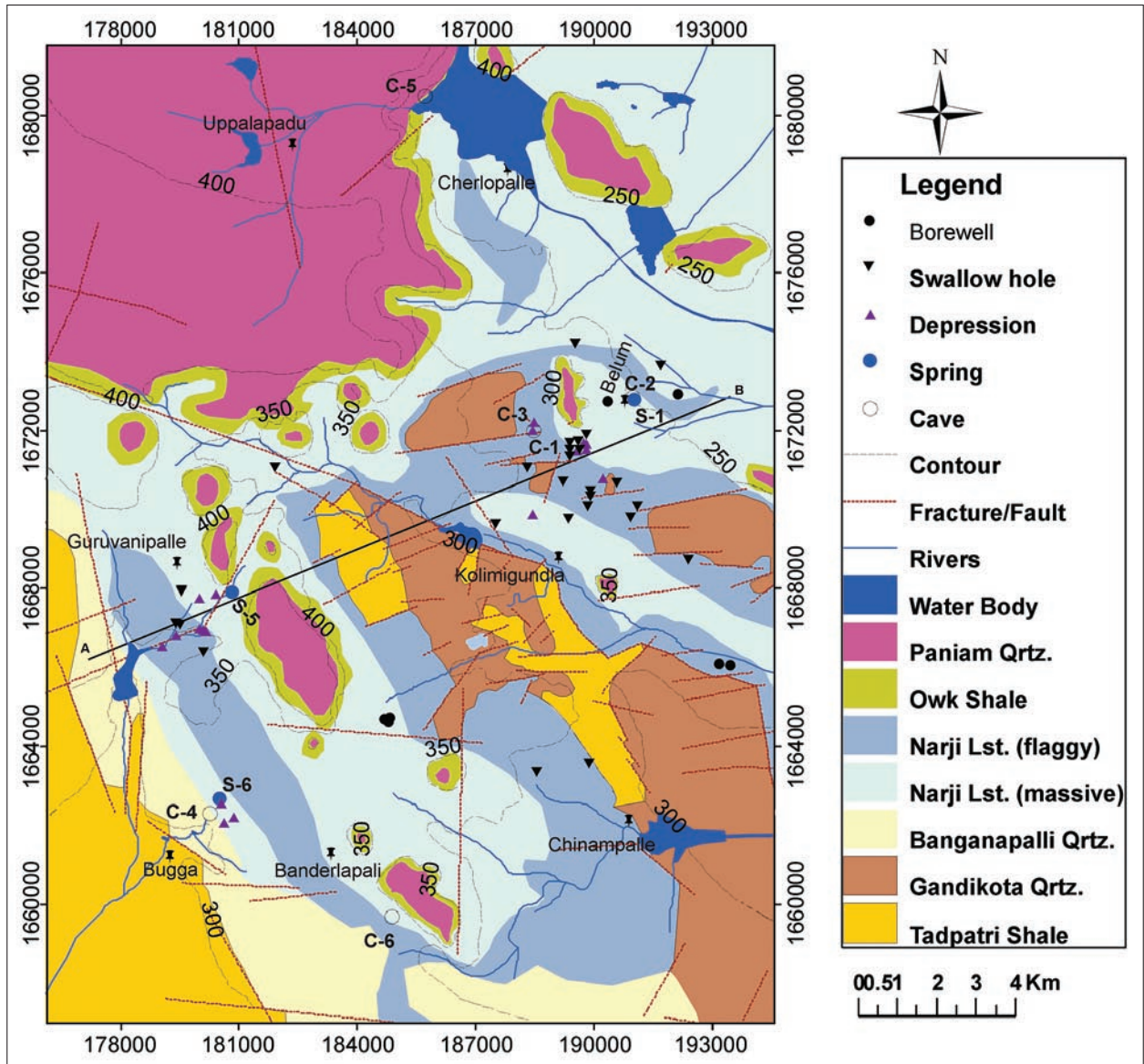


Fig. 6: Geological and geomorphological map of the Narji limestone plateau in Belum area with localization of observed karst features.

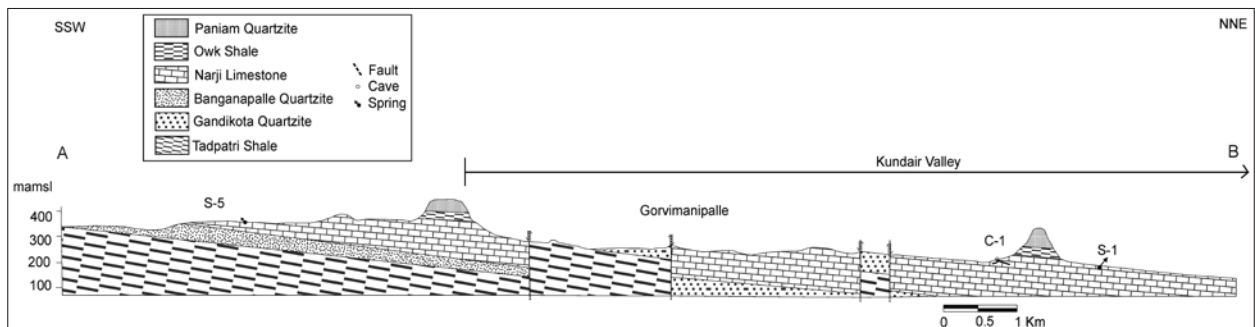


Fig. 7: Geological cross-section across the Narji limestone plateau, Belum area (the trace of the cross-section is indicated in Fig. 6).

rapid recession, typical of karst aquifers with high transmissivity in conduits (Fig. 9). Some depressions may

store temporary water bodies that are used by livestock. It is also observed that point recharge occurs within the

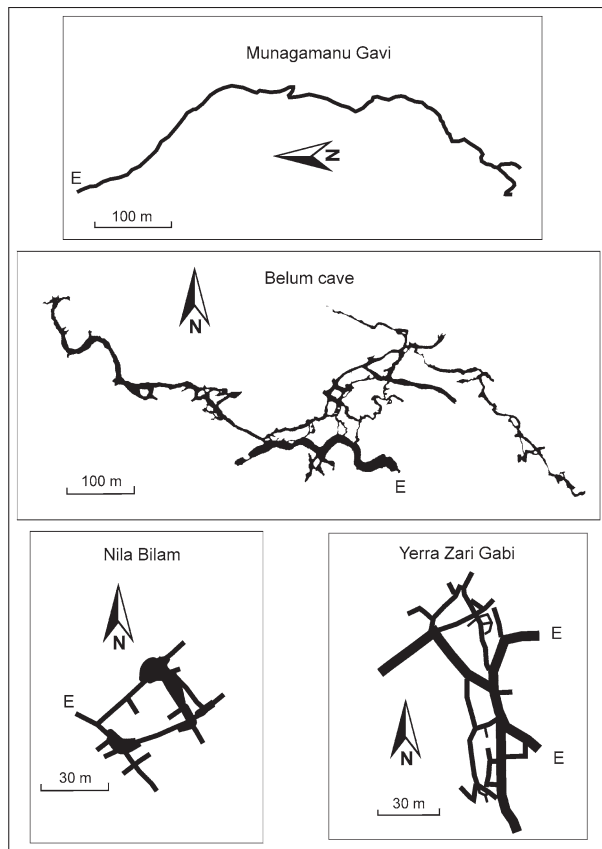


Fig. 8: Representative cave patterns that have developed in the Narji limestone.

limestone away from quartzite hills (e.g. the entrance of Belum cave acts as sinking points after heavy rainfall); it means that runoff is generated within the limestone plateau itself.

Seasonal streams have been observed in several caves: in Munugamanu cave (Figs. 5 & 8: C7), the stream can be followed over several hundreds of meters in a canyon-type vadose gallery; peak discharge should be several l/s and flow is maintained >0.1 l/s several weeks after the end of the monsoon. In Bandarlapalle Guha (Fig. 6: C6), the stream can be followed in a phreatic conduit

over 100 m between two sumps and has a discharge of several l/s during the monsoon season. Finally, in Belum cave (Figs. 6, 7 & 8: C1) at the end of the touristic part, the temporary stream can be followed in phreatic conduits over several hundred meters. It flows after each recharge event (several l/s) but dries up quite rapidly after.

Diffuse recharge seems to be limited as indicated by the absence of active speleothems (one exception in Munagamanu cave) even after rainfall events and the rapid decrease in spring discharges. However, epikarstic features are clearly observed in the massive limestone (Fig. 10) and they may have developed under more humid climatic conditions. This hypothesis can be supported by the relative abundance of inactive speleothems that are recorded in the Belum cave. These observations indicate that the limestone aquifer is mostly recharged by concentrated flow through swallow-holes and limited diffuse flow through the epikarst.



Fig. 10: Picture showing epikarst development in the Narji limestone: karrenfields in the massive unit.

Discharge of the aquifer occurs through seasonal and perennial karst springs (Tab. 2) and it is possible that significant flow feeds the confined limestone aquifer that develops to the East. Most springs (temporary as well as permanent) are observed on the western side of the Narji limestone plateau at or near the contact with the Tadipatri shale (free draining springs, Ford & Williams 2007) (Fig. 6); on the eastern side, the Narji

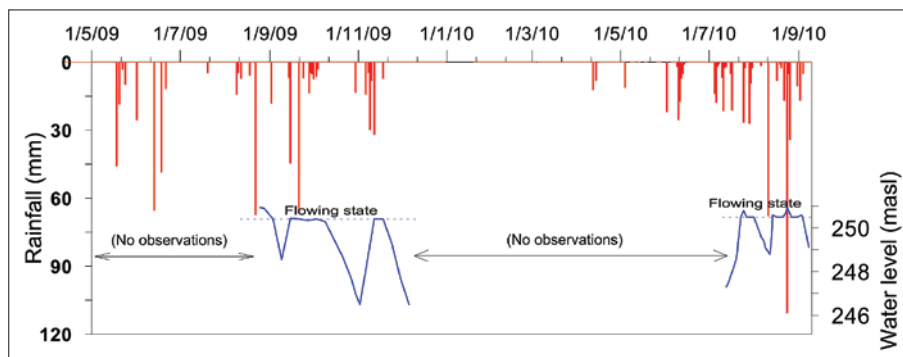


Fig. 9: Belum seasonal spring hydrograph (S2) showing a sharp response to the rainfall events typical of a karst aquifer. In general "no observations" correspond to periods when the spring was either dry or no data was collected. For location, refer to Fig. 1 & 6.

Tab. 2: Surveyed karst springs in the study area. Minimum and maximum discharges along with average electrical conductivity (at 25 °C) are indicated. The springs are located either on Fig. 1 or Fig. 6.

ID	Spring name	Longitude	Latitude	Geology	Discharge [l/s]		Average EC [uS/cm]	Specific Discharge [l/s/km ²]	Reference
					Min.	Max.			
S1	Belum Spring	78°07'30.0"	15°06'47.2"	Narji lim.	-	50	674.6	-	Gebauer 1983
S2	Kona Spring-K1	77°54'24.54"	15°08'56.5"	Narji lim.	1.15	6.3	576.2	0.74	Gebauer 1985
S3	Kona Spring-K2	77°54'49.09"	15°08'40.4"	Narji lim.	0.31	0.83	628.4	-	
S4	Kona Spring-K3	77°54'26.89"	15°09'33.47"	Narji lim.	0	5*	708*	-	
S5	Rati Spring	78°01'44.06"	15°03'50.35"	Narji lim.	0	15	594	-	
S6	Bugga Spring	78°01'37.61"	15°01'05.66"	Narji lim.	0	13.8	1105	-	
S7	Yaganti Spring	78°08'23.27"	15°21'03.07"	Narji lim.	4.2	8.72	789.2	-	
S8	Chintalayapalli Spring	77°56'39.29"	15°05'43.14"	Banganapalle qrtz./Narji lim.	?	5.5*	485*	-	
S9	Kundanakota Spring	77°57'03.21"	15°05'45.05"	Banganapalle qrtz./Narji lim.	?	11.5*	431*	-	
S10	Masanupalli Spring	77°58'10.01"	15°05'38.11"	Banganapalle qrtz./Narji lim.	?	9.4*	545*	-	

*data based on single value.



Fig. 11: Sinkhole in the Narji limestone that has opened in 2003 probably as a consequence of increased aquifer pumping, Nossam area.



Fig. 13: Karrenfield developed below the soil zone in the Koilkuntla limestone as an indicator of epikarst development.

limestone is progressively buried under younger formations and this setting favors confining flow conditions: only the seasonal spring of Belum (Tab. 2: S1) is known. It is observed that groundwater flow occurs

within the Narji limestone and the underlying Banganapalle quartzite at the base of which permanent and temporary springs are located (Tab. 2: S2, S8, S9 & S10). Springs within the limestone flow seasonally as a

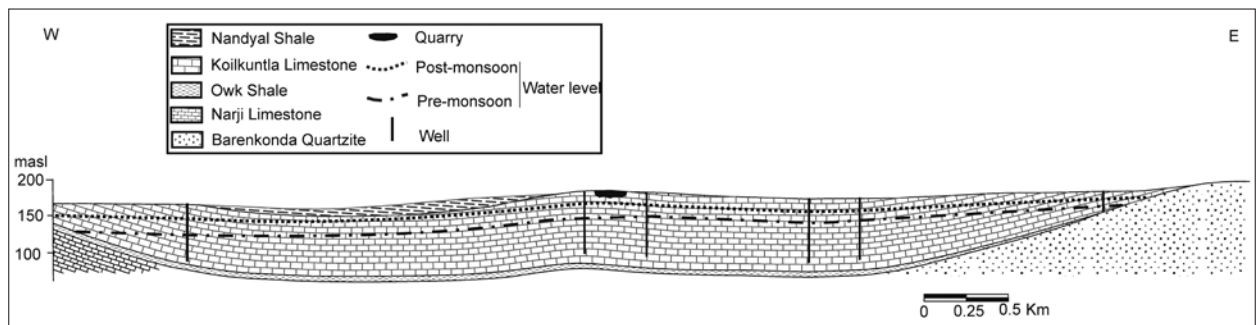


Fig. 12: Cross-section across the Koilkuntla limestone formation (the indicated quarry is also the location of Fig. 13).

Tab. 3: Statistics of 1-year bimonthly data (abstraction rates (Q), static water levels (SWL), pumped water levels) from 84 irrigation wells drilled in the Koilkuntla limestone.

		Average	Stand. Deviation	Coeff. Variation	N
	Qmean [l/s]	9.4	2.6	0.27	84
	Qmin [l/s]	7.8	2.1	0.27	84
	Qmax [l/s]	11.7	3.9	0.33	84
Post-monsoon 2005	SWL [m b.g.l]	12.8	8.0	0.63	79
	Drawdown [m]	7.7	5.6	0.72	79
	Sp. Capacity [l/s/m]	2.8	3.2	1.15	79
Pre-monsoon 2006	SWL [m b.g.l]	26.5	11.7	0.44	79
	Drawdown [m]	8.4	6.1	0.73	79
	Sp. Capacity [l/s/m]	1.7	1.6	0.98	79

result of piezometric surface rise (i.e. overflow) (Tab. 2: S5 & S6). The spring S4 is located at higher level in the unsaturated zone of the Narji limestone at the floor of a surface drainage channel; in this case it may possibly drain the epikarst instead of being directly connected to the saturated zone. The aquifer is also tapped as wells for domestic use and irrigation. In Nossam area, a few sinkholes have developed since 2003–2004 with diameter between 2–5 m and depth 2–3 m, partly filled with

water after monsoon (Fig. 11); some show an increase in diameter and depth with time.

KARST FEATURES IN THE KOILKUNTLA LIMESTONE

The Koilkuntla limestone has an average thickness of 90 m and bedding is nearly horizontal; it is underlain by Paniam quartzite and overlain by Nandyal shale (Fig. 12). The unit is well karstified as observed in quarries and an epikarst has developed (Fig. 13). However no caves are known possibly because of the absence of hilly terrains and the location of the water table close to the surface. The soil cover thickness varies from 0.5 to >2 m and contains abundant pisoliths.

The aquifer is intensively exploited for irrigation as well as domestic use (Fig. 12). A database of 84 irrigation wells located in the limestone show high average discharge of ~9 l/s, (Tab. 3) and a very significant water table fluctuation between post-monsoon (average water table 12.8 m b.g.s.) and pre-monsoon (average water table 26.5 m b.g.s.). In addition to the drop in water table, the average specific capacity of the wells decreases significantly. This decrease may be partly due to larger head differentials which reduces pump discharge and also partly due to the desaturation of the upper part of the limestone aquifer. For instance, out of all the dataset, 14 wells have a specific capacity (i.e. the discharge divided by the drawdown) higher than 5 l/s/m. For 13 of these wells, the static water level (SWL) is <20 m b.g.s., for 8 of them the SWL is <11 m. These data suggest a quite high permeability in the top 10 m of the limestone, possibly corresponding to the epikarst layer.

DISCUSSION

Field observations of caves, karst springs, swallow-holes, and karrenfields clearly indicate that the three carbonate formations of the Cuddapah sedimentary basin are karstified.

A specific question to be answered in semi-arid environments is to know whether observed karst has developed under present conditions or is inherited from past humid periods (Jennings 1983). The observed cave systems, being mostly inactive or only seasonally active, have developed during the Quaternary and possibly even earlier and it has been established that more humid conditions have prevailed during part of this period (Durand *et al.* 2007); these conditions have probably enhanced karstification processes. However, present hydrological observations in the Narji limestone indicate

active flow in conduits feeding permanent and seasonal springs. This strongly suggests ongoing karst development and dissolution processes. It is not possible to be as assertive for the two other carbonate units because of lack of field evidence, however it is likely that dissolution processes are equally active since these carbonate aquifers are located in very similar contexts than the Narji limestone aquifer.

Combining geological, geomorphological, and cave patterns information, it is possible to propose a tentative history of karstification for the Narji limestone (Fig. 14) which is the unit having the largest accessible cave system. In the earlier stage, it is inferred that network maze caves have developed in a confined limestone aquifer setting where diffuse infiltration took place across

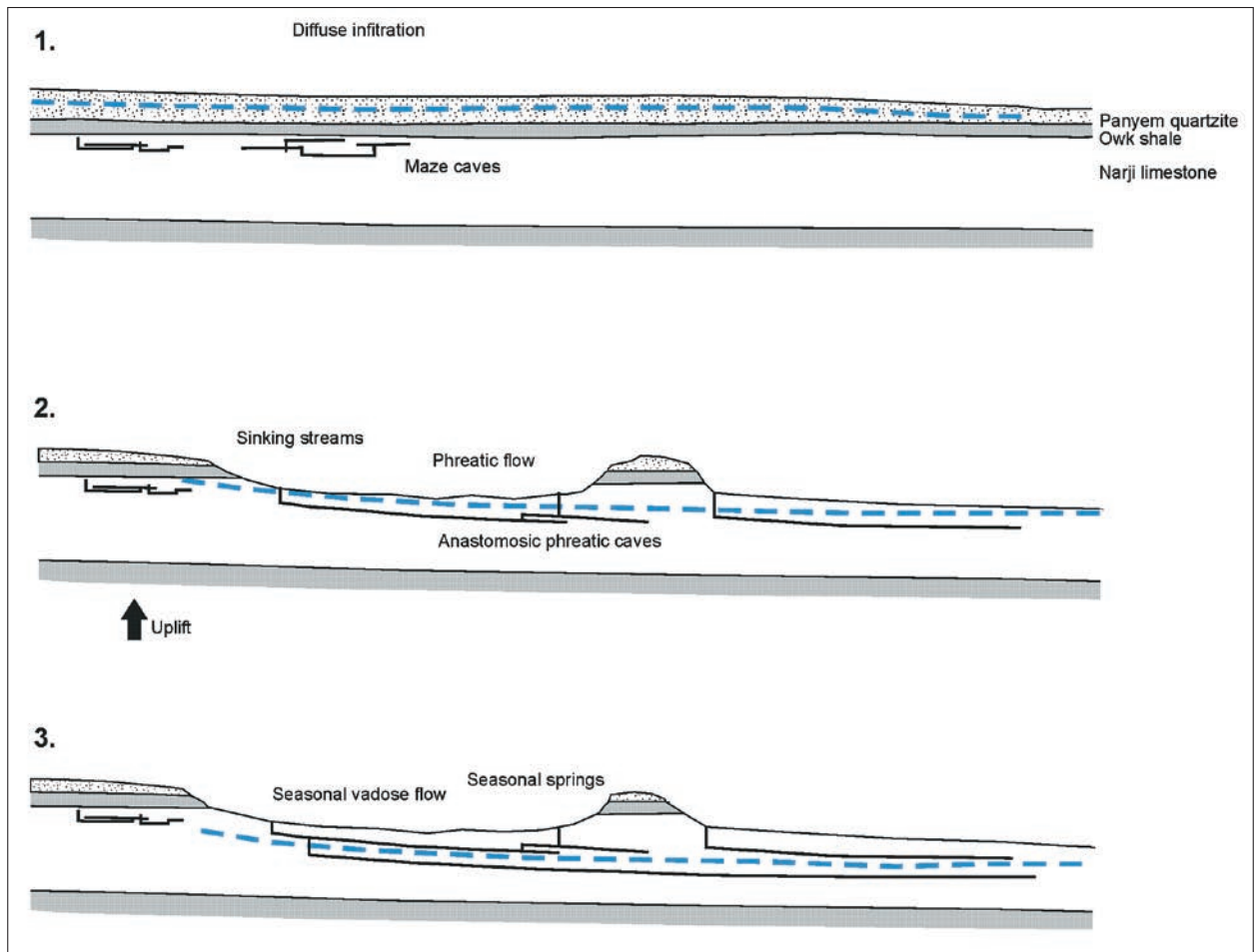


Fig. 14: A karstification conceptual model of the Narji limestone: 1) initial phase with development of maze cave system in a confined setting; 2) following tectonic uplift, the limestone is progressively exposed to the surface and anastomosing phreatic cave systems develop; 3) the water table gets progressively lower inducing a lower level of karstification (present state).

quartzite and shale layers similarly to the conceptual model of Palmer (1991, 2007). This event is believed to be Pre-Pliocene during more humid conditions prior to the onset of monsoonal conditions and Western Ghats uplifting at ~8 Ma. During this period, the sea level was more than ~100 m higher than the present level (Haq *et al.* 1987).

The fact that these relict maze caves (Nila Bilam, Yerra Zari Gabi, Fig. 8) are located near the top of the limestone series seems to corroborate this type of development. This model requires a significant permeability of the quartzite and shale, possibly initiated by the pre-lifting compressional forces, so as diffuse infiltration can take place. After Early-Pliocene, a eustatic fall in sea-level along with the Western Ghats denudational rebound (uplift and tilting of relief to the east (Radhakrishna 1952; Vaidyanadhan 1964) occurred. This event is believed to cause structural compartmentalization and fragmentation that enhanced denudation rates along

the Eastern Ghats margin controlled by the structural pattern of the resistant rock outcrops viz, Charnokites, Cuddapah sandstones and quartzites (Gunnell 1998a). The entire instability event caused a ~300m surface uplift in the Western Ghats (Gunnell & Fleitout 1998), with the harder rocks being comparatively more uplifted (Gunnell & Louchet 1998) than their softer counterparts.

Following tectonic uplifting, a positive relief favored surface runoff and progressive erosion of the quartzite and shale which resulted in the exposure of Narji limestone at the earth surface. The uplifting of Western Ghats and the onset of monsoon (~8 Ma), caused more humidity on the west coast of India, while the entire southern India was subjected to a long lasting aridification and developed characteristics of semi-arid landscapes (Gunnell 1998b).

Thus, piezometric surfaces readjusted to lower base levels, maze cave systems became inactive (relict caves), and the limestone aquifer became unconfined. This set-

ting supported the development of phreatic conduits (e.g. Belum cave) fed by sinking streams issued from quartzite hills and diffuse infiltration through the limestone plateau. However, the aridification was itself responsible for the initiation of seasonal contrasts and more intense precipitation regimes (Gunnell 1998a). During rapid and frequent sea level fluctuating Quaternary, more humid conditions (e.g. Durand *et al.* 2007) may have promoted the incision of deeper cave systems and the development of the existing ones. Further erosion of the land surface resulted in additional lowering of piezometric surfaces and the readjustment of the conduit systems (vadose conditions in the upper part of the limestone with associated development of canyon type conduits, progressive dissolution of a deeper level of phreatic conduits). This stage is still ongoing nowadays with an active inaccessible conduit network at greater depth and a seasonally active vadose flow in the explored caves.

Ford & Williams (2007) propose a linear relationship between electrical conductivity (EC) and total hardness (TH). Using this relationship and the average EC measured at Kona springs (Tab. 2: S2 & S3), average TH is 296 mg/l as CaCO₃. For the same spring, the specific discharge is estimated to be 0.98 l/s/km² (or 23.3 mm/a). Using Corbel formula (e.g. Ford & Williams 2007), the denudation rate is therefore 3.7 mm/ka. Even if this data should be taken as a crude estimate, it is in the same range as denudation rates estimated in arid climatic conditions in Australia (e.g. Stone *et al.* 1994).

It is proposed to consider these three carbonate formations as karstified and undergoing active karstification processes. This has an important bearing on the hydrological functioning of these aquifers which need to be discussed in more detail. Recharge of the limestone aquifers occur during the monsoon months (June to November) only after significant rainfall (average 5–7 recharge events per year): runoff on non-carbonated hilly terrains (mostly quartzite) is the main source of point recharge through swallow-holes located in the limestone plateau near the foothills. Significant runoff is also generated within the limestone areas and may recharge the aquifer through swallow-holes (as seen near the entrance of Belum cave) but also contribute to surface flow (a well developed drainage pattern can be observed on the limestone/dolomite areas indicating significant surface runoff). Finally some recharge may occur as diffuse infiltration through the soil zone and epikarst; this type of recharge seem to be quite limited as very few drip flow is observed in cave systems even after significant rain events.

In the Narji limestone, a large part of the aquifer transmissivity occurs as conduit flow feeding karstic springs. In the massive part of the limestone, it seems

that conduits provide the predominant permeability as indicated by several dry wells drilled by farmers and during the touristic development of Belum cave; in the flaggy part of the Narji limestone and in more fractured zones (e.g. near the contact with quartzite), additional permeability by bedding planes and joints is likely since irrigation wells with good sustained flow (average discharge 7–8 l/s) have been implemented.

The permanent springs (Fig. 1: S2, S3, S8, S9 & S10) are situated only at the western foothills of the limestone plateau, with no such permanent spring existing in the nearby eastern foothills where the human activities have significantly modified the natural landscape: a high density of paddy fields irrigated by canal water issued from a river/reservoir. Either pre-existing springs are presently concealed by these modifications or a regional flow system has developed (i.e. deeper circulation in the Narji Limestone to the east) with no local discharge.

In the Koilkuntla limestone, it seems clear that the fracture system provide significant permeability because of the large number of irrigation wells with moderate yields that are observed; the role of conduit flow is unclear but probably contributes to the larger yields observed on some wells. Data show that a significant part of well discharge is provided by the upper part of the limestone aquifer, which is indicative of a higher permeability. This may be partly attributed to the existence of a well-developed epikarst layer as suggested by Fig. 13.

The studied karst region presents several characteristics of karst in arid and semi-arid regions as described by Ford & Williams 2007. The karstic landscape is less developed than in more humid setting with a limited number of dolines, preponderance of runoff and evaporation over infiltration, which results in modest spring flow and even of a majority of springs being seasonal (Tab. 2), predominance of point recharge over diffuse infiltration, and a lower density of caves. The specific geological setting of the studied area with widespread distribution of quartzite hillocks creates favourable conditions for karstification: significant runoff generated on the hillocks provides aggressive water (i.e. dilute runoff water with low pH) which will infiltrate the karst through swallow-holes and have a good potential for active limestone dissolution. Diffuse infiltration taking place across the CO₂-rich soil zone will also contribute to limestone dissolution within the underlying epikarst layer. However, due to the present climatic conditions combining low rainfall with high evaporation rates, diffuse infiltration and dissolution fluxes are believed to be quite limited.

Because of the flashy nature of rainfall events (high rainfall intensity), a significant part of the generated runoff will also remain as surface flow as indicated by the surface drainage pattern observed on the limestone

plateau. As a result, the general morphology has a strong fluvial component and the karst morphology is limited to specific areas.

Field data suggest the presence of a well-developed epikarst in the Narji and Koilkuntla limestone. However,

its role on the hydrological functioning of the aquifer is not clear and it may well not control significantly present recharge conditions.

CONCLUSIONS

Field observations indicate the extensive karstification of the three carbonate formations present within the Cuddapah sedimentary basin, namely the Vempalle dolomite, the Narji and Koilkuntla limestone, which together cover about 17% of this basin. The karstic nature of these formations need to be acknowledged and considered in future development/management activities such as civil engineering work, water management, land management, etc.

A widespread concern in semi-arid regions is the scarcity of water resources and the need to have adequate water resource management tools. Due to intensive irrigated agriculture, parts of the limestone aquifers of the Cuddapah sedimentary basin are overexploited (e.g. Rao *et al.* 2001). The management tools needed to reverse these observed water table declining trends have to be based on an adequate understanding of the aquifer hydrogeological characteristics (recharge, permeability, storage).

Another striking feature of the region is the abundance of quarries either for extraction of construction

slabs (in Belum area their extent increased from 9.7 km² in 1983 to 25.6 km² in 2010) or for cement factories. Their impact on groundwater recharge and balance is being assessed in an ongoing project but additional impacts on land surface temperature (Xiao & Weng 2007), landscape and water quality (Gunn *et al.* 1993) are expected to occur.

There is a need for more detailed studies on karstification and the structure and functioning of these karst aquifers. A better understanding of these aquifers is essential for the adequate estimation of groundwater reserve, their sustainable exploitation, and also for the implementation of management policies aiming at protecting the quantity and quality of the resource. These karst water resources are essential to the local communities for domestic use and agricultural production.

Dams for irrigation are being built in the region to capture runoff from quartzite hills and the impoundments are at least partly in contact with karstified rocks; in this case, important and unexpected leakage may occur due to karst permeability.

ACKNOWLEDGMENTS

The first author is thankful to the Director, NGRI (CSIR) Hyderabad for permitting to publish this work. Farooq Ahmad Dar is grateful to UGC and French embassy for fellowship. Authors thank Dr. Krishniah, Mr. Nagmuniah, Mr. Babu (Belum cave employees) and Mr. Wajidud-Din for their continued support in the field work ac-

tivities. The NGO BIRDS agreed to share data from their APFAMGS project.

The authors also thank Dr. Paul Williams and an anonymous reviewer for their helpful and constructive comments in reviewing the paper.

REFERENCES

- Anand, M., Gibson, S.A., Subbarao, K.V., Kelley S.P. & A.P. Dickin, 2003: Early Proterozoic Melt Generation Processes beneath the Intra-cratonic Cuddapah Basin, Southern India.- *Journal of Petrology*, 44, 12, 2139–2171.
- Balakrishna, S. & B.E. Vijayam, 1968: Sedimentation of non-clastics in the western part of the Cuddapah basin.- *Bull. Nat. Geophys. Res. Inst.*, 6, 2, 51–67.
- Chandra, P.C., Satyanarayana T. & K.C.B. Raju, 1987: Geoelectrical response of cavities in limestones: An experimental field study from Kurnool District, Andhra Pradesh, India.- *Geoexploration*, 24, 6, 483–502.
- Coward, J.M.H., Waltham, A.C. & R.J. Bowser, 1972: Karst springs in the Vale of Kashmir.- *Journal of Hydrology*, 16, 213–233.
- Crawford, A.R., & W. Compston, 1973: The Age of the Cuddapah and Kurnool Systems, Southern India.- *Journal of the Geological Society of Australia*, 19, 4, 453–464.
- Dubey, D.P., Tiwari, R.N. & U. Dwivedi, 2006: Evaluation of Pollution Susceptibility of Karst Aquifers of Rewa Town (Madhya Pradesh) Using “DRASTIC” Approach.- *Journal of Environ. Science & Engg.* 48, 2, 113–118.
- Durand, N., Gunnell, Y., Curmi, P. & S.M. Ahmad, 2007: Pedogenic carbonates on Precambrian silicate rocks in South India: Origin and palaeoclimate significance.- *Quaternary International*, 162–163, 35–49.
- Dutt, N.V.B.S., 1962: Geology of Kurnool System of rocks in Cuddapah and the Southern part of Kurnool District.- *Rec. Geol. Surv. India*, 87, 549–694.
- Dutt, N.V.B.S., 1975: *Geology and mineral resources of Andhra Pradesh*.- Ramesh Publ., pp. 205, Hyderabad.
- Ford, D.C. & P. Williams, 2007: *Karst Hydrogeology and Geomorphology*.- John Wiley & Sons, Ltd, pp. 562, Chichester.
- Gebauer, H.D. & A. Abele, 1983: *Caves of India and Nepal / Höhlen von India und Nepal*.- Schwäbisch Gmünd & Ölmühle: Gebauer, pp. 166.
- Gebauer, H.D., 1985: *Kurnool 1984: Report of the speleological expedition to the district of Kurnool, Andhra Pradesh, India*.- *Abhandlungen zur Karst und Höhlenkunde*, 21, pp. 77.
- Gebauer, H.D., 1997: Indien 1996/97: Kurnool, Jaypur-Jagdulpur und Meghalaya.- *Mitt. Verb. dt. Höhlen- u. Karstforsch.* 43, 4, 104–111.
- Geological Survey of India, 1997: *Cuddapah geological quadrangle map series, 1:250,000*.- Kolkata.
- Gunn, J. & D. Bailey, 1993: Limestone quarrying and quarry reclamation in Britain.- *Environmental Geology*, 21, 3, 167–72.
- Gunnell, Y., 1998a: The interaction between geological structure and global tectonics in multistoried landscape development: a denudation chronology of the South Indian shield.- *Basin Research*, 10, 281–310.
- Gunnell, Y., 1998b: Passive margin uplifts and their influence on climatic change and weathering patterns of tropical shield regions.- *Glob. Planet. Change*, 18, 47–57.
- Gunnell, Y. & A. Louchet, 1998: The influence of rock hardness and divergent weathering on the interpretation of apatite fission track denudation rates: evidence from charnockites in South India and Sri Lanka.- *Zeitschrift für. Geomorphologie*, 44, 4, 481–504.
- Gunnell, Y. & L. Fleitout, 1998: Morphotectonic evolution of the Western Ghats, India.- In: Summerfield, M.A. (ed.) *Geomorphology and Global Tectonics*.- John Wiley & Sons, pp. 368, Chichester.
- Haq, B.H., Hardenbol, J. & P.R. Vail, 1987: The chronology of fluctuating sea level since the Triassic.- *Science*, 235, 1156–1167.
- Jeelani, G., 2008: Aquifer response to regional climate variability in part of Kashmir Himalaya in India.- *Hydrogeology Journal*, 16, 1625–1633.
- Jennings, J.N., 1983: The disregarded karst of the arid and semiarid domain.- *Karstologia*, 1, 61–73.
- Jhanwar, M.L., Rajurkar, S.T. & P.N. Phadtere, 1964: Stratigraphy of the Vempalle formation of Cuddapah basin.- *J. Indian Geosc. Ass.*, 4, 43–62.
- Kaila, K.L., Roy Chowdhury, K., Reddy, P.R., Krishna, V.G., Narain, H., Sabbotin, S.I., Sollogub, V.B., Chekunov, A.V., Kharetechko, G.E., Lazarenko, M.A. & T.N. Ilchenko, 1979: Crustal structure along Kavali--Udipi profile in the Indian Peninsular shield from Deep Seismic Sounding.- *J. Geol. Soc. India*, 20, 307–333.
- Kaila, K.L. & H.C. Tewari, 1985: Structural trends in the Cuddapah basin from deep seismic soundings (DSS) and their tectonic implications.- *Tectonophysics*, 115, 69–86.
- Kailasam, L.N., 1976: Geophysical studies of the major sedimentary basins of the Indian craton, their deep structural features and evolution.- *Tectonophysics*, 36, 1–3, 225–245.
- Kale, V., 1991: Constraints on the evolution of the Purana basins of peninsular India.- *J. Geol. Soci. India*, 38, 231–252.

- Kamal, M.Y., 1974: *Sedimentology and Sedimentary tectonics of the Kurnool system, near Kurnool*.- Unpublished PhD thesis, Osmania University, Hyderabad.
- Kamal, M.Y. & B.E. Vijayam, 1981: *Sedimentary tectonics of the Kurnool Cuddapah basin*.- In: *Fourth workshop on status, problems and programmes in Cuddapah basin*. Indian Inst. Peninsular Geol., pp. 75–85, Hyderabad.
- Kasipathi, C., Arjunudu, K., Rao, K.S. & M.S. Rao, 2008: *Cuddapah Formations of Andhra Pradesh, India. A New Report of Prospects for Rich Banded Iron Ore Formation*.- *Canadian Journal of Pure and Applied Sciences*, 2, 1, 227–233.
- King, W., 1872: *Kadapah and Kurnool formations in the Madras presidency*.- *Geol. Surv. Ind. Mem.*, 8.
- Kumar, J.V., 1983: *Geological and hydrogeological studies of part of Cuddapah basin*.- PhD thesis. Osmania University, Hyderabad.
- Meijerink, A.M.J., Rao, D.P. & J. Rupke, 1984: *Stratigraphic and structural development of the Precambrian Cuddapah Basin, SE India*.- *Precambrian Research*, 26, 57–104.
- Murty, K.S., 1988: *Karst Hydrogeology: India*.- In: *Karst Hydrogeology and Karst Environment Protection*. IAH, 21st Congress, 10–15 October 1988, 446–450, Guilin, China.
- Murthy, Y.G.K., Setti, T.L.N., Rajurkar, S.T., Meoloi, S.H., Nagaraja Rao, B.K., Ramaligaswami, G., Madan Mohan, B. & R. Ravindra Babu, 1979: *Salient features of the revised geological map of the Cuddapah basin*.- In: *Third workshop on status and problems in Indian Peninsular shield*, Inst. Of Indian Peninsular Geology, Hyderabad.
- Murthy, Y.G.K., 1981: *The Cuddapah Basin- A Review of Basin Development and Basement Framework Relations*.- In: *Fourth workshop on status, problems and programs in Cuddapah Basin*, Inst. Of Indian Peninsular Geology, 51–73, Hyderabad.
- Nagaraja Rao, B.K., Rajaurkar, S.T. & G. Ramalingaswamy, 1987: *Stratigraphy, Structure and Evolution of the Cuddapah Basin*.- *Mem. Geol. Soc. India*, 6, 33–86.
- Narayanaswami, S., 1966: *Tectonics of Cuddapah Basin*.- *J. Geol. Soc. Ind.*, 7, 33–50.
- Palmer, A.N., 1991: *Origin and morphology of limestone caves*.- *Geol. Soc. Am. Bull.*, 103, 1–21.
- Palmer, A.N., 2007: *Cave Geology*.- Cave Books, pp. 454, Dayton, Ohio.
- Pascoe, E.H., 1950: *A Manual of the Geology of India and Burma*.- Delhi, Govt., 1–3rd ed.
- Qureshi, M.N., Krishna-Brahman, N., Aravamadhu, P.S. & S.M. Naqvi, 1968: *Role of granitic intrusions in reducing the density of the crust and other related problems as illustrated from a gravity study of the Cuddapah Basin, India*.- *Proc. R. Soc.*, 304, 449–464.
- Radhakrishna, B.P., 1952: *The Mysore Plateau, its structural and physiographic evolution*.- *Bull. Mysore Geologists Assoc*, 3, 1–53.
- Raju, R.D., 2009: *Cuddapah Basin: India's Emerging Uranium-Hub*.- *Jour. Indian Association of Sedimentologists*, 28, 2, 15–24.
- Ramam, P.K. & V.N. Murthy, 1997: *Purana basins: Cuddapah, Pakhal, Bhima*.- In: *Geology of Andhra Pradesh*, Geological Society of India, 119–136, Bangalore.
- Rao, P.B., Subrahmanyam, K. & R.L. Dhar, 2001: *Geoenvironmental effects of groundwater regime in Andhra Pradesh, India*.- *Environmental Geology*, 40, 4–5, 632–642.
- Riding, R. & M. Sharma, 1998: *Late Palaeoproterozoic (~1800–1600 Ma) stromatolites, Cuddapah Basin, southern India: cyanobacterial or other bacterial microfabrics?*- *Precambrian Research*, 92, 21–35.
- Roy, A.K., 1947: *Geology of the Dhone taluk and neighbouring parts, Kurnool districts*.- Unpublished Geological Survey of India Progress Report (1945–1946).
- Sen, S.N. & R. Narsimha, 1968: *Igneous activity in Cuddapah Basin and adjacent areas and suggestions on the palaeogeography of the Basin*. In: *Proc. Symp. Upper Mantle Project*, January 1967, Hyderabad (India), Session V, 261–285.
- Shibasaki, T., Balakrishna, S., Yoshimura, T., Venkatanarayana, B., Furukama, H., Venkateswara, R.T., Chuman, N., Ramanohan, R.Y. & K. Venkateswaralu, 1985: *Karstification process of carbonate rocks in the Cuddapah sedimentary Basin, Indian Peninsular Shield*.- *J. Fac. Mar. Sci. Technol., Tokai Univ.*, 21, 31–45.
- Singh, Y. & D.P. Dubey, 2001: *Quality of groundwater in shallow and deep karst and other associated aquifer zones of central India*.- In: *8th Multidisciplinary Conference on Sinkholes and the Engineering and Environmental Impacts of Karst*, April 2001, USA, AA Balkema publishers, 259–264.
- Singh, A.P. & D.C. Mishra, 2002: *Tectonosedimentary evolution of Cuddapah basin and Eastern Ghats mobile belt (India) as Proterozoic collision: gravity, seismic and geodynamic constraints*.- *Journal of Geodynamics*, 33, 249–267.

- Stone, J., Allan, G.L. & L.K. Fifield, 1994: Limestone erosion measurements with cosmogenic chlorine-36 in calcite – preliminary results from Australia.- Nuclear Instruments and Methods in Physics Research, Series B, 92, 311–316.
- UNEP, 1992: *World Atlas of Desertification*.- Edward Arnold, pp. 182, London.
- Vaidyanathan, R., 1961: Stromatolites in lower Cuddapah limestones (Precambrian).- *Current Science*, 30, 221.
- Vaidyanadhan R., 1964: Recognition and correlation of erosion surfaces in and around the southern part of the Cuddapah Basin.- *J. Geol. Soc. Ind.*, 5.
- Venkatanarayana, B. & T.V. Rao, 1989: Geological and geophysical investigations for delineating karstic structures of the southwestern portion of Cuddapah basin, Andhra Pradesh, India.- In: Berry, B.F. (ed.) *Proc. of 3rd Multidisciplinary Conference on Sinkholes and the Engineering and Environmental Impacts of Karst*, Oct. 1989, USA, AA Balkema publishers, 59–64.
- Venkatanarayana, B., Ahmed, S. & V. Agnihotri, 1999: The hydrogeology of the Kuteshwar limestone deposits, Madhya Pradesh, India.- *Journal of Environmental Hydrology*, 7, 5, 1–13.
- Vijayam, B.E., 1968: Worm burrows in Narji Limestone near Govindine.- *Current science*, 37, 5, 142.
- Vijayam, B.E., Kamal, M.Y. & K. Veeriah, 1981: Sedimentation in the Kurnool group.- In: *Fourth workshop on status, problems and programmes in Cuddapah basin*, Indian Inst. Peninsular Geol., Hyderabad.
- Vittal, K.P.R., Basu, M.S., Chary, G.R., Sankar, G.R.M., Srijaya, T., Ramakrishna, Y.S., Samra, J.S. & G. Singh, 2004: District wise Promising Technologies for Rainfed Groundnut based Production System in India. In: *All India Coordinated Research Project for Dryland Agriculture Central Research Institute for Dryland Agriculture Santoshnagar*, Hyderabad.
- Xiao, H. & Q. Weng, 2007: The impact of land use and land cover changes on land surface temperature in a karst area of China.- *Journal of Environmental Management*, 85, 245–257.



Farooq A Dar <farooq.dar1@gmail.com>

AJGS: A manuscript number has been assigned to Hydrogeochemical characteristics of Karst Aquifer from a semi-arid region of South India and impact of rainfall recharge on groundwater chemistry

1 message

Arabian Journal of Geosciences <jovelyn.ortiz@springer.com>

Wed, Jun 19, 2013 at 2:55 AM

To: Farooq Ahmad Dar <farooq.dar1@gmail.com>

Dear Mr Dar,

Your submission entitled "Hydrogeochemical characteristics of Karst Aquifer from a semi-arid region of South India and impact of rainfall recharge on groundwater chemistry" has been assigned the following manuscript number: AJGS-D-13-00568.

You will be able to check on the progress of your paper by logging on to Editorial Manager as an author. The URL is <http://ajgs.edmgr.com/>.

Thank you for submitting your work to this journal.

Kind regards,

Editorial Office
Arabian Journal of Geosciences